Development and Manipulation of Photoresponsive Polymer Networks Through Light-Mediated Polymerizations

By

Michael Wade Lampley

Dissertation

Submitted to the Faculty of the

Graduate School of Vanderbilt University

in partial fulfillment of the requirements

for the degree of

DOCTOR OF PHILOSOPHY

in

Chemistry

August 9, 2019

Nashville, Tennessee

Approved:

Eva M. Harth, PhD

John A. McLean, PhD

Steven D. Townsend, PhD

G. Kane Jennings, PhD

To my amazing parents,

My brother and sister,

And my adorable niece.

We are all in the gutter,

But some of us are looking at the stars.

-Oscar Wilde

ACKNOWLEDGEMENTS

I would first like to thank my advisor, Professor Eva Harth, for giving me the opportunity to continue my education, for the guidance that you have given me, and for supporting and encouraging me over the years. Thank you for being a constant source of positivity and excitement, and for pushing me to be better. I would also like to thank the members of the Harth Research Group, past and present, for their support and comradery. I am eternally grateful for all the knowledge and friendships that I have obtained working with you.

I would also like to thank the members of my PhD committee: Professors John McLean, Steve Townsend, and Kane Jennings. Thank you for all the criticisms, insights, encouragements, and wisdom. I truly appreciate the time and guidance that you have given me over the years. I would like to thank the sources of financial support that made this research possible: the National Science Foundation, the Welch Foundation, the University of Houston Center of Excellence in Polymer Chemistry, and the Vanderbilt Department of Chemistry.

To Professor Norma Dunlap, I will be forever thankful. Your passion for teaching and chemistry inspired me to begin this journey, and with your knowledge and encouragement I built an invaluable scientific foundation that allowed me to complete it. To the members of the Dunlap Research Group during my time there, thank you for the support and the friendships that helped me get through the hard times.

I would like to extend a very special thanks to my family and friends who helped me on this journey with their love, understanding, and encouragement. This was all made possible with your love and support. Thank you for always listening. You will never know how much all of you mean to me.

TABLE OF CONTENTS

Page

DEDICATION ii

ACKNOWLEDGEMENTS iv

LIST OF FIGURES vii

LIST OF SCHEMES xiii

LIST OF TABLES xiv

Chapter

I. Introduction 1

Dissertation Overview 9
References 11

II. Photocontrolled Growth of Crosslinked Nanonetworks 23

Introduction 23
Results and Discussion 24
Preparation of Photogrowable Nanonetworks 24
Expansion of Nanonetworks Through Direct Photolysis 28
Promoted Disassembly of Nanonetworks After Direct Photolysis Expansion 30
Expansion of Nanonetworks by a Photoredox Catalyzed Polymerization 30
Promoted Disassembly of Nanonetworks After Photoredox Mediated Expansion 32
Conclusion 33
Experimental 33
References 59

III. Nanonetwork Photogrowth Expansion: Tailoring Nanoparticle Networks' Chemical Structure and Local Topology 64

Introduction 64
Results and Discussion 67
Model Polymerizations 69
Homopolymer Incorporation 70
Aminolysis of Homopolymer ENNs 73
Thermoresponsive Behavior of PNIPAAM ENNs 74

Incorporation of Statistical Copolymers 76
Incorporation of ABA tri- and ABABA Pentablock Copolymers 78
Aminolysis of ABA tri- and ABABA Pentablock ENNs 81
Conclusions 82
Experimental 83
References 118

IV. Progress Towards Site Selective Expansions of Diels-Alder Crosslinked Photogrowable Nanonetworks 122

Introduction 122
Results and Discussion 124
Photogrowable Nanonetwork Formation 125
RAFT Photocatalyst Selectivity 127
Conclusion 131
Experimental 131
References 149

V. Progress Towards the Preparation and Photocontrolled Growth of Self-Assembled Photoresponsive Materials 152

Introduction 152
Results and Discussion 155
Synthesis of a Bis-Ureidopyrimidinone-Urea-Trithiocarbonate 155
Conclusion 158
Experimental 158
References 162

VI. Future Directions 167

Appendix

A. Curriculum Vitae 169

LIST OF FIGURES

Figure Page

I-1. UV photoinduced reshuffling of trithiocarbonates....2

I-2. Comparison of the mechanisms of an iniferter RAFT polymerization vs a photoredox catalyzed RAFT polymerization....4

I-3. Schematic description of the surface modification of nanoparticles through (A) thiol-ene click and (B) surface-initiated polymerization....8

II-1. (A) Schematic description of nanonetwork expansion by direct photolysis. (B) Size and dispersity of nanonetworks before, PGNN, and after expansion, ENNs, by TEM, DLS, and GPC. (C) TEM images of nanonetworks before and after expansion. (D) GPC traces of nanonetworks before and after expansion. (E) Schematic description of the selective cleavage of nanonetwork by aminolysis to produce branched polymers (BP). (F) GPC traces of linear thiolated polymer scaffold 5, BP1 generated from PGNN and BP2-4 generated from ENN1-3. (G) GPC analysis of linear polymer and branched polymers from PGNN (BP1) and ENNs (BP2-4)....29

II-2. (A) Schematic description of nanonetwork expansion by photoredox catalysis using PTH. (B) Size and dispersity of nanonetworks before, PGNN, and after expansion, ENNs, by TEM, DLS, and GPC. (C) TEM images of nanonetworks before and after expansion. (D) GPC traces of nanonetworks before and after expansion. (E) Schematic description of the selective cleavage of nanonetwork by aminolysis to produce branched polymers (BP). (F) GPC traces of linear thiolated polymer scaffold 5, BP1 generated from PGNN and BP5-6 generated from ENN4-5. (G) GPC analysis of linear polymer and branched polymers from PGNN (BP1) and ENNs (BP5-6)....31

II-S1. 1H NMR spectrum of the purified maleimide TTC 1....43

II-S2. 13C NMR spectrum of the purified maleimide TTC 1....44

II-S3. 1H NMR spectrum of the thiol-maleimide compatibility experiment....45

II-S4. 13C NMR spectrum of the thiol-maleimide compatibility experiment....46

II-S5. 1H NMR spectrum of polymer 2....47

II-S6. 1H NMR spectrum of polymer 3. 48

II-S7. 1H NMR spectrum of polymer 4. 49

II-S8. 1H NMR spectrum of polymer 5. 50

II-S9. 1H NMR spectrum of photogrowable nanonetwork. 51

II-S10. 1H NMR spectrum of model DA reaction. 52

II-S11. 13C NMR spectrum of model DA reaction. 53

II-S12. 1H NMR spectrum of furan capped nanonetwork. 54

II-S13. 1H NMR spectrum of expanded nanonetwork after 1 hour of irradiation. 55

II-S14. 1H NMR spectrum of expanded nanonetwork after 6 hours of irradiation. 56

II-S15. GPC traces of polymers synthesized from maleimide TTC 1a. 57

II-S16. GPC traces of polymers synthesized from maleimide TTC 1a in the presence of 0.02 mol% PTH. 58

II-S17. GPC traces of nanonetworks before expansion (PGNN), after expansion for 6 hours (ENN), and after expansion for 30 minutes in the presence of PTH (ENN PTH). 59

III-1. (A) Structure and expansion of nanonetworks through the incorporation of various monomers, and the list of polymers incorporated into the networks. (B) The general structure of expanded networks with incorporated homopolymers, statistical copolymers, and block copolymers. 66

III-2. (A) Schematic description of homopolymer expansions of nanonetworks. GPC traces of homopolymer expansions with (B) MA, (C) tBA, (D) TFEA, (E) HEA, and (F) NIPAAM at 30 and 60 minutes irradiation times. 70

III-3. (A) Schematic description of the selective cleavage of nanonetworks to produce branched polymers. GPC traces of the resulting branched polymers from homopolymer expansions of (B) MA, (C) tBA, (D) TFEA, (E) HEA, and (F) NIPAAM. 73

III-4. (A) DLS diameter measurements of NIPAAM and HEA ENNs across 25-45°C. (B) Schematic description of PNIPAAM chain collapse above 32°C producing shrunken nanonetworks. (C) Images of solutions of NIPAAM and HEA ENNs at 25°C and 40°C. 75

III-5. (A) Schematic description and (B) GPC traces of statistical copolymer expansions of nanonetworks 77

III-6. (A) Schematic description of ABA block copolymer expansion of nanonetworks. GPC traces of block copolymer expansions with (B) tBA, (C) HEA, (D) TFEA, and (E) NIPAAM. 79

III-7. (A) Schematic description of the selective cleavage of nanonetworks to produce branched polymers. GPC traces of the resulting block copolymer expansions with (B) tBA, (C) HEA, (D) NIPAAM, and (E) TFEA. 81

III-S1. GPC traces of model homopolymerizations 96

III-S2. GPC traces of model statistical copolymerizations. 97

III-S3. GPC traces of model block copolymerizations with MA and A) tBA, B) HEA, C) TFEA, D) PNIPAAM. 98

III-S4. ^{1}H NMR spectrum of polymer 2. 99

III-S5. ^{1}H NMR spectrum of polymer 3. 100

III-S6. ^{1}H NMR spectrum of polymer 4. 101

III-S7. ^{1}H NMR spectrum of polymer 5. 102

III-S8. ^{1}H NMR spectrum of photogrowable nanonetwork. 103

III-S9. ^{1}H NMR spectrum of parent photogrowable nanonetwork. 104

III-S10. ^{1}H NMR spectrum of expanded nanonetwork with MA after 30 minutes of irradiation. 105

III-S11. ^{1}H NMR ($CDCl_3$, 600 MHz) spectrum of expanded nanonetwork with tBA after 30 minutes of irradiation. 106

III-S12. ^{1}H NMR ($CDCl_3$, 600 MHz) spectrum of expanded nanonetwork with TFEA after 30 minutes of irradiation. 107

III-S13. ^{1}H NMR (DMSO-d_6, 600 MHz) spectrum of expanded nanonetwork with HEA after 30 minutes of irradiation. 108

III-S14. ^{1}H NMR ($CDCl_3$, 600 MHz) spectrum of expanded nanonetwork with NIPAAM after 30 minutes of irradiation. 109

III-S15. ^{1}H NMR ($CDCl_3$, 600 MHz) spectrum of statistical copolymer expanded nanonetwork with MA and tBA after 30 minutes of irradiation. 110

III-S16. ^{1}H NMR ($CDCl_3$, 600 MHz) spectrum of statistical copolymer expanded nanonetwork with MA and TFEA after 30 minutes of irradiation. 111

III-17. ^{1}H NMR ($CDCl_3$, 600 MHz) spectrum of statistical copolymer expanded nanonetwork with MA and HEA after 30 minutes of irradiation. 112

III-18. ^{1}H NMR ($CDCl_3$, 600 MHz) spectra of ABABA block copolymer expanded nanonetwork progression with MA and TFEA. 113

III-S19. ^{1}H NMR ($CDCl_3$, 600 MHz) spectra of ABABA block copolymer expanded nanonetwork progression with MA and tBA. 114

III-S20. ^{1}H NMR ($CDCl_3$, 600 MHz) spectra of ABABA block copolymer expanded nanonetwork progression with MA and NIPAAM.. 115

III-S21. ^{1}H NMR (DMSO-d_6, 600 MHz) spectra of ABABA block copolymer expanded nanonetwork progression with MA and HEA. 116

III-S22. TEM images of the progression of ABA triblock, ABABA pentablock copolymer, and microparticle expansions. 117

IV-1. Schematic description of the proposed work to prepare differentiated nanonetworks through selective polymerizations from either scaffold polymer end groups (RAFT or ATRP) or crosslinker TTC. 124

IV-2. (A) Schematic description of the preparation of PGNNs from previous works. (B) Schematic description of the proposed work to prepare a second generation of PGNNs bearing RAFT or ATRP end groups from a furan functionalized scaffold polymer through a Diels-Alder reaction. 126

IV-3. (A) Structures of trithiocarbonates. (B) Comparison of symmetric and asymmetric TTC fragmentation pathways. 129

IV-S1. GPC traces of RAFT and ATRP statistical copolymers with FMA 136

IV-S2. GPC trace of RAFT-PMMA-*co*-PFMA chain extension with MMA. 137

IV-S3. GPC trace of ATRP-PMMA-*co*-PFMA chain extension with MMA. 138

IV-S4. GPC trace of RAFT-PMMA-*co*-PFMA chain extension with MMA in the presence of **1b**. 139

IV-S5. GPC trace of RAFT-PGNN. 140

IV-S6. GPC traces of MA polymerizations from **1b** mediated by ZnTPP 141

IV-S7. GPC trace of PMA chain extension with MA and 0.00625 mol% ZnTPP 142

IV-S8. TEM image of RAFT-PGNN. 143

IV-S9. ^{1}H NMR of RAFT-PMMA-*co*-PFMA. 144

IV-S10. ^{1}H NMR of ATRP-PMMA-*co*-PFMA. 145

IV-S11. ^{1}H NMR of RAFT-PGNN. 146

IV-S12. ^{1}H NMR of RAFT-PMMA-*co*-PFMA-*b*-PMMA produced in the presence of **1b**.....147

IV-S13. Crude ^{1}H NMR of concentrated supernatant produced from the chain extension of RAFT-PMMA-*co*-PFMA in the presence of **1b**. 148

V-1. (A) General structures of ureidopyrimidinone (UPy) and its dimer. (B) General structure of UPy with urea or urethane moieties and the illustration of dimerization and lateral stacking. (C) General structure of a Bis-Upy with urea or urethane and the illustration of self-dimerization and lateral stacking. 153

V-2. General structure of the proposed Bis-UPy-Urea-TTC and the schematic description of the proposed transformation from a self-assembled gel to a self-assembled fiber facilitated by polymerization from the TTC. 154

LIST OF SCHEMES

Scheme Page

I-1. Preparation of end-linked gels and the photoinduced network growth.....3

I-2. Preparation of crosslinked STEM gels and the photoinduced network modification.....7

II-1. Synthesis scheme of the photocontrolled growth of photoresponsive nanonetworks 25

II-S1. Model thiol-maleimide reaction (A). Synthesis of thiolated polymers (B).....35

III-1. Synthesis of thiolated polymer 67

III-2. Synthesis of photogrowable nanonetwork 68

III-S1. Model polymerization of various monomers. 85

IV-S1. Model polymerization of MA from **1b** mediated by ZnTPP. 135

V-1. Steps to the synthesis of Bis-UPy-Urea-TTC **7**. 155

V-2. Steps to the synthesis of a Bis-UPy-Urea-TTC 156

V-3. Steps to the synthesis of Bis-UPy-Urea-TTC **17**. 157

.

LIST OF TABLES

Table Page

II-1. Syntheses of photogrowable nanonetworks (PGNNs) through thiol-maleimide click chemistry....27

II-S1. GPC analysis of polymers synthesized from maleimide TTC 1a....57

II-S2. GPC analysis of polymers synthesized from maleimide TTC 1a in the presence of 0.02 mol% PTH. 58

III-1. Homopolymer expansions of PGNNs 71

III-2. Aminolysis of homopolymer nanonetwork expansions 73

III-3. Statistical copolymer expansions of PGNNs....77

III-4. Block copolymer expansions of PGNNs 80

III-5. Aminolysis of block copolymer nanonetwork expansions 82

III-S1. Model homopolymerizations with TTC 1a 96

III-S2. Model statistical copolymerizations with TTC 1a 97

III-S3. Model block copolymerizations with TTC 1a 98

IV-S1. GPC analysis of RAFT and ATRP statistical copolymers with FMA.....136

IV-S2. GPC analysis of RAFT-PMMA-*co*-PFMA chain extension with MMA. 137

IV-S3. GPC analysis of ATRP-PMMA-*co*-PFMA chain extension with MMA. 138

IV-S4. GPC analysis of RAFT-PMMA-*co*-PFMA chain extension with MMA in the presence of **1b** 139

IV-S5. GPC analysis of MA polymerizations from **1b** mediated by ZnTPP. 141

IV-S6. GPC analysis of PMA chain extension with MA and 0.00625 mol% ZnTPP. 142

IV-S7. GPC analysis and comparison of MA polymerization
with BTPA mediated by ZnTPP 142

CHAPTER I

INTRODUCTION

Polymer networks are the structural foundation for a number of polymeric materials including nanoparticles, microparticles, thin films and bulk gels. These networks are comprised of either physical connections[1-3] or covalent bonds[4-6] and can be constructed with a wide range of chemical building blocks engineer materials with specific physical and chemical properties. There is immense interest in these materials due to their versatile connections and structural diversity which has seen them utilized in a wide range of technological areas such as biomedical applications in the way of tissue engineering,[7-9] drug delivery,[10-12] and antifouling[13-15] as well as in areas such as stretchable electronics[16-18] and soft robotics.[19] The rise of polymer networks can in part be attributed to crosslinking chemistries that enable controlled and facile connections such as click chemistries (e.g. thiol-ene, thiol-yne, azide-alkyne).[20] Controlling and finely tuning network properties (e.g. swelling capacity, hydrophilicity, elasticity, conductivity, etc.) is of the utmost importance when preparing materials for specific applications. However, most traditional networks are static, and the bulk properties cannot be manipulated once a crosslinked network has formed. Additionally, current polymer network architectures are heterogenous and contain network defects that affect the physical network properties, especially for cases in which free radical polymerizations are used due to the uncontrolled nature of these processes. In order to reach a higher level of precision and more specialized applications, a higher level of control over network formation, architecture, and material properties is required.

In the past decade, polymeric networks have become increasingly more dynamic through the incorporation of reversible linkages such as cycloaddition adducts,[21-25] disulfide bonds,[26-27] and

oximes,[28-30] or stimuli responsive moieties such as dithiocarbamates,[31] thiuram disulfides,[32] and trithiocarbonates (TTCs) within the network architecture.[6, 33-34] In particular, TTCs have emerged as a powerful tool to develop dynamic and photo-responsive materials due to their ability to act as initiators, chain transfer agents, and terminators, known as "iniferters,"[35] in controlled radical polymerizations (CRPs). For this reason, materials produced with embedded TTCs have been shown to possess photoresponsive properties such as photocontrolled growth,[36-38] photoinduced self-healing,[39] photoinduced network alterations,[40] and photo-degradation.[41-42] Of particular interest, are photoinduced self-healing and photocontrolled growth as these two examples demonstrate the photoinduced manipulation of network architecture and properties that can be achieved through the use of TTCs as dynamic covalent crosslinkers.

Photoinduced self-healing of crosslinked gels with integrated TTCs was first reported by the Matyjaszewski group. Methacrylate gels were prepared by crosslinking methacrylates with a methacrylate functionalized TTC. The self-healing properties arise from the TTC's ability to undergo a "reshuffling" reaction (**Figure I-1**).[39] Upon irradiation with ultra violet (UV) light the TTC acts as an initiator and fragments into two radical species. The carbon-centered radical is free to recombine with the TTC sulfur-centered radical or form an adduct with another TTC unit. Adduct formation ultimately results in the exchange of side chains between TTC units. Through this reshuffling reaction lacerated gels can be repeatedly healed, and severed pieces of gel can be mended together as the crosslinks exchange their old connections for new ones.

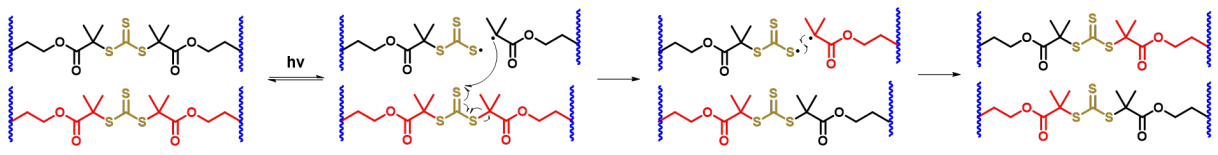

Figure I-1. UV photoinduced reshuffling of trithiocarbonates.

In 2013, the Johnson group demonstrated the first photoinduced addition of polymer chains to the crosslinks of an existing gel network. Pore size and composition of the photoresponsive polymer networks were manipulated through photo-CRPs with TTCs acting as iniferters.[37] End-linked polymer gels were prepared by a Diels-Alder reaction between a bis-norbornene functionalized TTC poly(N-isopropylacrylamide) (pNIPAAM) macromer and a tris-tetrazine crosslinker (**Scheme I-1**). UV or sunlight photoinduced iniferter polymerization of NIPAAM from the TTC resulted in an increase in molecular weight between polymer chains, bulk network growth, and an increase in swelling capacity.

Scheme I-1. Preparation of end-linked gels and the photoinduced network growth.

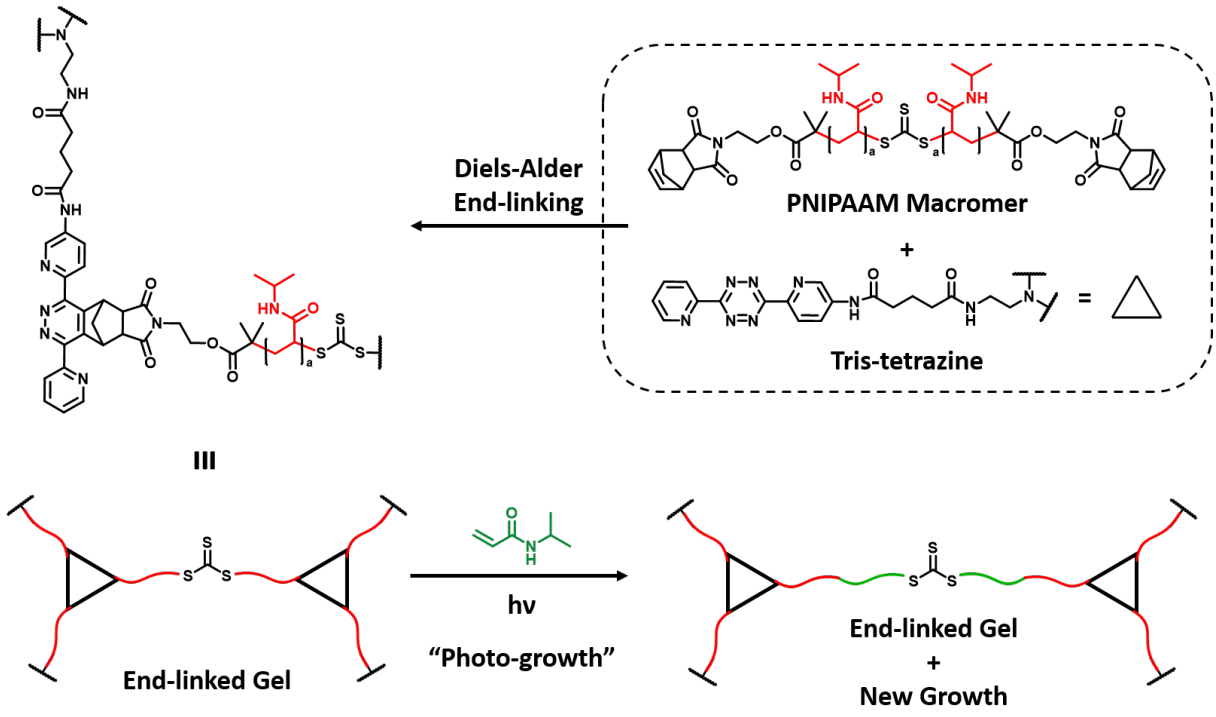

Parallel to the discovery of these network manipulations, the field of CRPs was experiencing a renaissance in the way of light-mediated polymerizations. Indeed, light-mediated polymerizations have been developed for the most well-known CRPs such as reversible addition-

fragmentation chain-transfer (RAFT),[43-45] atom transfer radical polymerization (ATRP),[46-50] and single electron transfer living radical polymerization (SET-LRP),[51-53] as well as other types of polymerizations including ring opening polymerization (ROP)[54] and ring opening metathesis polymerization (ROMP).[55] Traditional CRPs rely on exogenous radical initiators to produce radical species and initiate polymerization, and while UV induced photolysis iniferter polymerizations were known[35] and require no exogenous radical source, they often suffer from side reactions that diminish control as a result of prolonged exposure to UV light.[56-57] These detriments stimulated the investigation into lower energy visible light-mediated polymerization methods that required no external radical initiator.

Inspired by the seminal works of the Hawker group,[46] Boyer et al. developed photoinduced electron transfer (PET)-RAFT polymerization techniques that rely on the use of photocatalysts and lower energy visible light to provide greater spatiotemporal control over their thermal polymerization counterparts.[45] In this process a photocatalyst is excited by a wavelength of visible light and is able to transfer an electron to the chain transfer agent (CTA) producing two radical ion

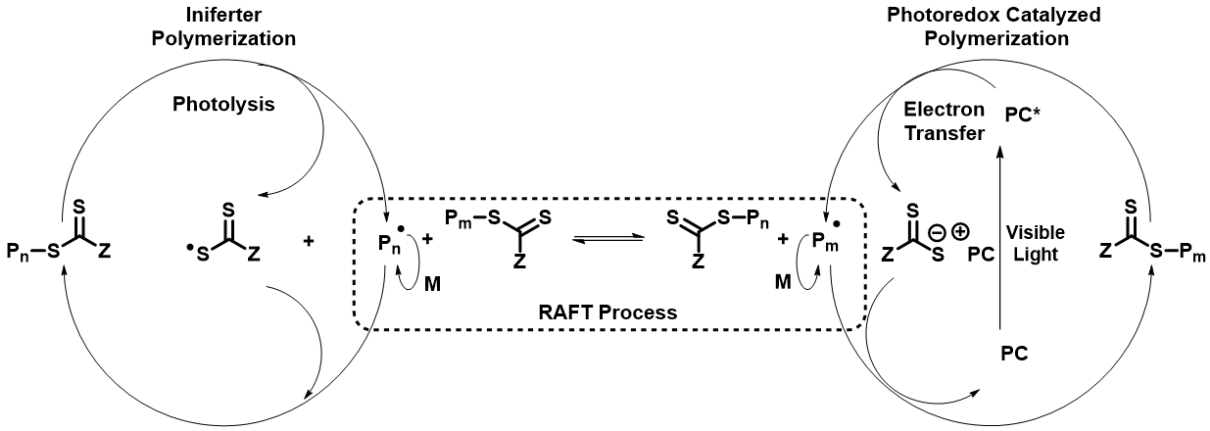

Figure I-2. Comparison of the mechanisms of an iniferter RAFT polymerization vs a photoredox catalyzed RAFT polymerization.

species (**Figure I-2**). The CTA is able to then dissociate producing a CTA anion and a carbon-centered radical that is free to propagate. The CTA anion and the photocatalyst radical ion can deactivate the propagating polymer chain to generate the ground state photocatalyst and a polymeric CTA. Additionally, the CTA anion is more stable than the sulfur-centered radical that is produced in photoinduced iniferter polymerizations which allows for fewer side reactions and increases the livingness of the polymerization.

PET-RAFT boasts a high level of control over molecular weight and dispersity, while demonstrating equally substantial versatility, orthogonality, and functional group compatibility.[58-62] This technique has been shown to work with numerous photoredox catalysts and various wavelengths of light.[43, 63-64] It is also tolerant of oxygen,[45, 50, 65-67] compatible with a wide range of monomers, and fully orthogonal with other types of polymerizations such as ROP[68] and ATRP.[69] Through the use of specific photoredox catalysts, a PET-RAFT polymerization can be specific to a single type of RAFT agent (e.g dithiobenzoate or TTC).[44, 70] This specificity has allowed for the synthesis of grafted copolymers utilizing a dithiobenzoate RAFT agent with pheophorbide A (PheoA) to grow the main methacrylate polymer chain and a TTC RAFT agent inimer (an initiator functionalized with a polymerizable monomer handle) with zinc tetraphenylporphyrin (ZnTPP) to graft acrylate polymer branches.

The success of PET-RAFT inspired the development of new organo-photocatalysts and the advancement of other CRP techniques.[48-49, 71] For example, Hawker et al. developed the first metal free ATRP approach using an organic-based photocatalyst 10-phenylphenothiazine (PTH).[47] The method eliminated the issue of metal contamination commonly found in traditional ATRP reactions while still maintaining the characteristics of a controlled ATRP polymerization (i.e. low dispersity, molecular weight control, and high end group fidelity). PTH was later adopted by the

Johnson group to develop a metal free photoredox catalyzed photo-CRP mediated by TTCs.[72] This photoredox method provides control over a variety of monomers with narrow dispersities and good molecular weight control.

Development and advancement of these light-mediated polymerizations allowed for the evolution of Johnson et al.'s work on the photogrowth of end-linked gels.[37] A new gel system was prepared from a tetra functional polyethylene glycol polymer functionalized with a dibenzocyclooctyne and a symmetric bis-azide functionalized TTC crosslinker. With the use of a photoredox catalyst, PTH, a new living additive manufacturing method was developed.[36] This work demonstrated improved control over the previous UV light catalyzed iniferter approach and was able to produce differentiated "daughter" gels from dormant "parent" gels. Daughter gels could be produced to have various properties (e.g. increased softness or stiffness, thermoresponsiveness, polarity responsiveness) through the introduction of new polymer chains within the crosslinks.

Similarly, the Matyjaszewski group developed photoactivated structurally tailored and engineered macromolecular (STEM) gels.[73-77] In these works, crosslinked methacrylate gels were prepared through RAFT polymerization between a methacrylate monomer, crosslinker, and an ATRP inimer. Incorporation of the ATRP inimer resulted in gels containing an ATRP initiator that could be activated through a light-mediated polymerization to graft polymer chains off the existing architecture of the gel. Addition of new polymer chains acted to alter the mechanical properties of the gels with the properties being tunable by varying the grafting density and the polymer chain lengths. Additionally, these materials were shown to be capable of producing single-piece materials with both hard and soft domains using a photomask during polymerization. STEM gels have recently been further developed to demonstrate a metal free approach which relies

on the incorporation of RAFT inimers into a crosslinked methacrylate network prepared through a RAFT polymerization with a methacrylate functionalized TTC crosslinker (**Scheme I-2**).[78] The method hinges on the selective activation of the scaffold polymer RAFT chain end and the inimer/crosslinker TTCs through the use of either blue or green light. Through this method three different types of gels based off the amount of incorporated inimer and the type of crosslinker used are produced. The mechanical properties were then manipulated to alter the stiffness or the softness through polymerizations from either the crosslinker, inimer, or chain end.

Scheme I-2. Preparation of crosslinked STEM gels and the photoinduced network modification.

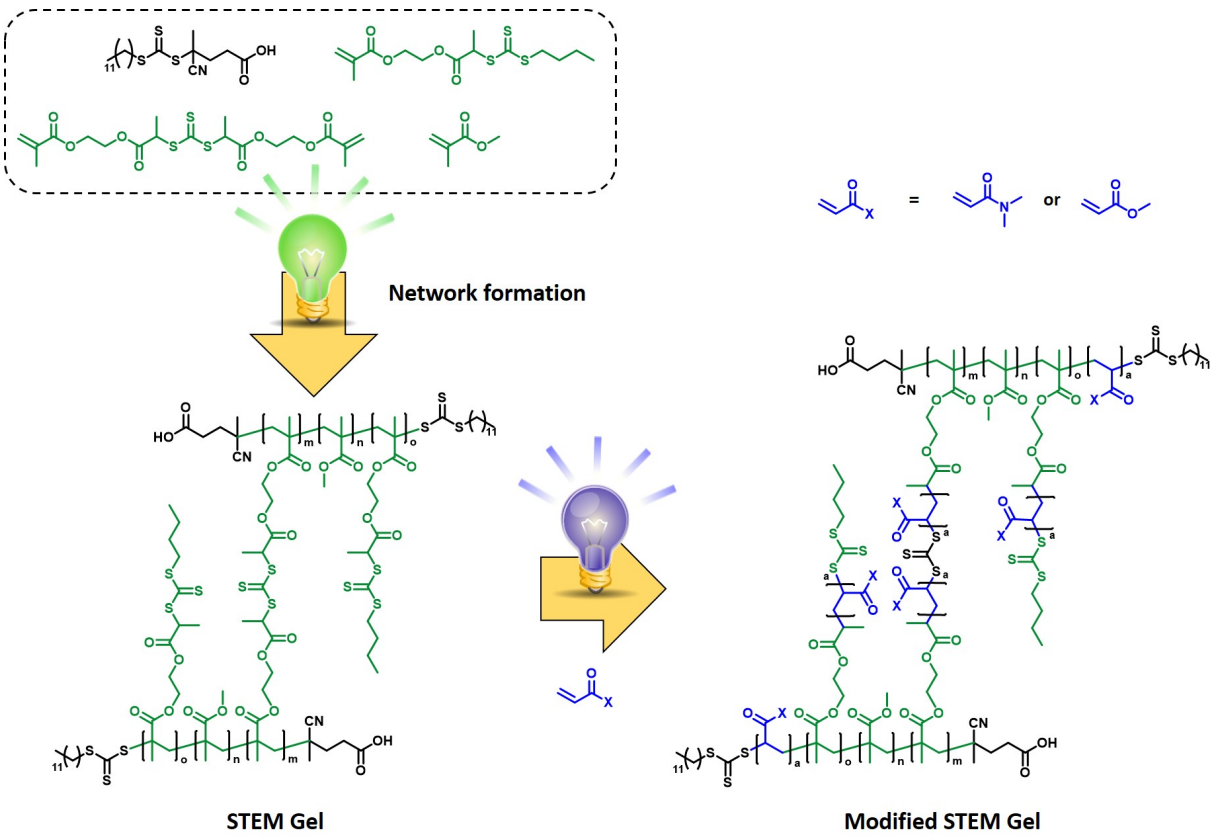

These examples of the manipulation of bulk gel mechanical and chemical properties provide a means to the production of highly tunable materials in the bulk, however; there was previously no examples of these kinds of manipulations on the nanoscale. Modifications to

nanoparticles primarily occur on the surface of the particle through the use of click chemistries or surface-initiated polymerizations (**Figure I-3**).[79-82]

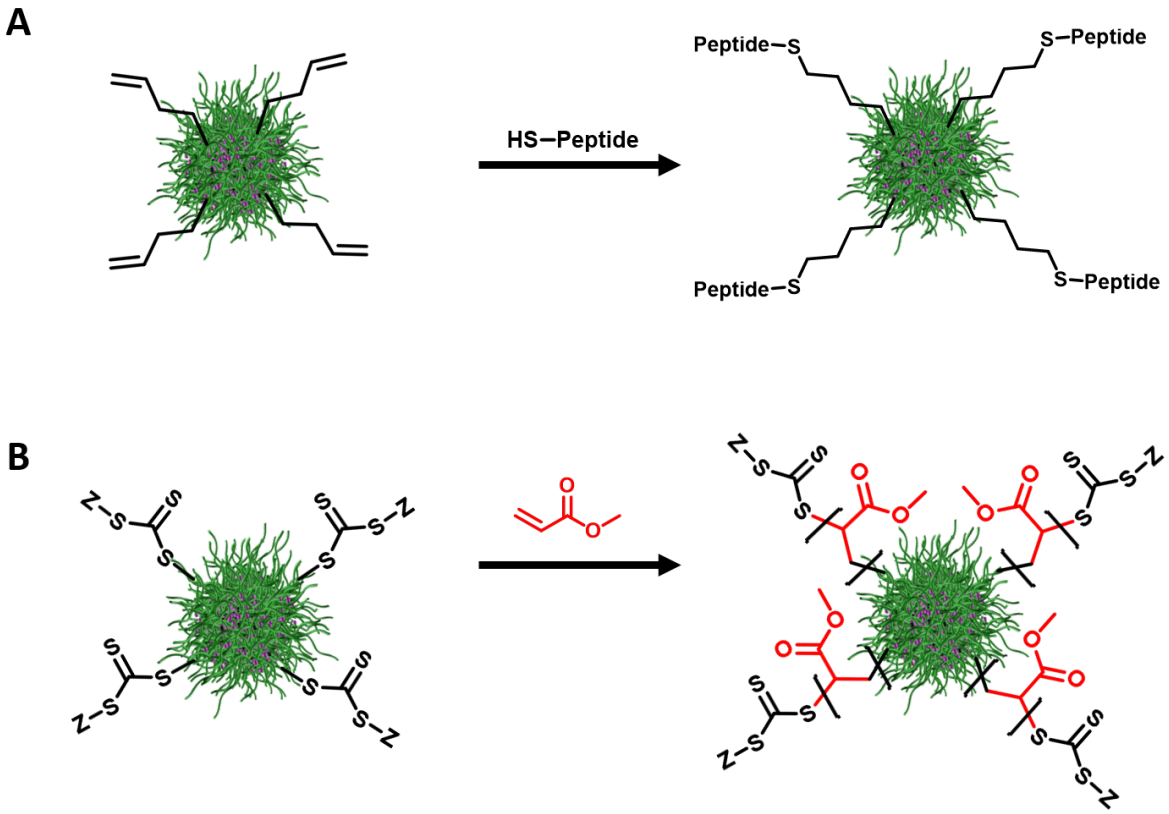

Figure I-3. Schematic description of the surface modification of nanoparticles through (A) thiol-ene click and (B) surface initiated polymerization.

While there are examples of nanoparticles or microparticles increasing in size, the changes only occur on the particle periphery and no intentional changes are made to the core architecture.[83-84] For these reasons, we aimed to develop a method which would allow for the precise manipulation of size, architecture, and properties in nanomaterials as a means to better understand how existing nanoscale networks behave to the introduction of new polymer chains within the network crosslinks.

DISSERTATION OVERVIEW

There is a great and increasing interest in the modification of existing network architectures and properties to prepare new materials in a controlled manner. Advances in light mediated polymerizations have facilitated the preparation of such materials; however, previous modifications of networks have primarily been investigated with bulk gel materials and there exists a need to explore these manipulations on the nanoscale. The aim of this body of work is to develop a nanoparticle system capable of experiencing precise manipulations in size, architecture, and network properties through light-mediated polymerizations.

Chapter II details the synthesis and post modification of "living", crosslinked nanoparticles, deemed photogrowable nanonetworks (PGNNs). Manipulations of PGNNs' size and morphology were explored through two approaches (1) a direct photolysis iniferter polymerization and (2) a photoredox catalyzed polymerization in the presence of 10-phenylphenothiazine (PTH). PGNNs were examined before and after each polymerization to evaluate the change in size and morphology. Successful incorporation of methyl acrylate (MA) polymer chains into the network crosslinks resulted in nanonetworks with greater diameters than the parent PGNN in both types of polymerizations, and networks expanded in the presence of PTH displayed an improved dispersity when compared to those expanded through the iniferter polymerization. This study demonstrates the ability to manipulate the size and chemical composition of living, crosslinked nanonetworks providing the potential to prepare highly tailored nanomaterials from a single parent network.

Chapter III reports the advancement of the controlled photogrowth of crosslinked nanonetworks through the expansion of the monomer scope and the manipulation of network properties. Monomers from different families (i.e. acrylate and acrylamide) with hydrophobic (i.e.

methyl acrylate (MA), t-butyl acrylate (tBA), trifluoroethyl acrylate (TFEA)) or hydrophilic (i.e. hydroxyethyl acrylate (HEA), N-isopropylacrylamide (NIPAAM)) character were chosen to explore the scope of monomers that can be successfully utilized in the photogrowth process. Polymerization conditions were developed for each monomer through model polymerizations and then optimized conditions were applied to the PGNN expansions. Monomers were successfully incorporated in each case and the diameters of daughter nanonetworks is increased from those of the parent. Incorporation of hydrophilic monomers (HEA, NIPAAM) produced water soluble daughter networks from water insoluble parent networks. Addition of NIPAAM provided expanded networks with a thermoresponsive behavior capable of shrinking the network to a smaller diameter when heated. Lastly, network refractive indices were altered through the polymerization of TFEA. The successful incorporation of a variety of monomers and the demonstrated manipulation of network properties allows this photogrowth process to be a powerful tool to develop and study highly engineerable nanomaterials.

After successfully demonstrating the expansion of nanonetworks' size and the tailoring of their properties, we were interested in investigating how the size, morphology, and properties of networks could be altered if a selective polymerization were to occur from the scaffold polymer chain end in addition to the previously developed photogrowth process. Chapter IV explores the progress towards the design and preparation of a living crosslinked nanoparticle capable of facilitating orthogonal polymerizations from the scaffold chain end and from the crosslinker. To achieve this the scaffold polymer end group must remain intact and must possess properties such that it can be activated independently of the crosslinker TTC. These conditions can be realized through the use of either a dithiobenzoate or ATRP bromine end group on the scaffold polymer in conjunction with selective catalysts and a crosslinking chemistry compatible with the desired end

group. A Diels-Alder (DA) reaction between furfuryl methacrylate (FMA) and the previously prepared bis-maleimide TTC proved to be compatible with both the dithiobenzoate and the ATRP bromine end groups. Nanonetworks can be prepared through a DA crosslinking with a poly(methyl methacrylate-*co*-furfruyl methacrylate), synthesized through either RAFT or ATRP and the bis-maleimide TTC. Model selectivity studies were conducted to examine if the chosen catalysts could selectively activate one CTA in the presence of another.

Chapter 5 explores the progress towards the design and synthesis of a symmetrical TTC RAFT agent functionalized with ureidopyrimidinone hydrogen bond donor/acceptors to produce photoresponsive self-assembled materials capable of experiencing morphological changes as result of light-mediated polymerizations.

REFERENCES

(1) W., D. P. Y.; M., B. J.; Huizinga-van, d. V. A.; M., S. F. M.; C., H. M.; A., v. L. M. J., The Use of Fibrous, Supramolecular Membranes and Human Tubular Cells for Renal Epithelial Tissue Engineering: Towards a Suitable Membrane for a Bioartificial Kidney. *Macromolecular Bioscience* **2010,** *10* (11), 1345-1354.

(2) Bastings, M. M. C.; Koudstaal, S.; Kieltyka, R. E.; Nakano, Y.; Pape, A. C. H.; Feyen, D. A. M.; van Slochteren, F. J.; Doevendans, P. A.; Sluijter, J. P. G.; Meijer, E. W.; Chamuleau, S. A. J.; Dankers, P. Y. W., A Fast pH-Switchable and Self-Healing Supramolecular Hydrogel Carrier for Guided, Local Catheter Injection in the Infarcted Myocardium. *Advanced Healthcare Materials* **2014,** *3* (1), 70-78.

(3) Miao, T.; Miller, E. J.; McKenzie, C.; Oldinski, R. A., Physically crosslinked polyvinyl alcohol and gelatin interpenetrating polymer network theta-gels for cartilage regeneration. *Journal of Materials Chemistry B* **2015,** *3* (48), 9242-9249.

(4) Döhler, D.; Peterlik, H.; Binder, W. H., A dual crosslinked self-healing system: Supramolecular and covalent network formation of four-arm star polymers. *Polymer* **2015,** *69*, 264-273.

(5) Cromwell, O. R.; Chung, J.; Guan, Z., Malleable and Self-Healing Covalent Polymer Networks through Tunable Dynamic Boronic Ester Bonds. *J. Am. Chem. Soc.* **2015,** *137* (20), 6492-6495.

(6) Kloxin, C. J.; Scott, T. F.; Adzima, B. J.; Bowman, C. N., Covalent Adaptable Networks (CANs): A Unique Paradigm in Cross-Linked Polymers. *Macromolecules* **2010,** *43* (6), 2643-2653.

(7) Pina, S.; Oliveira, J. M.; Reis, R. L., Natural-Based Nanocomposites for Bone Tissue Engineering and Regenerative Medicine: A Review. *Adv. Mater.* **2015,** *27* (7), 1143-1169.

(8) Annabi, N.; Tamayol, A.; Uquillas, J. A.; Akbari, M.; Bertassoni, L. E.; Cha, C.; Camci-Unal, G.; Dokmeci, M. R.; Peppas, N. A.; Khademhosseini, A., 25th Anniversary Article: Rational Design and Applications of Hydrogels in Regenerative Medicine. *Adv. Mater.* **2014,** *26* (1), 85-124.

(9) Yang, J.-A.; Yeom, J.; Hwang, B. W.; Hoffman, A. S.; Hahn, S. K., In situ-forming injectable hydrogels for regenerative medicine. *Prog. Polym. Sci.* **2014,** *39* (12), 1973-1986.

(10) Qi, X.; Wei, W.; Li, J.; Liu, Y.; Hu, X.; Zhang, J.; Bi, L.; Dong, W., Fabrication and Characterization of a Novel Anticancer Drug Delivery System: Salecan/Poly(methacrylic acid) Semi-interpenetrating Polymer Network Hydrogel. *ACS Biomaterials Science & Engineering* **2015,** *1* (12), 1287-1299.

(11) Aminabhavi, T. M.; Nadagouda, M. N.; More, U. A.; Joshi, S. D.; Kulkarni, V. H.; Noolvi, M. N.; Kulkarni, P. V., Controlled release of therapeutics using interpenetrating polymeric networks. *Expert Opinion on Drug Delivery* **2015,** *12* (4), 669-688.

(12) Bajpai, S. K.; Chand, N.; Agrawal, A., Microwave-assisted synthesis of carboxymethyl psyllium and its development as semi-interpenetrating network with poly(acrylamide) for gastric delivery. *Journal of Bioactive and Compatible Polymers* **2015,** *30* (3), 241-257.

(13) Kim, S.; Dehlinger, D.; Peña, J.; Seol, H.; Shusteff, M.; Collette, N. M.; Elsheikh, M.; Davenport, M.; Naraghi-Arani, P.; Wheeler, E., Virus concentration and purification by a microfluidic filtering system with an integrated PEGylated antifouling membrane. *Microfluidics and Nanofluidics* **2019,** *23* (1), 9.

(14) He, B.; Ding, Y.; Wang, J.; Yao, Z.; Qing, W.; Zhang, Y.; Liu, F.; Tang, C. Y., Sustaining fouling resistant membranes: Membrane fabrication, characterization and mechanism understanding of demulsification and fouling-resistance. *Journal of Membrane Science* **2019,** *581*, 105-113.

(15) Zhao, X.; Zhang, R.; Liu, Y.; He, M.; Su, Y.; Gao, C.; Jiang, Z., Antifouling membrane surface construction: Chemistry plays a critical role. *Journal of Membrane Science* **2018,** *551*, 145-171.

(16) Tugui, C.; Stiubianu, G.; Iacob, M.; Ursu, C.; Bele, A.; Vlad, S.; Cazacu, M., Bimodal silicone interpenetrating networks sequentially built as electroactive dielectric elastomers. *Journal of Materials Chemistry C* **2015,** *3* (34), 8963-8969.

(17) Zhang, G.; McBride, M.; Persson, N.; Lee, S.; Dunn, T. J.; Toney, M. F.; Yuan, Z.; Kwon, Y.-H.; Chu, P.-H.; Risteen, B.; Reichmanis, E., Versatile Interpenetrating Polymer Network Approach to Robust Stretchable Electronic Devices. *Chem. Mater.* **2017,** *29* (18), 7645-7652.

(18) Zhou, Y.; Wan, C.; Yang, Y.; Yang, H.; Wang, S.; Dai, Z.; Ji, K.; Jiang, H.; Chen, X.; Long, Y., Highly Stretchable, Elastic, and Ionic Conductive Hydrogel for Artificial Soft Electronics. *Adv. Funct. Mater.* **2019,** *29* (1), 1806220.

(19) Whitesides, G. M., Soft Robotics. *Angew. Chem. Int. Ed.* **2018,** *57* (16), 4258-4273.

(20) Xu, Z.; Bratlie, K. M., Click Chemistry and Material Selection for in Situ Fabrication of Hydrogels in Tissue Engineering Applications. *ACS Biomaterials Science & Engineering* **2018,** *4* (7), 2276-2291.

(21) Nimmo, C. M.; Owen, S. C.; Shoichet, M. S., Diels−Alder Click Cross-Linked Hyaluronic Acid Hydrogels for Tissue Engineering. *Biomacromolecules* **2011,** *12* (3), 824-830.

(22) Stewart, S. A.; Backholm, M.; Burke, N. A. D.; Stöver, H. D. H., Cross-Linked Hydrogels Formed through Diels–Alder Coupling of Furan- and Maleimide-Modified Poly(methyl vinyl ether-alt-maleic acid). *Langmuir* **2016,** *32* (7), 1863-1870.

(23) Kawamoto, K.; Grindy, S. C.; Liu, J.; Holten-Andersen, N.; Johnson, J. A., Dual Role for 1,2,4,5-Tetrazines in Polymer Networks: Combining Diels–Alder Reactions and Metal Coordination To Generate Functional Supramolecular Gels. *ACS Macro Lett.* **2015,** *4* (4), 458-461.

(24) García-Astrain, C.; Algar, I.; Gandini, A.; Eceiza, A.; Corcuera, M. Á.; Gabilondo, N., Hydrogel synthesis by aqueous Diels-Alder reaction between furan modified methacrylate and polyetheramine-based bismaleimides. *J. Polym. Sci., Part A: Polym. Chem.* **2015,** *53* (5), 699-708.

(25) Tsurkan, M. V.; Jungnickel, C.; Schlierf, M.; Werner, C., Forbidden Chemistry: Two-Photon Pathway in [2+2] Cycloaddition of Maleimides. *J. Am. Chem. Soc.* **2017,** *139* (30), 10184-10187.

(26) Bracchi, M. E.; Dura, G.; Fulton, D. A., The synthesis of poly(arylthiols) and their utilization in the preparation of cross-linked dynamic covalent polymer nanoparticles and hydrogels. *Polym. Chem.* **2019,** *10* (10), 1258-1267.

(27) Barcan, G. A.; Zhang, X.; Waymouth, R. M., Structurally Dynamic Hydrogels Derived from 1,2-Dithiolanes. *J. Am. Chem. Soc.* **2015,** *137* (17), 5650-5653.

(28) Kendrick-Williams, L. L.; Harth, E., Second-Generation Nanosponges: Nanonetworks in Controlled Dimensions via Backbone Ketoxime and Alkoxyamine Cross-Links for Controlled Release. *Macromolecules* **2018,** *51* (24), 10160-10166.

(29) Mukherjee, S.; Hill, M. R.; Sumerlin, B. S., Self-healing hydrogels containing reversible oxime crosslinks. *Soft Matter* **2015,** *11* (30), 6152-6161.

(30) Nadgorny, M.; Collins, J.; Xiao, Z.; Scales, P. J.; Connal, L. A., 3D-printing of dynamic self-healing cryogels with tuneable properties. *Polym. Chem.* **2018,** *9* (13), 1684-1692.

(31) Gordon, M. B.; French, J. M.; Wagner, N. J.; Kloxin, C. J., Dynamic Bonds in Covalently Crosslinked Polymer Networks for Photoactivated Strengthening and Healing. *Adv. Mater.* **2015,** *27* (48), 8007-8010.

(32) Amamoto, Y.; Otsuka, H.; Takahara, A.; Matyjaszewski, K., Self-Healing of Covalently Cross-Linked Polymers by Reshuffling Thiuram Disulfide Moieties in Air under Visible Light. *Adv. Mater.* **2012,** *24* (29), 3975-3980.

(33) Picchioni, F.; Muljana, H., Hydrogels Based on Dynamic Covalent and Non Covalent Bonds: A Chemistry Perspective. *Gels* **2018,** *4* (1), 21.

(34) Kloxin, C. J.; Bowman, C. N., Covalent adaptable networks: smart, reconfigurable and responsive network systems. *Chem. Soc. Rev.* **2013,** *42* (17), 7161-7173.

(35) Otsu, T.; Yoshida, M., Role of initiator-transfer agent-terminator (iniferter) in radical polymerizations: Polymer design by organic disulfides as iniferters. *Die Makromolekulare Chemie, Rapid Communications* **1982,** *3* (2), 127-132.

(36) Chen, M.; Gu, Y.; Singh, A.; Zhong, M.; Jordan, A. M.; Biswas, S.; Korley, L. T. J.; Balazs, A. C.; Johnson, J. A., Living Additive Manufacturing: Transformation of Parent Gels into Diversely Functionalized Daughter Gels Made Possible by Visible Light Photoredox Catalysis. *ACS Central Science* **2017,** *3* (2), 124-134.

(37) Zhou, H.; Johnson, J. A., Photo-controlled Growth of Telechelic Polymers and End-linked Polymer Gels. *Angew. Chem. Int. Ed.* **2013,** *52* (8), 2235-2238.

(38) Singh, A.; Kuksenok, O.; Johnson, J. A.; Balazs, A. C., Tailoring the structure of polymer networks with iniferter-mediated photo-growth. *Polym. Chem.* **2016,** *7* (17), 2955-2964.

(39) Amamoto, Y.; Kamada, J.; Otsuka, H.; Takahara, A.; Matyjaszewski, K., Repeatable Photoinduced Self-Healing of Covalently Cross-Linked Polymers through Reshuffling of Trithiocarbonate Units. *Angew. Chem. Int. Ed.* **2011,** *50* (7), 1660-1663.

(40) Amamoto, Y.; Otsuka, H.; Takahara, A.; Matyjaszewski, K., Changes in Network Structure of Chemical Gels Controlled by Solvent Quality through Photoinduced Radical Reshuffling Reactions of Trithiocarbonate Units. *ACS Macro Lett.* **2012,** *1* (4), 478-481.

(41) Ercole, F.; Thissen, H.; Tsang, K.; Evans, R. A.; Forsythe, J. S., Photodegradable Hydrogels Made via RAFT. *Macromolecules* **2012,** *45* (20), 8387-8400.

(42) Li, Q.; Hu, X.; Bai, R., Synthesis of Photodegradable Polystyrene with Trithiocarbonate as Linkages. *Macromol. Rapid Commun.* **2015,** *36* (20), 1810-1815.

(43) Xu, J.; Shanmugam, S.; Duong, H. T.; Boyer, C., Organo-photocatalysts for photoinduced electron transfer-reversible addition-fragmentation chain transfer (PET-RAFT) polymerization. *Polym. Chem.* **2015,** *6* (31), 5615-5624.

(44) Xu, J.; Shanmugam, S.; Fu, C.; Aguey-Zinsou, K.-F.; Boyer, C., Selective Photoactivation: From a Single Unit Monomer Insertion Reaction to Controlled Polymer Architectures. *J. Am. Chem. Soc.* **2016,** *138* (9), 3094-3106.

(45) Xu, J.; Jung, K.; Atme, A.; Shanmugam, S.; Boyer, C., A Robust and Versatile Photoinduced Living Polymerization of Conjugated and Unconjugated Monomers and Its Oxygen Tolerance. *J. Am. Chem. Soc.* **2014,** *136* (14), 5508-5519.

(46) Fors, B. P.; Hawker, C. J., Control of a Living Radical Polymerization of Methacrylates by Light. *Angew. Chem. Int. Ed.* **2012,** *51* (35), 8850-8853.

(47) Treat, N. J.; Sprafke, H.; Kramer, J. W.; Clark, P. G.; Barton, B. E.; Read de Alaniz, J.; Fors, B. P.; Hawker, C. J., Metal-Free Atom Transfer Radical Polymerization. *J. Am. Chem. Soc.* **2014,** *136* (45), 16096-16101.

(48) Miyake, G. M.; Theriot, J. C., Perylene as an Organic Photocatalyst for the Radical Polymerization of Functionalized Vinyl Monomers through Oxidative Quenching with Alkyl Bromides and Visible Light. *Macromolecules* **2014,** *47* (23), 8255-8261.

(49) McCarthy, B.; Miyake, G. M., Organocatalyzed Atom Transfer Radical Polymerization Catalyzed by Core Modified N-Aryl Phenoxazines Performed under Air. *ACS Macro Lett.* **2018,** *7* (8), 1016-1021.

(50) Theriot, J. C.; Lim, C.-H.; Yang, H.; Ryan, M. D.; Musgrave, C. B.; Miyake, G. M., Organocatalyzed atom transfer radical polymerization driven by visible light. *Science* **2016,** *352* (6289), 1082-1086.

(51) Vorobii, M.; de los Santos Pereira, A.; Pop-Georgievski, O.; Kostina, N. Y.; Rodriguez-Emmenegger, C.; Percec, V., Synthesis of non-fouling poly[N-(2-hydroxypropyl)methacrylamide] brushes by photoinduced SET-LRP. *Polym. Chem.* **2015,** *6* (23), 4210-4220.

(52) Vorobii, M.; Pop-Georgievski, O.; de los Santos Pereira, A.; Kostina, N. Y.; Jezorek, R.; Sedláková, Z.; Percec, V.; Rodriguez-Emmenegger, C., Grafting of functional methacrylate polymer brushes by photoinduced SET-LRP. *Polym. Chem.* **2016,** *7* (45), 6934-6945.

(53) Laun, J.; Vorobii, M.; de los Santos Pereira, A.; Pop-Georgievski, O.; Trouillet, V.; Welle, A.; Barner-Kowollik, C.; Rodriguez-Emmenegger, C.; Junkers, T., Surface Grafting via Photo-Induced Copper-Mediated Radical Polymerization at Extremely Low Catalyst Concentrations. *Macromol. Rapid Commun.* **2015,** *36* (18), 1681-1686.

(54) Fu, C.; Xu, J.; Boyer, C., Photoacid-mediated ring opening polymerization driven by visible light. *Chem. Commun.* **2016,** *52* (44), 7126-7129.

(55) Ogawa, K. A.; Goetz, A. E.; Boydston, A. J., Metal-Free Ring-Opening Metathesis Polymerization. *J. Am. Chem. Soc.* **2015,** *137* (4), 1400-1403.

(56) Lu, L.; Zhang, H.; Yang, N.; Cai, Y., Toward Rapid and Well-Controlled Ambient Temperature RAFT Polymerization under UV−Vis Radiation: Effect of Radiation Wave Range. *Macromolecules* **2006,** *39* (11), 3770-3776.

(57) Chen, M.; Zhong, M.; Johnson, J. A., Light-Controlled Radical Polymerization: Mechanisms, Methods, and Applications. *Chem. Rev.* **2016,** *116* (17), 10167-10211.

(58) Jung, K.; Xu, J.; Zetterlund, P. B.; Boyer, C., Visible-Light-Regulated Controlled/Living Radical Polymerization in Miniemulsion. *ACS Macro Lett.* **2015,** *4* (10), 1139-1143.

(59) McKenzie, T. G.; Fu, Q.; Uchiyama, M.; Satoh, K.; Xu, J.; Boyer, C.; Kamigaito, M.; Qiao, G. G., Beyond Traditional RAFT: Alternative Activation of Thiocarbonylthio Compounds for Controlled Polymerization. *Advanced Science* **2016**, n/a-n/a.

(60) Fu, C.; Xu, J.; Tao, L.; Boyer, C., Combining Enzymatic Monomer Transformation with Photoinduced Electron Transfer − Reversible Addition–Fragmentation Chain Transfer for the Synthesis of Complex Multiblock Copolymers. *ACS Macro Lett.* **2014,** *3* (7), 633-638.

(61) Xu, J.; Jung, K.; Corrigan, N. A.; Boyer, C., Aqueous photoinduced living/controlled polymerization: tailoring for bioconjugation. *Chemical Science* **2014,** *5* (9), 3568-3575.

(62) Xu, J.; Shanmugam, S.; Boyer, C., Organic Electron Donor–Acceptor Photoredox Catalysts: Enhanced Catalytic Efficiency toward Controlled Radical Polymerization. *ACS Macro Lett.* **2015,** *4* (9), 926-932.

(63) Shanmugam, S.; Xu, J.; Boyer, C., Light-Regulated Polymerization under Near-Infrared/Far-Red Irradiation Catalyzed by Bacteriochlorophyll a. *Angew. Chem. Int. Ed.* **2016,** *55* (3), 1036-1040.

(64) Shanmugam, S.; Xu, J.; Boyer, C., Utilizing the electron transfer mechanism of chlorophyll a under light for controlled radical polymerization. *Chemical Science* **2015,** *6* (2), 1341-1349.

(65) Corrigan, N.; Rosli, D.; Jones, J. W. J.; Xu, J.; Boyer, C., Oxygen Tolerance in Living Radical Polymerization: Investigation of Mechanism and Implementation in Continuous Flow Polymerization. *Macromolecules* **2016,** *49* (18), 6779-6789.

(66) Xu, J.; Jung, K.; Boyer, C., Oxygen Tolerance Study of Photoinduced Electron Transfer–Reversible Addition–Fragmentation Chain Transfer (PET-RAFT) Polymerization Mediated by Ru(bpy)3Cl2. *Macromolecules* **2014,** *47* (13), 4217-4229.

(67) Shanmugam, S.; Xu, J.; Boyer, C., Photoinduced Electron Transfer–Reversible Addition–Fragmentation Chain Transfer (PET-RAFT) Polymerization of Vinyl Acetate and N-Vinylpyrrolidinone: Kinetic and Oxygen Tolerance Study. *Macromolecules* **2014,** *47* (15), 4930-4942.

(68) Fu, C.; Xu, J.; Kokotovic, M.; Boyer, C., One-Pot Synthesis of Block Copolymers by Orthogonal Ring-Opening Polymerization and PET-RAFT Polymerization at Ambient Temperature. *ACS Macro Lett.* **2016,** *5* (4), 444-449.

(69) Theriot, J. C.; Miyake, G. M.; Boyer, C. A., N,N-Diaryl Dihydrophenazines as Photoredox Catalysts for PET-RAFT and Sequential PET-RAFT/O-ATRP. *ACS Macro Lett.* **2018,** *7* (6), 662-666.

(70) Shanmugam, S.; Xu, J.; Boyer, C., Exploiting Metalloporphyrins for Selective Living Radical Polymerization Tunable over Visible Wavelengths. *J. Am. Chem. Soc.* **2015,** *137* (28), 9174-9185.

(71) Ramsey, B. L.; Pearson, R. M.; Beck, L. R.; Miyake, G. M., Photoinduced Organocatalyzed Atom Transfer Radical Polymerization Using Continuous Flow. *Macromolecules* **2017,** *50* (7), 2668-2674.

(72) Chen, M.; MacLeod, M. J.; Johnson, J. A., Visible-Light-Controlled Living Radical Polymerization from a Trithiocarbonate Iniferter Mediated by an Organic Photoredox Catalyst. *ACS Macro Lett.* **2015,** *4* (5), 566-569.

(73) Mpoukouvalas, A.; Li, W.; Graf, R.; Koynov, K.; Matyjaszewski, K., Soft Elastomers via Introduction of Poly(butyl acrylate) “Diluent” to Poly(hydroxyethyl acrylate)-Based Gel Networks. *ACS Macro Lett.* **2013,** *2* (1), 23-26.

(74) Beziau, A.; Fortney, A.; Fu, L.; Nishiura, C.; Wang, H.; Cuthbert, J.; Gottlieb, E.; Balazs, A. C.; Kowalewski, T.; Matyjaszewski, K., Photoactivated Structurally Tailored and Engineered Macromolecular (STEM) gels as precursors for materials with spatially differentiated mechanical properties. *Polymer* **2017,** *126*, 224-230.

(75) Cuthbert, J.; Zhang, T.; Biswas, S.; Olszewski, M.; Shanmugam, S.; Fu, T.; Gottlieb, E.; Kowalewski, T.; Balazs, A. C.; Matyjaszewski, K., Structurally Tailored and Engineered Macromolecular (STEM) Gels as Soft Elastomers and Hard/Soft Interfaces. *Macromolecules* **2018,** *51* (22), 9184-9191.

(76) Cuthbert, J.; Beziau, A.; Gottlieb, E.; Fu, L.; Yuan, R.; Balazs, A. C.; Kowalewski, T.; Matyjaszewski, K., Transformable Materials: Structurally Tailored and Engineered Macromolecular (STEM) Gels by Controlled Radical Polymerization. *Macromolecules* **2018,** *51* (10), 3808-3817.

(77) Cuthbert, J.; Martinez, M. R.; Sun, M.; Flum, J.; Li, L.; Olszewski, M.; Wang, Z.; Kowalewski, T.; Matyjaszewski, K., Non-Tacky Fluorinated and Elastomeric STEM Networks. *Macromol. Rapid Commun.* **2019,** *0* (0), 1800876.

(78) Shanmugam, S.; Cuthbert, J.; Flum, J.; Fantin, M.; Boyer, C.; Kowalewski, T.; Matyjaszewski, K., Transformation of gels via catalyst-free selective RAFT photoactivation. *Polym. Chem.* **2019**.

(79) Yi, G.; Son, J.; Yoo, J.; Park, C.; Koo, H., Application of click chemistry in nanoparticle modification and its targeted delivery. *Biomaterials Research* **2018,** *22* (1), 13.

(80) Ling, D.; Hackett, M. J.; Hyeon, T., Surface ligands in synthesis, modification, assembly and biomedical applications of nanoparticles. *Nano Today* **2014,** *9* (4), 457-477.

(81) Li, N.; Binder, W. H., Click-chemistry for nanoparticle-modification. *J. Mater. Chem.* **2011,** *21* (42), 16717-16734.

(82) Hore, M. J. A., Polymers on nanoparticles: structure & dynamics. *Soft Matter* **2019,** *15* (6), 1120-1134.

(83) McKenzie, T. G.; Wong, E. H. H.; Fu, Q.; Sulistio, A.; Dunstan, D. E.; Qiao, G. G., Controlled Formation of Star Polymer Nanoparticles via Visible Light Photopolymerization. *ACS Macro Lett.* **2015,** *4* (9), 1012-1016.

(84) Tan, J.; Zhao, G.; Lu, Y.; Zeng, Z.; Winnik, M. A., Synthesis of PMMA Microparticles with a Narrow Size Distribution by Photoinitiated RAFT Dispersion Polymerization with a Macromonomer as the Stabilizer. *Macromolecules* **2014,** *47* (19), 6856-6866.

CHAPTER II

PHOTOCONTROLLED GROWTH OF CROSSLINKED NANONETWORKS

INTRODUCTION

The progress of photo-controlled radical polymerization (photo-CRP) methodologies[1-3] has tremendously enhanced the availability and versatility of spatiotemporally controlled polymers,[4] high molecular weight polymers,[5] and nanomaterials,[6-8] as well as photoresponsive materials.[9-15] This rapidly expanding area has enabled impressive examples of polymeric materials applying the advantages provided by these techniques. Of particular significance is the use of trithiocarbonates (TTCs) in photoresponsive materials which can act as "iniferters";[16] requiring no exogenous source of radical initiator in the presence of an appropriate light source. For this reason, several photoresponsive properties including photocontrolled growth,[9-11] photoinduced self-healing,[12] photoinduced network alterations,[13] and photo-degradation[14-15] could be facilitated in polymeric materials through the incorporation of TTCs. In a proof-of-concept study reported by Johnson and co-workers, a series of photoresponsive polymeric networks (PRPNs)[9] were developed using TTCs. Implementation of TTC's into the gel network led to an increase in swelling capacity and molecular weight between crosslinks after the introduction of new polymer chains through light-mediated polymerizations activated by sunlight.

Light-mediated polymerization techniques such as photoinduced electron transfer-reversible addition-fragmentation chain-transfer (PET-RAFT)[17-18] and photoinduced atom transfer radical polymerization (ATRP)[19-20] have continued to improve photo-CRP methods[1] and enable increasingly robust polymerization reactions by providing advantages such as a higher tolerance

towards oxygen,[21] smaller sample sizes,[22] the ability to irradiate at different wavelengths of light,[23-25] and the ability to work in aqueous environments.[5, 20, 26] Improvements in photo-CRPs and the introduction of new photocatalysts has resulted in the improved manipulation of bulk networks with integrated TTC's and the development of a living additive manufacturing method.[10] While the manipulation of crosslinked bulk networks have been reported, a photoinduced expansion of nanonetworks is still in demand as it would allow for the preparation of new daughter particles diverse in both size and composition stemming from one parent particle. This concept is in contrast to known post-polymerization methods of nano- and microparticles that add polymer chains to particles' periphery,[27-28] but in which changes to the network structure are not intended. In this contribution, we sought to develop a strategy to enable precise manipulations of size, architecture and integrated functionalities in nanomaterials by utilizing controlled light-initiated polymerizations.

RESULTS AND DISCUSSION

Preparation of Photogrowable Nanonetworks

Our strategy included the design of nanonetworks that can experience photogrowth by implementing a two-component crosslinking mechanism involving a functionalized polymer and a bifunctional crosslinker containing a TTC unit. For a successful nanomaterial capable of photogrowth we pursued a crosslinking chemistry that is orthogonal to a variety of polymers with a diverse set of functional groups and a suitable TTC crosslinker capable of mediating photo-CRP of acrylate monomers by either direct photolysis of the TTC or through a photoredox catalyzed polymerization. Although we have extensive experience to form nanonetworks through amine-

Scheme II-1. Synthesis scheme of the photocontrolled growth of photoresponsive nanonetworks

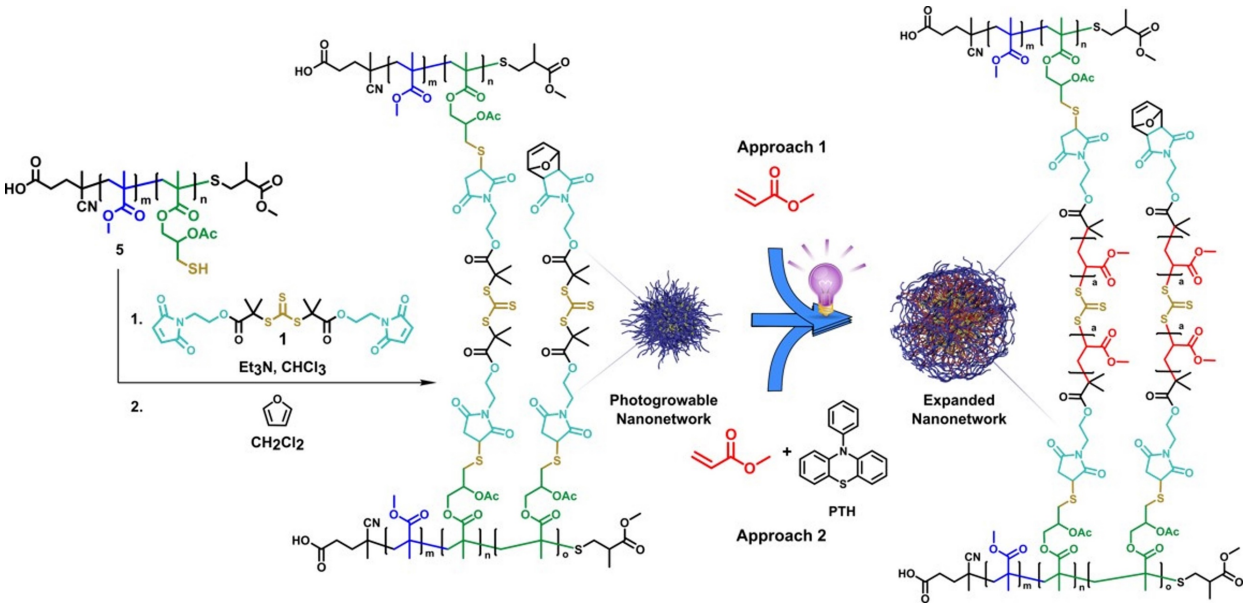

epoxy crosslinking[29-30] we tested a nucleophilic thiol-maleimide crosslinking reaction, envisioning that nanonetworks could be formed by utilizing a thiolated polymer scaffold and a symmetrical maleimide functionalized TTC crosslinker (**Scheme II-1**), thereby avoiding the deleterious effect of amines on TTC units. While it is known that thiol nucleophiles can also induce the degradation of TTC's, we reasoned that the crosslinking reaction could proceed without degradation given that the reaction occurs at near neutral pH and provides quantitative yields within minutes. To confirm this hypothesis, we synthesized a model compound, a symmetrical TTC, bearing two maleimides **1** to react with 1-propanethiol in the presence of a catalytic amount of triethylamine (**Scheme II-S1A**). ^{1}H and ^{13}C NMR spectroscopy (**Figure II-S3, II-S4**) of the reaction after 15 minutes indicated the complete reaction of the maleimide to produce the expected product without degradation of the TTC as evidenced by the TTC carbonyl shift and the absence of signals corresponding to the formation of an undesired TTC. This experiment motivated us to investigate an adaptable strategy for the synthesis of the desired thiolated polymer scaffolds.

In our previous work, we have prepared polyester[29] and polycarbonate[30] polymer species bearing epoxide pendant groups that were accessed efficiently from alkene precursors through a facile meta-chloroperbenzoic acid (mCPBA) epoxidation. Utilizing similar epoxides as a handle, we proposed that a thiolated polymer scaffold could be achieved through the nucleophilic ring opening by a protected thiol followed by deprotection. In detail, the copolymerization of methyl methacrylate and glycidol methacrylate utilizing 4-cyanopentanoic acid dithiobenzoate (CPADB) to produce 80/20 poly(methyl methacrylate-*co*-glycidol methacrylate) (PMMA-*co*-GMA) copolymers **2** provided a direct access to epoxide pendant polymers (**Scheme II-S1B**). Dithiobenzoate moieties of **2** were removed by aminolysis with piperidine and the resulting thiol was capped through a thiol-Michael addition to provide thioether **3**. The removal of the RAFT end group ensured that chain growth could only occur between the crosslinks of the envisioned nanonetworks. Thioacetate ester **4** was obtained by ring opening the epoxide with thioacetic acid. Deprotection of the thioacetate would provide the desired thiol; however, the typical conditions used to deprotect acetates could lead to unwanted transesterification reactions. In light of this, we decided to take advantage of the neighboring alcohol produced from the ring opening to perform an intramolecular acetyl migration. Exploring the conditions of Han and coworkers.[31] we were able to successfully deprotect over 90% of the thiols through a sulfur to oxygen acetyl migration to yield the thiolated polymer scaffold **5** (**Scheme II-S1**).

With the thiolated polymers in hand, we advanced to explore the construction of the photogrowable nanonetworks (PGNN) through thiol-maleimide crosslinking reactions. Equivalent to nanonetworks we formed via amine-epoxy reactions in our previous work, the concentration of the pendant functional unit of the linear polymer in solution, here the thiol functionality, was kept constant (0.005 or 0.025 mmol/mL) and particles in increasing sizes were formed by adding

Table II-1. Syntheses of photogrowable nanonetworks (PGNNs) through thiol-maleimide click chemistry

Entry	$M_{n,GPC}$[a] (g/mol)	PDI[a]	% thiol[b]	Crosslinker eq	M[c] (mmol/mL)	Size[d] (nm)
1	8,330	1.15	20	1	0.005	45±7.0
2	8,330	1.15	20	2	0.005	58±10
3	8,330	1.15	20	4	0.005	147±50
4	8,330	1.15	20	1	0.025	142±30
5	8,330	1.15	20	2	0.025	165±30
6	8,330	1.15	20	4	0.025	186±20

[a] Molecular weight and polydispersity of the thiolated polymer scaffold 5 measured by GPC at 40°C and a flow rate of 1mL/min. Tetrahydrofuran (THF) was used as the eluent. [b] Percent functionalization of the thiolated polymer scaffold as determined by the ^{1}H NMR integration. [c] Concentration of thiol functionality in mmol to mL of chloroform. [d] Average nanoparticle size measured by TEM after purification by dialysis.

increasing equivalents of maleimide crosslinker (**Table II-1**). Crosslinking reactions were always conducted with an excess of maleimide groups towards the thiol groups, for example 1 eq. of crosslinker is equivalent to two maleimide units per thiol functionality to ensure that all thiol units, which could potentially interfere with the future expansion process, are consumed in the reaction. However, the high reactivity of the thiol group is prone to form disulfide bonds during the particle formation and is detected as high molecular weight shoulder in PGNNs gel permeation chromatography (GPC) (**Figure II-1D**) traces. Moreover, the resulting nanonetworks contain free maleimide groups on their particle surface. In model expansion polymerization reactions with the TTC crosslinker **1**, we observed a high dispersity of the polymers in contrast to ones in which the maleimide units were not present. Following this study, to prevent any unwanted side reactions during the photogrowth polymerization caused by the maleimide units, maleimides were capped through Diels-Alder reactions with furan to eliminate the reactive group.

Expansion of Nanonetworks Through Direct Photolysis

In the first approach to network expansion (Approach 1), we decided to investigate the polymerization through the direct photolysis of the TTC. Representative model polymerizations of a 2 M methyl acrylate (MA) in dimethyl sulfoxide (DMSO) were performed with crosslinker **1a** (**Scheme II-S1A**) under irradiation with violet light (400 nm) (**Figure II-S15, Table II-S1**) achieving good control throughout the polymerization. Adaptation of these experimental conditions to the crosslinked nanonetworks should lead to an increase in both molecular weight and size of the PGNNs producing expanded nanonetworks (ENNs) as a result of the newly incorporated MA polymer chains. We choose to test the expansion of a PGNN with the size of 58 nm (**Table II-1**) as a means to better illustrate the differences in sizes of nanonetworks before and after photogrowth.

After irradiation of the reaction for 1, 3 or 6 hours in DMSO, the reaction mixture was dialyzed to remove unreacted monomer and DMSO. We observed that not only the parent PGNN but also the ENN reaction products, were fully soluble in organic solvents and we were able to confirm the incorporation of MA monomer units by ^{1}H NMR (**Figure II-S13, II-S14**). Additionally, expanded nanonetworks were analyzed by GPC, TEM and dynamic light scattering (DLS) to determine the increase in particle size. After 1 hour reaction time, the PGNNs experienced a growth from ~58 nm to ~77nm, irradiation for 3 hours further increased the size to ~ 156 nm, and finally 6 hours of irradiation resulted in ENNs with diameters of ~ 358 nm as measured by TEM (**Figure II-1**). Sizes determined by DLS were ~ 10-20% larger and is attributed to the difference between the solution and dry states of the nanonetworks. Control experiments performed in the absence of monomer or in the absence of light showed no change in particle size. GPC traces of the ENNs were shifted to higher molecular weights throughout the series when

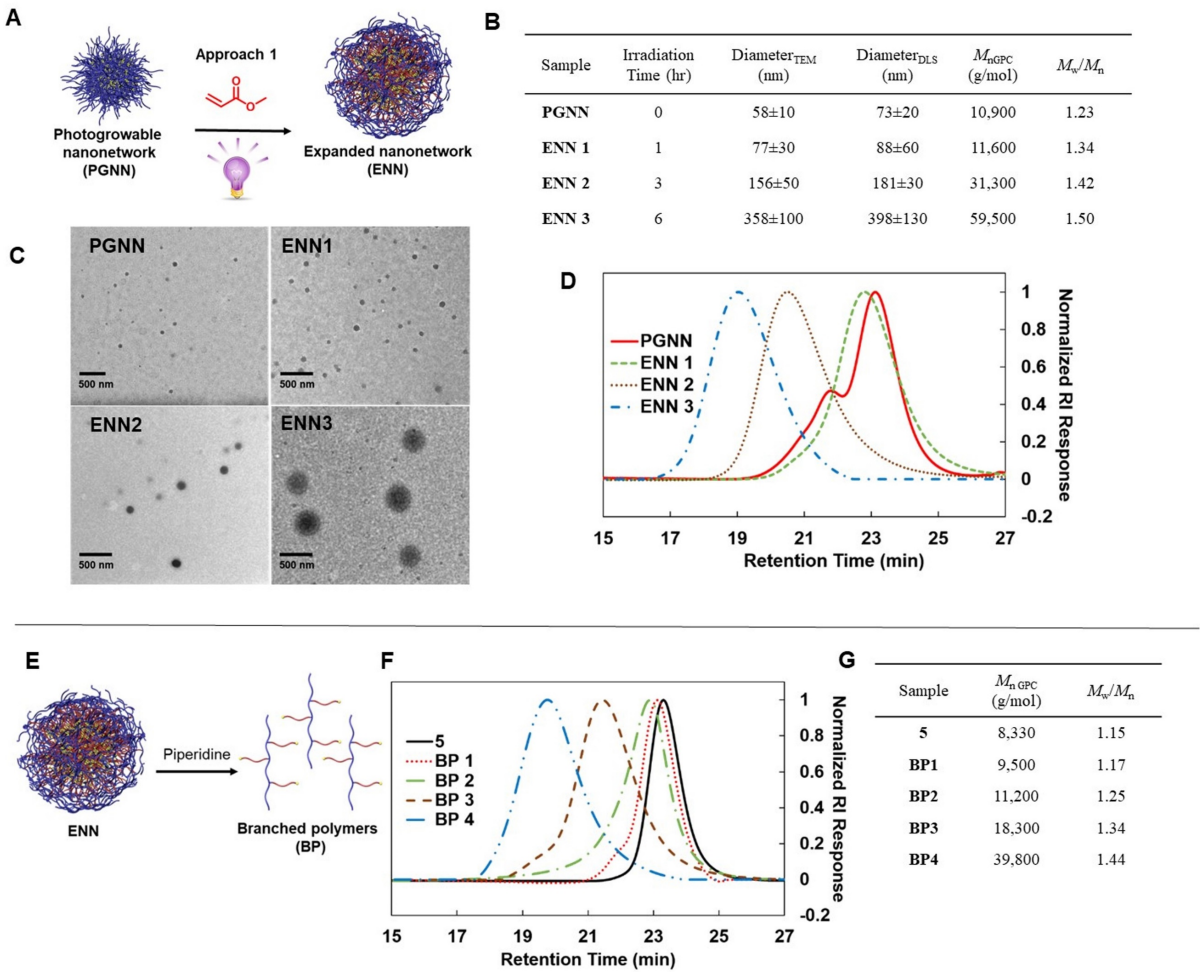

Sample	Irradiation Time (hr)	$Diameter_{TEM}$ (nm)	$Diameter_{DLS}$ (nm)	M_{nGPC} (g/mol)	M_w/M_n
PGNN	0	58±10	73±20	10,900	1.23
ENN 1	1	77±30	88±60	11,600	1.34
ENN 2	3	156±50	181±30	31,300	1.42
ENN 3	6	358±100	398±130	59,500	1.50

Sample	$M_{n\,GPC}$ (g/mol)	M_w/M_n
5	8,330	1.15
BP1	9,500	1.17
BP2	11,200	1.25
BP3	18,300	1.34
BP4	39,800	1.44

Figure II-1. (A) Schematic description of nanonetwork expansion by direct photolysis. (B) Size and dispersity of nanonetworks before, PGNN, and after expansion, ENNs, by TEM, DLS, and GPC. (C) TEM images of nanonetworks before and after expansion. (D) GPC traces of nanonetworks before and after expansion. (E) Schematic description of the selective cleavage of nanonetwork by aminolysis to produce branched polymers (BP). (F) GPC traces of linear thiolated polymer scaffold 5, BP1 generated from PGNN and BP2-4 generated from ENN1-3. (G) GPC analysis of linear polymer and branched polymers from PGNN (BP1) and ENNs (BP2-4). All GPC measurements were conducted at 40°C and a flow rate of 1mL/min with tetrahydrofuran as the eluent.

compared to the PGNN and the high molecular weight shoulder of the PGNN, attributed to disulfide coupling during particle formation, disappeared with the addition of polymers into the nanonetwork and resulted in unimodal distributions.

Promoted Disassembly of Nanonetworks After Direct Photolysis Expansion

While the GPC traces indicate a polymer growth throughout the network, we intended to gain a better understanding of the composition of the nanonetwork before and after the photogrowth expansion. Similar to the analysis of bulk networks where a promoted disassembly is the only option to gain information about the added polymer after photogrowth, the disassembly of the ENNs is equally informative to examine the extent and control of polymerization over the course of the expansion. The TTC network crosslinks were selectively cleaved with piperidine to produce branched polymers (BPs) (**Figure II-1E**) which were treated with dithiothreitol (DTT) before analysis to reduce disulfide bonds that are formed as a result of the cleavage.

Exposure of PGNN to piperidine resulted in BP 1 with in an average increase of 1,170 g/mol from the original linear polymer scaffold **5** which arises from the attached crosslinker (**Figure II-1F-G).** Cleavage of expanded networks after 1 hour of irradiation yielded BP 2 with M_n=11,200 g/mol and an increased dispersity of 1.25. In agreement with a living polymerization, further irradiation led to an increase of 28,600 g/mol from BP 2 to BP 4 and a relatively low dispersity of 1.44 (**Figure II-1G**). We concluded that the photogrowth process led to a successful insertion of monomer units into the network crosslinks and that the insertion is responsible for the growth in nanonetwork size.

Expansion of Nanonetworks by a Photoredox Catalyzed Polymerization

Encouraged by the successful expansion of the nanonetworks, we intended to test if a photoredox catalyzed polymerization could provide improved control over the photogrowth process. Organic photocatalysts have been shown to enhance the control and livingness of polymerizations with TTCs and have accelerated the development of additive manufacturing

methods from parent bulk gels.[10, 24] To explore this catalyzed approach, we first conducted model polymerization reactions with TTC crosslinker **1a** in the presence of 0.02 mol% 10-phenylphenothiazine (PTH). These conditions yielded rapid propagations and near full conversions in 30 minutes with good control over dispersity (M_n=31,900 g/mol, M_w/M_n =1.09) (**Figure II-S16**).

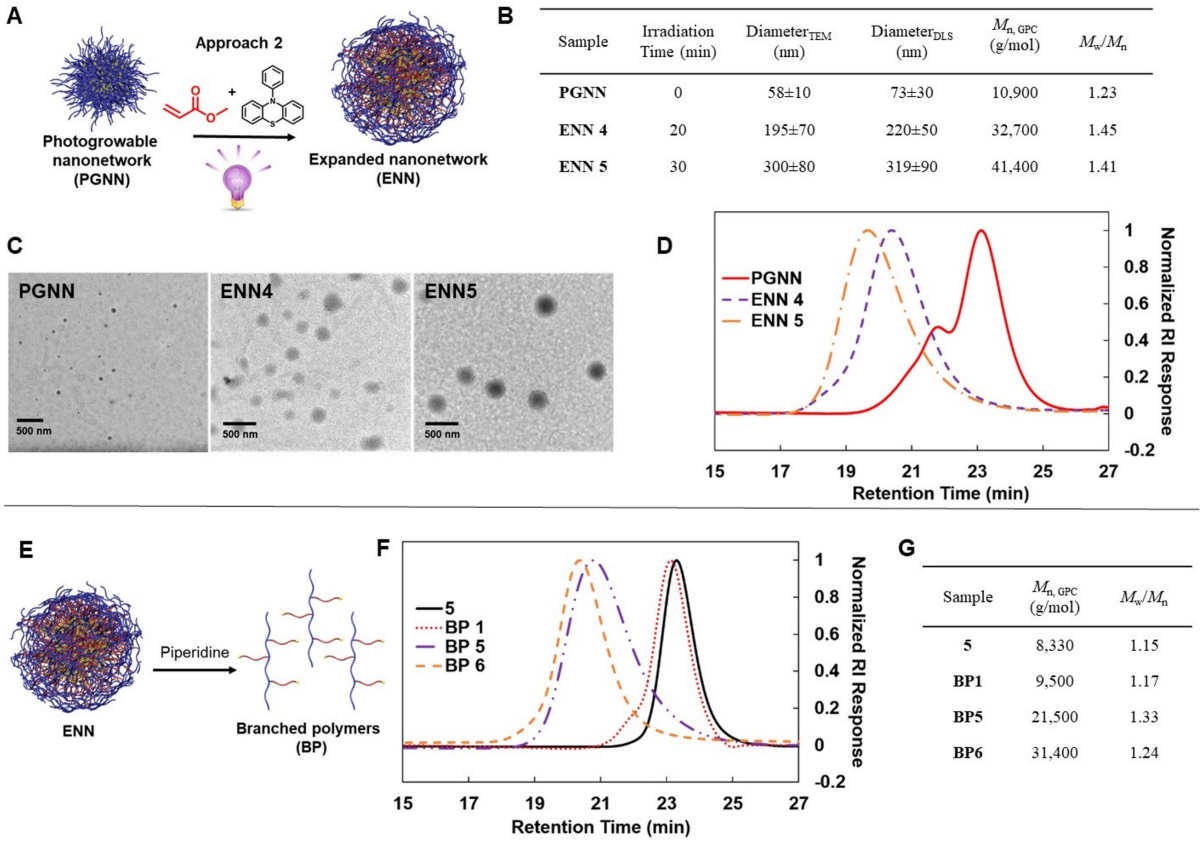

Sample	Irradiation Time (min)	Diameter$_{TEM}$ (nm)	Diameter$_{DLS}$ (nm)	$M_{n,GPC}$ (g/mol)	M_w/M_n
PGNN	0	58±10	73±30	10,900	1.23
ENN 4	20	195±70	220±50	32,700	1.45
ENN 5	30	300±80	319±90	41,400	1.41

Sample	$M_{n,GPC}$ (g/mol)	M_w/M_n
5	8,330	1.15
BP1	9,500	1.17
BP5	21,500	1.33
BP6	31,400	1.24

Figure II-2. (A) Schematic description of nanonetwork expansion by photoredox catalysis using PTH. (B) Size and dispersity of nanonetworks before, PGNN, and after expansion, ENNs, by TEM, DLS, and GPC. (C) TEM images of nanonetworks before and after expansion. (D) GPC traces of nanonetworks before and after expansion. (E) Schematic description of the selective cleavage of nanonetwork by aminolysis to produce branched polymers (BP). (F) GPC traces of linear thiolated polymer scaffold 5, BP1 generated from PGNN and BP5-6 generated from ENN4-5. (G) GPC analysis of linear polymer and branched polymers from PGNN (BP1) and ENNs (BP5-6). All GPC measurements were conducted at 40°C and a flow rate of 1mL/min with tetrahydrofuran as the eluent.

Following approach 2 (**Figure II-2**), PGNNs dissolved in a 2M MA solution in DMSO with 0.02 mol% PTH, were irradiated for 20 minutes, however; these conditions resulted in the unwanted formation of gels. Therefore, we conducted the reaction at a lower monomer concentration of 1 MA and no gel formation was observed after 20 minutes of irradiation time. In a second set of reactions, we extended the polymerization time to 30 minutes and both ENNs were characterized by NMR spectroscopy, TEM and DLS measurements. The particle size increased to an average of ~195 nm and ~300 nm after 20 min and 30 min respectively. Again, the addition of polymers into the network was witnessed by a shift to higher molecular weights and unimodal traces. Despite the accelerated insertion and growth caused by the photoredox initiated polymerization, no adverse effect on the dispersity of the ENNs was observed. Additionally, dispersities of ENNs from catalyzed reactions are slightly improved in contrast to expansion reactions without the addition of PTH.

Promoted Disassembly of Nanonetworks After Photoredox Mediated Expansion

Utilizing a promoted disassembly of the ENNs, we selectively cleaved these networks to investigate if a higher control over the expansion polymerization process was achieved. ENN 4 and 5 resulted in branched polymers with M_n=21,500, M_w/M_n=1.33 (BP 5) and M_n=31,400, M_w/M_n=1.23 (BP 6) respectively (**Figure II-2 F-G**). Interestingly, the cleaved networks showed a narrowing in dispersity with increased reaction times which is attributed to a higher control of polymerization using the photoredox catalyst and a greater ratio of well controlled linear polymers as part of the nanonetwork architecture. Furthermore, it emphasizes the significance and possibilities of CRPs in combination with photoredox catalysts for the incorporation of polymers

into parent particles to adjust functionalities, properties and even improve the dispersities of nanoscale structures.

CONCLUSION

In summary, we have developed a method to prepare nanonetworks in a variety of sizes, with a TTC unit as a crosslinking and iniferter element based on a thiol-maleimide crosslinking process. The engagement of the TTC through direct photolysis or a photoredox mechanism successfully integrated methyl acrylate polymers into the network elements of the particle and demonstrated the ability to expand nanonetworks to reach defined sizes. The presence of a photoredox catalyst significantly accelerated particle growth and achieved a higher level of control over the polymerization in contrast to the direct photolysis, suggesting that an increase in size through addition of controlled linear polymers could generate particles with improved dispersities in comparison to the parent particle.

EXPERIMENTAL

Materials:

All reagents and solvents were purchased from Sigma Aldrich and used as received unless otherwise stated. 4-cyanopentanoic acid dithiobenzoate (CPADB)[32], S,S'-bis(α,α'-dimethyl-α''-acetic acid)trithiocarbonate (BDMAT)[33], N-(2-Hydroxyethyl)maleimide[34-35], and 10-phenylphenothiazine (PTH)[19] were prepared according to the literature. Acrylate monomers methylmethacrylate (MMA), glycidol methacrylate (GMA), and methyl acrylate (MA) were purified immediately before use by passing through a short column of inhibitor removers purchased from Sigma Aldrich.

Characterization:

All ^{1}H and ^{13}C spectra were obtained using a Bruker AV-I 400 MHz, JEOL ECA 400 (400 MHz), or ECA-600 (600 MHz) spectrometer. Chemical shifts were measured relative to residual solvent peaks as an internal standard set to δ 7.26 and δ 77.16 (CDCl3) for 1H and 13C respectively. TEM imaging was performed using a JEOL 2000 FX Transmission Electron Microscope at 200 kV. Gel permeation chromatography (GPC) was performed using a Tosoh high performance GPC system HLC-8320 equipped with an auto injector, a dual differential refractive index detector and TSKgel G series columns connected in series (7.8×300 mm TSKgel G5000Hxl, TSKgel G4000Hxl, TSKgel G3000Hxl). GPC analysis was carried out in HPLC grade tetrahydrofuran with a flow rate of 1.0 mL/min at 40 °C. Molecular weights (Mn and Mw) and molecular weight distributions were calculated from polymethyl methacrylate (PMMA) standards with molecular weights of 800 to 2.2×106 g mol-1 provided by Polymer Standard Service (PSS). Dynamic light scattering (DLS) was measured on a Malvern Zetasizer Nano ZS in THF at 25°C with an angle of 173° and at appropriate sample concentrations.

Synthetic Methods:

Scheme II-S1. Model thiol-maleimide reaction (A). Synthesis of thiolated polymers (B).

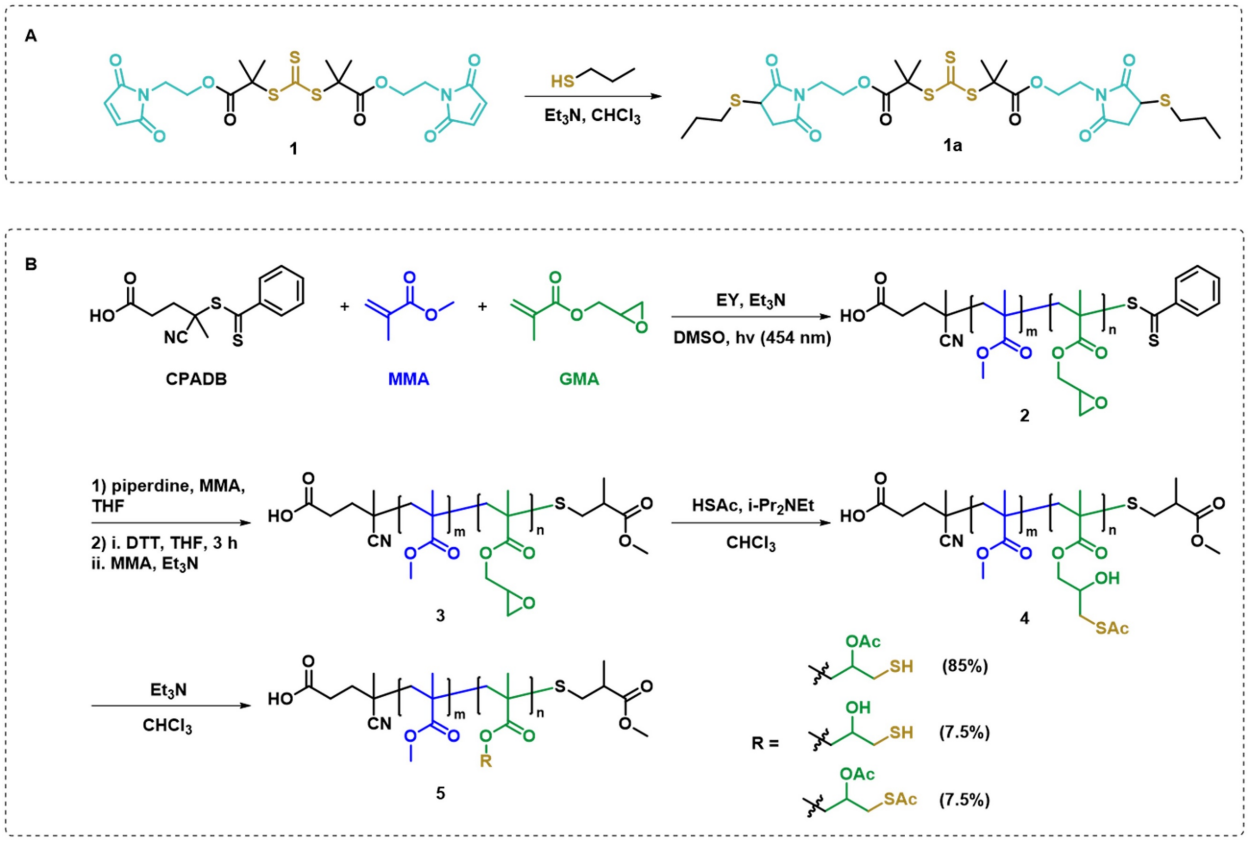

Synthesis of maleimide TTC (1)

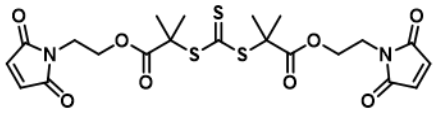

BDMAT (232 mg, 0.82 mmol) was dissolved in thionyl chloride (6 mL) and refluxed for 3 h. Excess thionyl chloride was removed and the resulting yellow solid (BDMAT-Cl) was used without further purification. BDMAT-Cl in CH_2Cl_2 (2 mL) was added dropwise to a stirring solution of N-(2-Hydroxyethyl)maleimide (254 mg, 1.8 mmol), pyridine (0.15 mL, 1.8 mmol), CH_2Cl_2 (8 mL) under nitrogen at 0°C. The reaction stirred for 3 h at room temperature and was then diluted with 5 mL CH_2Cl_2 and washed with 1M HCl, Sat. $NaHCO_3$, and water. The organic layer was dried over anhydrous $MgSO_4$, and the solvent evaporated to give the crude product as a

brown solid. The product was recrystallized from ethyl acetate to provide the product as a yellow solid (261 mg, 60%) ^{1}H NMR (400 MHz, $CDCl_3$) δ 6.72 (s, 4H), 4.21 (t, J = 4 Hz, 4H), 3.80 (t, J = 4 Hz, 4H), 1.60 (s, 12H). ^{13}C NMR (400 MHz, $CDCl_3$) δ 218.72, 172.32, 170.23, 134.13, 62.77, 56.06, 36.47, 24.94. (Figure II-S1, II-S2)

Trithiocarbonate compatibility with thiol-maleimide (1a)

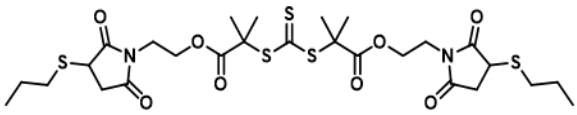

Triethylamine (4.3 μL, 0.031 mmol) was added to a solution of 1-propane thiol (5.8 μL, 0.062 mmol) and **1** (15 mg, 0.028 mmol) in $CDCl_3$ (0.75 mL). The reaction stirred for 15 minutes and an NMR was taken without purification of the reaction mixture. ^{1}H NMR (400 MHz, $CDCl_3$) δ 4.24 (t, J = 4 Hz, 4H), 3.78 (m, 6H), 3.18 (dd, J = 12 Hz, 2H), 2.87 (m, 2H), 2.72 (m, 2H), 2.54 (dd, J = 16 Hz, 2H), 1.67 (m, 4H), 1.62 (s, 12H). ^{13}C NMR (400 MHz, $CDCl_3$) δ 218.88, 176.26, 174.45, 172.35, 62.19, 56.22, 39.01, 37.72, 36.12, 33.75, 24.97, 24.95, 22.33, 13.33. (Figure II-S3, II-S4)

General procedure for the preparation of PMMA-co-GMA (2)

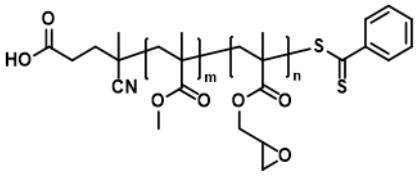

Reactions were prepared using the ratio (MMA/GMA/CPADB/EY/Et_3N) (80/20/1/0.02/1) in a 1:1 monomer:DMSO ratio. Reactions were irradiated with a 3.5 W blue light for the desired amount of time and then precipitated twice in diethyl ether. (Mn=7.60 kDa, PDI=1.09, MMA=77%, GMA=23%) (Figure II-S5)

General aminolysis procedure of PMMA-co-GMA (3)

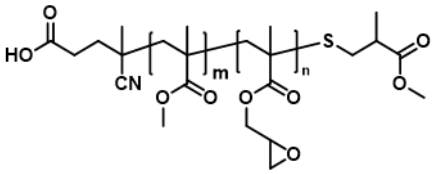

To a sealed 1 dram vial **2** (300 mg) was added and covered with a nitrogen atmosphere, and then dissolved in degassed THF (3 mL). MMA (100 µL) and piperidine (50 µL) were added under nitrogen. After 6 hours the reaction was precipitated into diethyl ether. The product was dissolved in THF (3mL) and treated with DTT for 3 hours under nitrogen. MMA (100 µL) and triethylamine (10 µL) were added to the solution and the reaction stirred for 3 hours under nitrogen. The reaction was precipitated into diethyl ether twice and dried under vacuum to give 284 mg of a colorless product. (Figure II-S6)

General thiolation procedure of aminolyzed PMMA-co-GMA (4)

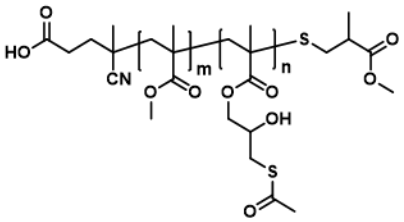

Thioacetic acid (59 µL, 0.82 mmol) and *i*-Pr_2NEt (10 µL, 0.058 mmol) were added to a solution of **3** (274 mg, 0.41 mmol epoxide) in $CDCl_3$ (1.5 mL). The reaction stirred for 18 hours. The product was then precipitated twice in diethyl ether and dried under vacuum to give 230 mg of the protected thiolated product. (Figure II-S7)

General acetyl migration procedure of thiolated PMMA-co-GMA (5)

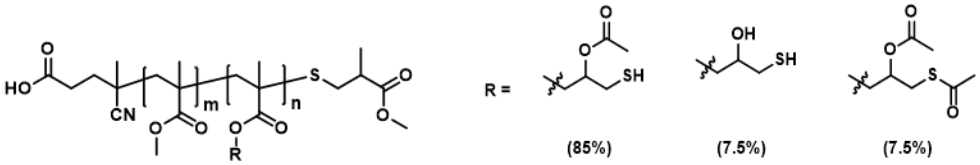

Triethylamine (2.3 mL) was added dropwise to a vigorously stirring solution of **4** (115 mg) under nitrogen. After 18 hours the reaction was concentrated and precipitated twice in diethyl ether to give 93 mg of the deprotected product. The pure product was stored in $CHCl_3$ at 2°C to prevent the formation of an insoluble gel. (Figure II-S8)

General procedure for thiol-maleimide nanonetwork formation

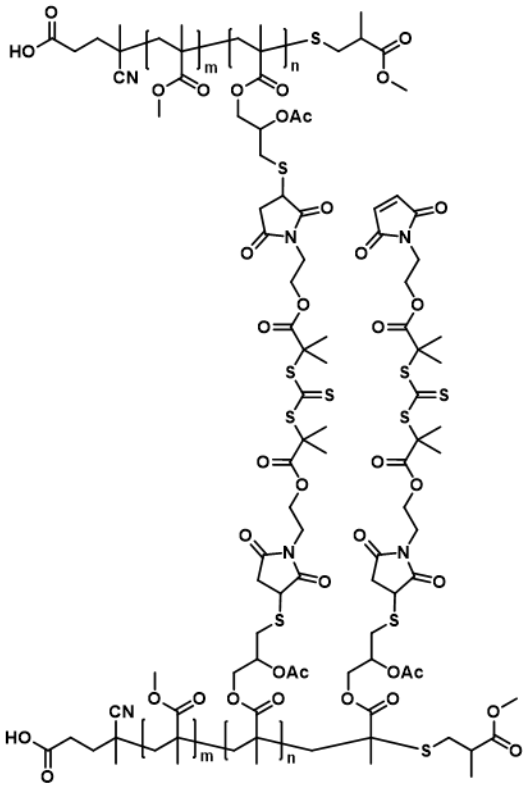

A solution of **5** in THF and stirred with DTT for 3 hours to reduce any disulfide bonds. The polymer was purified with Sephadex LH-20. The polymer was dried and then dissolved in the desired amount of $CHCl_3$ under a nitrogen atmosphere. The desired amount of **1** (1, 2, or 4 equivalents to thiols) and Et_3N (0.2 equivalents to thiols) in $CHCl_3$ (20% of the total reaction volume) were added dropwise to the vigorously stirring solution of **5** in $CHCl_3$ under nitrogen. After 18 hours the reaction was diluted with CH_2Cl_2 and dialyzed for two days in 10 kDa MWCO snakeskin tubing against a 1:1 mixture of ACN:THF. (Figure II-S9)

Model Diels-Alder reaction

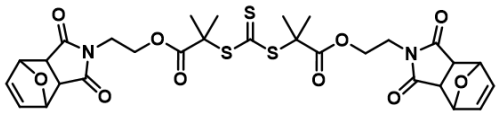

Maleimide TTC **1** (100 mg, 0.19 mmol) was dissolved in furan (2 mL) and stirred for 24 hours. The reaction was concentrated under vacuum to give a mixture of endo/exo products as a yellow solid (120 mg, 95%). ^{1}H NMR (600 MHz, $CDCl_3$) δ 6.51, 6.42 (s, 4H), 5.33, 5.25 (s, 4H), 4.20, 4.09 (q, J = 5.4 Hz, 4H), 3.76, 3.58 (s, J=5.4 Hz, 4H), 3.55, 2.88 (d, 4H), 1.61 (m, 12H). ^{13}C NMR (600 MHz, $CDCl_3$) δ 219.02, 175.97, 174.67, 172.36, 136.64, 134.58, 80.89, 79.42, 62.30, 56.30, 47.56, 46.09, 37.64, 37.38, 25.04 (Figure II-S10, II-S11)

General procedure for the Diels-Alder reaction of nanonetwork maleimides

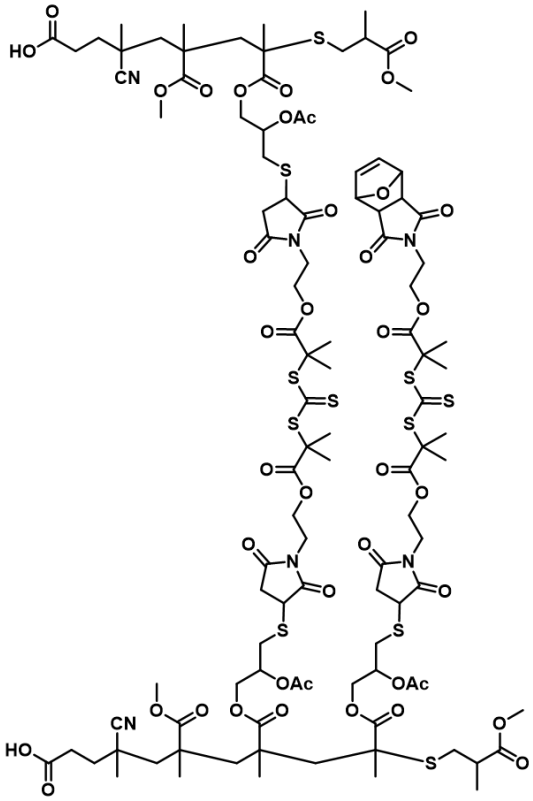

An excess of furan (1.5 mL) was added to a solution of nanonetworks (50 mg) in CH_2Cl_2 (1 mL). The reaction mixture was stirred for 24 hours and concentrated under vacuum to give the product as a yellow solid. (Figure II-S12)

General procedure for controlled photo-growth of nanonetworks

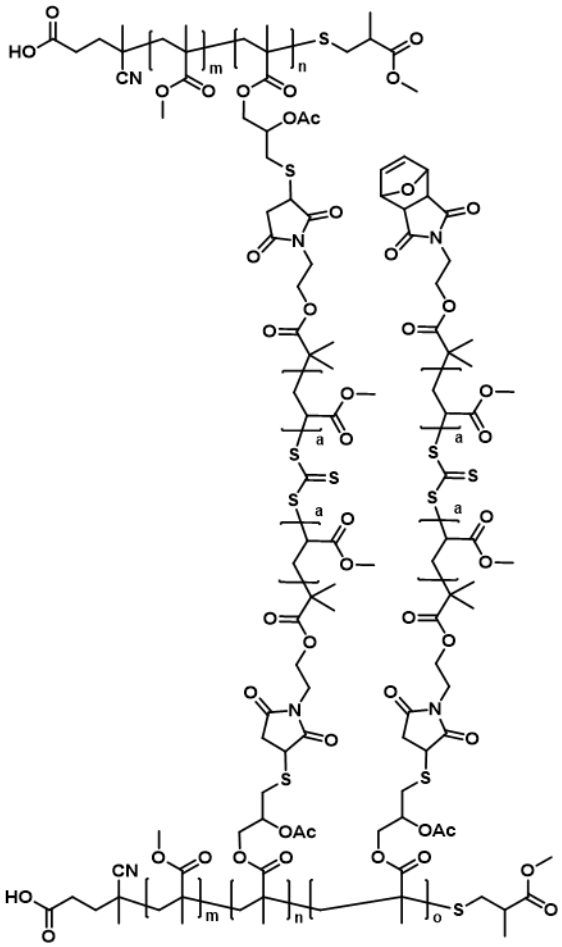

Nanonetworks (4 mg) were sealed in a 1 dram vial, covered with a nitrogen atmosphere, and dissolved in degassed MA (300 μL) with PTH (0 or 0.02 mol%) for 1 hour. DMSO (1.6 or 3.2 mL) was added under argon. The reaction was then placed 2 cm from a 400 nm light source and irradiated for the desired amount of time. The crude product was diluted with CH_2Cl_2 and dialyzed

in 10 kDa MWCO snakeskin tubing against a 1:1:1 mixture of CH_2Cl_2:ACN:THF for 2 days. (Figure II-S13, II-S14)

General procedure for the aminolysis of expanded nanonetworks

Piperidine (10 uL) was added to a solution of expanded nanonetworks (10 mg) in THF (0.5 mL). The reaction was stirred for 18 hours and then treated with DTT for 3 hours before dialysis in 10 kDa MWCO snakeskin tubing against 1:1 ACN:THF for 24 hours. The purified product was concentrated, dissolved in HPLC grade THF, filtered and analyzed by GPC.

Polymerization mediated by 1a

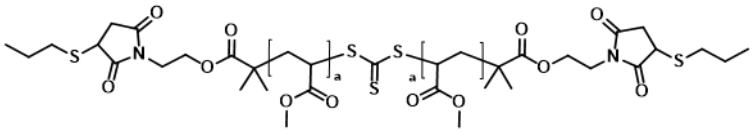

TTC **1a** (4.2 mg, 0.0062 mmol) was dissolved in a degassed solution of DMSO (1.55 mL) and MA (277 µL, 3.1 mmol) with PTH (0 or 0.02mol%). The reaction vessel was sealed and sparged with nitrogen for 30 minutes. The reaction was then placed 2 cm form a 400 nm led light source and irradiated for the desired amount of time. (Figure II-S15, II-S16) (Table II-S1, II-S2)

NMR Spectra

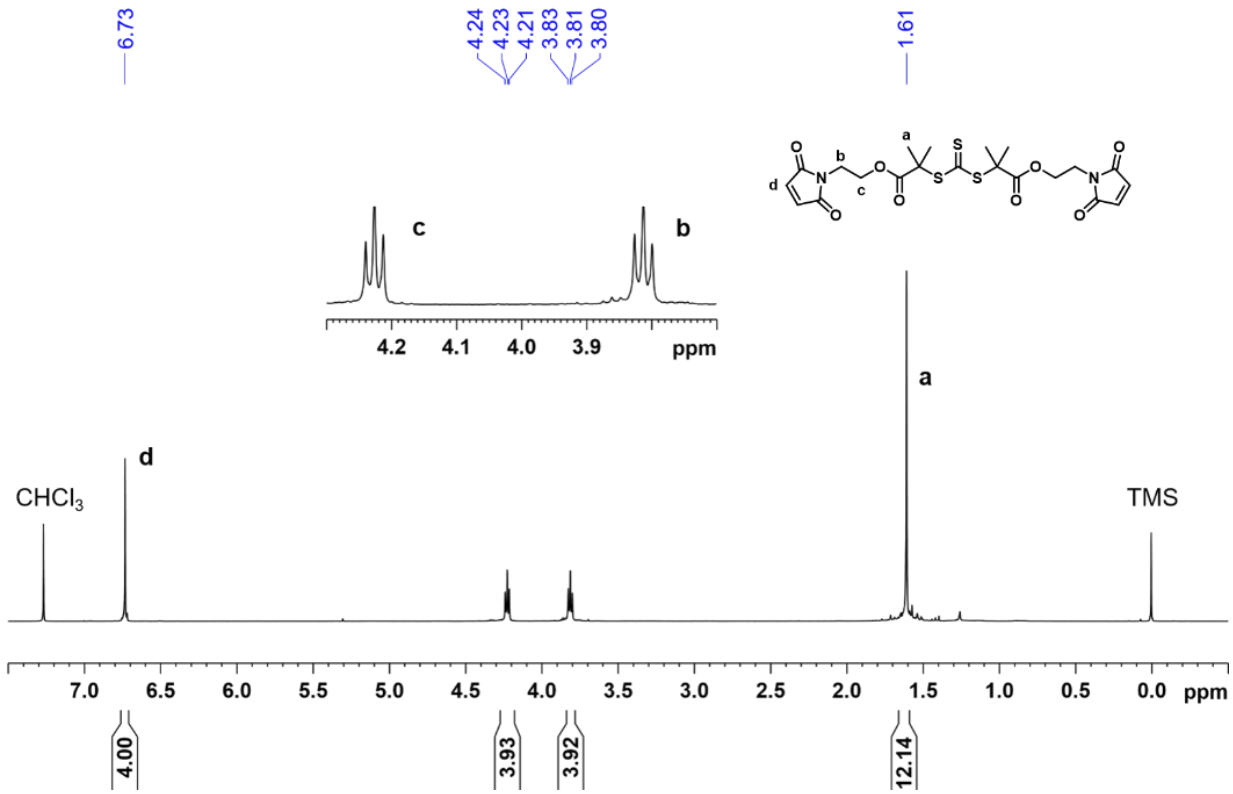

Figure II-S1. ^{1}H NMR ($CDCl_3$, 400 MHz) spectrum of the purified maleimide TTC **1**.

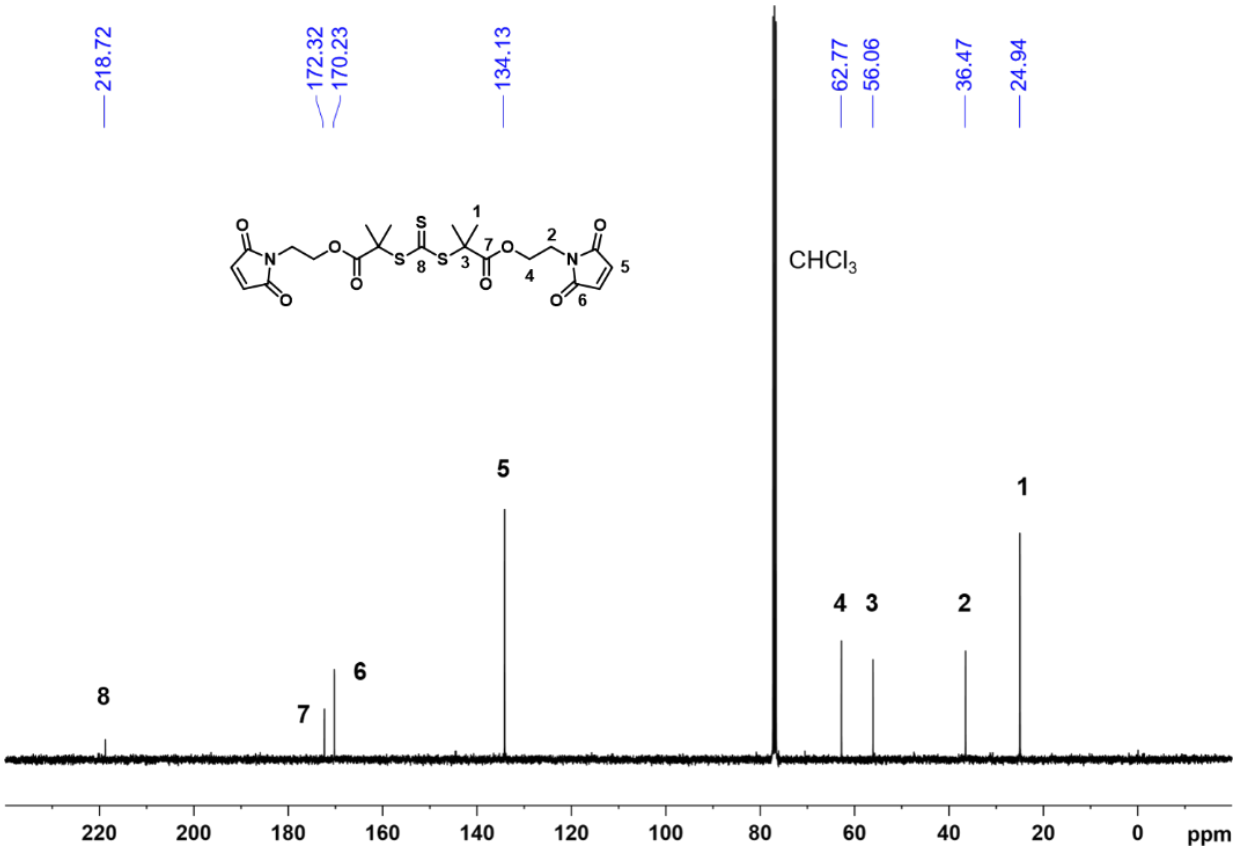

Figure II-S2. ^{13}C NMR ($CDCl_3$, 400 MHz) spectrum of the purified maleimide TTC **1**.

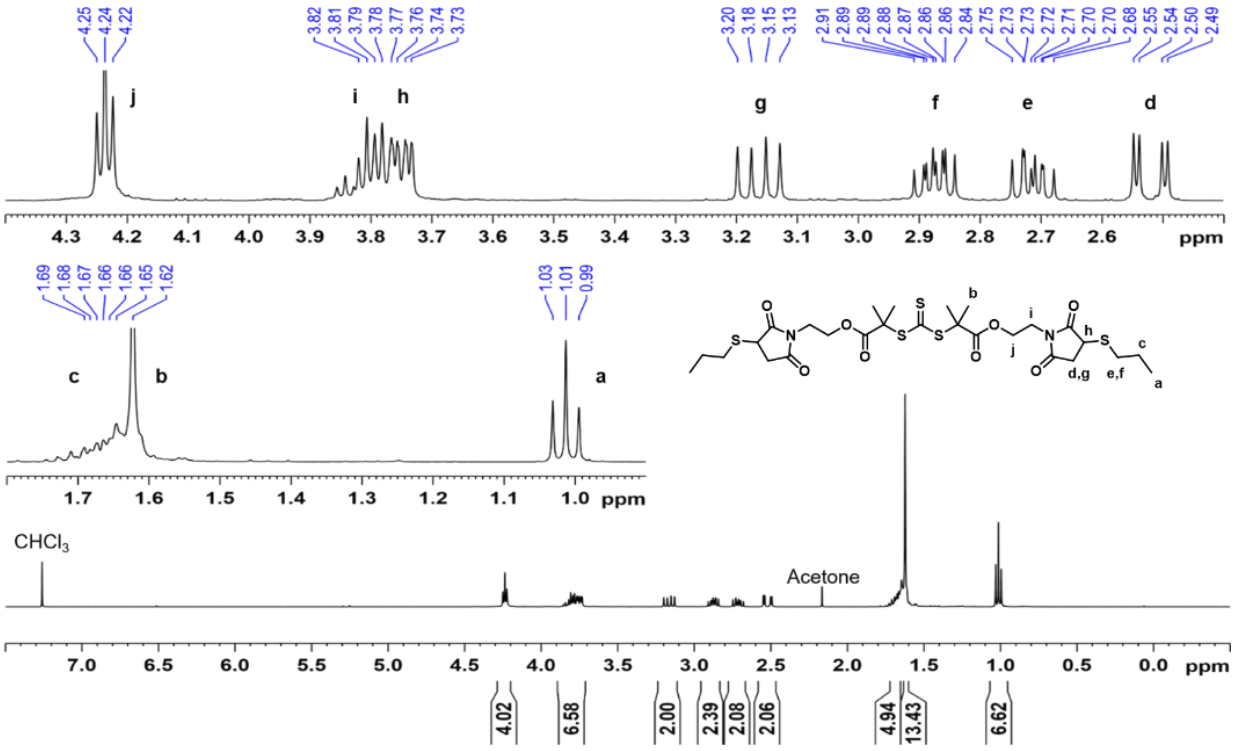

Figure II-S3. ^{1}H NMR ($CDCl_3$, 400 MHz) spectrum of the thiol-maleimide compatibility experiment.

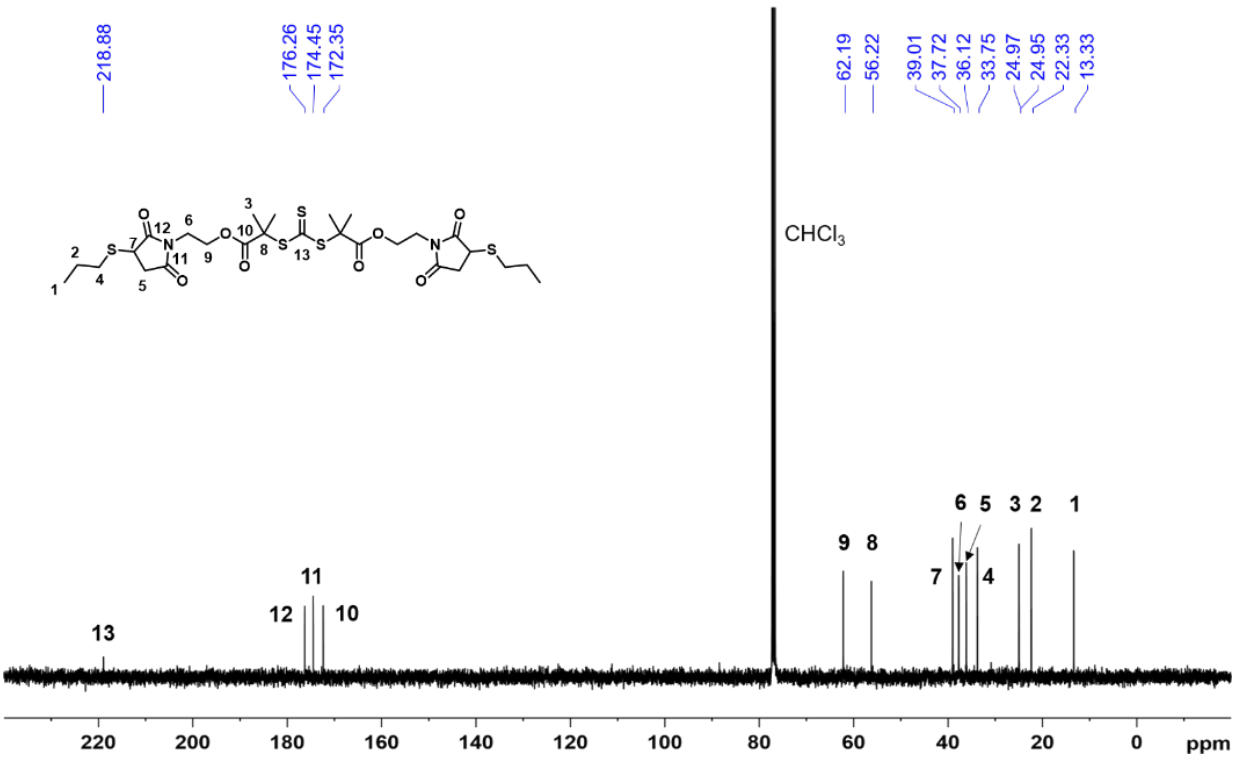

Figure II-S4. ^{13}C NMR ($CDCl_3$, 400 MHz) spectrum of the thiol-maleimide compatibility experiment.

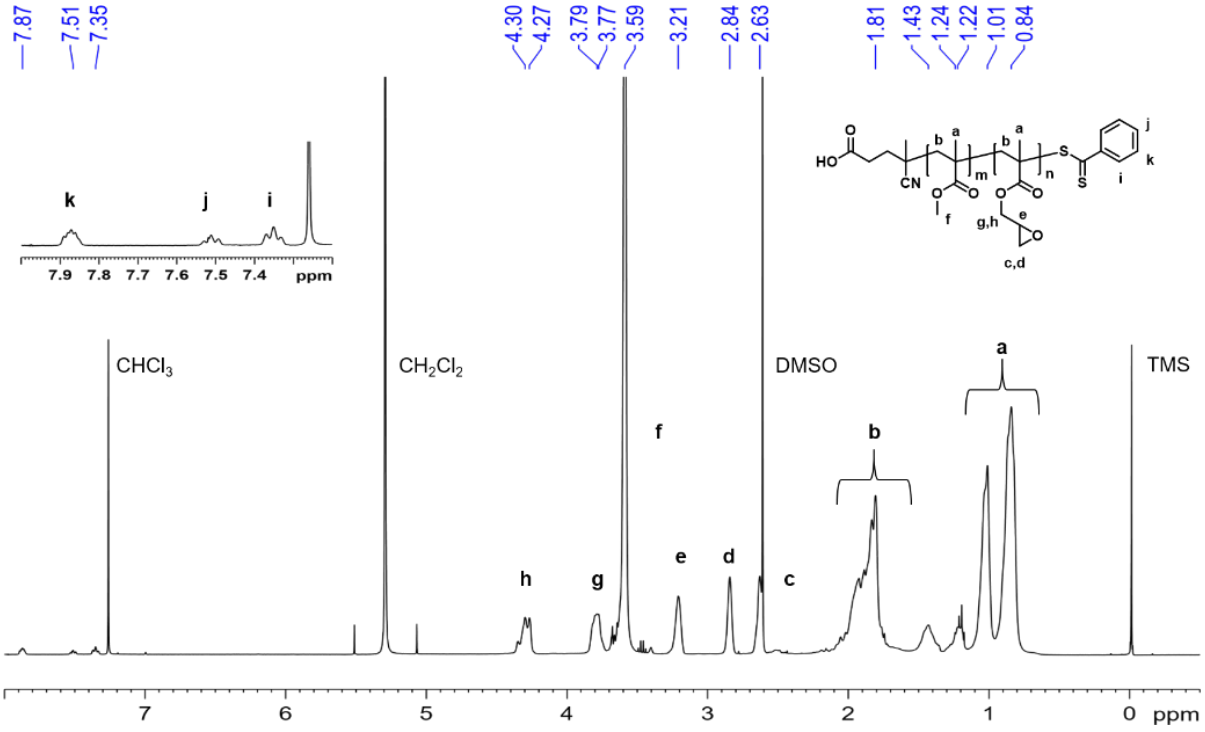

Figure II-S5. ^{1}H NMR ($CDCl_3$, 400 MHz) spectrum of polymer **2**.

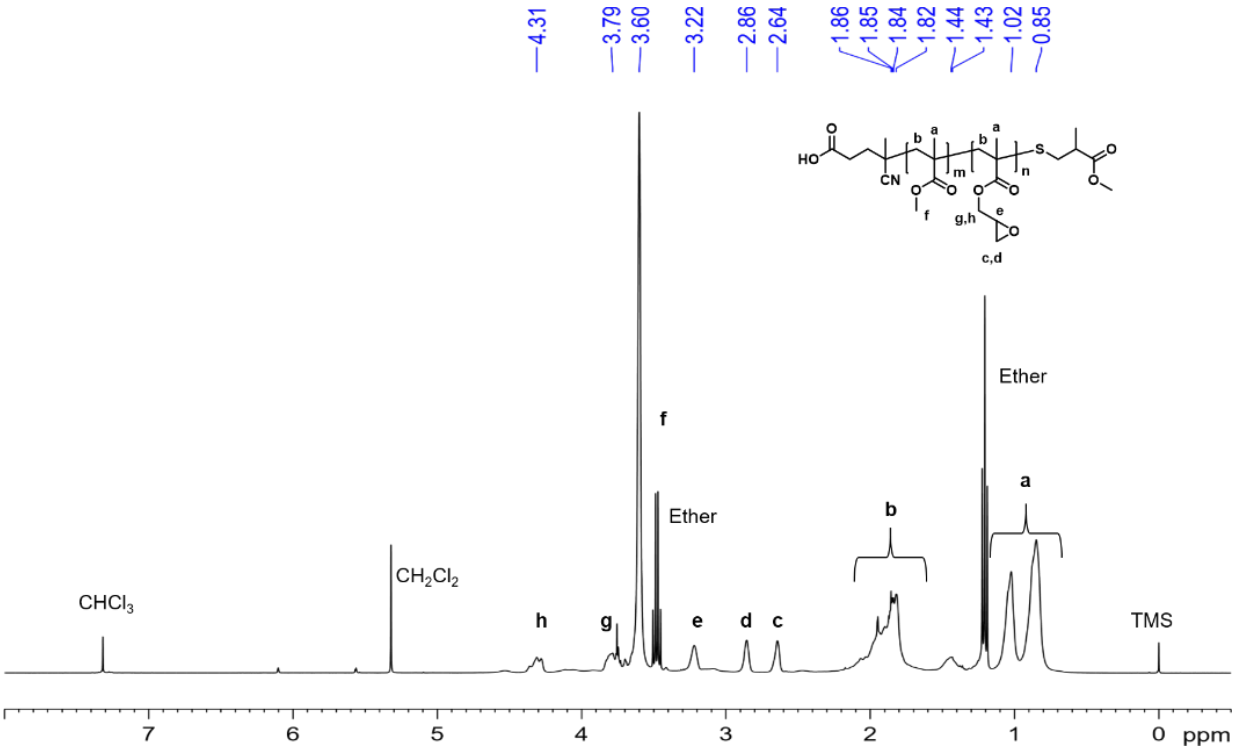

Figure II-S6. ^{1}H NMR ($CDCl_3$, 400 MHz) spectrum of polymer **3**.

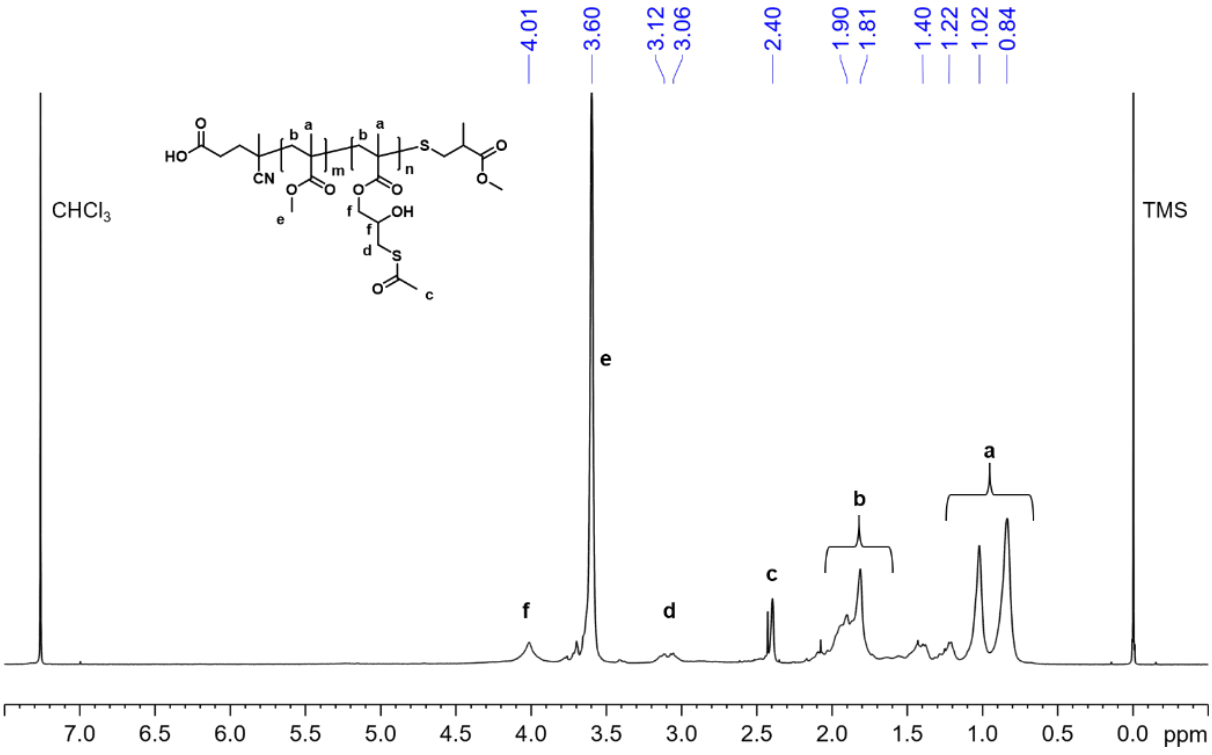

Figure II-S7. ^{1}H NMR ($CDCl_3$, 400 MHz) spectrum of polymer **4**.

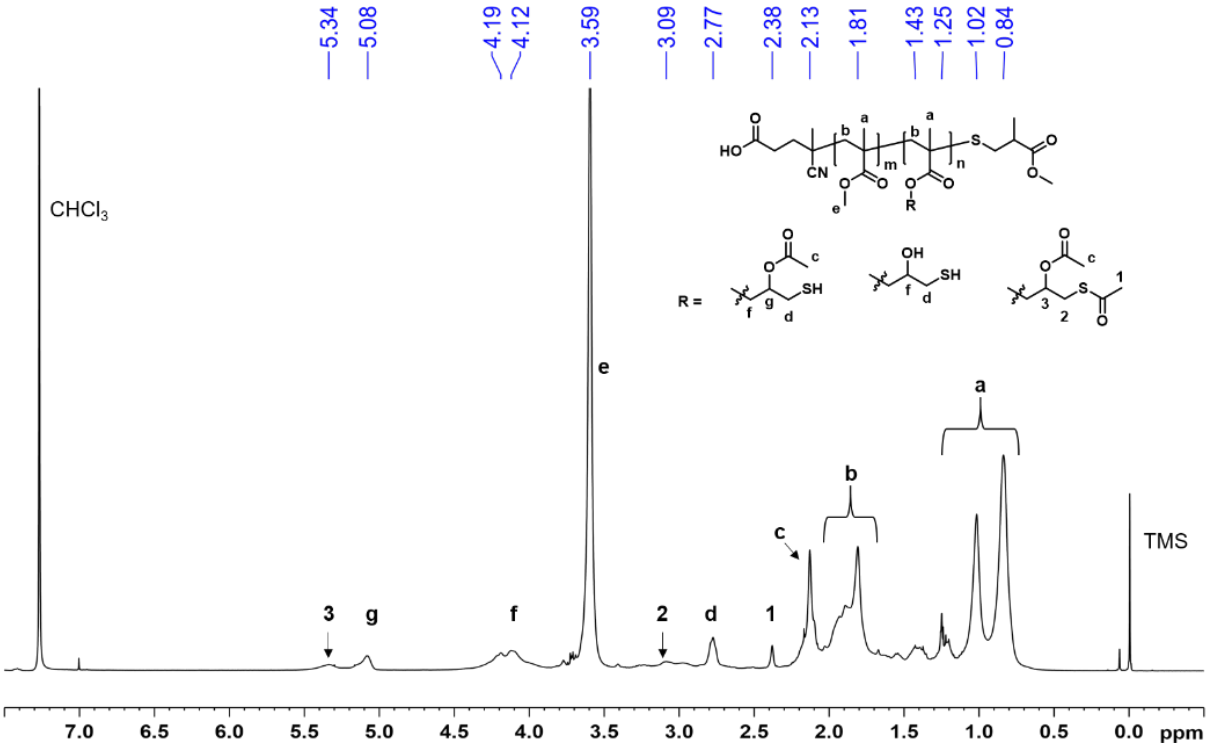

Figure II-S8. ^{1}H NMR ($CDCl_3$, 400 MHz) spectrum of polymer **5**.

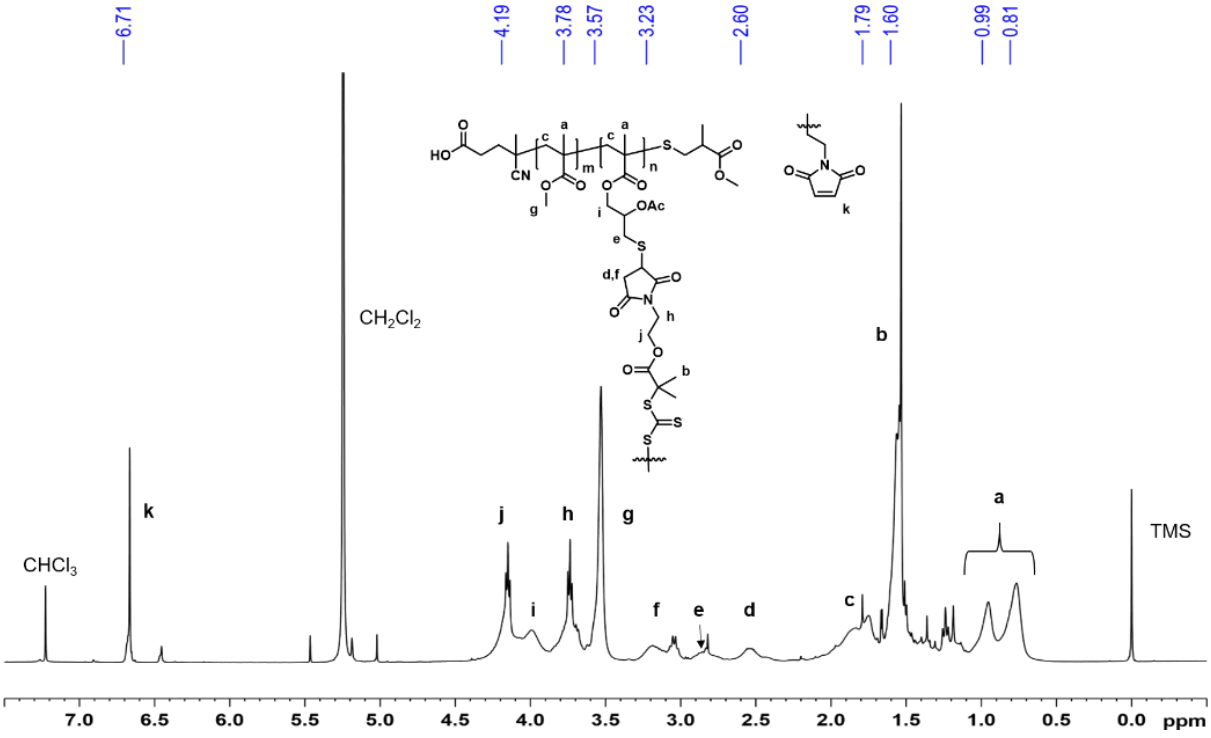

Figure II-S9. ^{1}H NMR ($CDCl_3$, 400 MHz) spectrum of photogrowable nanonetwork.

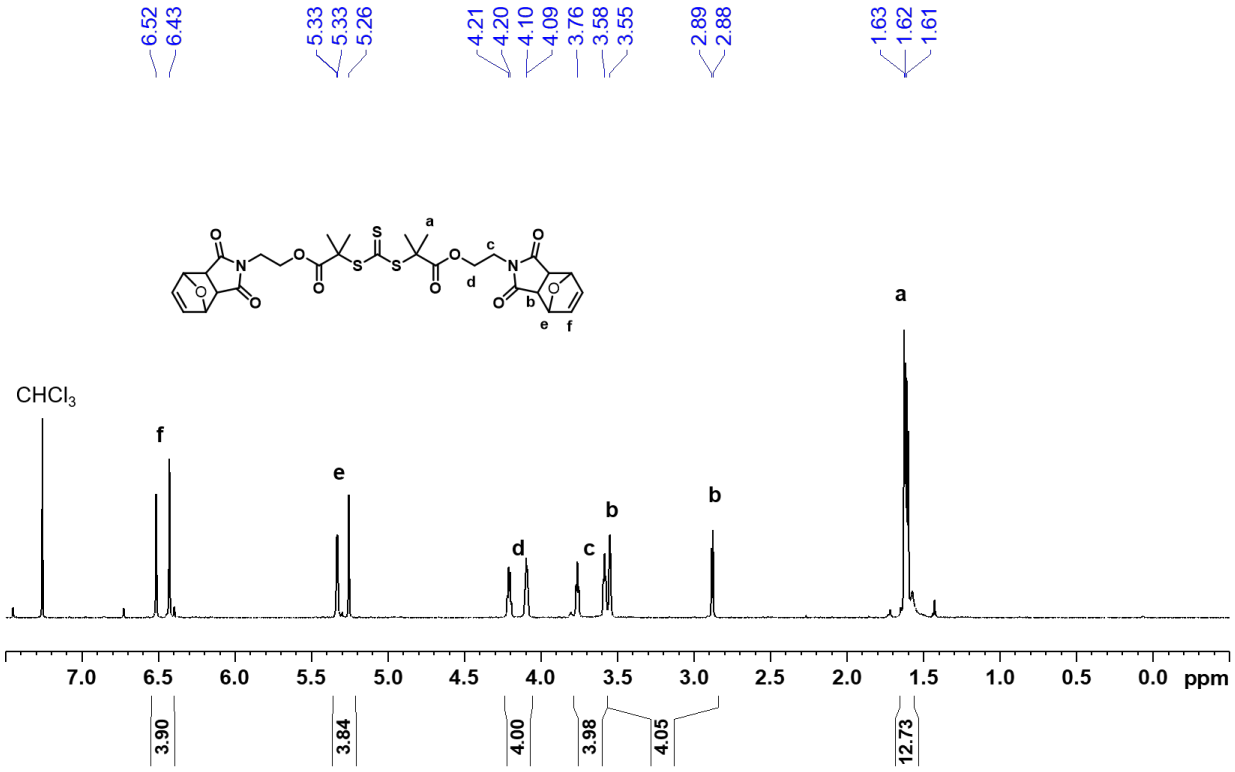

Figure II-S10. ^{1}H NMR ($CDCl_3$, 600 MHz) spectrum of model DA reaction.

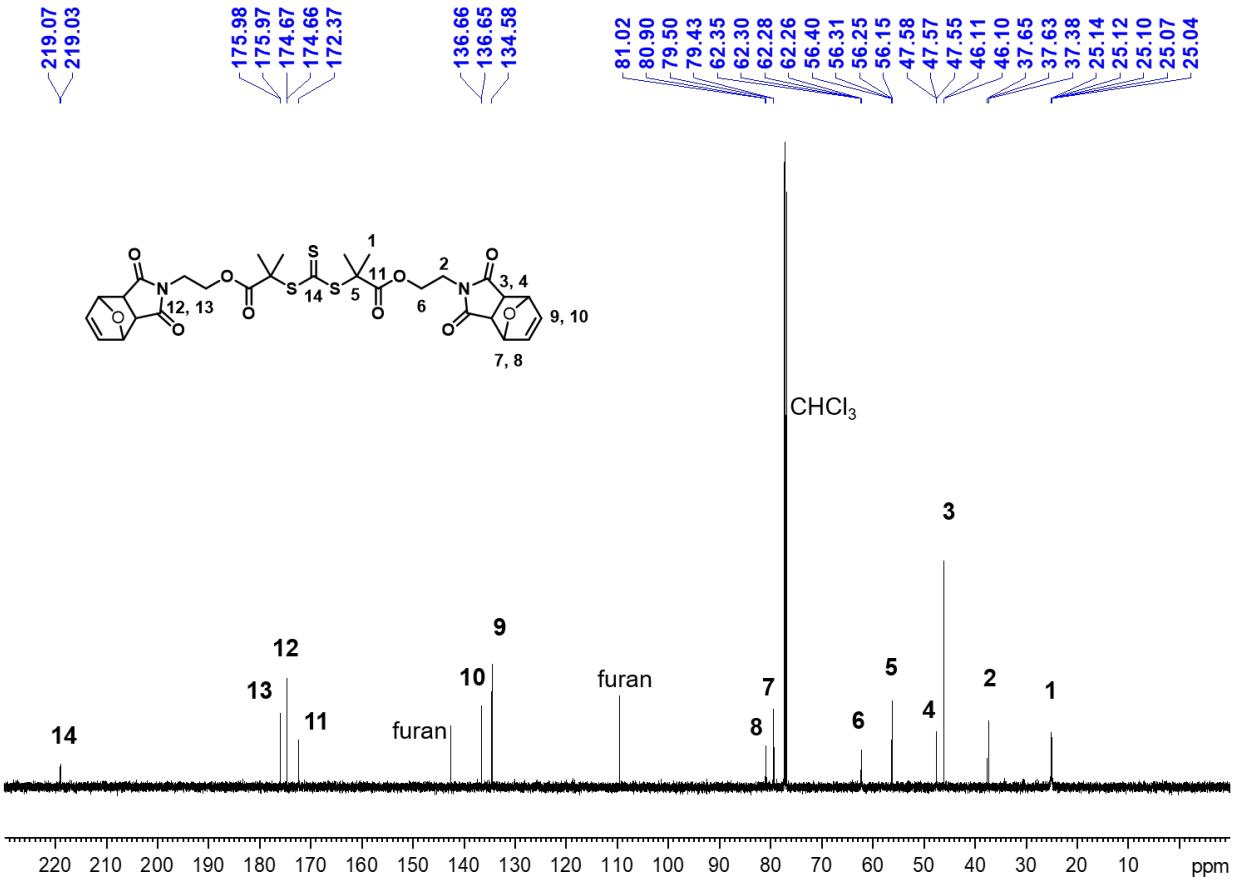

Figure II-S11. ^{13}C NMR ($CDCl_3$, 600 MHz) spectrum of model DA reaction.

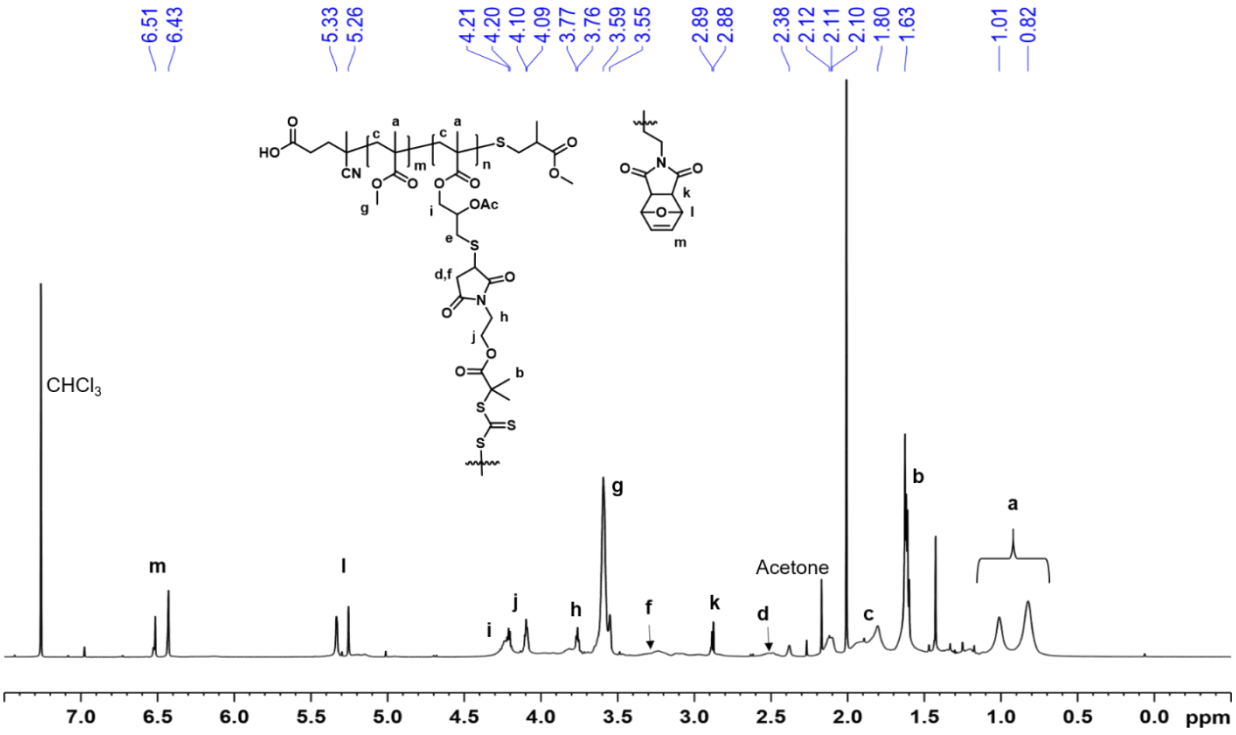

Figure II-S12. ^{1}H NMR ($CDCl_3$, 600 MHz) spectrum of furan capped nanonetwork.

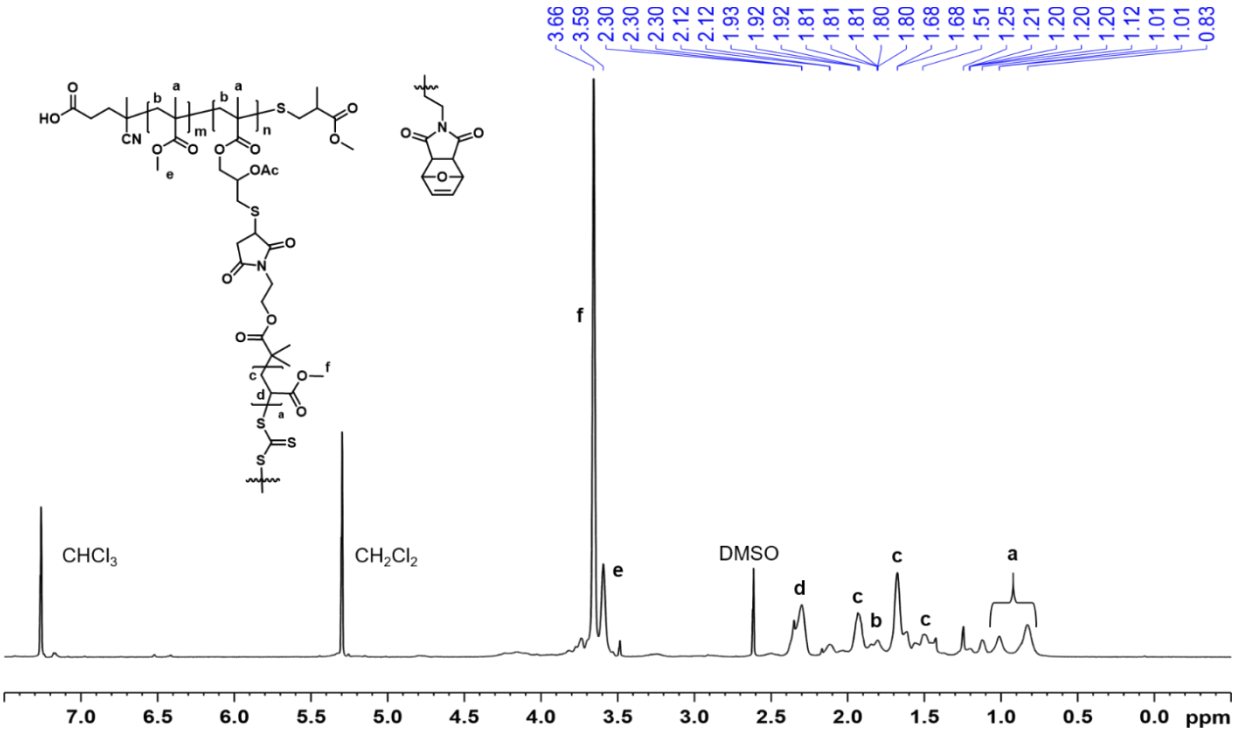

Figure II-S13. ^{1}H NMR ($CDCl_3$, 600 MHz) spectrum of expanded nanonetwork after 1 hour of irradiation.

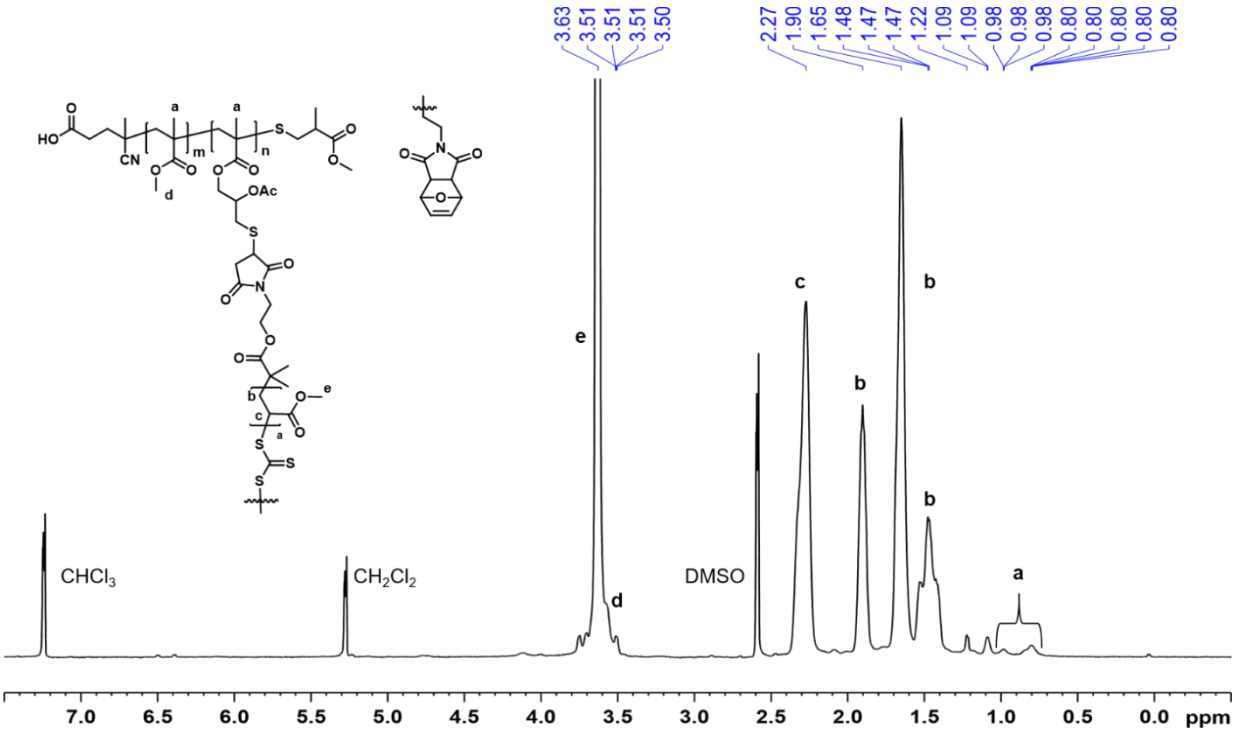

Figure II-S14. ^{1}H NMR ($CDCl_3$, 600 MHz) spectrum of expanded nanonetwork after 6 hours of irradiation.

GPC Analysis

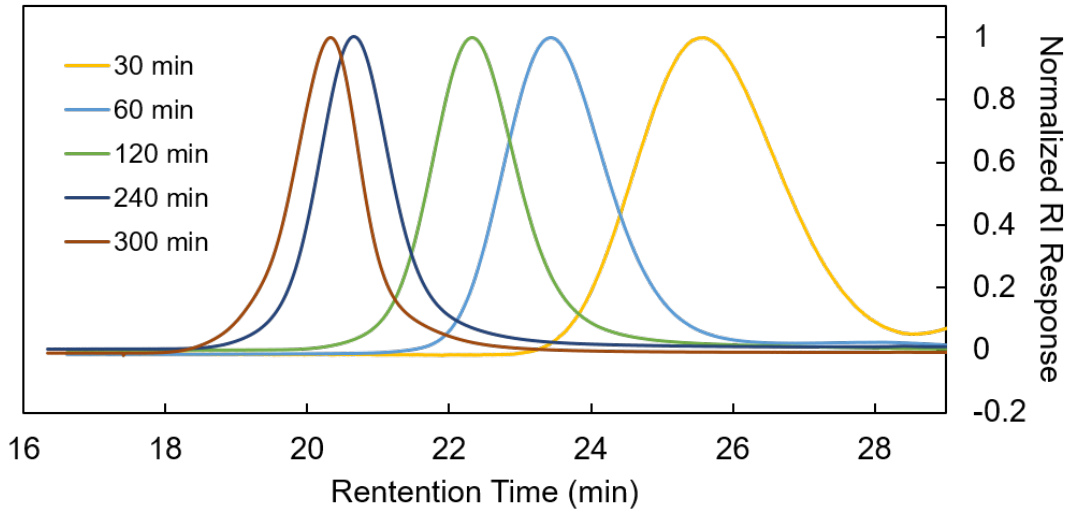

Figure II-S15. GPC traces of polymers synthesized from maleimide TTC **1a**.

Table II-S1. GPC analysis of polymers synthesized from maleimide TTC **1a**.

Irradiation Time (min)	M_n[a] (kDa)	M_w[a](kDa)	M_w/M_n[a]
30	3.10	3.65	1.17
60	7.91	8.69	1.09
120	12.84	14.24	1.11
240	29.32	32.80	1.11
300	36.42	41.65	1.14

[a] Molecular weight and polydispersity measured by GPC in THF at 40°C and a flow rate of 1mL/min.

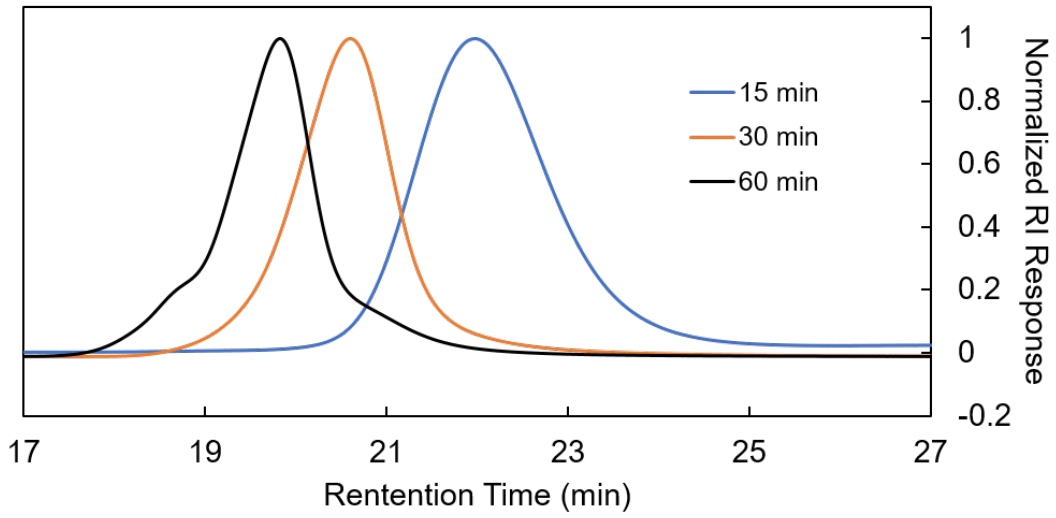

Figure II-S16. GPC traces of polymers synthesized from maleimide TTC **1a** in the presence of 0.02 mol% PTH.

Table II-S2. GPC analysis of polymers synthesized from maleimide TTC **1a** in the presence of 0.02 mol% PTH.

Irradiation Time (min)	M_n[a] (kDa)	M_w[a](kDa)	M_w/M_n[a]
15	14.80	16.87	1.14
30	31.90	34.77	1.09
60	49.64	59.73	1.20

[a] Molecular weight and polydispersity measured by GPC in THF at 40°C and a flow rate of 1mL/min.

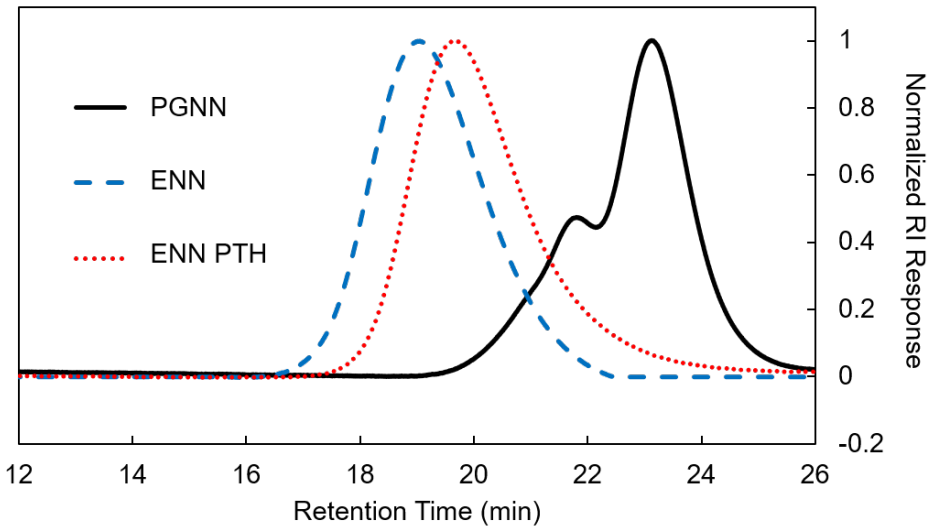

Figure II-S17. GPC traces of nanonetworks before expansion (PGNN), after expansion for 6 hours (ENN), and after expansion for 30 minutes in the presence of PTH (ENN PTH).

REFERENCES

(1) Chen, M.; Zhong, M. J.; Johnson, J. A., Light-Controlled Radical Polymerization: Mechanisms, Methods, and Applications. *Chem Rev* **2016,** *116* (17), 10167-10211.

(2) McKenzie, T. G.; Fu, Q.; Uchiyama, M.; Satoh, K.; Xu, J. T.; Boyer, C.; Kamigaito, M.; Qiao, G. G., Beyond Traditional RAFT: Alternative Activation of Thiocarbonylthio Compounds for Controlled Polymerization. *Adv Sci* **2016,** *3* (9).

(3) Dadashi-Silab, S.; Doran, S.; Yagci, Y., Photoinduced Electron Transfer Reactions for Macromolecular Syntheses. *Chem Rev* **2016,** *116* (17), 10212-10275.

(4) Xu, J.; Fu, C.; Shanmugam, S.; Hawker, C. J.; Moad, G.; Boyer, C., Synthesis of Discrete Oligomers by Sequential PET-RAFT Single-Unit Monomer Insertion. *Angew. Chem. Int. Ed.* **2017,** *56* (29), 8376-8383.

(5) Carmean, R. N.; Becker, T. E.; Sims, M. B.; Sumerlin, B. S., Ultra-High Molecular Weights via Aqueous Reversible-Deactivation Radical Polymerization. *Chem* **2017,** *2* (1), 93-101.

(6) Tan, J.; Sun, H.; Yu, M.; Sumerlin, B. S.; Zhang, L., Photo-PISA: Shedding Light on Polymerization-Induced Self-Assembly. *ACS Macro Lett.* **2015,** *4* (11), 1249-1253.

(7) Yeow, J.; Xu, J.; Boyer, C., Polymerization-Induced Self-Assembly Using Visible Light Mediated Photoinduced Electron Transfer–Reversible Addition–Fragmentation Chain Transfer Polymerization. *ACS Macro Lett.* **2015,** *4* (9), 984-990.

(8) Gao, P.; Cao, H.; Ding, Y.; Cai, M.; Cui, Z. G.; Lu, X. H.; Cai, Y. L., Synthesis of Hydrogen-Bonded Pore-Switchable Cylindrical Vesicles via Visible-Light-Mediated RAFT Room-Temperature Aqueous Dispersion Polymerization. *Acs Macro Lett* **2016,** *5* (12), 1327-1331.

(9) Zhou, H.; Johnson, J. A., Photo-controlled Growth of Telechelic Polymers and End-linked Polymer Gels. *Angew. Chem. Int. Ed.* **2013,** *52* (8), 2235-2238.

(10) Chen, M.; Gu, Y.; Singh, A.; Zhong, M.; Jordan, A. M.; Biswas, S.; Korley, L. T. J.; Balazs, A. C.; Johnson, J. A., Living Additive Manufacturing: Transformation of Parent Gels into Diversely Functionalized Daughter Gels Made Possible by Visible Light Photoredox Catalysis. *ACS Central Science* **2017,** *3* (2), 124-134.

(11) Singh, A.; Kuksenok, O.; Johnson, J. A.; Balazs, A. C., Tailoring the structure of polymer networks with iniferter-mediated photo-growth. *Polym. Chem.* **2016,** *7* (17), 2955-2964.

(12) Amamoto, Y.; Kamada, J.; Otsuka, H.; Takahara, A.; Matyjaszewski, K., Repeatable Photoinduced Self-Healing of Covalently Cross-Linked Polymers through Reshuffling of Trithiocarbonate Units. *Angew. Chem. Int. Ed.* **2011,** *50* (7), 1660-1663.

(13) Amamoto, Y.; Otsuka, H.; Takahara, A.; Matyjaszewski, K., Changes in Network Structure of Chemical Gels Controlled by Solvent Quality through Photoinduced Radical Reshuffling Reactions of Trithiocarbonate Units. *ACS Macro Lett.* **2012,** *1* (4), 478-481.

(14) Ercole, F.; Thissen, H.; Tsang, K.; Evans, R. A.; Forsythe, J. S., Photodegradable Hydrogels Made via RAFT. *Macromolecules* **2012,** *45* (20), 8387-8400.

(15) Li, Q.; Hu, X.; Bai, R., Synthesis of Photodegradable Polystyrene with Trithiocarbonate as Linkages. *Macromol. Rapid Commun.* **2015,** *36* (20), 1810-1815.

(16) Otsu, T.; Yoshida, M., Role of initiator-transfer agent-terminator (iniferter) in radical polymerizations: Polymer design by organic disulfides as iniferters. *Die Makromolekulare Chemie, Rapid Communications* **1982,** *3* (2), 127-132.

(17) Xu, J.; Shanmugam, S.; Duong, H. T.; Boyer, C., Organo-photocatalysts for photoinduced electron transfer-reversible addition-fragmentation chain transfer (PET-RAFT) polymerization. *Polym. Chem.* **2015,** *6* (31), 5615-5624.

(18) Xu, J.; Jung, K.; Atme, A.; Shanmugam, S.; Boyer, C., A Robust and Versatile Photoinduced Living Polymerization of Conjugated and Unconjugated Monomers and Its Oxygen Tolerance. *J. Am. Chem. Soc.* **2014,** *136* (14), 5508-5519.

(19) Treat, N. J.; Sprafke, H.; Kramer, J. W.; Clark, P. G.; Barton, B. E.; Read de Alaniz, J.; Fors, B. P.; Hawker, C. J., Metal-Free Atom Transfer Radical Polymerization. *J. Am. Chem. Soc.* **2014,** *136* (45), 16096-16101.

(20) Pan, X. C.; Malhotra, N.; Simakova, A.; Wang, Z. Y.; Konkolewicz, D.; Matyjaszewski, K., Photoinduced Atom Transfer Radical Polymerization with ppm-Level Cu Catalyst by Visible Light in Aqueous Media. *J Am Chem Soc* **2015,** *137* (49), 15430-15433.

(21) Corrigan, N.; Rosli, D.; Jones, J. W. J.; Xu, J.; Boyer, C., Oxygen Tolerance in Living Radical Polymerization: Investigation of Mechanism and Implementation in Continuous Flow Polymerization. *Macromolecules* **2016,** *49* (18), 6779-6789.

(22) Yeow, J.; Chapman, R.; Xu, J.; Boyer, C., Oxygen tolerant photopolymerization for ultralow volumes. *Polym. Chem.* **2017**.

(23) Xu, J.; Shanmugam, S.; Fu, C.; Aguey-Zinsou, K.-F.; Boyer, C., Selective Photoactivation: From a Single Unit Monomer Insertion Reaction to Controlled Polymer Architectures. *J. Am. Chem. Soc.* **2016,** *138* (9), 3094-3106.

(24) Chen, M.; MacLeod, M. J.; Johnson, J. A., Visible-Light-Controlled Living Radical Polymerization from a Trithiocarbonate Iniferter Mediated by an Organic Photoredox Catalyst. *ACS Macro Lett.* **2015,** *4* (5), 566-569.

(25) Costa, L. P. D.; McKenzie, T. G.; Schwarz, K. N.; Fu, Q.; Qiao, G. G., Observed Photoenhancement of RAFT Polymerizations under Fume Hood Lighting. *Acs Macro Lett* **2016,** *5* (11), 1287-1292.

(26) Shi, Y.; Liu, G. H.; Gao, H.; Lu, L. C.; Cai, Y. L., Effect of Mild Visible Light on Rapid Aqueous RAFT Polymerization of Water-Soluble Acrylic Monomers at Ambient Temperature: Initiation and Activation. *Macromolecules* **2009,** *42* (12), 3917-3926.

(27) McKenzie, T. G.; Wong, E. H. H.; Fu, Q.; Sulistio, A.; Dunstan, D. E.; Qiao, G. G., Controlled Formation of Star Polymer Nanoparticles via Visible Light Photopolymerization. *ACS Macro Lett.* **2015,** *4* (9), 1012-1016.

(28) Tan, J.; Zhao, G.; Lu, Y.; Zeng, Z.; Winnik, M. A., Synthesis of PMMA Microparticles with a Narrow Size Distribution by Photoinitiated RAFT Dispersion Polymerization with a Macromonomer as the Stabilizer. *Macromolecules* **2014,** *47* (19), 6856-6866.

(29) Ende, A. E. v. d.; Kravitz, E. J.; Harth, E., Approach to Formation of Multifunctional Polyester Particles in Controlled Nanoscopic Dimensions. *J. Am. Chem. Soc.* **2008,** *130* (27), 8706-8713.

(30) Stevens, D. M.; Tempelaar, S.; Dove, A. P.; Harth, E., Nanosponge Formation from Organocatalytically Synthesized Poly(carbonate) Copolymers. *ACS Macro Lett.* **2012,** *1* (7), 915-918.

(31) Wang, G.; Peng, L.; Zheng, Y.; Gao, Y.; Wu, X.; Ren, T.; Gao, C.; Han, J., Novel triethylamine catalyzed S →O acetyl migration reaction to generate candidate thiols for construction of topological and functional sulfur-containing polymers. *RSC Adv.* **2015,** *5* (8), 5674-5679.

(32) Mitsukami, Y.; Donovan, M. S.; Lowe, A. B.; McCormick, C. L., Water-Soluble Polymers. 81. Direct Synthesis of Hydrophilic Styrenic-Based Homopolymers and Block Copolymers in Aqueous Solution via RAFT. *Macromolecules* **2001,** *34* (7), 2248-2256.

(33) Zuo, Y.; Guo, N.; Jiao, Z.; Song, P.; Liu, X.; Wang, R.; Xiong, Y., Novel reversible thermoresponsive nanogel based on poly(ionic liquid)s prepared via RAFT crosslinking copolymerization. *J. Polym. Sci., Part A: Polym. Chem.* **2016,** *54* (1), 169-178.

(34) Klein, R.; Übel, F.; Frey, H., Maleimide Glycidyl Ether: A Bifunctional Monomer for Orthogonal Cationic and Radical Polymerizations. *Macromol. Rapid Commun.* **2015,** *36* (20), 1822-1828.

(35) Salewska, N.; Milewska, M. J., Efficient Method for the Synthesis of Functionalized Basic Maleimides. *J. Heterocycl. Chem.* **2014,** *51* (4), 999-1003.

CHAPTER III

NANONETWORK PHOTOGROWTH EXPANSION: TAILORING NANOPARTICLE NETWORKS' CHEMICAL STRUCTURE AND LOCAL TOPOLOGY

INTRODUCTION

Amorphous polymer networks are one of the most fundamental materials in polymer science with applications that are governed by their complex dynamics, linear elasticity,[1] network topology,[2-3] and mechanical properties.[4-5] It is accepted that heterogeneous crosslinking events occur during network formation creating imperfections that ultimately affect a network's connectivity and its resulting dynamics.[6-10] Controlling crosslinking chemistry and allowing for the repair and restructuring of networks through integrated moieties is an increasing field of interest as it allows for control over a network's structure both during and after formation.[11-16] Recently, post-synthetic modifications of polymer gels' chemical compositions and network properties have been achieved through either the incorporation of atom transfer radical polymerization (ATRP) initiator sites within the parent gel network producing structurally tailored and engineered macromolecular (STEM) gels,[17-20] or through the incorporation of trithiocarbonates (TTCs) in the parent network crosslinks[21] which, with the advancement of photo-controlled radical polymerizations and new photocatalysts,[22-24] resulted in the development of a living additive manufacturing method.[25] In each case properties of the parent gels were manipulated by growing secondary polymer chains into the existing network from the embedded initiators, and the

produced daughter gels possessed new properties provided by and dependent upon the newly introduced polymer chains.

In our recent communication, we adapted this concept to the expansion of nanonetwork materials, which in contrast to the above material is not a gel but rather a macromolecular network fully soluble in organic solvents.[26] In a proof-of-concept study, the photocontrolled growth of nanonetworks was achieved through polymerizations from the integrated trithiocarbonate crosslinker by either direct photolysis or by photoredox catalysis. Integration of linear polymers into the nanonetwork yielded improved dispersities in contrast to the parent nanonetworks and improved control over the polymerization was achieved by performing the polymerizations with 10-phenylphenothiazine (PTH) as a photocatalyst.[26] These results along with the successful reports of property manipulations in polymer gels encouraged us to further test the controlled modification of our nanonetwork system by altering the network composition, architecture, and properties.

Herein, we sought to investigate the controlled manipulation of photogrowable nanonetworks' (PGNNs) sizes and properties by utilizing a breadth of monomer families to form homopolymers with hydrophilic or hydrophobic character from acrylates, acrylamides and fluorinated monomers such as tert-butyl acrylate (tBA), trifluoroethyl acrylate (TFEA), hydroxyethyl acrylate (HEA), and stimuli responsive N-isopropyl acrylamide (NIPAAM). Control provided by this process allows for the preparation of other polymer compositions in the form of statistical copolymers containing methyl acrylate (MA) (PMA-*co*-PTFEA, PMA-*co*-PtBA, and PMA-*co*-PHEA) and block copolymers. The symmetrical nature of the trithiocarbonate is ideal to grow ABA triblock

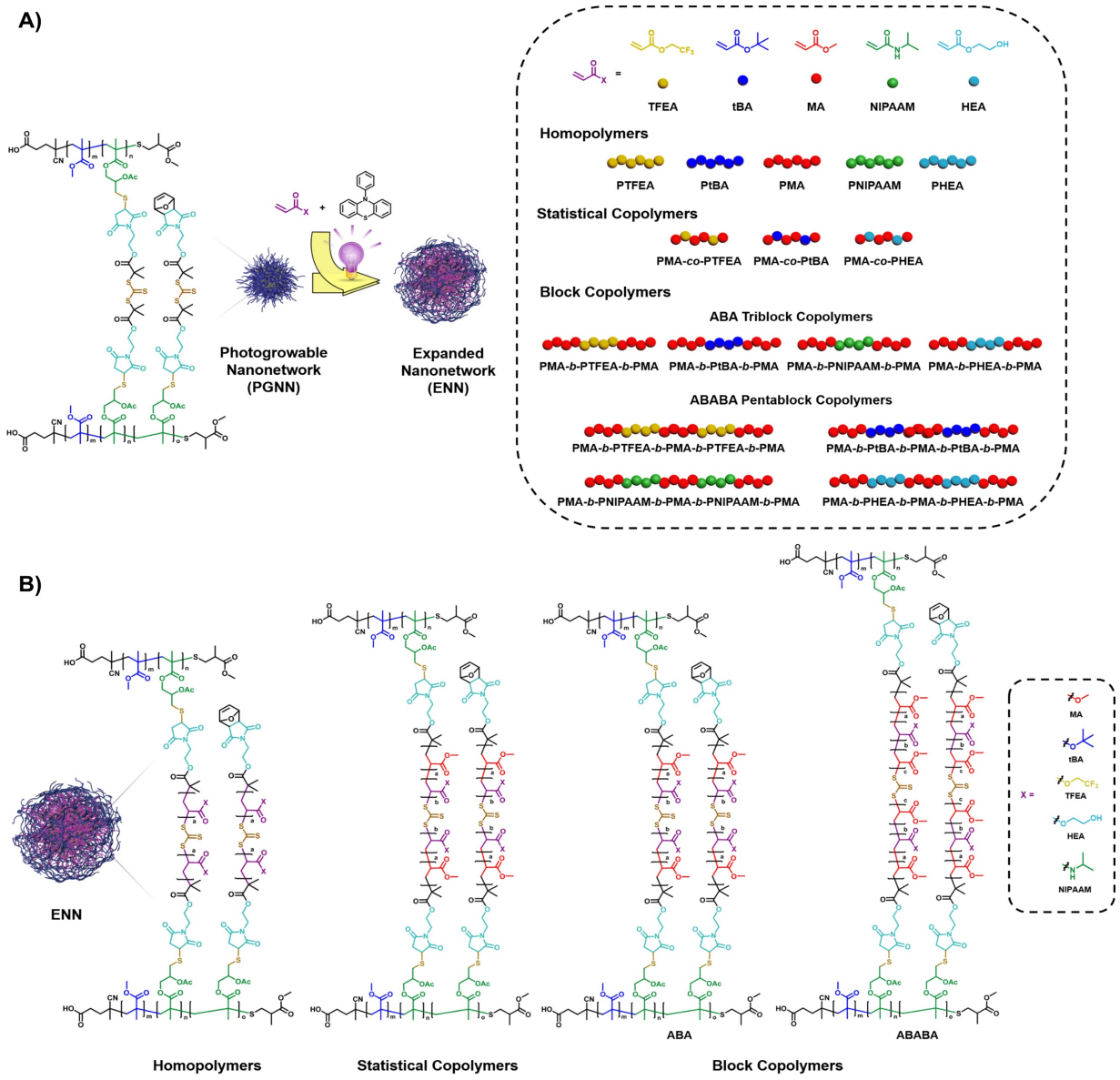

Figure III-1. (A) Structure and expansion of nanonetworks through the incorporation of various monomers, and the list of polymers incorporated into the networks. (B) The general structure of expanded networks with incorporated homopolymers, statistical copolymers, and block copolymers.

and ultimately ABABA pentablock copolymers through the addition of three monomers to form PMA-*b*-PTFEA-*b*-PMA-*b*-PTFEA-*b*-PMA, PMA-*b*-PtBA-*b*-PMA-*b*-PtBA-*b*-PMA, PMA-*b*-PNIPAAM-*b*-PMA-*b*-PNIPAAM-*b*-PMA, and PMA-*b*-PHEA-*b*-PMA-*b*-PHEA-*b*-PMA pentablock copolymers. Utilizing this controlled photogrowth process we are able

to tailor multiple progeny networks with homogenously altered network compositions, sizes, and properties stemming from a single parent network on the nanoscale.

RESULTS AND DISCUSSION

Crosslinked nanonetworks derived from our developed intermolecular chain crosslinking process with integrated trithiocarbonates[26] (PGNNs) are ideal candidates for photoredox mediated polymerizations with the aim to extend the network architecture through linear polymers, as the parent and resulting particles are soluble in organic solvents which allows for advantageous conditions during polymerization and characterization.[26] To further develop and investigate the scope of possible nanonetwork modifications, representative monomers such as tert-butyl acrylate (tBA), trifluoroethyl acrylate (TFEA), hydroxyethyl acrylate (HEA), N-isopropyl acrylamide (NIPAAM) and polymer compositions in the form of homopolymers, statistical copolymers, and ABA tri- and ABABA pentablock copolymers were integrated into the crosslinker of the network structure (**Figure III-1**).

Scheme III-1. Synthesis of thiolated polymer.[26]

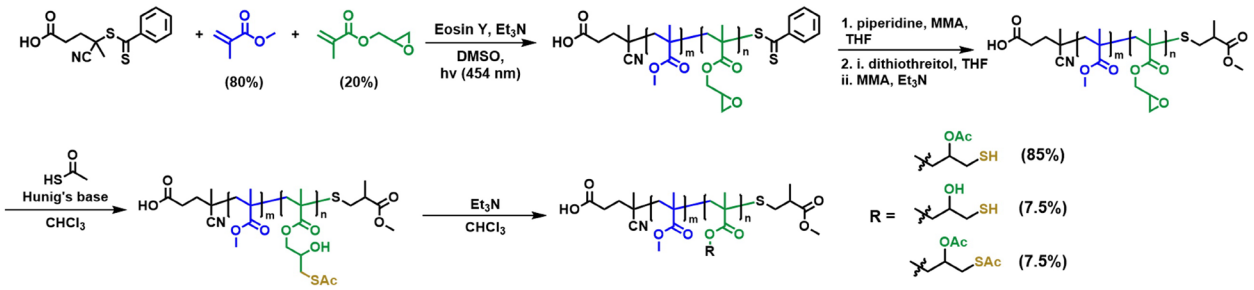

Parent PGNNs were prepared as previously described; briefly a poly (methyl methacrylate-co-glycidol methacrylate) copolymer was synthesized through reversible

addition-fragmentation chain-transfer (RAFT) polymerization as one of the nanoparticle components with MW = 6,200 g/mol, $Đ$ = 1.09 and 19 % incorporation of glycidyl methacrylate (**Scheme III-1**). The dithiobenzoate RAFT end group was removed by aminolysis and the resulting thiol was capped with methyl methacrylate to ensure polymerization could only occur from the TTC crosslinker. Pendant epoxides were ring opened with thioacetic acid followed by a triethylamine promoted sulfur to oxygen acetyl migration to provide a thiolated polymer. Parent PGNNs were then prepared through thiol maleimide click chemistry using the thiolated polymer at a concentration of 0.005 M with 2 equivalents (with respect to mmol of thiol) of the symmetrical bis-maleimide crosslinker[26] with integrated trithiocarbonate producing nanonetworks with a size of 43±10 nm by TEM and 66±11 nm by DLS (**Scheme III-2**). As the concentration of the active unit in the polymer and the equivalents of the crosslinking unit determines the size of the nanoparticle, we used a ratio that gives particles well below 100 nm for the investigation of the photogrowth process as a means to better illustrate the range of nanonetwork dimensions that can be achieved. Free maleimides on the nanonetwork surface were then reacted with

Scheme III-2. Synthesis of photogrowable nanonetwork.[26]

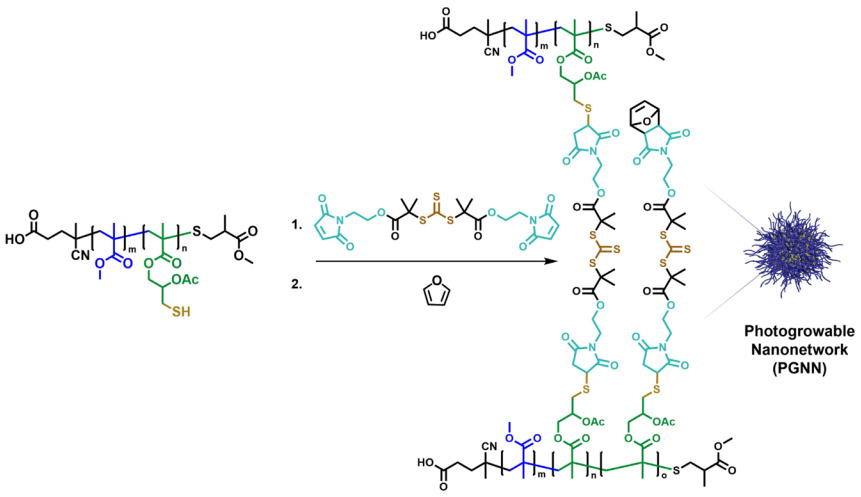

furan in a Diels-Alder reaction to prevent the maleimides from interfering in future polymerizations. Although only an intermolecular crosslinking is desired during our network formation, intramolecular crosslinking is unavoidable and will result in the formation of loops. While the number of loops present within a network and the behavior of loops during the photogrowth process is currently unknown, it may be an interesting subject for future studies.

Model Polymerizations

A series of model photoredox polymerizations were performed with PTH as a photocatalyst and a thiol capped crosslinker **1a** (**Scheme III-S1**) to obtain optimized conditions to produce homopolymers, copolymers, and block copolymers with the desired monomers. Model homopolymerizations revealed that a high level of control over dispersity ($Đ \leq 1.14$) can be obtained for each monomer with the exception of HEA ($Đ = 1.31$) and that polymerizations in acetonitrile (MeCN) progress slower than in dimethyl sulfoxide (DMSO) (**Figure III-S1**) as demonstrated by the polymerization of MA. Additionally, homopolymers of TFEA produce a negative refractive index (RI) response in GPC with dimethyl formamide (DMF) as the eluent which is expected when fluorinated polymers have a smaller refractive index than the eluent.[27] Model copolymerizations produced good control over dispersity ($Đ \leq 1.17$) for each copolymer pair (MA-tBA, MA-TFEA, MA-HEA) (**Figure III-S2**). As expected, the small incorporation of TFEA randomly in a copolymer with MA does not produce a negative RI response in GPC. Lastly, model polymerizations to produce ABA triblock and ABABA pentablock copolymers with MA (A) and another monomer (B) demonstrated excellent control over dispersity with tBA

and TFEA ($Đ \leq 1.14$), while block copolymers that incorporated HEA or NIPAAM displayed increased dispersity ($Đ \leq 1.33$) (**Figure III-S3**). Interestingly, PMA-**b**-PTFEA-*b*-PMA triblock copolymers display both a weak negative and a weak positive RI response as opposed to the expected negative response. GPC analysis of molecular weight and dispersity of this polymer were not reported due to the disruption of the baseline and the presence of these overlapping responses. Further chain extension with MA to produce the PMA-*b*-PTFEA-*b*-PMA-*b*-PTFEA-*b*-PMA pentablock yields only a positive response. This reversion to a single positive peak can be explained by the increase in refractive index provided by the new PMA block.

Homopolymer Incorporation

Next, optimized experimental conditions were applied to PGNNs to investigate the expansion of nanonetworks with various monomers (**Figure III-2, Table III-1**). Parent

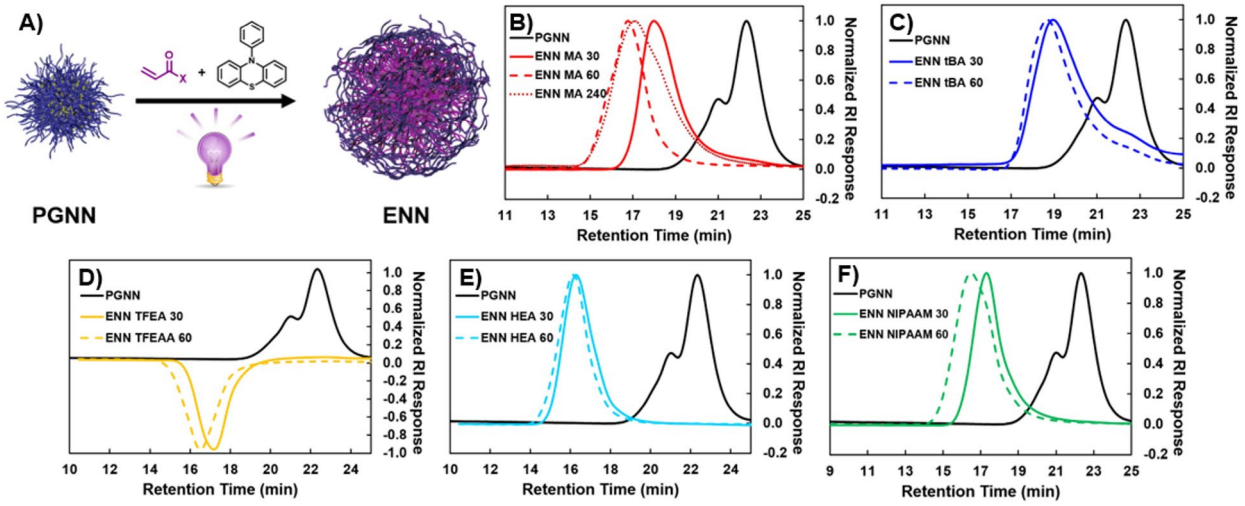

Figure III-2. (A) Schematic description of homopolymer expansions of nanonetworks. GPC traces of homopolymer expansions with (B) MA, (C) tBA, (D) TFEA, (E) HEA, and (F) NIPAAM at 30 and 60 minutes irradiation times.

Table III-1. Homopolymer expansions of PGNNs

#	sample	monomer	irradiation time (min)	PTH (mol%)	solvent	$M_{n\ GPC}$[a] (g/mol)	$Đ$[a]	$diameter_{TEM}$ (nm)	$diameter_{DLS}$ (nm)
1	**PGNN**	-	0	-	-	9,800	1.53	43 ± 10	66 ± 11
2	**ENN MA 30**	MA	30	0.02	DMSO	47,200	1.79	250 ± 60	290 ± 95
3	**ENN MA 60**	MA	60	0.02	DMSO	132,000	1.84	584 ± 146	612 ± 165
4	**ENN MA 240**	MA	240	0.10	MeCN	81,400	2.10	1022 ± 327	1354 ± 567
5	**ENN tBA 30**	tBA	30	0.10	MeCN	21,000	1.60	182 ± 56	231 ± 118
6	**ENN tBA 60**	tBA	60	0.10	MeCN	25,900	1.63	225 ± 70	263 ± 115
7	**ENN TFEA 30**	TFEA	30	0.02	MeCN	102,000	1.42	266 ± 47	300 ± 71
8	**ENN TFEA 60**	TFEA	60	0.02	MeCN	153,000	1.80	361 ± 85	395 ± 101
9	**ENN HEA 30**	HEA	30	0.02	DMSO	173,000	1.74	162 ± 78	193 ± 84
10	**ENN HEA 60**	HEA	60	0.02	DMSO	226,000	1.87	241 ± 90	283 ± 130
11	**ENN NIPAAM 30**	NIPAAM	30	0.005	MeCN	62,000	1.86	197 ± 75	250 ± 65
12	**ENN NIPAAM 60**	NIPAAM	60	0.005	MeCN	119,000	2.31	319 ± 95	372 ± 90

[a] Molecular weight and polydispersity were determined by GPC analysis with DMF as eluent at 1 ml/min at 60 °C.

nanonetworks were exposed to the desired monomer (1 M) and solvent and were then irradiated for 30, 60 or 240 minutes in the presence of PTH. Expansion reactions were then purified by dialysis. Given that the parent PGNN and all the produced daughter ENNs are soluble in organics, nanonetworks were analysed by GPC and NMR to confirm the successful incorporation of new monomer units. While GPC analysis of these nanonetworks does not yield true reflections of their molecular weights, it does offer easily accessible evidence that a change has occurred within the network that is a direct result of the incorporation of new monomer units. GPC analysis of all homopolymer ENNs revealed a shift towards higher molecular weight and an increase in dispersity ($Đ \leq 1.86$) when compared to the parent PGNN ($Đ = 1.53$) (**Figure III-2**). The average change in dispersity across all monomers, after 30 minutes of irradiation, ($\Delta Đ_{avg} \approx 0.22$) agrees with our previous findings for MA homopolymerizations ($\Delta Đ_{avg} \approx 0.18$)[26]. Irradiation with the photocatalyst produced an increase in the diameter of the parent PGNN in the case of each monomer, with longer irradiation times producing larger daughter ENNs as confirmed by

TEM and DLS measurements. Homopolymer expansion of PGNNs with tBA proceeded slower than other monomers investigated. This was attributed in part to the steric hinderance provided by the tert-butyl ester which may hinder the incorporation of additional monomers within the network structure (**Table III-1**). Expansions with TFEA produced ENNs that displayed a negative RI response on GPC as expected from the model polymerization. This negative response is indicative that the RI of the nanonetwork has changed as a result of the formation of new polymer chains and points toward the possibility of being able to produce nanonetworks with tuneable RIs. Samples irradiated for 60 min, showed an increased molecular weight, size, and in most cases slight increases in dispersities were observed. In order to probe the limits of the expansion process, an expansion with MA was performed for 240 min which resulted in ENNs with sizes around 1000 nm. Irradiation times longer than 240 min yielded no further increase in network diameter.

Aminolysis of Homopolymer ENNs

To gain a better understanding of the control over polymerizations within the nanonetworks, a promoted network disassembly was performed on each ENN. Promoted network disassembly proceeds through aminolysis of the crosslinker TTC with piperidine resulting in branched polymers (BPs) (**Figure III-3**). Exposure of the parent **PGNN** to piperidine resulted in **BP** with M_n = 7,600 g/mol and $Đ$ = 1.14. GPC analysis of the promoted disassembly of each homopolymer ENN after 30 minutes reveals an increase in molecular weight in comparison to **BP** for each monomer. Dispersity of these BPs remains relatively low ($Đ \leq 1.42$) in each case except for HEA which displayed a higher dispersity

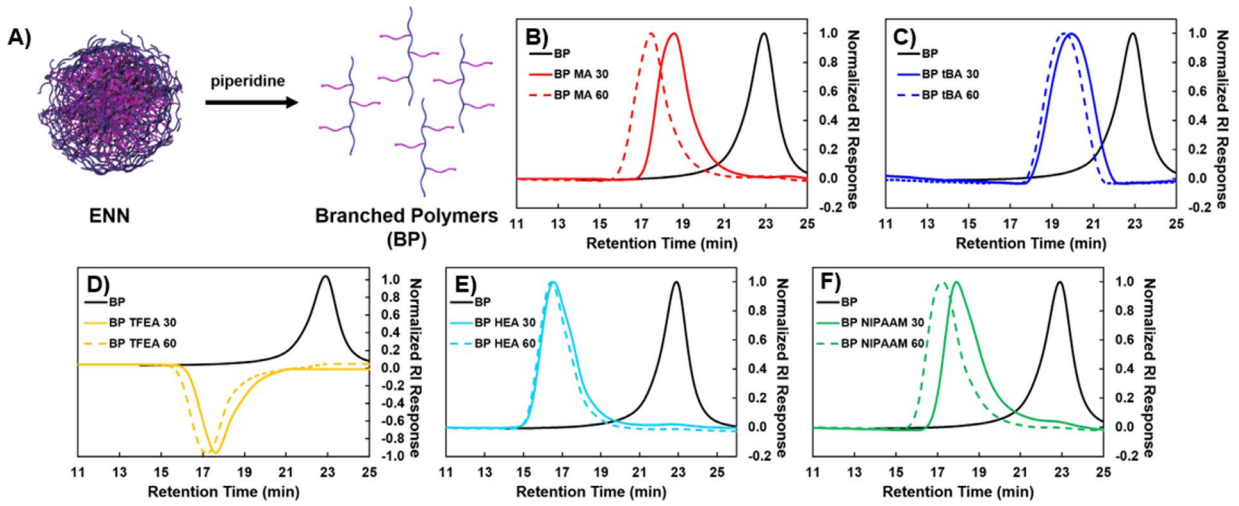

Figure III-3. (A) Schematic description of the selective cleavage of nanonetworks to produce branched polymers. GPC traces of the resulting branched polymers from homopolymer expansions of (B) MA, (C) tBA, (D) TFEA, (E) HEA, and (F) NIPAAM.

Table III-2. Aminolysis of homopolymer nanonetwork expansions

#	sample	$M_{n\ GPC}$[a] (g/mol)	$Đ$[a]
1	**BP**	7,600	1.14
2	**BP MA 30**	31,900	1.30
3	**BP MA 60**	112,000	1.38
4	**BP tBA 30**	19,000	1.22
5	**BP tBA 60**	23,300	1.21
6	**BP TFEA 30**	85,000	1.42
7	**BP TFEA 60**	136,500	1.37
8	**BP HEA 30**	168,000	1.60
9	**BP HEA 60**	209,000	1.55
10	**BP NIPAAM 30**	58,000	1.37
11	**BP NIPAAM 60**	106,000	1.55

[a] Molecular weight and polydispersity were determined by GPC analysis (DMF as eluent).

of 1.60. In all cases BPs produced after 60 minutes of irradiation show an increase in molecular weight when compared to those produced at 30 minutes. BPs produced from tBA, TFEA, and HEA after 60 minutes display a narrowing of dispersity from 30 minutes, while MA and NIPAAM display a slight increase at this extended reaction time (**Figure**

III-3, Table III-2). Although all BPs displayed a higher dispersity when compared to the parent BP, it should be noted that the difference in dispersity from 30 to 60 minutes is small ($\Delta Đ < 0.1$) in all cases except for NIPAAM, the dispersity decreases from 30 to 60 minutes in the majority of cases, and in all cases the dispersity remains relatively low ($Đ \leq 1.60$).

Thermoresponsive Behavior of PNIPAAM ENNs

Encouraged by the successful incorporation of these monomer families, we sought to explore the properties that can arise as a result from the altered chemical composition of these daughter nanonetworks. For example, we evidenced a change of the tailorable nanonetwork RI through the polymerization of TFEA, and we explored the effects that the introduction of HEA would have on nanonetwork solubility. Parent PGNNs are insoluble in water; however, by incorporating PHEA chains within the nanonetwork a fully water soluble ENN can be produced. Likewise, water soluble nanonetworks can be prepared through the incorporation of PNIPAAM chains within the nanonetwork.

Armed with the knowledge that PNIPAAM ENNs are water soluble we aimed to investigate if these daughter networks inherited the thermoresponsive behavior of PNIPAAM. It is well known that PNIPAAM has a lower critical solution temperature (LCST) at 32°C in water above which PNIPAAM expunges water and experiences a chain collapse resulting in a shrunken polymer.[28] We reasoned that if a daughter network expanded with PNIPAAM possessed these thermoresponsive properties then it could be feasible to induce a chain collapse that results in the shrinkage of PNIPAAM polymers and ultimately the ENN itself by merely heating the ENN above 32°C. To probe this, we designed an experiment in which PNIPAAM ENNs after 30 (**ENN NIPAAM 30**) and 60

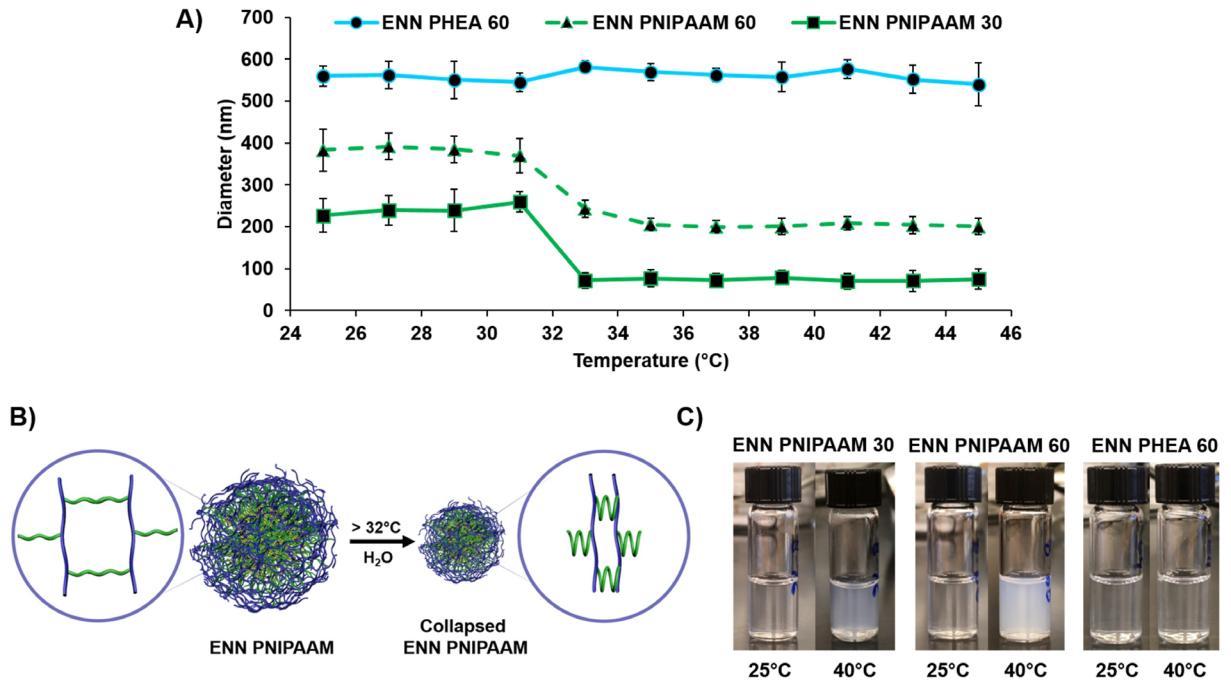

Figure III-4. (A) DLS diameter measurements of NIPAAM and HEA ENNs across 25-45°C. (B) Schematic description of PNIPAAM chain collapse above 32°C producing shrunken nanonetworks. (C) Images of solutions of NIPAAM and HEA ENNs at 25°C and 40°C.

(**ENN NIPAAM 60**) minute irradiation times were dissolved in water and the diameter measured by DLS every two degrees over a temperature range of 25°C - 45°C. The average size of each ENN was first determined in water at 25°C resulting in an average size of ~239 nm for **ENN NIPAAM 30** and ~383 nm for **ENN NIPAAM 60**. Upon heating above 32°C we observe a sharp decrease in diameter for **ENN NIPAAM 30** to ~70 nm and a more gradual decrease for **ENN NIPAAM 60** to ~200 nm (**Figure III-4**). Additional heating to 45°C provided no changes nanonetwork diameters. To ensure that the observed change in diameter was due to the formation of PNIPAAM chains and was independent of the properties of the parent nanonetwork, a control experiment was performed. Because, the parent PGNN is insoluble in water, but HEA ENNs are water soluble and should not possess thermoresponsive properties, the HEA ENNs (**ENN HEA 60**) were used as control

networks. The average size of **ENN HEA 60** was found to be ~560 nm, and heating through 32°C to 45°C produced no meaningful change in diameter. Thus, we can conclude that the change in diameter at 32°C is indeed caused by the incorporation of PNIPAAM. To further illustrate the thermoresponsive behavior of PNIPAAM ENNs, images displaying the nanonetworks fully dissolved in water at 25°C are compared to images of nanonetworks after being heated above the LCST (40°C) (**Figure III-4**). It is clear that HEA ENNs are unaffected by the change in temperature, while the NIPAAM ENNs display increased turbidity as a result of the increase in temperature, with the change in turbidity being more apparent with larger nanonetworks. The success of these experiments is encouraging as it demonstrates the potential to produce highly tailorable and stimuli responsive nanomaterials.

Incorporation of Statistical Copolymers

After having successfully demonstrated the addition of each monomer into the parent PGNN, we aimed to explore the introduction of polymer compositions in the form of statistical copolymers or block copolymers from these investigated monomer families. First, we examined the incorporation of copolymers from MA/tBA, MA/TFEA, and MA/HEA with MA being the major monomer component. MA was chosen as the major component in each composition due to its flexibility to be polymerized in either MeCN or DMSO and still provide good control over dispersity. Copolymer ENNs were prepared by first exposing the parent PGNN to a 1 M solution of MA and the desired comonomer in an 80/20 ratio respectively with the appropriate solvent. Nanonetworks were then irradiated in the presence of PTH for 30 minutes and then purified by dialysis. Analysis of the

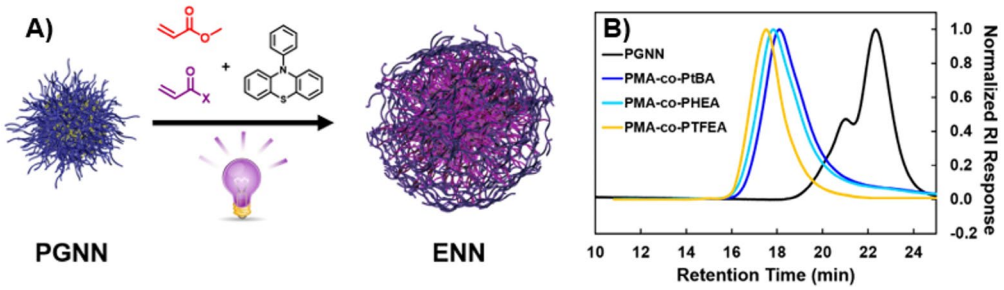

Figure III-5. (A) Schematic description and (B) GPC traces of statistical copolymer expansions of nanonetworks.

Table III-3. Statistical copolymer expansions of PGNNs

#	sample	monomers (MA/X)	irradiation time (min)	solvent	$M_{n\ GPC}$[a] (g/mol)	$Đ$[a]	monomer incorporation[b] (MA/X)	$diameter_{TEM}$ (nm)	$diameter_{DLS}$ (nm)
1	PGNN	-	0	-	9,800	1.53	-	43 ± 10	66 ± 11
2	PMA-*co*-PtBA	MA/tBA (80/20)	30	MeCN	26,000	1.58	67/33	220 ± 112	283 ± 130
3	PMA-*co*-PHEA	MA/HEA (80/20)	30	DMSO	63,700	1.58	69/31	381 ± 103	420 ± 135
4	PMA-*co*-PTFEA	MA/TFEA (80/20)	30	DMSO	87,000	1.59	74/26	302 ± 100	332 ±140

Reactions were performed with 0.02 mol % PTH. [a] Molecular weight and polydispersity were determined by GPC analysis (DMF as eluent). [b] Monomer incorporation was determined by ^{1}H NMR.

produced copolymer ENN by GPC reveals a shift toward higher molecular weight and a slight increase in dispersity in each case (**Figure III-5**). Interestingly, the dispersity observed for copolymers ENNs with MA ($Đ \leq 1.59$) is less than the dispersity observed for homopolymer ENNs of MA ($Đ = 1.79$). Analysis by TEM and DLS showed an increase in the diameter from the parent PGNN with sizes similar to those produced from MA homopolymer ENNs (**Table III-3**). NMR analysis displayed incorporations of tBA and HEA to be elevated compared to those observed in the model copolymerizations, while incorporations of TFEA closely matched those of the model (**Table III-S2**). These successful copolymerizations demonstrate the potential to incorporate controllable quantities of a desired functional group which can facilitate further chemical modifications.

Incorporation of ABA tri- and ABABA Pentablock Copolymers

Next, we examined the possibility of producing ABA triblock and ABABA pentablock copolymers as the incorporation of block copolymer structures into these nanonetworks could produce particles that exhibit microphase separation behavior providing an interesting opportunity to examine the effects this would have on a pre-existing nanonetwork. Given ENNs still have the integrated TTCs after expansion, ENNs can be used as macroinitiators to produce further expanded nanonetworks rendering them capable of producing block copolymers. For the production of ABA and ABABA block copolymers MA was chosen as the "A" block for both its solvent and monomer compatibility and the desired monomer as the "B" block. Pentablock ENNs were prepared by first preparing a MA homopolymer ENN (**ENN 1**) as previously described. **ENN 1** was then used to prepare ABA triblock copolymers with each monomer (tBA, TFEA, HEA, NIIPAAM) by exposing **ENN 1** to the appropriate conditions determined in the model block copolymerizations. Further expansion from **ENN 1** with each monomer results in four ABA triblock copolymers: PMA-*b*-PtBA-*b*-PMA (**ENN 2**), PMA-*b*-PHEA-*b*-PMA (**ENN3**), PMA-*b*-PNIPAAM-*b*-PMA (**ENN 4**), and PMA-*b*-PTFEA-*b*-PMA (**ENN 5**). Utilizing the triblock ENNs as macroinitiators, ABABA pentablock ENNs can be prepared by performing chain extensions with MA. Chain extensions from each tri block results in four pentablock copolymer ENNs: PMA-*b*-PtBA-*b*-PMA-*b*-PtBA-*b*-PMA (**ENN 6**), PMA-*b*-PHEA-*b*-PMA-*b*-PHEA-*b*-PMA (**ENN 7**), PMA-*b*-PNIPAAM-*b*-PMA-*b*-PNIPAAM-*b*-PMA (**ENN 8**), and PMA-*b*-PTFEA-*b*-PMA-*b*-PTFEA-*b*-PMA (**ENN 9**).

Analysis of **ENN 1** reveals the expected increase in diameter, molecular weight, and dispersity that was observed in the previous homopolymerizations. GPC analysis of ABA

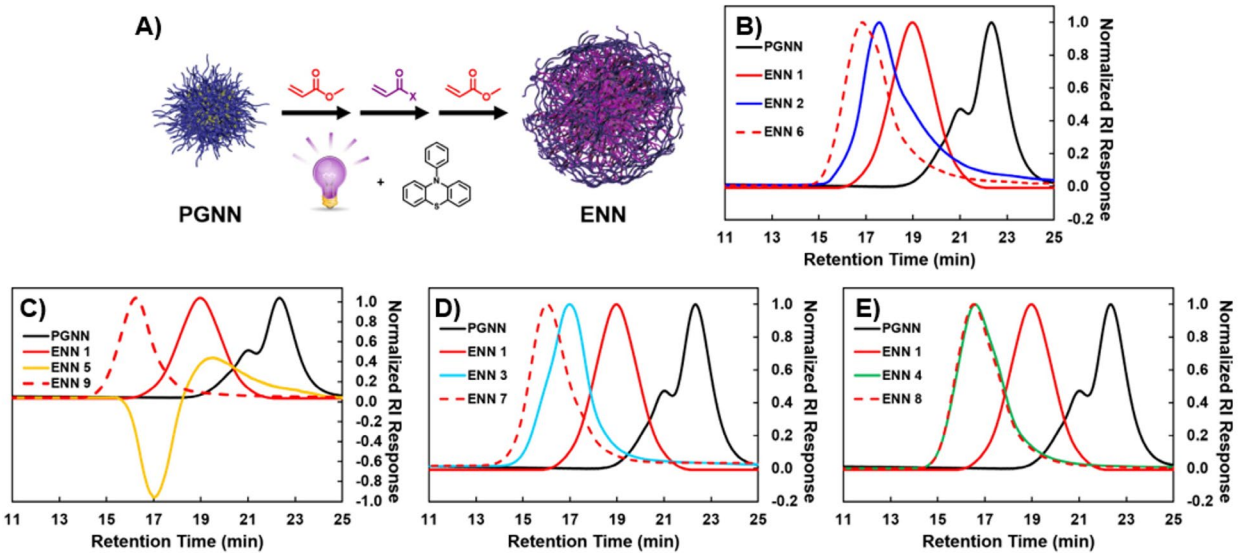

Figure III-6. (A) Schematic description of ABA block copolymer expansion of nanonetworks. GPC traces of block copolymer expansions with (B) tBA, (C) HEA, (D) TFEA, and (E) NIPAAM.

triblocks displays a shift towards higher molecular weight and increased dispersity (**Figure III-6**). Both HEA and NIPAAM triblocks experience slight increases in dispersity ($Đ$ = 1.81) compared to **ENN 1** ($Đ$ = 1.72) (**Table III-4**). **ENN 5** produces the same weak negative and weak positive RI response in GPC that were observed in the model block copolymerizations with TFEA and so molecular weight and dispersity were not reported for this nanonetwork. **ENN 2**, prepared from tBA, experiences a more pronounced increase in dispersity ($Đ$ = 2.38) than the other ENNs when compared to **ENN 1** ($Đ$ = 1.72). Closer examination of the GPC trace reveals low molecular weight tailing which is attributed to only partial polymerization participation of **ENN 1** with tBA. Size characterization by TEM and DLS showed an increase in diameter with each triblock ENN when compared to **ENN 1**. Characterization of triblocks by ^{1}H NMR confirmed the successful production of new polymer chains through the appearance of peaks unique to the desired monomers such

Table III-4. Block copolymer expansions of PGNNs

#	sample	macro-initiator (MI)	MI $M_{n,GPC}$[a] (g/mol)	MI $Đ$[a]	monomer	$M_{n\,GPC}$[a] (g/mol)	$Đ$[a]	diameter$_{TEM}$ (nm)	diameter$_{D}$ (nm)
1	**PGNN**	-	9,800	1.53	-	9,800	1.53	43 ± 10	66 ± 11
2	**ENN 1** (PMA)	PGNN	9,800	1.53	MA	30,000	1.72	273 ± 60	302 ± 98
3[b,c]	**ENN 2** (PMA-*b*-PtBA-*b*-PMA)	ENN 1	30,000	1.72	tBA	50,500	2.38	325 ± 131	355 ± 15
4	**ENN 3** (PMA-*b*-PHEA-*b*-PMA)	ENN 1	30,000	1.72	HEA	118,000	1.81	347 ± 86	387 ± 92
5[b,d]	**ENN 4** (PMA-*b*-PNIPAAM-*b*-PMA)	ENN 1	30,000	1.72	NIPAAM	149,000	1.81	375 ± 77	413 ± 97
6[b]	**ENN 5** (PMA-*b*-PTFEA-*b*-PMA)	ENN 1	30,000	1.72	TFEA	-	-	482 ± 55	518 ± 98
7[b,c]	**ENN 6** (PMA-*b*-PtBA-*b*-PMA-*b*-PtBA-*b*-PMA)	ENN 2	50,500	2.38	MA	119,000	1.98	420 ± 103	482 ± 14
8	**ENN 7** (PMA-*b*-PHEA-*b*-PMA-*b*-PHEA-*b*-PMA)	ENN 3	118,000	1.81	MA	289,000	1.96	452 ± 122	493 ± 14
9	**ENN 8** (PMA-*b*-PNIPAAM-*b*-PMA-*b*-PNIPAAM-*b*-PMA)	ENN 4	149,000	1.81	MA	175,000	1.87	402 ± 115	438 ± 16
10	**ENN 9** (PMA-*b*-PTFEA-*b*-PMA-*b*-PTFEA-*b*-PMA)	ENN 5	-	-	MA	272,000	1.74	613 ± 151	651 ± 18

Reactions were performed in DMSO with 0.02 mol % PTH unless otherwise indicated. [a] Molecular weight and polydispersity were determined by GPC analysis (DMF as eluent). [b] Reactions were performed in MeCN. [c] Reactions were performed with 0.1 mol % PTH. [d] Reactions were performed with 0.005 mol % PTH.

as the tert-butyl, isopropyl, fluorinated ester, and hydroxy ethyl ester moieties (**Figure III-S18-S21**).

As expected, GPC analysis of ABABA pentablock ENNs shows a shift towards higher molecular weight and in the case of HEA and NIPAAM a slight increase in dispersity. Interestingly, **ENN 6**, experienced a narrowing of dispersity to $Đ$ = 1.98 from its macroinitiator's, **ENN 2**, dispersity of 2.38. Accompanying this narrowing was a reduction in the lower molecular weight tailing that was previously observed. This suggests that the nanonetworks that comprised the tailing were still capable of mediating radical polymerizations and thus capable of experiencing the photocontrolled growth process. As demonstrated in the model block copolymerizations, **ENN 9** experiences a reversion to a

positive RI response in GPC from **ENN 5** as a result of the new PMA block. Remarkably, the dispersity of all pentablock ENNs remained lower than 2.0, which is a strong indication of the fidelity and control of the photoredox mediated polymerizations. Further characterization of pentablock ENNs by ^{1}H NMR confirms the installation of a new PMA block within the nanonetwork as we can observe a clear increase in the intensity of the methyl ester peak in each pentablock ENN.

Aminolysis of ABA tri- and ABABA Pentablock ENNs

Once again, we implemented a promoted disassembly to gain a clearer understanding of the control obtained during the expansion process of ABA and ABABA block copolymer ENNs (**Figure III-7**). Aminolysis products of the PMA ENN macroinitiator (**BP 1**) displayed an increase of 20,000 g/mol and $Đ$ = 1.24 compared to the parent PGNN (**BP**) with M_n = 7,600 g/mol and $Đ$ = 1.14 (**Table III-5**). Disassembly

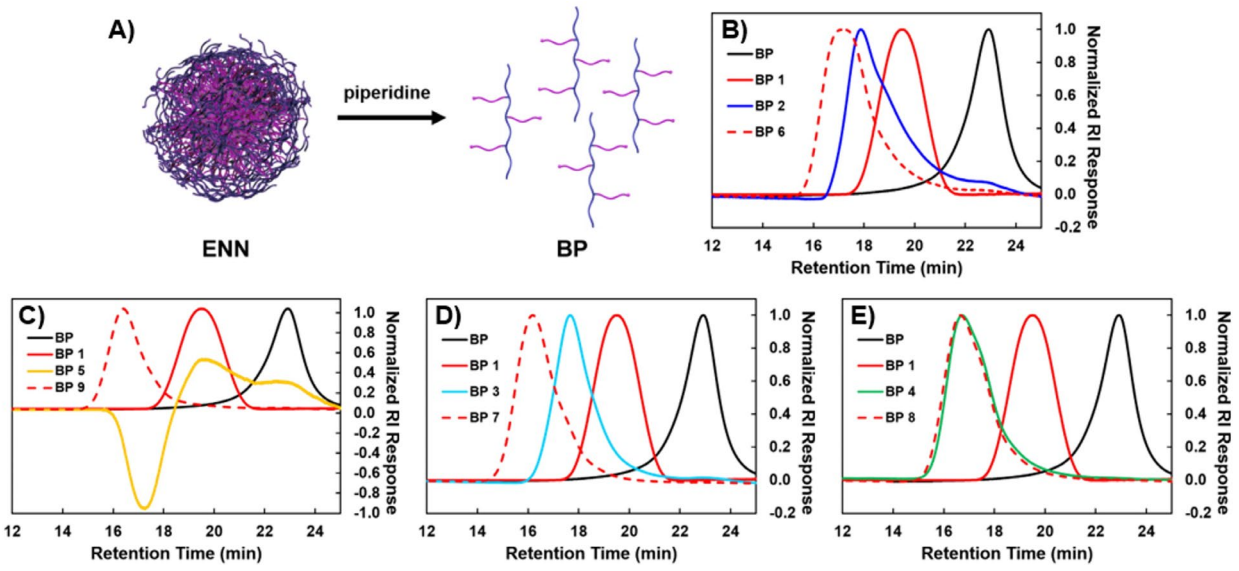

Figure III-7. (A) Schematic description of the selective cleavage of nanonetworks to produce branched polymers. GPC traces of the resulting block copolymer expansions with (B) tBA, (C) HEA, (D) NIPAAM, and (E) TFEA.

Table III-5. Aminolysis of block copolymer nanonetwork expansions

#	sample[a]	$M_{n\ GPC}$[b] (g/mol)	$Đ$[b]
1	**BP**	7,600	1.14
2	**BP 1** (PMA)	27,000	1.24
3	**BP 2** (PMA-*b*-PtBA)	56,000	1.48
4	**BP 3** (PMA-*b*-PHEA)	100,000	1.67
5	**BP 4** (PMA-*b*-PNIPAAM)	132,000	1.69
6	**BP 5** (PMA-*b*-PTFEA)	-	-
7	**BP 6** (PMA-*b*-PtBA-*b*-PMA)	103,000	1.69
8	**BP 7** (PMA-*b*-PHEA-*b*-PMA)	231,000	1.79
9	**BP 8** (PMA-*b*-PNIPAAM-*b*-PMA)	139,000	1.79
10	**BP 9** (PMA-*b*-PTFEA-*b*-PMA)	265,000	1.34

[a] Branched block copolymers as they appear once cleaved from either the tri- or pentablock copolymer ENNs. [b] Molecular weight and polydispersity were determined by GPC analysis (DMF as eluent).

products of the triblock ENNs exhibited increases in molecular weight as well as increases in dispersity with $Đ < 1.70$. Aminolysis of the PMA-*b*-PTFEA-*b*-PMA triblock produces a PMA-*b*-PTFEA diblock copolymer which exhibits a similar positive and negative RI response in GPC therefore analysis of molecular weight and dispersity were not reported. Promoted disassembly of ABABA pentablock ENNs once again revealed an increase in both molecular weight and dispersity for blocks with tBA, NIPAAM, and HEA with $Đ < 1.8$. Interestingly, **BP 9** of the pentablock ENN containing TFEA possessed a relatively low dispersity of $Đ = 1.34$.

CONCLUSION

A developed photoexpansion process opens the possibility to significantly alter the chemical topology of a unique nanonetwork by integrating linear polymer chains with various compositions (homopolymers, statistical copolymers, block copolymer) from a

range of monomer families. Through this photoexpansion process a single parent nanonetwork can produce multiple differentiated progeny that inherit properties of the newly incorporated polymers which allows for the manipulation of RI, the transformation of water-insoluble parent particles into water soluble structures, and the transformation of thermally unresponsive parent networks into thermally responsive daughter networks. Furthermore, the integration of ABA and ABABA block copolymers, with their known microphase separation behavior, can prove beneficial to produce model systems to examine effects of introducing block copolymer architectures into an existing nanonetwork on network topology and organization. The ability to control and integrate a variety of linear homopolymers, statistical copolymers, or block copolymers into parent nanonetworks will allow for targeted manipulations of the chemical structure and physical properties to facilitate investigations of network topologies.

EXPERIMENTAL

Materials:

All reagents and solvents were purchased from Sigma Aldrich and used as received unless otherwise stated. Methyl acrylate (MA, 99%), t-butyl acrylate (tBA, 98%), 2,2,2-trifluoroethyl acrylate (TFEA, 99%) were purified immediately before use by passing through a short column of inhibitor removers purchased from Sigma Aldrich. N-isopropylacrylamide (NIPAAM, 97%) was recrystallized from hexanes. 2-Hydroxyethyl acrylate (HEA, 96%) was purified by first dissolving the monomer in water (25% by volume). The solution was extracted with hexanes six times to remove diacrylate and with ether six times to remove acrylic acid. $MgSO_4$ drying agent was used

to remove traces of water in the ether phase before evaporation. The monomer was then passed through short column of inhibitor removers immediately before use. The monomer was then dried under high vacuum for 20 minutes before use. 10-phenylphenothiazine (PTH)[29] was prepared according to literature. TTC **1a** and PGNNs were synthesized as previously reported.[26] All photogrowth polymerizations were performed in a circular glass dish lined with a 400 nm LED strip (390 nm - 405 nm, 24W/5m) and cooled by compressed air (showed below).

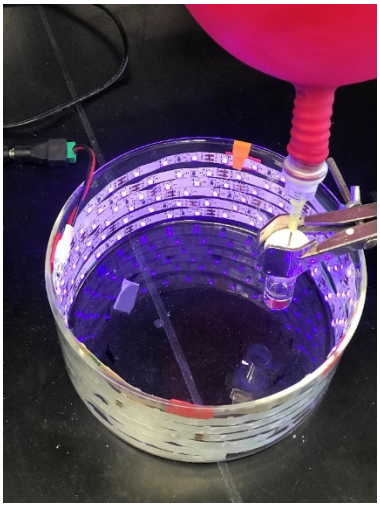

Material Characterization:

All ^{1}H and ^{13}C spectra were obtained using a JEOL ECA 400 (400 MHz), JEOL ECA 500 (500 MHz), or ECA-600 (600 MHz) spectrometer. Chemical shifts were measured relative to residual solvent peaks as an internal standard. TEM imaging was performed using either a JEOL 2000 FX or JEOL 2010 F Transmission Electron Microscope at 200 kV with formvar coated or holey carbon coated copper grids. Gel permeation chromatography (GPC) was performed using a Tosoh high performance GPC system HLC-8320 equipped with an auto injector, a dual differential refractive index detector and TSKgel G series columns connected in series (7.8×300 mm TSKgel G5000Hxl, TSKgel G4000Hxl, TSKgel G3000Hxl). GPC analysis was carried out in HPLC grade

tetrahydrofuran (THF) with a flow rate of 1.0 mL/min at 40 °C or N,N-dimethylformamide (DMF) with a flow rate of 1.0 mL/min at 60 °C. Molecular weights (Mn and Mw) and molecular weight distributions were calculated from polymethyl methacrylate (PMMA) standards with molecular weights of 800 to 2.2×106 g mol-1 provided by Polymer Standard Service (PSS). Dynamic light scattering (DLS) was measured on a Malvern Zetasizer Nano ZS in THF, methanol, or water at 25°C with an angle of 173° and at appropriate sample concentrations.

Acknowledgement: All experiments were conducted alongside coauthor Enkhjargal Tsogtgerel.

Synthesis:

All model polymerizations conducted used TTC:monomer ratio of 1:500. Model Polymerizations. TTC **1a** (4.0 mg, 0.0059 mmol) was dissolved in 2M monomer solution in DMSO or MECN with PTH (0.02-0.1 mol%) in a 1-dram vial. The reaction vessel was sealed and sparged with nitrogen for 20 minutes. The reaction was then placed 2 cm from a 400 nm led light source and irradiated for 30 minutes. The polymers were precipitated in cold diethyl ether, unless otherwise stated, and then analyzed by GPC.

Scheme III-S1. Model polymerization of various monomers.

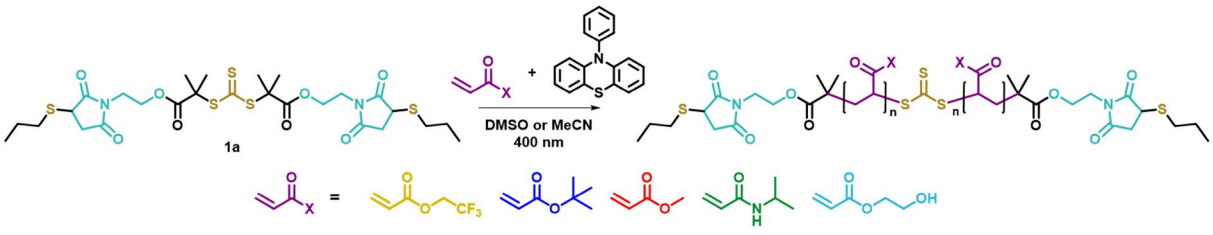

Polymerization of ABA and ABCBA block copolymers were conducted following the same procedure with macroinitiator and PTH (0.02-0.1 mol%) in 1M monomer solution in DMSO or

MECN. (NOTE: MeCN was chosen as the solvent for tBA and NIPAAM, as PtBA is insoluble in DMSO and polymerizations of NIPAAM in DMSO yielded increased dispersities. TFEA can be polymerized in either DMSO or MeCN but produced lower dispersities in MeCN. PHEA has poor solubility in MeCN and was polymerized in DMSO. Solvents for the statistical copolymerizations were chosen to accommodate monomers with poor solubility. Copolymers of MA/tBA were performed in MeCN due to PtBA's poor solubility in DMSO. Copolymers of MA/HEA were performed in DMSO due to PHEA's poor solubility in MeCN. Copolymers of MA/TFEA were performed in DMSO as TFEA can be polymerized in both solvents and MA displayed lower dispersity when polymerized in DMSO. Solvents for the preparation of block copolymers were again chosen based off the solubilities of the previous block and the block that is to be added, or in the case of TFEA solvent was chosen based off conditions that produced the lowest dispersity.)

Procedure for results documented in Table S1.

Synthesis of PMA: TTC **1a** (4.0 mg, 0.0059 mmol) was dissolved in DMSO or MECN (1.47 mL) and MA (264 μL, 2.94 mmol) with PTH (0.02 mol%). The reaction vessel was sealed and sparged with nitrogen for 20 minutes (MECN solution in an ice bath). The reaction was then placed 2 cm from a 400 nm led light source and irradiated for 30 minutes.

Synthesis of PtBA: TTC **1a** (4.0 mg, 0.0059 mmol) was dissolved in MECN (1.47 mL) and MA (430 μL, 2.94 mmol) with PTH (0.1 mol%). The reaction vessel was sealed and sparged with nitrogen for 20 minutes in an ice bath. The reaction was then placed 2 cm from a 400 nm led light source and irradiated for 30 minutes. The polymer was precipitated in cold hexanes.

Synthesis of PNIPAAM: TTC **1a** (4.0 mg, 0.0059 mmol) was dissolved in MECN (1.47 mL) and MA (332 mg, 2.94 mmol) with PTH (0.05 mol%). The reaction vessel was sealed and sparged with nitrogen for 20 minutes (MECN solution in an ice bath). The reaction was then placed 2 cm from a 400 nm led light source and irradiated for 30 minutes.

Synthesis of PHEA: TTC **1a** (4.0 mg, 0.0059 mmol) was dissolved in DMSO (1.47 mL) and HEA (337 µL, 2.94 mmol) with PTH (0.02 mol%). The reaction vessel was sealed and sparged with nitrogen for 20 minutes. The reaction was then placed 2 cm from a 400 nm led light source and irradiated for 30 minutes.

Synthesis of PTFEA: TTC **1a** (4.0 mg, 0.0059 mmol) was dissolved in DMSO or MECN (1.47 mL) and TFEA (372 µL, 2.94 mmol) with PTH (0.02 mol%). The reaction vessel was sealed and sparged with nitrogen for 20 minutes (MECN solution in an ice bath). The reaction was then placed 2 cm from a 400 nm led light source and irradiated for 30 minutes. The polymer was precipitated in cold 1:1 mixture of hexanes : diethyl ether.

Procedure for results documented in Table S2.

Synthesis of PMA-*co*-PtBA(80/20): TTC **1a** (4.0 mg, 0.0059 mmol) was dissolved in MECN (1.47 mL) and MA (211 µL, 2.35 mmol) and tBA (86 µL, 0.59 mmol) with PTH (0.1 mol%). The reaction vessel was sealed and sparged with nitrogen for 20 minutes in an ice bath. The reaction was then placed 2 cm from a 400 nm led light source and irradiated for 30 minutes.

Synthesis of PMA-*co*-PHEA(80/20): TTC **1a** (4.0 mg, 0.0059 mmol) was dissolved in DMSO (1.47 mL) and MA (211 µL, 2.35 mmol) and HEA (67 µL, 0.59 mmol) with PTH (0.02 mol%). The reaction vessel was sealed and sparged with nitrogen for 20 minutes (MECN solution in an ice bath). The reaction was then placed 2 cm from a 400 nm led light source and irradiated for 30 minutes.

Synthesis of PMA-*co*-PTFEA (80/20): TTC **1a** (4.0 mg, 0.0059 mmol) was dissolved in DMSO (1.47 mL) and MA (211 µL, 2.35 mmol) and TFEA (74 µL, 0.59 mmol) with PTH (0.02 – 0.1 mol%). The reaction vessel was sealed and sparged with nitrogen for 20 minutes. The reaction was then placed 2 cm from a 400 nm led light source and irradiated for 30 minutes.

Procedure for results documented in Table S3.

Synthesis of PMA macroinitiator: TTC **1a** (36.0 mg, 0.0531 mmol) was dissolved in MECN (13.23 mL) and MA (2.38 mL, 26.46 mmol) with PTH (0.1 mol%). The reaction vessel was sealed and sparged with nitrogen for 30 minutes in an ice bath. The reaction was then placed 2 cm from a 400 nm led light source and irradiated for 30 minutes.

Synthesis of PMA-*b*-PtBA-*b*-PMA: PMA macroinitiator (40.0 mg, 0.0036 mmol) was dissolved in MECN (1.80 mL) and tBA (263 µL, 1.80 mmol) with PTH (0.02 mol%). The reaction vessel was sealed and sparged with nitrogen for 20 minutes in an ice bath. The reaction was then placed 2 cm from a 400 nm led light source and irradiated for 30 minutes.

Synthesis of PMA-*b*-PHEA-*b*-PMA: PMA macroinitiator (40.0 mg, 0.0036 mmol) was dissolved in DMSO (1.80 mL) and HEA (206 µL, 1.80 mmol) with PTH (0.02 mol%). The reaction vessel was sealed and sparged with nitrogen for 20 minutes. The reaction was then placed 2 cm from a 400 nm led light source and irradiated for 30 minutes.

Synthesis of PMA-*b*-PTFEA-*b*-PMA: PMA macroinitiator (20.0 mg, 0.0027 mmol) was dissolved in MECN (1.35 mL) and TFEA (171 µL, 1.35 mmol) with PTH (0.02 mol%). The reaction vessel was sealed and sparged with nitrogen for 20 minutes in an ice bath. The reaction was then placed 2 cm from a 400 nm led light source and irradiated for 30 minutes.

Synthesis of PMA-*b*-PNIPAAM-*b*-PMA: PMA macroinitiator (20.0 mg, 0.0023 mmol) was dissolved in MECN (1.58 mL) and NIPAAM (130 mg, 1.15 mmol) with PTH (0.005 mol%). The reaction vessel was sealed and sparged with nitrogen for 20 minutes in an ice bath. The reaction was then placed 2 cm from a 400 nm led light source and irradiated for 30 minutes.

Synthesis of PMA-*b*-PtBA-*b*-PMA-*b*-PtBA-*b*-PMA: PMA-*b*-PtBA-*b*-PMA macroinitiator (40.0 mg, 0.0021 mmol) was dissolved in MECN (1.04 mL) with PTH (0.1 mol%). The reaction vessel was sealed and sparged with nitrogen for 20 minutes in an ice bath. Degassed monomer MA (93 µL, 1.04 mmol) was added to the vessel. The reaction was then placed 2 cm from a 400 nm led light source and irradiated for 30 minutes.

Synthesis of PMA-*b*-PHEA-*b*-PMA-*b*-PHEA-*b*-PMA: PMA-*b*-PHEA-*b*-PMA macroinitiator (80.0 mg, 0.0013 mmol) was dissolved in DMSO (0.64 mL) with PTH (0.02 mol%). The reaction vessel was sealed and sparged with nitrogen for 20 minutes. Degassed monomer MA (58 μL, 0.64 mmol) was added to the vessel. The reaction was then placed 2 cm from a 400 nm led light source and irradiated for 30 minutes.

Synthesis of PMA-*b*-PTFEA-*b*-PMA-*b*-PTFEA-*b*-PMA: PMA-*b*-PHEA-*b*-PMA macroinitiator (21.0 mg, 0.0019 mmol) was dissolved in DMSO (0.94 mL) with PTH (0.02 mol%). The reaction vessel was sealed and sparged with nitrogen for 20 minutes. Degassed monomer MA (84 μL, 0.94 mmol) was added to the vessel. The reaction was then placed 2 cm from a 400 nm led light source and irradiated for 30 minutes.

Synthesis of PMA-*b*-PNIPAAM-*b*-PMA-*b*-PNIPAAM-*b*-PMA: PMA-*b*-PNIPAAM-*b*-PMA macroinitiator (40.0 mg, 0.0021 mmol) was dissolved in MECN (1.04 mL) with PTH (0.1 mol%). The reaction vessel was sealed and sparged with nitrogen for 20 minutes in an ice bath. Degassed monomer MA (93 μL, 1.04 mmol) was added to the vessel. The reaction was then placed 2 cm from a 400 nm led light source and irradiated for 30 minutes.

General Procedure for the Photogrowable Nanonetworks (PGNNs)

General procedure for the preparation of PMMA-co-GMA (2)

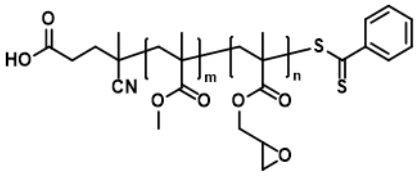

Reactions were prepared using the ratio (MMA/GMA/CPADB/EY/Et_3N) (80/20/1/0.02/1) in a 1:1 monomer:DMSO ratio. Reactions were irradiated with a 3.5 W blue light for the desired amount of time and then precipitated twice in diethyl ether. (Mn=6.20 kDa, PDI=1.09, MMA=81%, GMA=19%)

General aminolysis procedure of PMMA-co-GMA (3)

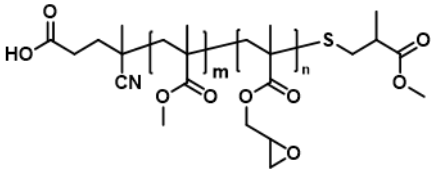

To a sealed 6 dram vial **2** (1.5 g) was added and covered with a nitrogen atmosphere, and then dissolved in degassed THF (15 mL). MMA (500 µL) and piperidine (250 µL) were added under nitrogen. After 6 hours the reaction was precipitated into diethyl ether. The product was dissolved in THF (10 mL) and treated with DTT for 3 hours under nitrogen. MMA (500 µL) and triethylamine (50 µL) were added to the solution and the reaction stirred for 3 hours under nitrogen. The reaction was precipitated into diethyl ether twice and dried under vacuum to give 1.44 g of a colorless product.

General thiolation procedure of aminolyzed PMMA-co-GMA (4)

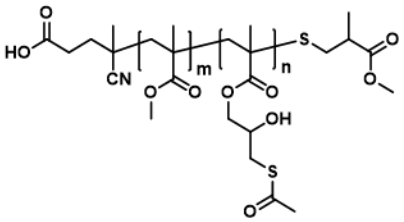

Thioacetic acid (207 µL, 2.9 mmol) and *i*-Pr_2NEt (84 µL, 0.48 mmol) were added to a solution of **3** (1.44 g, 2.42 mmol epoxide) in $CDCl_3$ (5 mL). The reaction stirred for 18 hours. The product was then precipitated twice in diethyl ether and dried under vacuum to give 1.39 g of the protected thiolated product.

General acetyl migration procedure of thiolated PMMA-co-GMA (5)

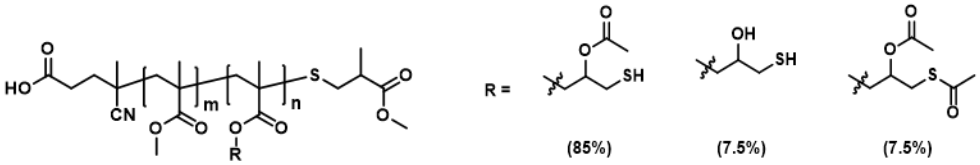

Triethylamine (10 mL) was added dropwise to a vigorously stirring solution of **4** (1.39 g) in $CHCl_3$ (50 mL) under nitrogen. After 18 hours the reaction was concentrated and precipitated twice in diethyl ether to give 1.35 g of the deprotected product.

General procedure for thiol-maleimide nano-network formation

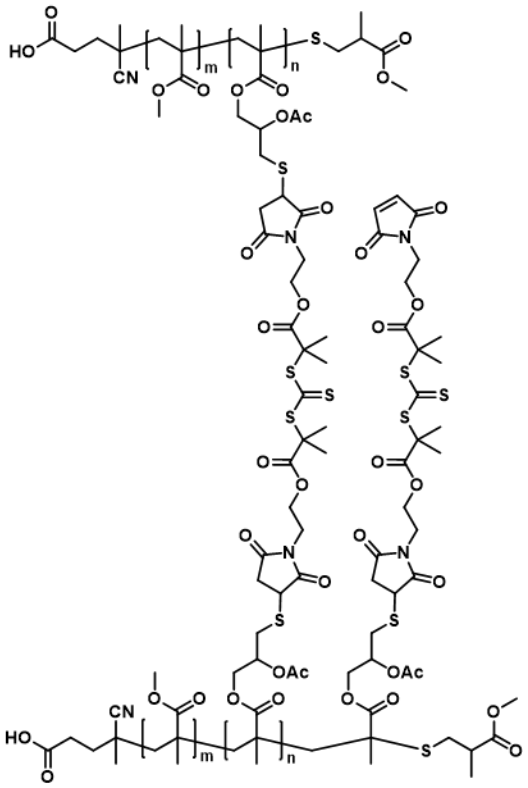

A solution of **5** in THF and stirred with DTT for 3 hours to reduce any disulfide bonds. The polymer was purified with Sephadex LH-20. The polymer (250 mg) was dried and then dissolved in $CHCl_3$ (50 mL) under a nitrogen atmosphere. Maleimide crosslinker **1** (327 mg, 2 equivalents to thiols) and Et_3N (73 uL, 0.2 equivalents to thiols) in $CHCl_3$ (12 mL) were added dropwise to the vigorously stirring solution of **5** under nitrogen. After 18 hours the reaction was diluted with CH_2Cl_2 and dialyzed for two days in 10 kDa MWCO snakeskin tubing against a 1:1 mixture of ACN:THF.

General Procedure for the Photogrowth of the PNN's

Nano-networks (4 mg) were sealed in a vial, covered with a nitrogen atmosphere, and dissolved in a solution of degassed monomer (MA, tBA, HEA, TFEA, NIPAAM) (3 mmol) in the appropriate solvent (MeCN or DMSO) (3 mL) with PTH (0.005 to 0.1 mol%). The reaction was then placed 2 cm from a 400 nm light source and irradiated for the desired amount of time. The crude product was diluted with CH_2Cl_2 or methanol and dialyzed in 10 kDa MWCO snakeskin tubing against a 1:1:1 mixture of CH_2Cl_2:MeCN:THF or a 1:1 mixture of methanol:MeCN for 2 days.

General procedure for controlled photo-growth of block copolymer nano-networks

PMA ENN macroinitiator (24 mg) was sealed in a vial and dissolved in a solution of degassed monomer (tBA, HEA, TFEA, NIPAAM) (3 mmol) in the appropriate solvent (MeCN or DMSO) (3 mL) with PTH (0.005 to 0.1 mol%). The reaction was then placed 2 cm from a 400 nm light source and irradiated for 30 minutes. The crude product was diluted with CH_2Cl_2 or methanol and dialyzed in 10 kDa MWCO snakeskin tubing against a 1:1:1 mixture of CH_2Cl_2:MeCN:THF or a 1:1 mixture of methanol:MeCN for 2 days.

PMA-*b*-X-*b*-PMA triblock ENN macroinitiator (50% of the total mg produced) was sealed in a vial and dissolved in a solution of degassed monomer (MA) (1.5 mmol) in the appropriate solvent (MeCN or DMSO) (1.5 mL) with PTH (0.005 to 0.1 mol%). The reaction was then placed 2 cm from a 400 nm light source and irradiated for 30 minutes. The crude product was diluted with CH_2Cl_2 or methanol and dialyzed in 10 kDa MWCO snakeskin tubing against a 1:1:1 mixture of CH_2Cl_2:MeCN:THF or a 1:1 mixture of methanol:MeCN for 2 days.

Procedure for the controlled photogrowth of nanonetworks into microparticles

Nanonetworks (4 mg) were sealed in a vial, covered with a nitrogen atmosphere, and dissolved in a solution of degassed MA (1.2 mL) in MeCN (13 mL) with PTH (0.1 mol%). The reaction was then placed 2 cm from a 400 nm light source and irradiated for the desired amount of time. The crude product was diluted with CH_2Cl_2 and dialyzed in 10 kDa MWCO snakeskin tubing against a 1:1 mixture of MeCN:THF for 2 days.

General procedure for the aminolysis of expanded nanonetworks

Piperidine (10 uL) was added to a solution of expanded nanonetworks (10 mg) in DMF (0.5 mL). The reaction was stirred for 18 hours and then treated with DTT for 3 hours before dialysis in 10 kDa MWCO snakeskin tubing against 1:1 MECN:THF for 24 hours. The purified product was concentrated, dissolved in HPLC grade DMF, filtered and analyzed by GPC.

General procedure for NIPAAM ENN thermoresponse graph

NIPAAM and HEA ENN solutions were prepared in appropriate concentrations in water. Diameter measurements were taken in triplicate every 2°C while heating from 25°C to 45°C. Samples were equilibrated to the new temperature for 5 minutes in between measurements.

GPC Analysis of Optimized Model Polymerizations

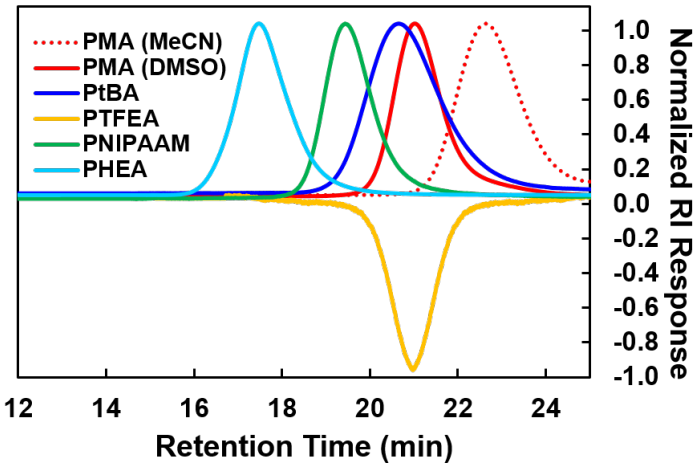

Figure III-S1. GPC traces of model homopolymerizations.

Table III-S1. Model homopolymerizations with TTC 1a

#	monomer	PTH (mol %)	solvent	M_n[a]	Đ[a]
1	MA	0.02	MeCN	6,400	1.06
2	MA	0.02	DMSO	11,100	1.09
3	tBA	0.10	MeCN	12,700	1.14
4	NIPAAM	0.005	MeCN	23,300	1.11
5	TFEA	0.02	MeCN	14,800	1.11
6	HEA	0.02	DMSO	75,600	1.31

[a] Molecular weight and polydispersity were determined by GPC analysis (DMF as eluent).

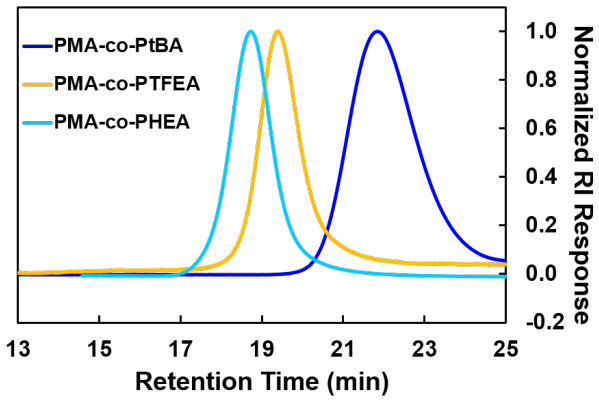

Figure III-S2. GPC traces of model statistical copolymerizations.

Table III-S2. Model statistical copolymerizations with TTC 1a

#	sample	monomers	monomer feed (MA/X)	PTH (mol %)	solvent	M_n[a]	Đ[a]	monomer incorporation (MA/X)
1	PMA-co-tBA	MA/tBA	80/20	0.10	MeCN	12,800	1.10	78/22
2	PMA-co-PTFEA	MA/TFEA	80/20	0.02	DMSO	24,200	1.12	76/24
3	PMA-co-PHEA	MA/HEA	80/20	0.02	DMSO	35,900	1.17	81/19

[a] Molecular weight and polydispersity were determined by GPC analysis (DMF as eluent).

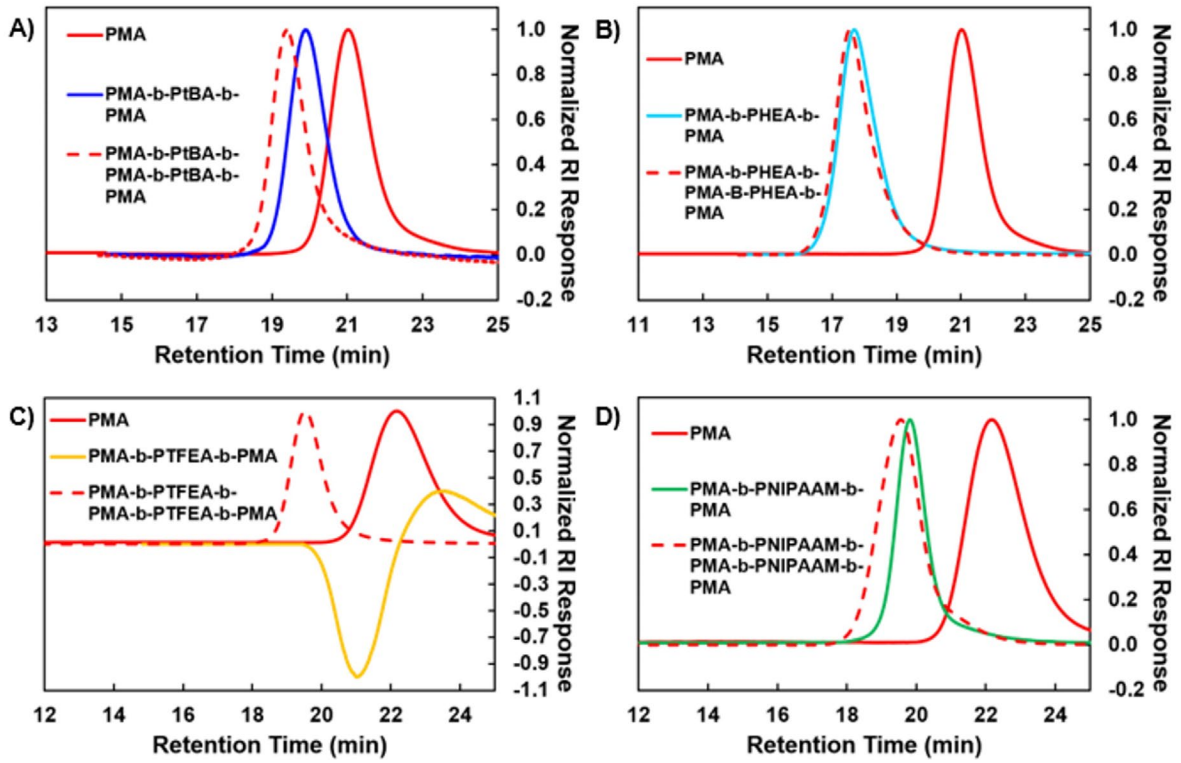

Figure III-S3. GPC traces of model block copolymerizations with MA and A) tBA, B) HEA, C) TFEA, D) PNIPAAM.

Table III-S3. Model block copolymerizations with TTC 1a

#	sample	Macroinitiator (MI)	MI M_n[a] (g/mol)	MI Đ[a]	monomer	PTH (mol%)	solvent	M_n[a] (g/mol)	Đ[a]
1	PMA-b-PtBA-b-PMA	PMA	11,100	1.09	tBA	0.10	MeCN	19,500	1.07
2	PMA-b-PHEA-b-PMA	PMA	11,100	1.09	HEA	0.02	DMSO	62,100	1.28
3	PMA-b-PTFEA-b-PMA	PMA	8,700	1.10	TFEA	0.02	MeCN	-	-
4	PMA-b-NIPAAM-b-PMA	PMA	8,700	1.10	NIPAAM	0.005	MeCN	24,900	1.14
5	PMA-b-PtBA-b-PMA- b-PtBA-b-PMA	PMA-b-PtBA-b-PMA	19,500	1.07	MA	0.10	MeCN	23,600	1.11
6	PMA-b-PHEA-b-PMA- b-PHEA-b-PMA	PMA-b-PHEA-b-PMA	62,100	1.28	MA	0.02	DMSO	65,500	1.33
7	PMA-b-PTFEA-b-PMA- b-PTFEA-b-PMA	PMA-b-PTFEA-b-PMA	-	-	MA	0.02	DMSO	29,000	1.14
8	PMA-b-NIPAAM-b-PMA- b-NIPAAM-b-PMA	PMA-b-PNiPAAm-b-PMA	24,900	1.14	MA	0.10	MeCN	28,400	1.24

[a] Molecular weight and polydispersity were determined by GPC analysis (DMF as eluent).

Selected NMR Spectra

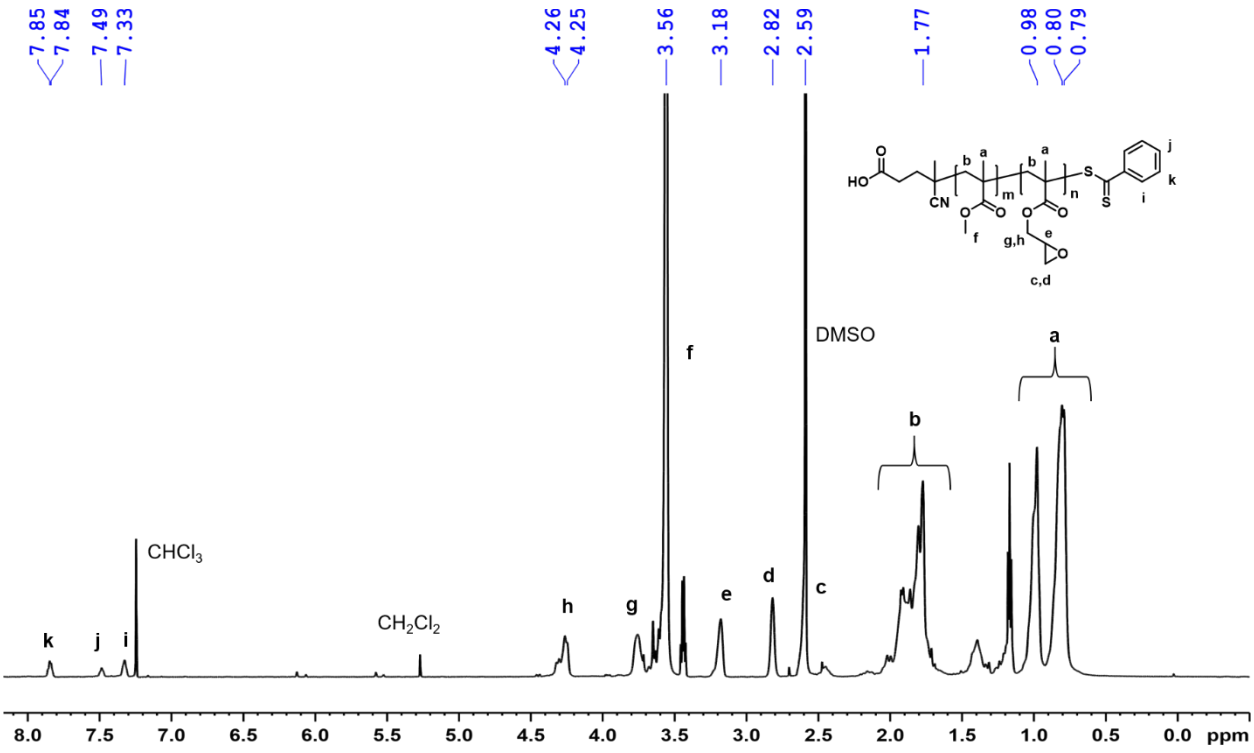

Figure III-S4. ^{1}H NMR ($CDCl_3$, 400 MHz) spectrum of polymer 2.

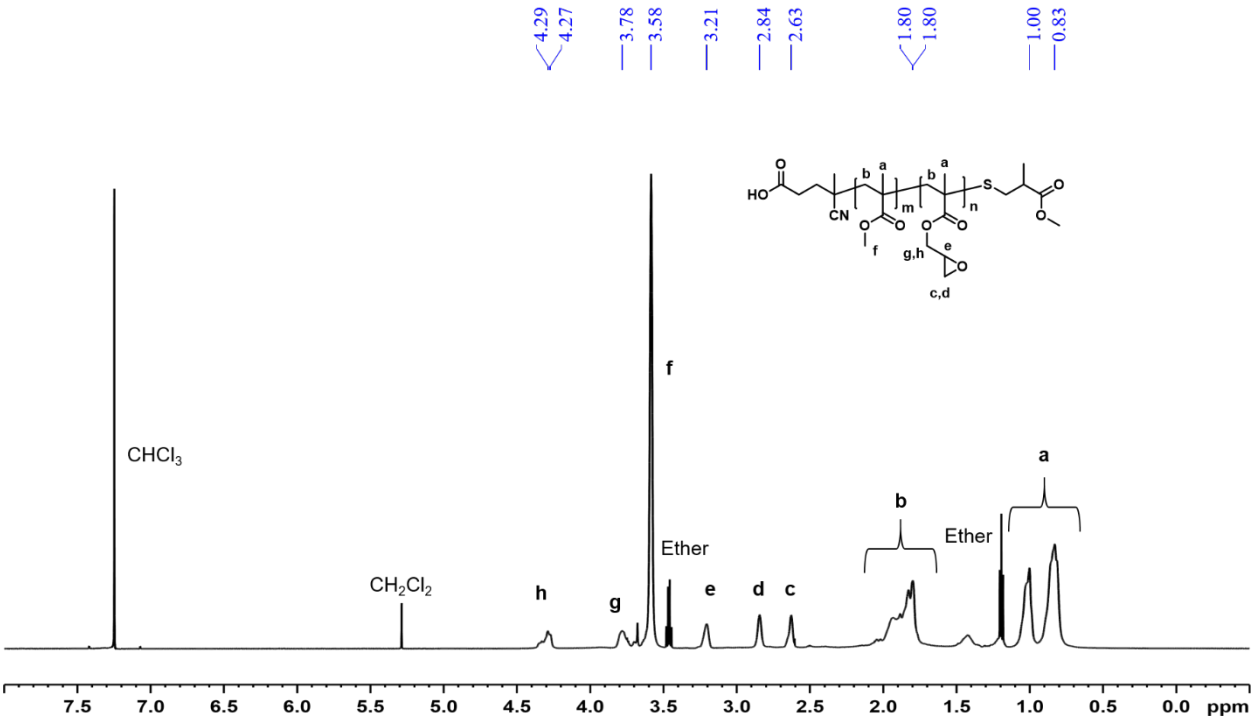

Figure III-S5. ^{1}H NMR ($CDCl_3$, 400 MHz) spectrum of polymer 3.

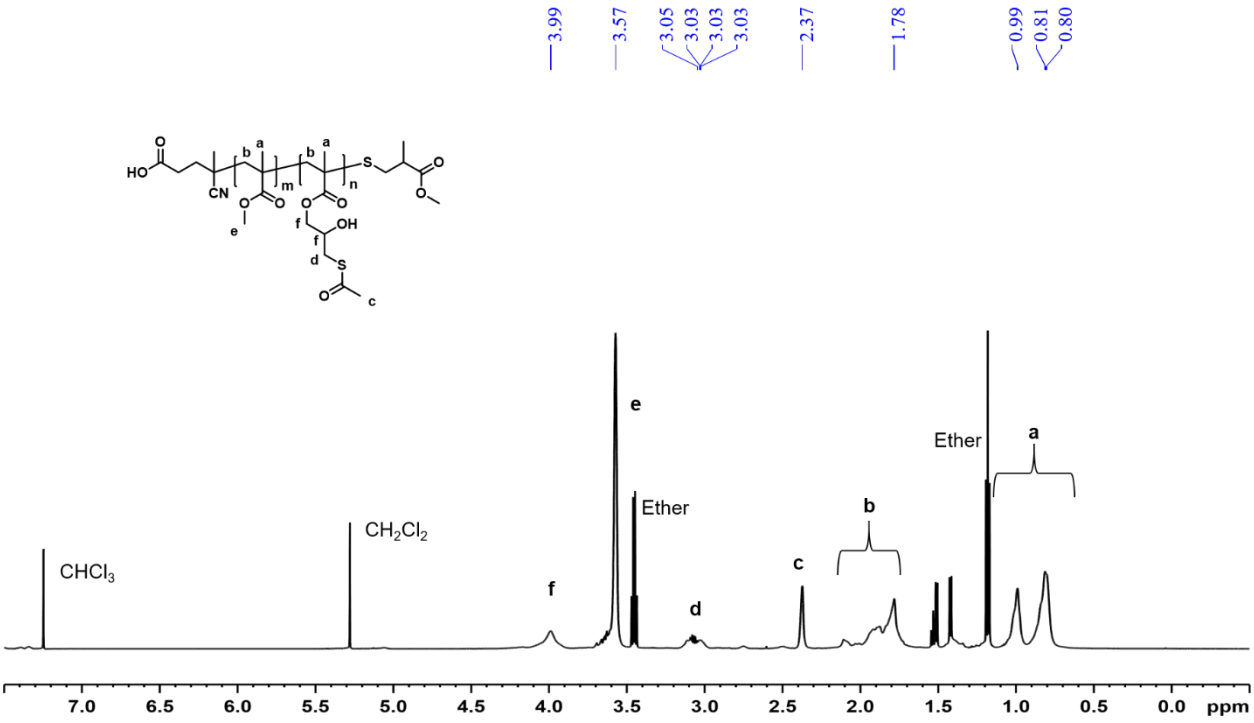

Figure III-S6. ^{1}H NMR ($CDCl_3$, 400 MHz) spectrum of polymer 4.

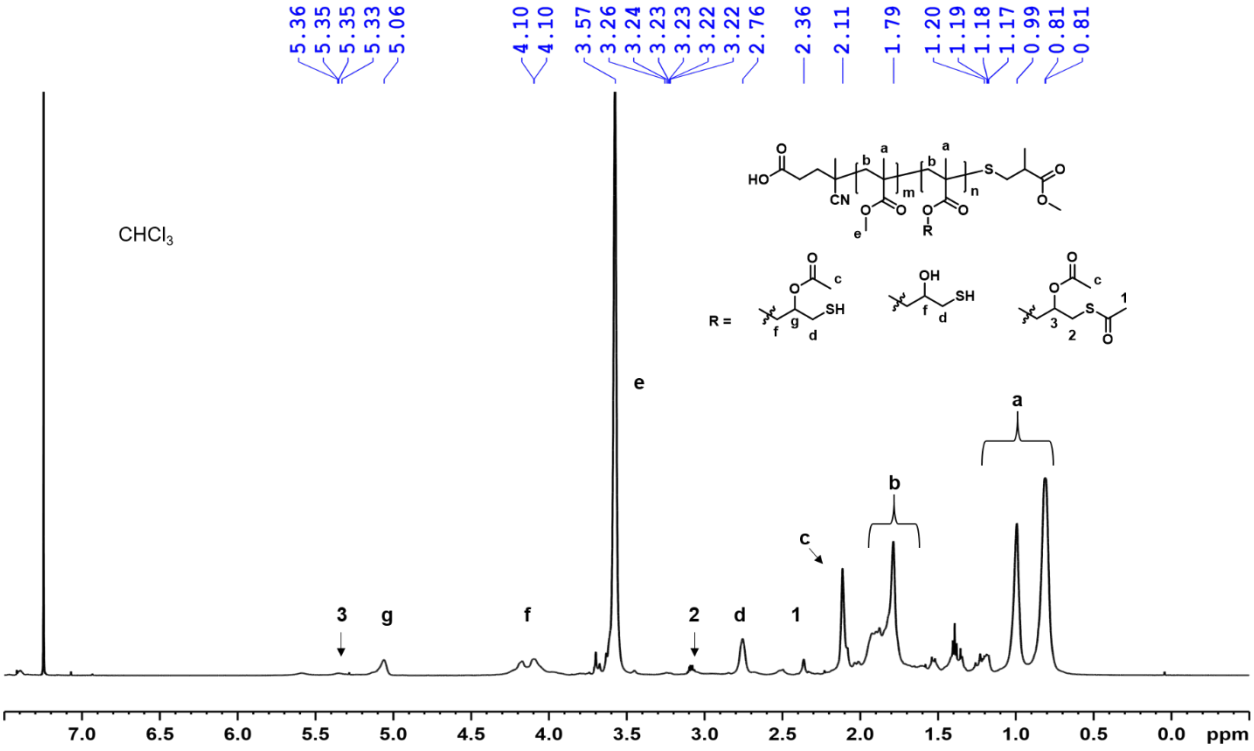

Figure III-S7. ^{1}H NMR ($CDCl_3$, 400 MHz) spectrum of polymer 5.

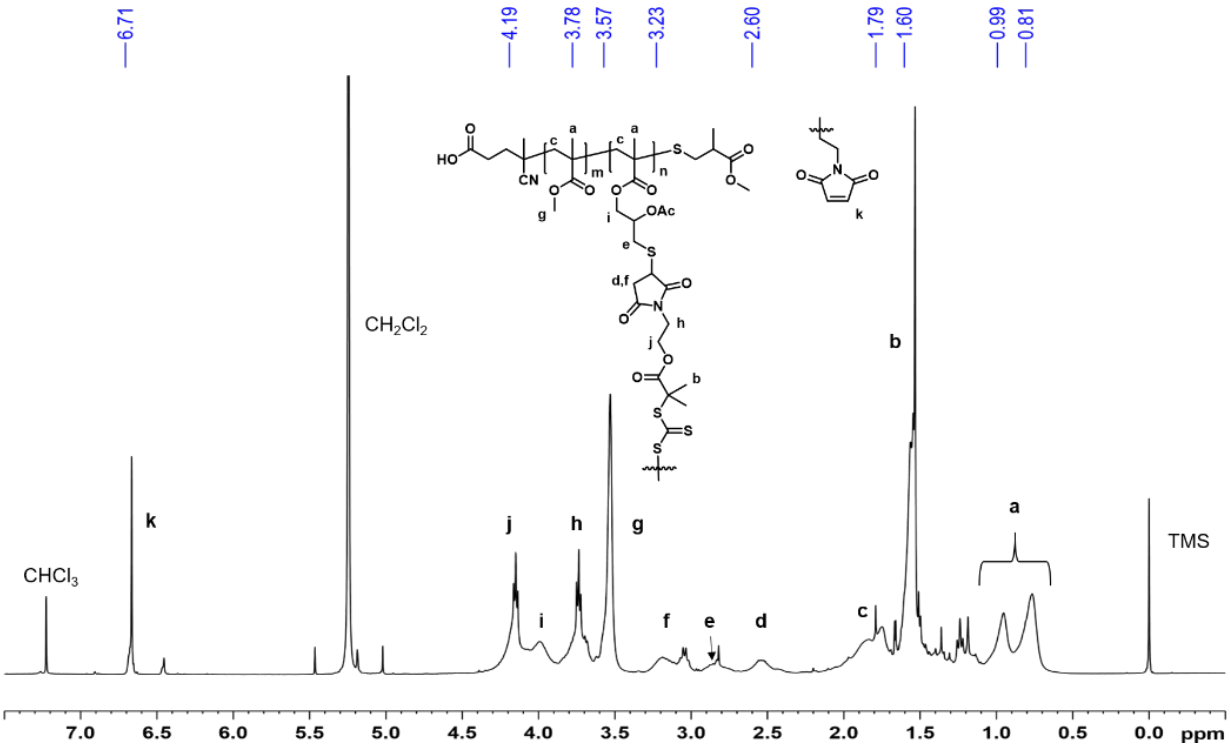

Figure III-S8. ^{1}H NMR ($CDCl_3$, 400 MHz) spectrum of photogrowable nanonetwork.

Parent PGNN Spectra

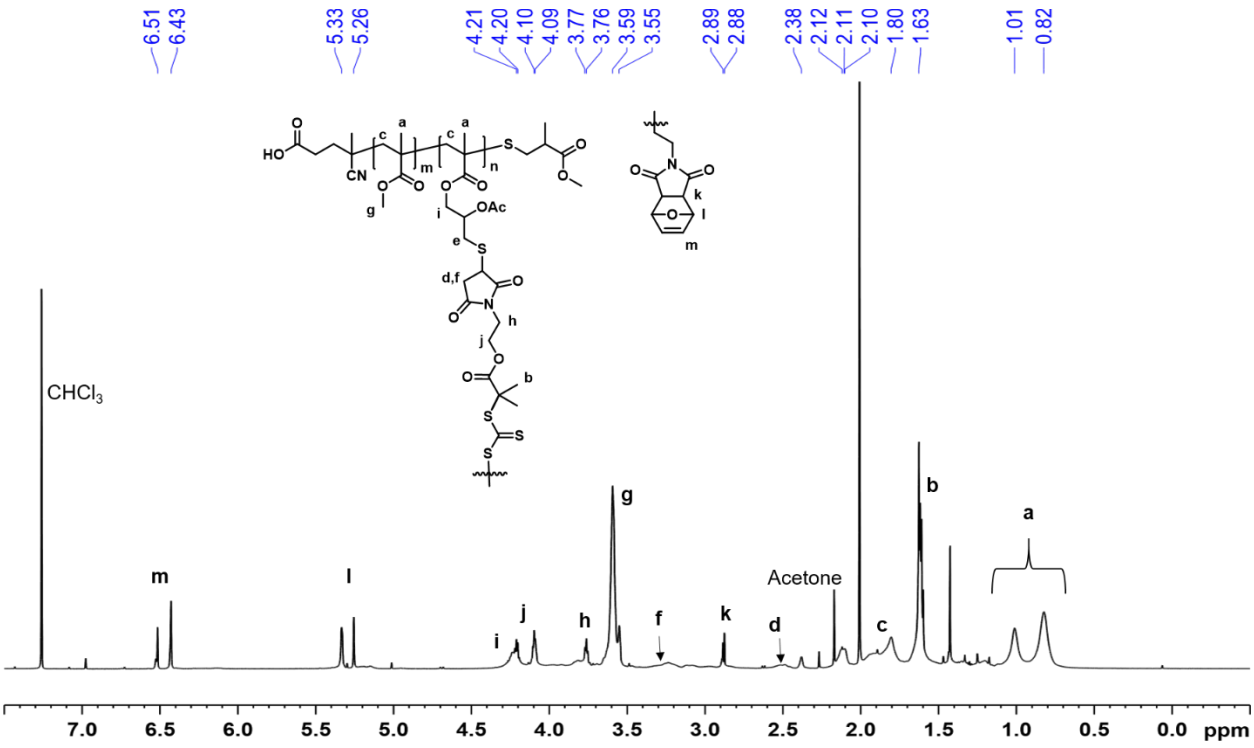

Figure III-S9. ^{1}H NMR ($CDCl_3$, 600 MHz) spectrum of parent photogrowable nanonetwork.

Homopolymer ENN Spectra

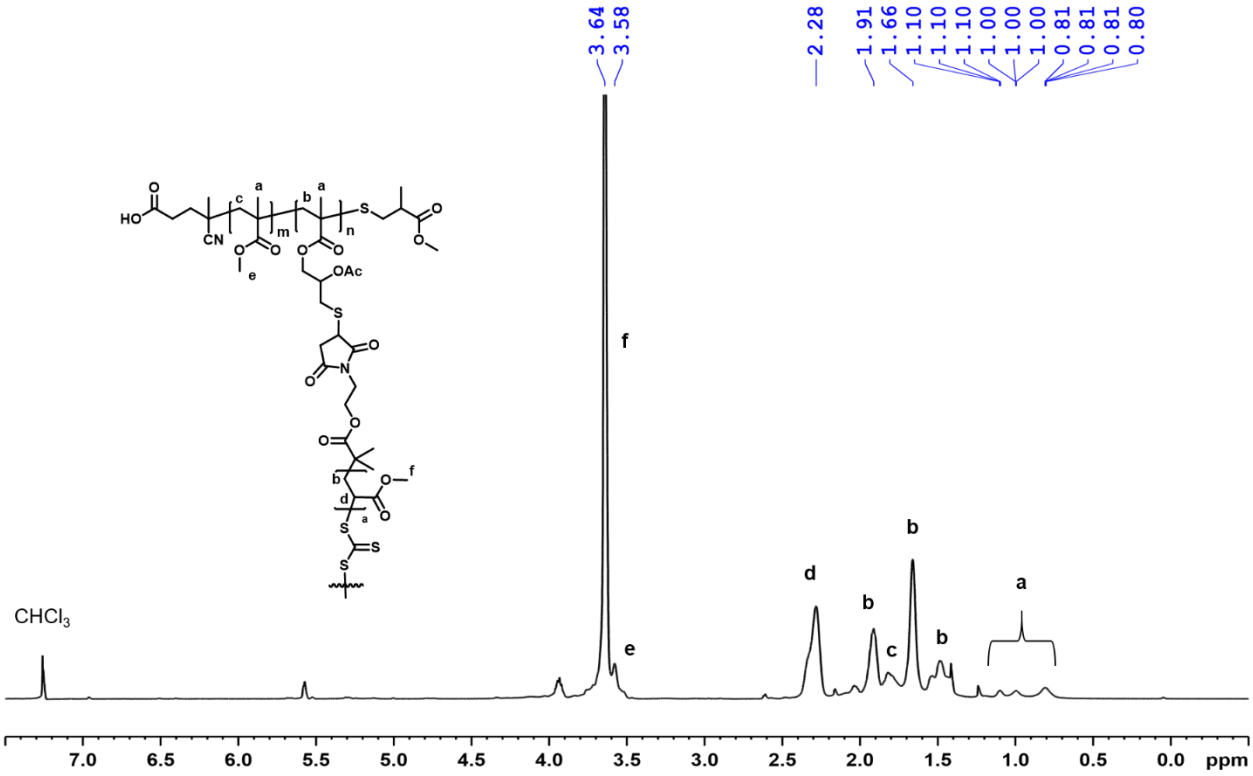

Figure III-S10. ^{1}H NMR ($CDCl_3$, 600 MHz) spectrum of expanded nanonetwork with MA after 30 minutes of irradiation.

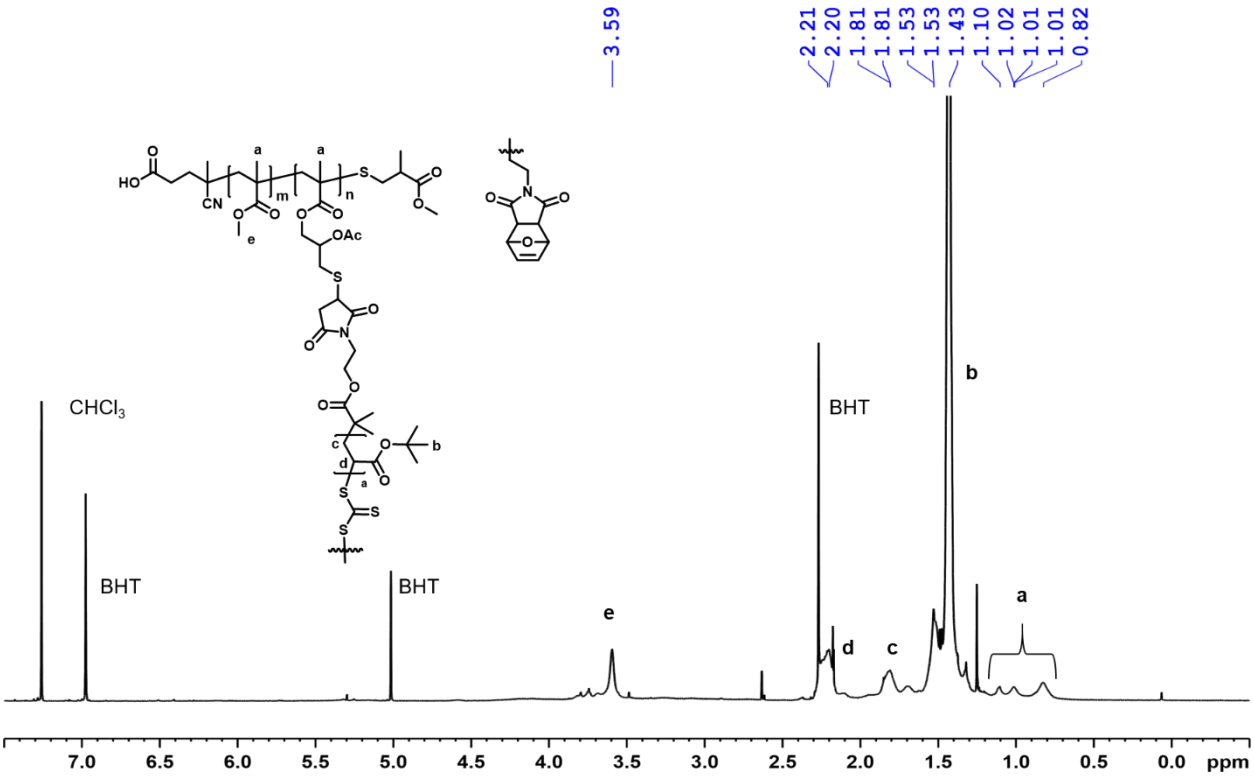

Figure III-S11. ^{1}H NMR ($CDCl_3$, 600 MHz) spectrum of expanded nanonetwork with tBA after 30 minutes of irradiation.

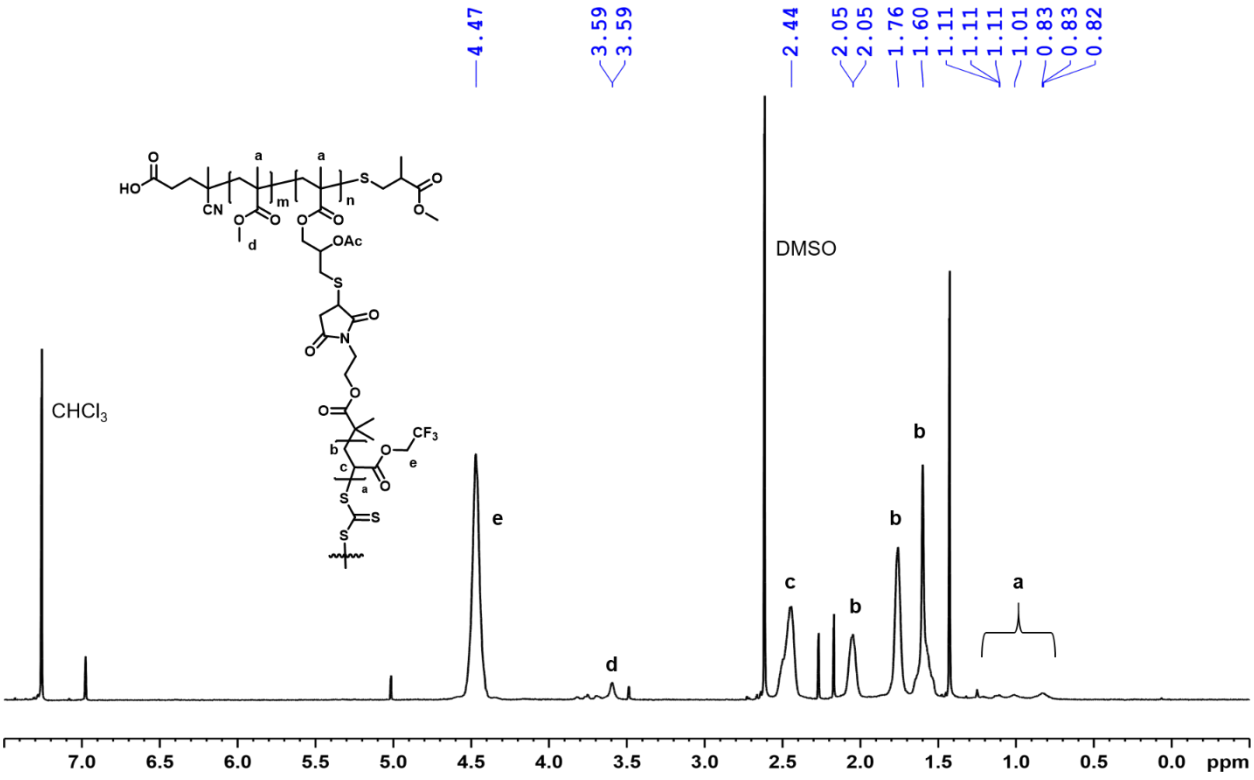

Figure III-S12. ^{1}H NMR ($CDCl_3$, 600 MHz) spectrum of expanded nanonetwork with TFEA after 30 minutes of irradiation.

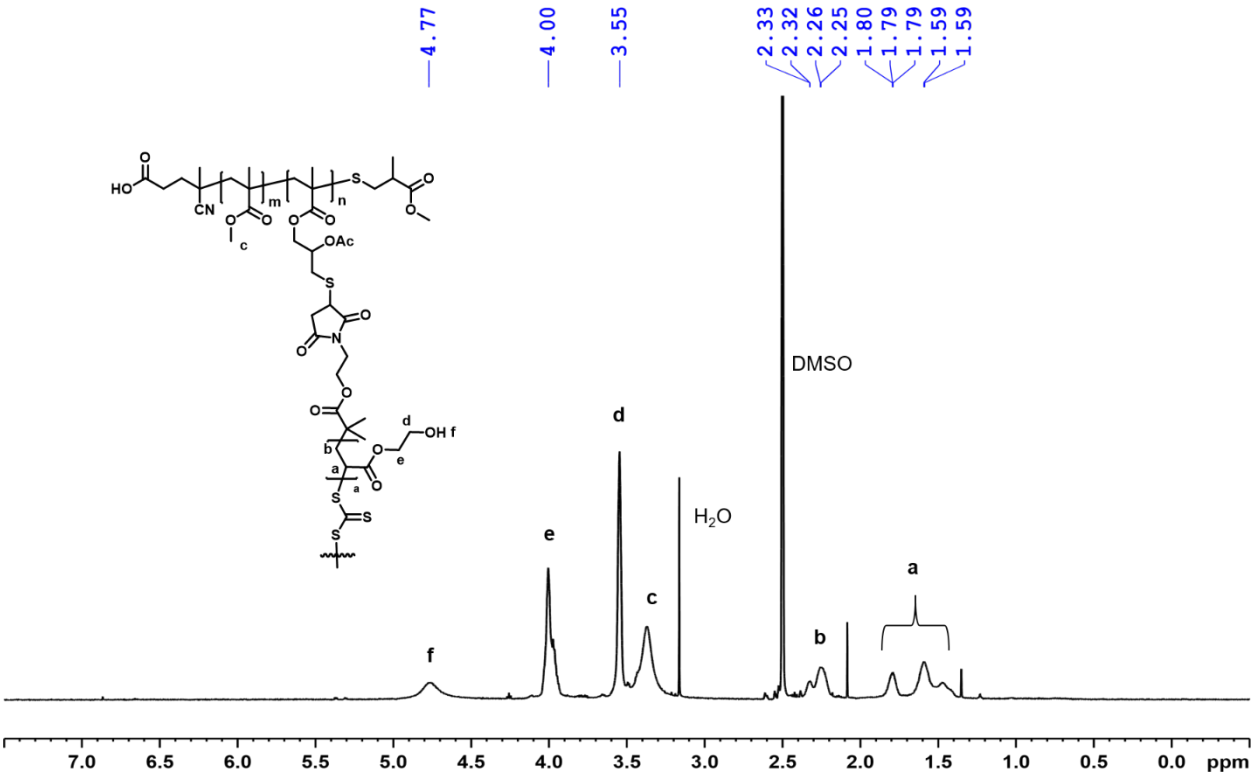

Figure III-S13. ^{1}H NMR (DMSO-d_6, 600 MHz) spectrum of expanded nanonetwork with HEA after 30 minutes of irradiation.

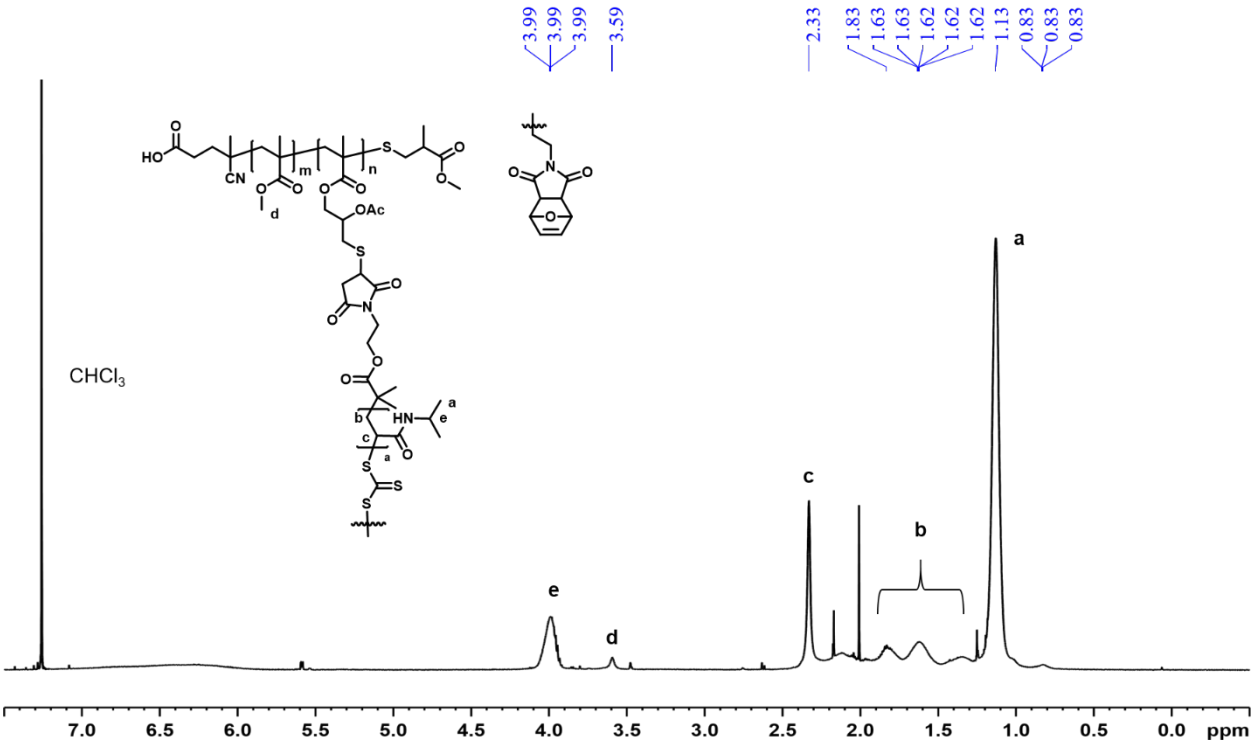

Figure III-S14. ^{1}H NMR ($CDCl_3$, 600 MHz) spectrum of expanded nanonetwork with NIPAAM after 30 minutes of irradiation.

Statistical Copolymer ENN Spectra:

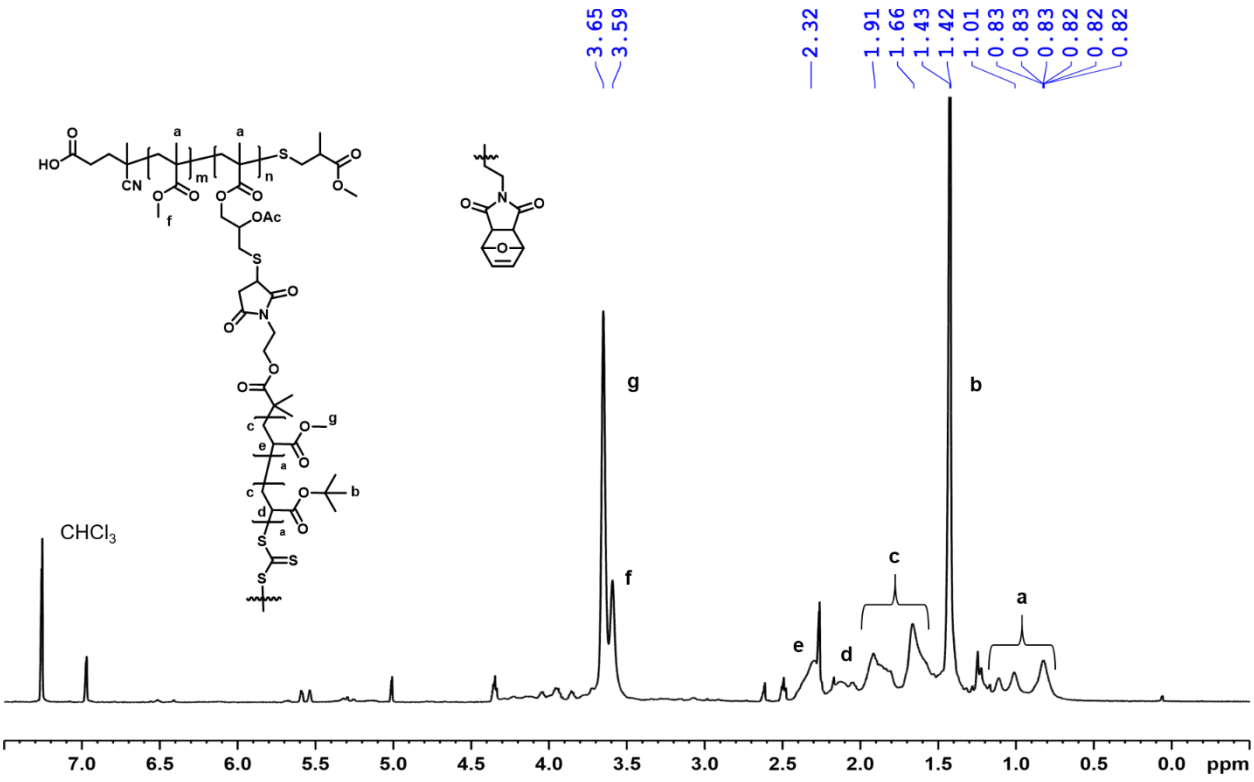

Figure III-S15. ^{1}H NMR ($CDCl_3$, 600 MHz) spectrum of statistical copolymer expanded nanonetwork with MA and tBA after 30 minutes of irradiation.

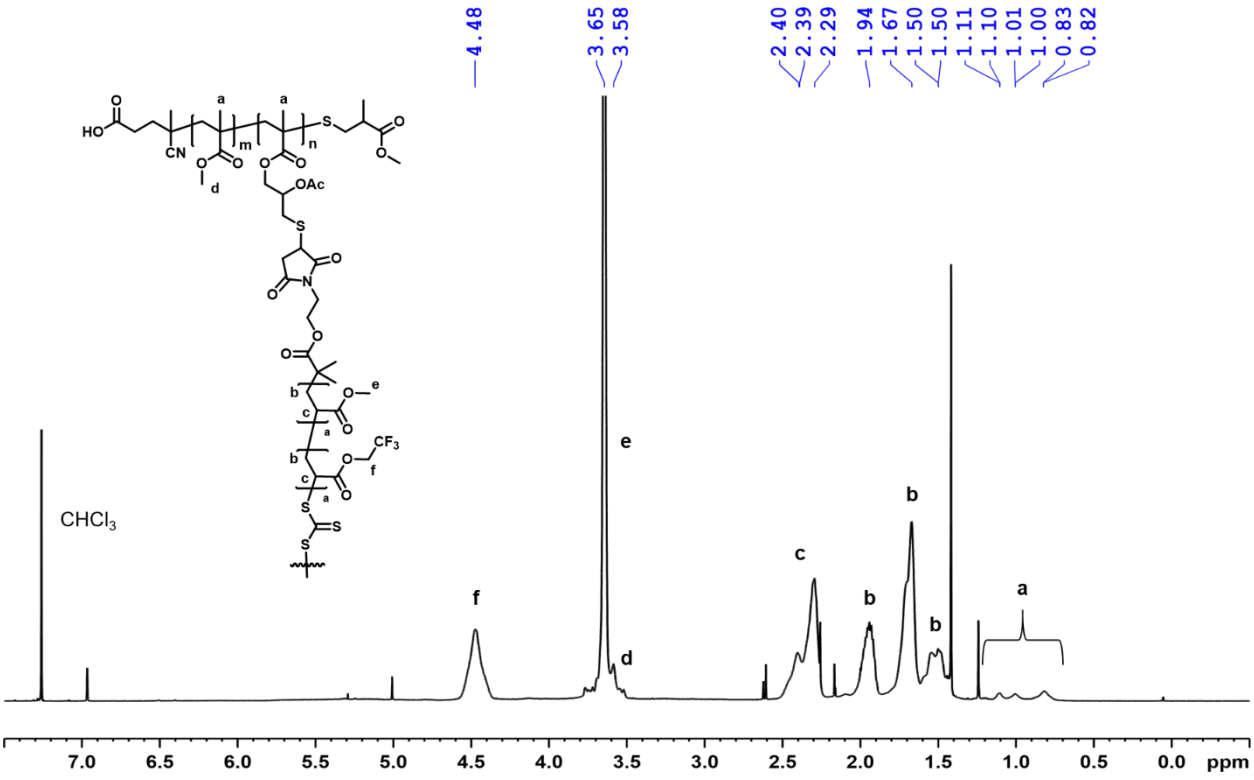

Figure III-S16. ^{1}H NMR ($CDCl_3$, 600 MHz) spectrum of statistical copolymer expanded nanonetwork with MA and TFEA after 30 minutes of irradiation.

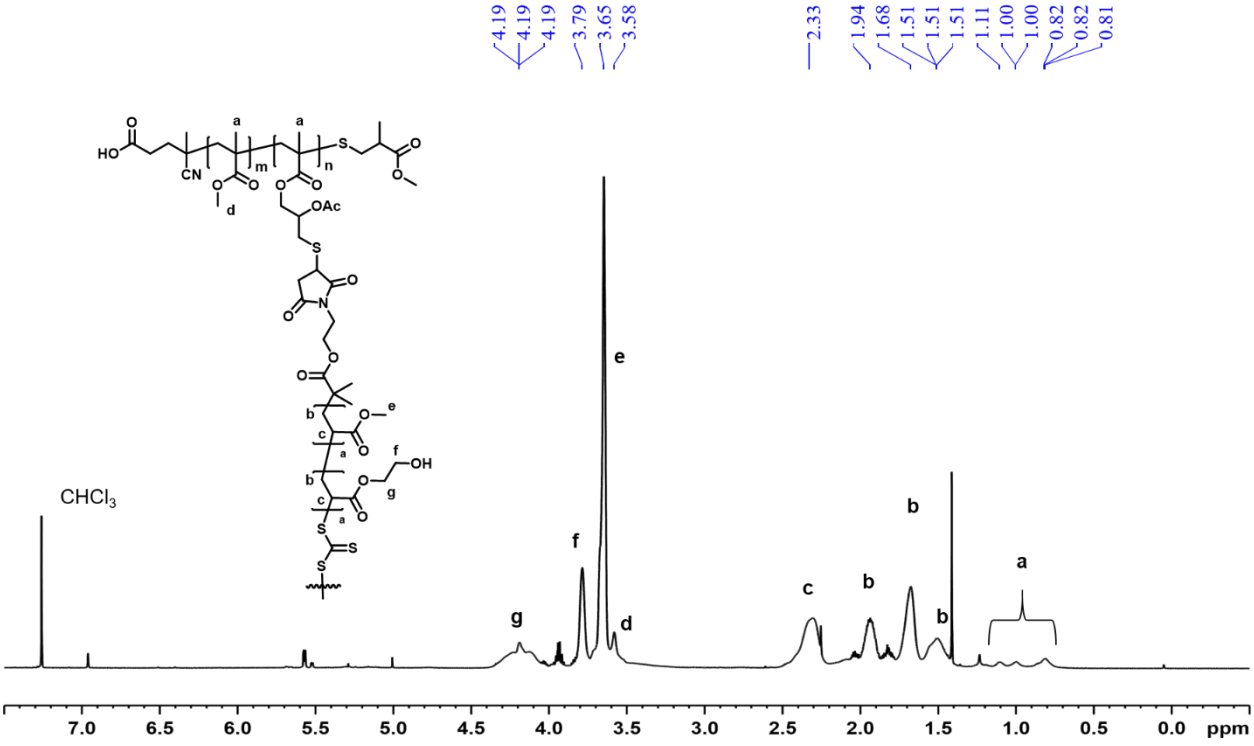

Figure III-S17. ^{1}H NMR ($CDCl_3$, 600 MHz) spectrum of statistical copolymer expanded nanonetwork with MA and HEA after 30 minutes of irradiation.

Block ENN Spectra:

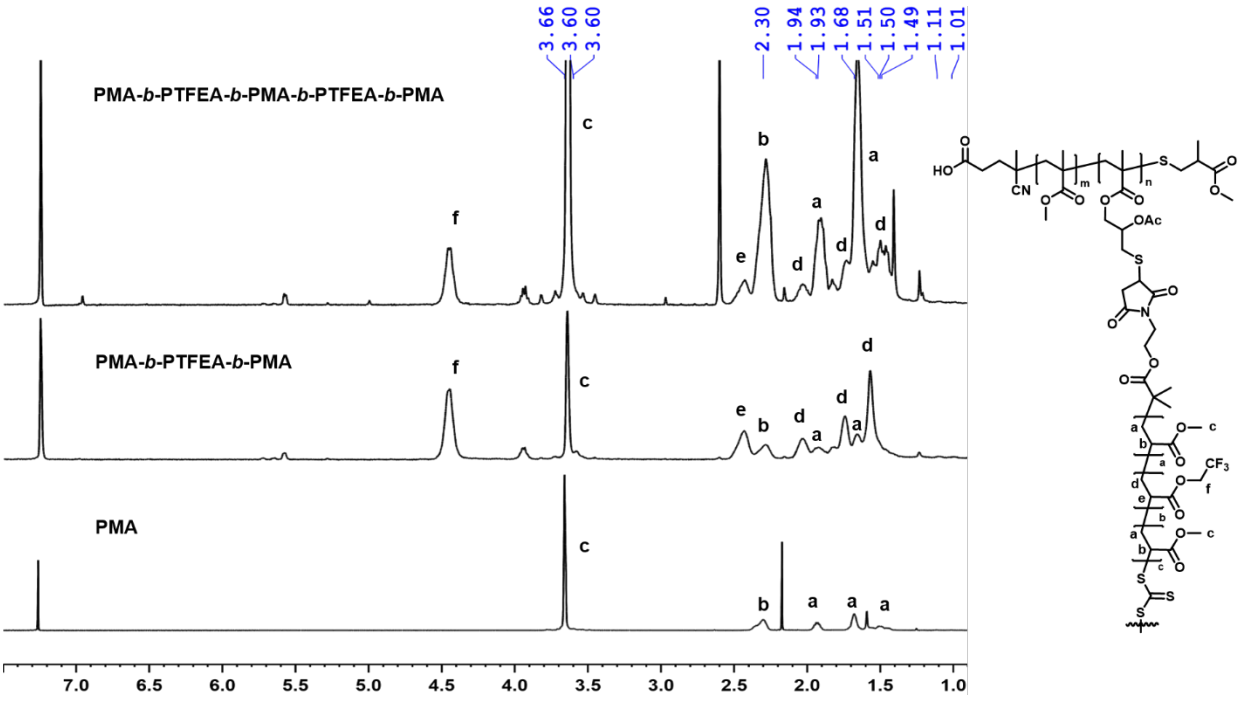

Figure III-S18. ^{1}H NMR ($CDCl_3$, 600 MHz) spectra of ABABA block copolymer expanded nanonetwork progression with MA and TFEA.

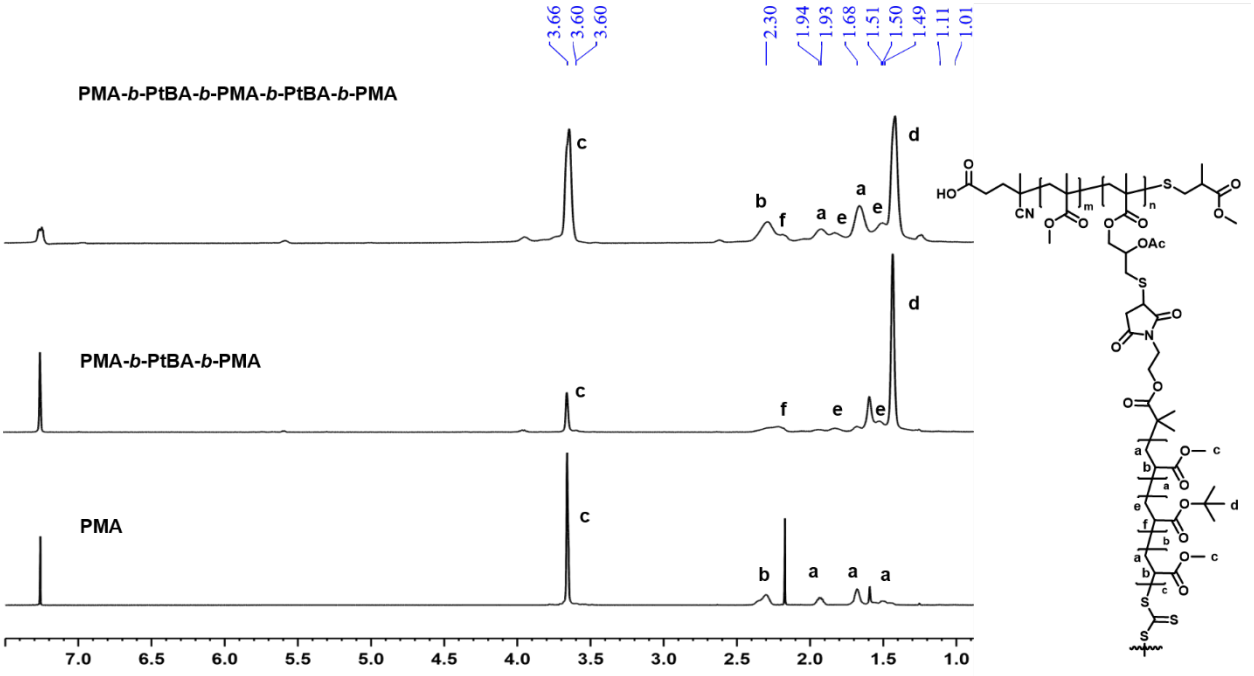

Figure III-S19. ^{1}H NMR ($CDCl_3$, 600 MHz) spectra of ABABA block copolymer expanded nanonetwork progression with MA and tBA.

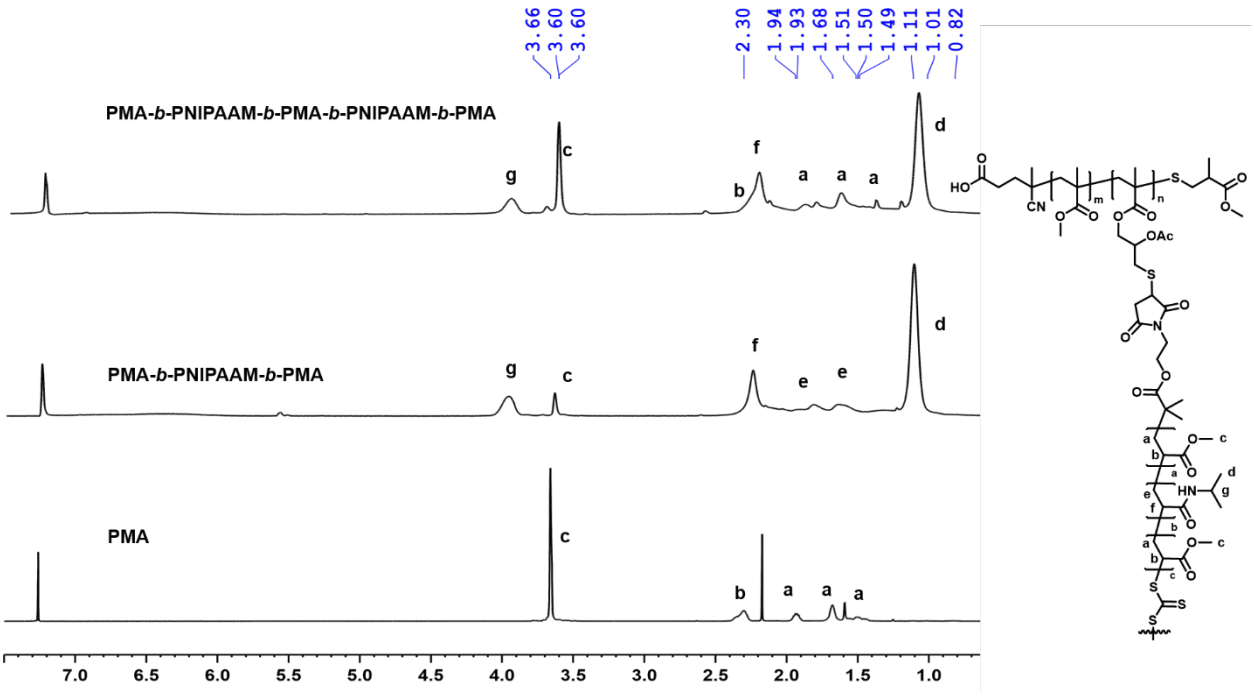

Figure III-S20. ^{1}H NMR ($CDCl_3$, 600 MHz) spectra of ABABA block copolymer expanded nanonetwork progression with MA and NIPAAM.

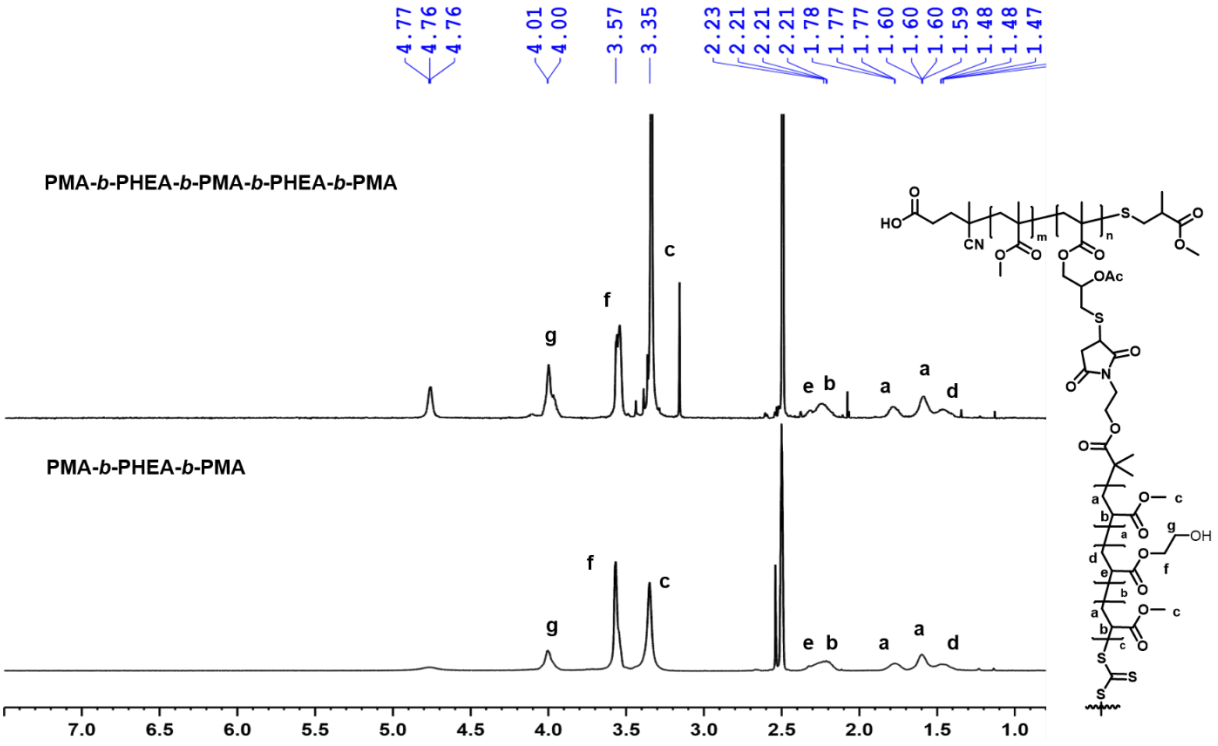

Figure III-S21. ^{1}H NMR (DMSO-d_6, 600 MHz) spectra of ABABA block copolymer expanded nanonetwork progression with MA and HEA.

Selected TEM Images

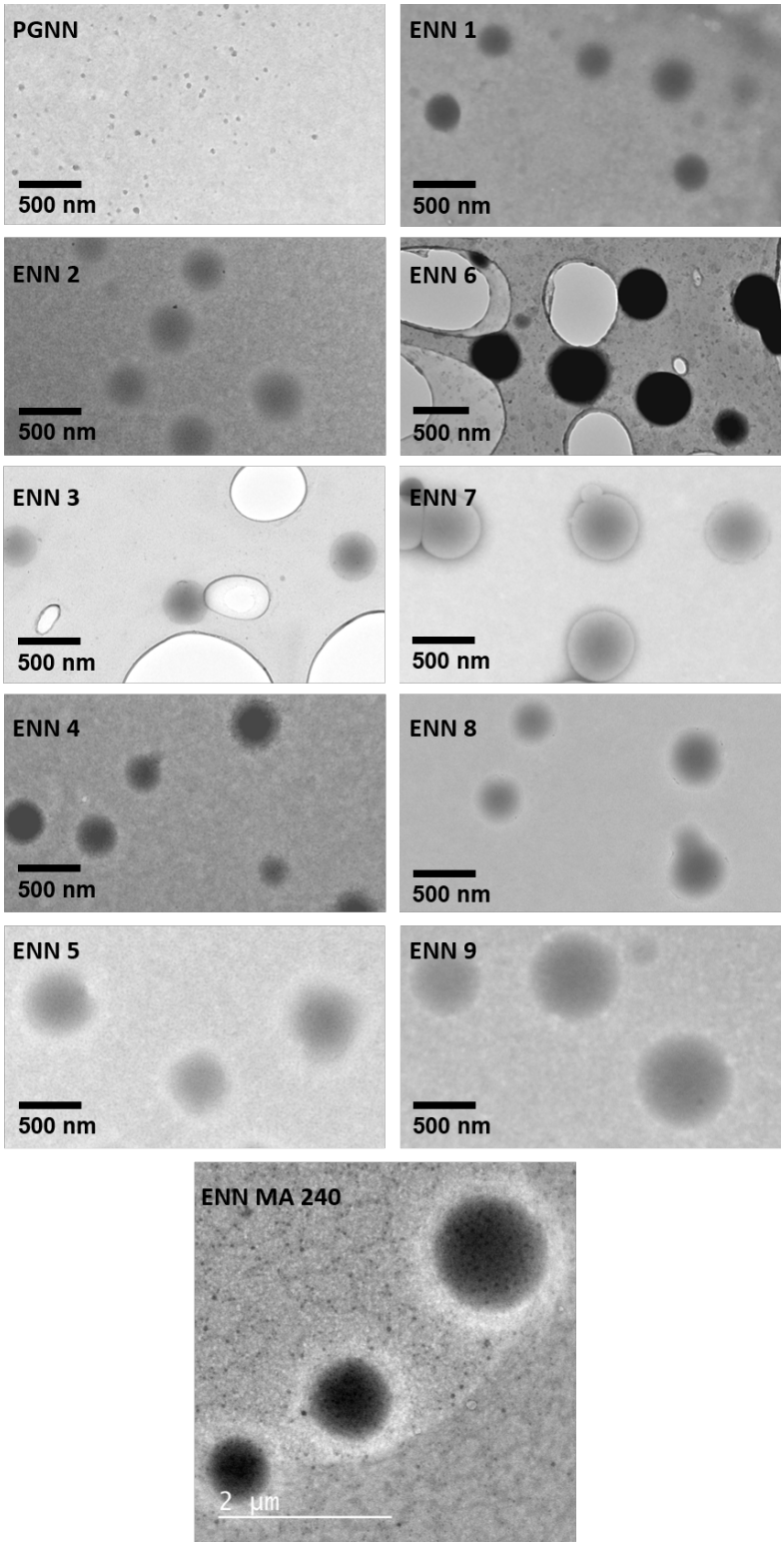

Figure III-S22. TEM images of the progression of ABA triblock, ABABA pentablock copolymer, and microparticle expansions.

REFERENCES

(1) Lin, T.-S.; Wang, R.; Johnson, J. A.; Olsen, B. D., Revisiting the Elasticity Theory for Real Gaussian Phantom Networks. *Macromolecules* **2019,** *52* (4), 1685-1694.

(2) Gu, Y.; Zhao, J.; Johnson, J. A., A (Macro)Molecular-Level Understanding of Polymer Network Topology. *Trends in Chemistry* **2019**.

(3) Wang, R.; Alexander-Katz, A.; Johnson, J. A.; Olsen, B. D., Universal Cyclic Topology in Polymer Networks. *Phys. Rev. Lett.* **2016,** *116* (18), 188302.

(4) Seiffert, S.; Sprakel, J., Physical chemistry of supramolecular polymer networks. *Chem. Soc. Rev.* **2012,** *41* (2), 909-930.

(5) Aoki, H.; Tanaka, S.; Ito, S.; Yamamoto, M., Nanometric Inhomogeneity of Polymer Network Investigated by Scanning Near-Field Optical Microscopy. *Macromolecules* **2000,** *33* (26), 9650-9656.

(6) Zhou, H.; Woo, J.; Cok, A. M.; Wang, M.; Olsen, B. D.; Johnson, J. A., Counting primary loops in polymer gels. *Proceedings of the National Academy of Sciences* **2012,** *109* (47), 19119.

(7) Lin, T.-S.; Wang, R.; Johnson, J. A.; Olsen, B. D., Topological Structure of Networks Formed from Symmetric Four-Arm Precursors. *Macromolecules* **2018,** *51* (3), 1224-1231.

(8) Di Lorenzo, F.; Seiffert, S., Nanostructural heterogeneity in polymer networks and gels. *Polym. Chem.* **2015,** *6* (31), 5515-5528.

(9) Wang, J.; Lin, T.-S.; Gu, Y.; Wang, R.; Olsen, B. D.; Johnson, J. A., Counting Secondary Loops Is Required for Accurate Prediction of End-Linked Polymer Network Elasticity. *ACS Macro Lett.* **2018,** *7* (2), 244-249.

(10) Wang, R.; Lin, T.-S.; Johnson, J. A.; Olsen, B. D., Kinetic Monte Carlo Simulation for Quantification of the Gel Point of Polymer Networks. *ACS Macro Lett.* **2017,** *6* (12), 1414-1419.

(11) Gordon, M. B.; French, J. M.; Wagner, N. J.; Kloxin, C. J., Dynamic Bonds in Covalently Crosslinked Polymer Networks for Photoactivated Strengthening and Healing. *Adv. Mater.* **2015,** *27* (48), 8007-8010.

(12) Amamoto, Y.; Otsuka, H.; Takahara, A.; Matyjaszewski, K., Changes in Network Structure of Chemical Gels Controlled by Solvent Quality through Photoinduced Radical Reshuffling Reactions of Trithiocarbonate Units. *ACS Macro Lett.* **2012,** *1* (4), 478-481.

(13) Amamoto, Y.; Otsuka, H.; Takahara, A.; Matyjaszewski, K., Self-Healing of Covalently Cross-Linked Polymers by Reshuffling Thiuram Disulfide Moieties in Air under Visible Light. *Adv. Mater.* **2012,** *24* (29), 3975-3980.

(14) Amamoto, Y.; Kamada, J.; Otsuka, H.; Takahara, A.; Matyjaszewski, K., Repeatable Photoinduced Self-Healing of Covalently Cross-Linked Polymers through Reshuffling of Trithiocarbonate Units. *Angew. Chem. Int. Ed.* **2011,** *50* (7), 1660-1663.

(15) Nicolaÿ, R.; Kamada, J.; Van Wassen, A.; Matyjaszewski, K., Responsive Gels Based on a Dynamic Covalent Trithiocarbonate Cross-Linker. *Macromolecules* **2010,** *43* (9), 4355-4361.

(16) Kloxin, C. J.; Scott, T. F.; Adzima, B. J.; Bowman, C. N., Covalent Adaptable Networks (CANs): A Unique Paradigm in Cross-Linked Polymers. *Macromolecules* **2010,** *43* (6), 2643-2653.

(17) Beziau, A.; Fortney, A.; Fu, L.; Nishiura, C.; Wang, H.; Cuthbert, J.; Gottlieb, E.; Balazs, A. C.; Kowalewski, T.; Matyjaszewski, K., Photoactivated Structurally Tailored

and Engineered Macromolecular (STEM) gels as precursors for materials with spatially differentiated mechanical properties. *Polymer* **2017,** *126*, 224-230.

(18) Cuthbert, J.; Beziau, A.; Gottlieb, E.; Fu, L.; Yuan, R.; Balazs, A. C.; Kowalewski, T.; Matyjaszewski, K., Transformable Materials: Structurally Tailored and Engineered Macromolecular (STEM) Gels by Controlled Radical Polymerization. *Macromolecules* **2018,** *51* (10), 3808-3817.

(19) Cuthbert, J.; Zhang, T.; Biswas, S.; Olszewski, M.; Shanmugam, S.; Fu, T.; Gottlieb, E.; Kowalewski, T.; Balazs, A. C.; Matyjaszewski, K., Structurally Tailored and Engineered Macromolecular (STEM) Gels as Soft Elastomers and Hard/Soft Interfaces. *Macromolecules* **2018,** *51* (22), 9184-9191.

(20) Cuthbert, J.; Martinez, M. R.; Sun, M.; Flum, J.; Li, L.; Olszewski, M.; Wang, Z.; Kowalewski, T.; Matyjaszewski, K., Non-Tacky Fluorinated and Elastomeric STEM Networks. *Macromol. Rapid Commun.* **2019,** *0* (0), 1800876.

(21) Zhou, H.; Johnson, J. A., Photo-controlled Growth of Telechelic Polymers and End-linked Polymer Gels. *Angew. Chem. Int. Ed.* **2013,** *52* (8), 2235-2238.

(22) Chen, M.; MacLeod, M. J.; Johnson, J. A., Visible-Light-Controlled Living Radical Polymerization from a Trithiocarbonate Iniferter Mediated by an Organic Photoredox Catalyst. *ACS Macro Lett.* **2015,** *4* (5), 566-569.

(23) Leibfarth, F. A.; Mattson, K. M.; Fors, B. P.; Collins, H. A.; Hawker, C. J., External Regulation of Controlled Polymerizations. *Angew. Chem. Int. Ed.* **2013,** *52* (1), 199-210.

(24) Trotta, J. T.; Fors, B. P., Organic Catalysts for Photocontrolled Polymerizations. *Synlett* **2016,** *27* (05), 702-713.

(25) Chen, M.; Gu, Y.; Singh, A.; Zhong, M.; Jordan, A. M.; Biswas, S.; Korley, L. T. J.; Balazs, A. C.; Johnson, J. A., Living Additive Manufacturing: Transformation of Parent Gels into Diversely Functionalized Daughter Gels Made Possible by Visible Light Photoredox Catalysis. *ACS Central Science* **2017,** *3* (2), 124-134.

(26) Lampley, M. W.; Harth, E., Photocontrolled Growth of Cross-Linked Nanonetworks. *ACS Macro Lett.* **2018**, 745-750.

(27) Discekici, E. H.; Anastasaki, A.; Kaminker, R.; Willenbacher, J.; Truong, N. P.; Fleischmann, C.; Oschmann, B.; Lunn, D. J.; Read de Alaniz, J.; Davis, T. P.; Bates, C. M.; Hawker, C. J., Light-Mediated Atom Transfer Radical Polymerization of Semi-Fluorinated (Meth)acrylates: Facile Access to Functional Materials. *J. Am. Chem. Soc.* **2017,** *139* (16), 5939-5945.

(28) Schild, H. G., Poly(N-isopropylacrylamide): experiment, theory and application. *Prog. Polym. Sci.* **1992,** *17* (2), 163-249.

(29) Treat, N. J.; Sprafke, H.; Kramer, J. W.; Clark, P. G.; Barton, B. E.; Read de Alaniz, J.; Fors, B. P.; Hawker, C. J., Metal-Free Atom Transfer Radical Polymerization. *J. Am. Chem. Soc.* **2014,** *136* (45), 16096-16101.

CHAPTER IV

PROGRESS TOWARDS SITE SELECTIVE EXPANSIONS OF DIELS-ALDER CROSSLINKED PHOTOGROWABLE NANONETWORKS

INTRODUCTION

In past years there has been an increasing interest in the post synthetic modification of functional materials.[1-6] In addition, several advances in this area were facilitated by the recent interest and developments in photochemistry and the selectivity and control it provides.[7-11] These advances have allowed for the production of bulk crosslinked networks capable of being mechanically or chemically differentiated through the introduction of new polymer chains either between network crosslinks or through integrated inimers. Indeed, we too have developed a crosslinked network capable of experiencing precise manipulations utilizing light-mediated polymerizations.[12] However, other examples have only produced bulk materials, whereas we have developed a crosslinked nanoparticle system deemed photogrowable nanonetworks (PGNNs). These PGNNs were demonstrated to controllably increase in size when polymer chains were introduced into the crosslinks through a photoredox mediated polymerization. More recently, the monomer scope was expanded to allow for the manipulation of network properties such as solubility, refractive index, and thermoresponsiveness. Additionally, more complex structures such as tri- and pentablock copolymer structures were realized. The success of our prior works has encouraged us to continue to investigate and improve our photogrowable nanonetworks.

In our previous investigations, we examined only the manipulation of a nanonetwork's size and properties through the expansion of the trithiocarbonate (TTC) crosslinker.[12] We now strive

to investigate what effects expanding the scaffold chain end has on nanonetwork morphology and size. To achieve this, two criteria must be met: 1) the scaffold chain end group must remain intact in order to initiate polymerization and 2) the scaffold chain end must be capable of a selective activation to initiate polymerization. We reasoned the second condition could be met through the use of selective photoactivation using two photocatalysts (i.e. zinc tetraphenylporphyrin (ZnTPP) and pheophorbide A (PheoA)) capable of selecting for specific types of reversible addition-fragmentation chain-transfer (RAFT) agents (i.e. dithiobenzoates and trithiocarbonates) as demonstrated by Boyer et al[13-14] or through orthogonal atom transfer radical polymerization (ATRP) and RAFT polymerizations with an ATRP initiator on the scaffold chain end.[15-16]

However, our first generation PGNN is incapable of satisfying the first requirement. While the scaffold chain end of the first generation PGNNs was purposefully rendered inert through an aminolysis reaction to ensure that new polymer chains could only grow from the crosslinker, the remaining synthetic steps, namely the thiolation and deprotection steps, ultimately result in the degradation of the dithiobenzoate through nucleophilic attack of the thiol. To circumvent this degradation a new generation of PGNNs needed to be designed utilizing a crosslinking chemistry compatible with either a dithiobenzoate or an ATRP bromine end group and a synthetic route that ideally required fewer synthetic steps than first generation PGNNs. Herein, we report the design of a second generation of PGNNs and the progress towards the selective expansion of crosslinked PGNNs with either RAFT or ATRP end groups (RAFT/ATRP-PGNN) present on the chain end of scaffold polymers.

RESULTS AND DISCUSSION

First generation PGNNs were manipulated to investigate controlled expansions of only the integrated TTC crosslinker. In this work, we aimed to develop a second generation of PGNN that possessed living chain ends on the scaffold polymer (either dithiobenzoate or ATRP bromine) as a means to investigate the effect expansion from the scaffold has on nanonetwork size and

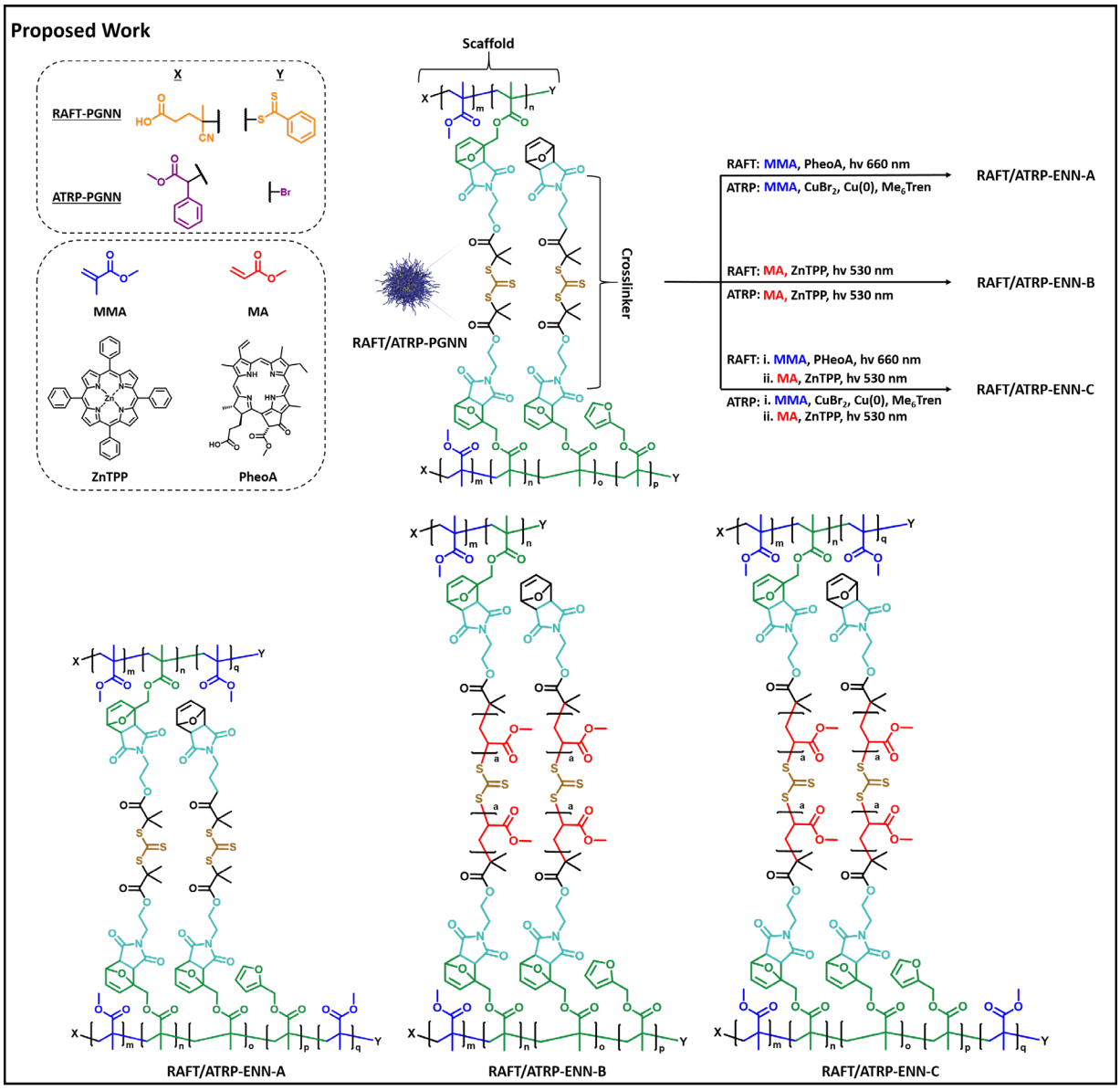

Figure IV-1. Schematic description of the proposed work to prepare differentiated nanonetworks through selective polymerizations from either scaffold polymer end groups (RAFT or ATRP) or crosslinker TTC.

morphology. To elucidate these effects RAFT-PGNNs or ATRP-PGNNs will be expanded to produce daughter networks that possess either an expanded scaffold (A), an expanded crosslinker (B), or both an expanded scaffold and crosslinker (C) (**Figure IV-1**). These site selective expansions can conceivably be achieved using selective polymerization techniques. Expansion of the crosslinker TTC with methyl acrylate (MA) could be mediated with ZnTPP under green light for both RAFT- and ATRP-PGNNs. Scaffold expansion with methyl methacrylate (MMA) of RAFT-PGNNs could proceed with PheoA under red light, while expansion of ATRP-PGNNs could proceed under ATRP conditions with the use of an appropriate ligand such as Tris[2-(dimethylamino)ethyl]amine (Me_6Tren).[16]

Photogrowable Nanonetwork Formation

First generation PGNNs were prepared through a thiol-maleimide crosslinking utilizing a thiol functionalized scaffold polymer that required several synthetic steps to produce (**Figure IV-2A**). Additionally, the synthetic route was not conducive to maintaining the integrity of the scaffold polymer end group. For these reasons, when designing the second generation of PGNNs we aimed to reduce the number of steps required to produce the PGNNs. In addition, crosslinking chemistries involving radicals or nucleophiles were avoided as they could induce degradation of both the crosslinker TTC and the scaffold polymer end group. In our previous works we have capped the free maleimides present in the nanonetworks through a Diels-Alder (DA) reaction with furan. Given the success and compatibility of this reaction we envisioned that the network formation could occur through a DA reaction between our existing symmetrical TTC maleimide crosslinker **1** and a furan functionalized polymer. Indeed, other bulk networks and nanoparticles

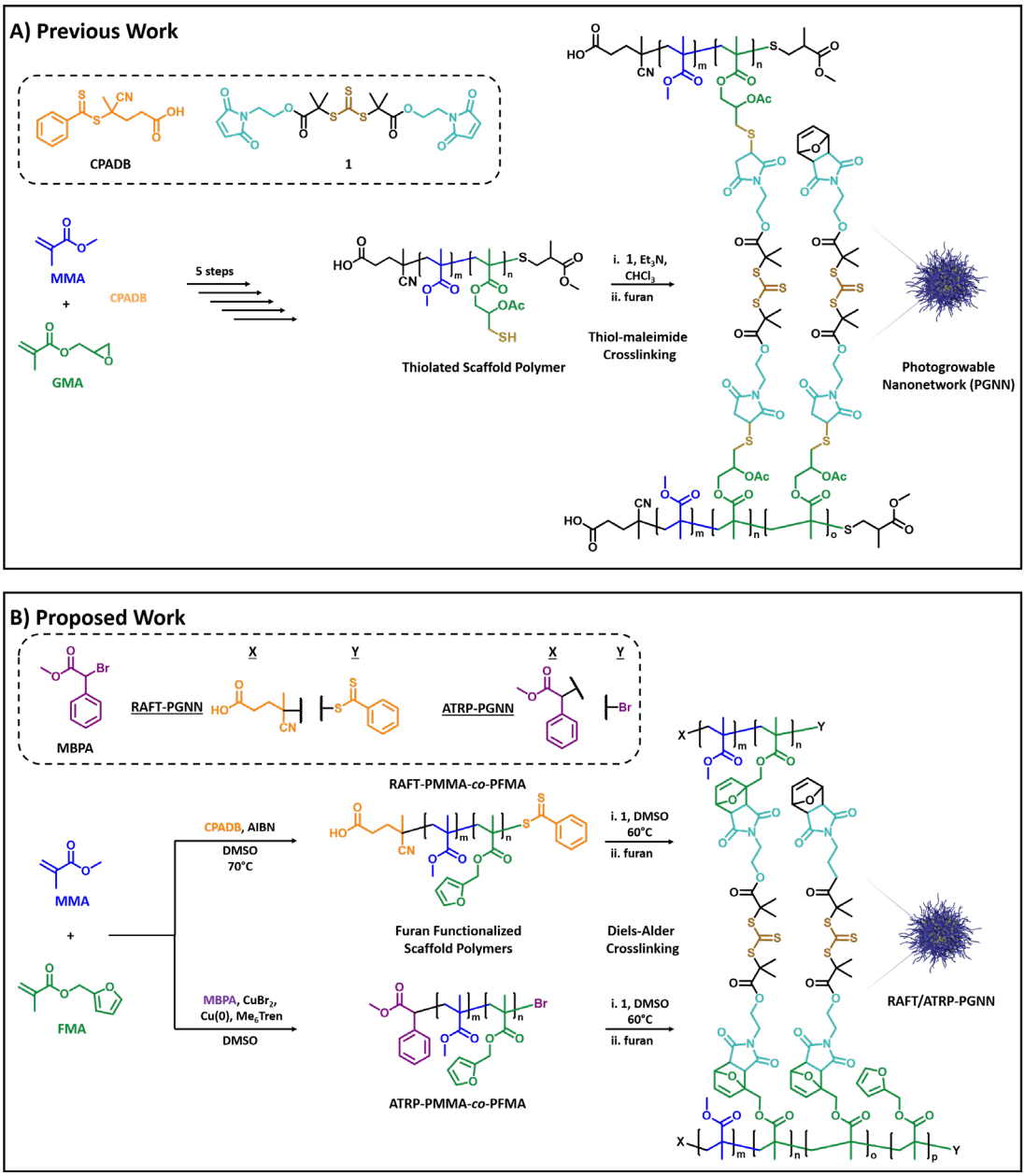

Figure IV-2. (A) Schematic description of the preparation of PGNNs from previous works. (B) Schematic description of the proposed work to prepare a second generation of PGNNs bearing RAFT or ATRP end groups from a furan functionalized scaffold polymer through a Diels-Alder reaction.

have been prepared through similar DA reactions with copolymers prepared from a commercially available, furan functionalized monomer, furfuryl methacrylate (FMA). [17-18]

Furan functionalized scaffold polymers with either dithiobenzoate or bromine end groups can be prepared in one step with low dispersities (**Table IV-S1**) through either RAFT or ATRP statistical copolymerization of MMA and FMA (**Figure IV-2B**). End group fidelity of both copolymers was explored through chain extensions with MMA, and in each case a PMMA block was successfully added with good control over dispersity (**Figure IV-S2, S3, Table IV-S2, S3**). With copolymers in hand PGNNs can be prepared through a DA reaction between RAFT- or ATRP-PMMA-*co*-PFMA scaffold polymer and TTC crosslinker **1** (**Figure IV-2B**). RAFT-PGNNs were prepared using a 4:1 maleimide:furan ratio in DMSO (0.02 M with respect to furan moieties) at 60°C for 6 hours after which the reaction was cooled to room temperature and excess furan was added to cap unreacted maleimide groups. PGNNs were then purified by dialysis and analyzed by transmission electron microscopy (TEM), nuclear magnetic resonance (NMR), and gel permeation chromatography (GPC). RAFT-PGNNs produced through this method produced sizes of 230 ± 56 nm as measured by TEM (**Figure IV-S8**). ^{1}H NMR analysis of RAFT-PGNNs confirms the presence of the dithiobenzoate as evidenced by the three aromatic signals (**Figure IV-S11**). Preparation of ATRP-PGNNs is still ongoing.

RAFT Photocatalysts Selectivity

To achieve the desired site selective network expansion, methods that can selectively activate the different initiators (i.e. dithiobenzoate, trithiocarbonate, and ATRP bromine) must be applied. Given that we have only demonstrated the successful production of RAFT-PGNNs, we began examining the feasibility of our selective RAFT expansions through a series of model polymerizations. ZnTPP and PheoA were chosen to selectively activate the TTC and the dithiobenzoate respectively as they have been previously demonstrated to be selective.[14]

First, we confirmed that PheoA could produce controlled polymers by performing chain extensions with MMA from our scaffold polymer (RAFT-PMMA-*co*-PFMA, Mn = 6,300 g/mol, $Đ$ = 1.13) to obtain a well-defined extended polymer (RAFT-PMMA-*co*-PFMA-*b*-PMMA, Mn = 14,600 g/mol, $Đ$ = 1.10). Second, we examined the selectivity of PheoA by performing a chain extension from RAFT-PMMA-*co*-PFMA (Mn = 6,300 g/mol, $Đ$ = 1.13) in the presence of furan capped crosslinker **1b**. Analysis by GPC revealed a monomodal trace with shift towards higher molecular weight (**Figure IV-S4**). ^{1}H NMR analysis of the precipitated polymer displayed no signals for crosslinker **1b** (**Figure IV-S12**), and ^{1}H NMR of the concentrated supernatant displayed signals for **1b** (**Figure IV-S13**). These results indicate that PheoA can selectively activate our dithiobenzoate to polymerize MMA in the presence of our TTC crosslinker.

Next, we moved on to determine if ZnTPP could selectively activate our TTC crosslinker. We began with a model polymerization of MA from TTC **1b** catalyzed by ZnTPP in green light (**Scheme IV-S1**). It was found that higher concentrations of ZnTPP produced polymers that displayed either bimodal or high molecular weight shouldering in GPC (**Figure IV-S6**). Lowering the catalyst amount from 0.00125 mol% to 0.000625 mol% with respect to MA produced well defined polymers after 30 minutes of irradiation. However, longer irradiation times produced polymers with high molecular weight shouldering in GPC. Additionally, chain extensions with ZnTPP of polymers produced after 30 minutes of irradiation yielded an increase in molecular weight, but also displayed high molecular weight shouldering (**Figure IV-S7**). Despite these flaws we endeavored to study whether or not the polymerization would be selective for the TTC in this limited reaction window. A model polymerization of MA from crosslinker **1b** in the presence of ZnTPP and RAFT-PMMA-*co*-PFMA was irradiated for 30 minutes under green light. Interestingly, no observable polymerization occurred. These results were surprising as ZnTPP has

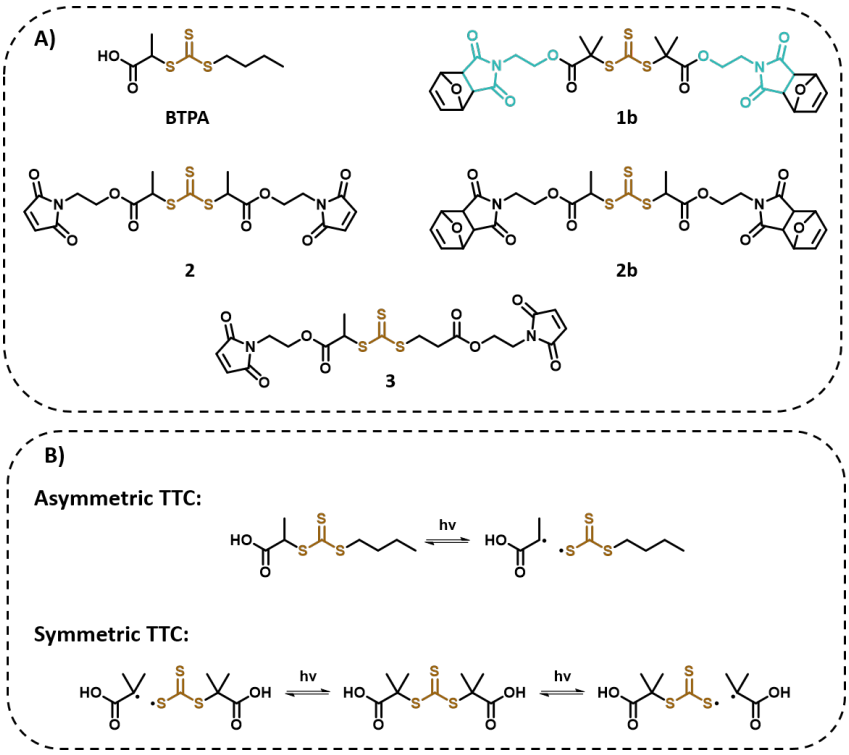

Figure IV-3. (A) Structures of trithiocarbonates. (B) Comparison of symmetric and asymmetric TTC fragmentation pathways.

been reported to function with a number of trithiocarbonates and there have been no reports of a similar loss of control after such a short amount of time.

To gain a better understanding of these results, a control experiment was conducted using conditions from a previously reported polymerization of MA with 2-(n-butyltrithiocarbonate) propionic acid (BTPA) (**Figure IV-3A**) as a TTC RAFT agent and ZnTPP as a photocatalyst.[13] Results obtained from this polymerization closely match those reported (**Table IV-S7**). This experiment seems to eliminate impurities in the catalyst or any potential differences of the light source as possible explanations for our observations. Furthermore, our TTC crosslinker has been shown to produce well defined polymers with 10-phenylphenothiazine (PTH) as a photocatalyst and has been demonstrated to perform multiple chain extensions in the presence of PTH which would eliminate the crosslinker as a potential problem. All of this data may suggest that it is the combination of ZnTPP and crosslinker **1b** that produces the observed loss of control.

To the best of our knowledge, all reports of utilizing ZnTPP as a photocatalyst with TTCs have been performed with asymmetric TTCs and there are no examples of ZnTPP activating a symmetrical TTC. Given that symmetrical TTCs can fragment from both sides of the TTC while asymmetric TTCs can only fragment from one side, it may be possible that there is a mechanistic explanation for our observations based off the structural differences between symmetric and asymmetric TTCs (**Figure IV-3B**). To investigate this hypothesis a symmetrical TTC with the same initiating group as BTPA **2b** could be examined for the ability to polymerize MA in the presence of ZnTPP as polymerizations with BTPA have been shown to be successful (**Table IV-S7**). If the polymerization of **2b** is successful, then the observed loss of control may be more specific to crosslinker **1b**. If the polymerization is unsuccessful, then it may be more evidence that ZnTPP has a negative interaction with symmetrical TTCs.

Regardless of the outcome of these experiments the fact remains that ZnTPP is not an ideal catalyst to achieve the desired site selective network expansions in either RAFT- or ATRP-PGNNs with our crosslinker TTC. To address this issue, further work must be done to develop a method that utilizes either a new catalyst that is selective for the TTC crosslinker **1b** or implements a new TTC crosslinker that can be selectively activated by either ZnTPP or by direct photolysis with visible light. However, to the best of our knowledge there are currently no reports of another photocatalyst that is selective for TTCs over dithiobenzoates. For this reason, selection of a new crosslinker may prove to be a more fruitful approach. To this end, if ZnTPP can be demonstrated to effectively control polymerization from **2b,** then bis-maleimide crosslinker **2** could replace **1** as the crosslinker (**Figure IV-3A**). Additionally, crosslinker **2** could be used under direct photolysis conditions with blue light if ZnTPP is unable to act as an effective catalyst. However, further selectivity experiments would need to be conducted if a photolysis iniferter polymerization was

pursued. Alternatively, asymmetric crosslinker **3** (**Figure IV-3**) could be utilized with ZnTPP. While it is unclear whether the asymmetric nature of this crosslinker will produce different results from a symmetrical crosslinker when it comes to network expansion, it still stands as a viable option to implement the site selective expansion of PGNNs.

CONCLUSION

Here we describe the preparation of a second generation of PGNNs functionalized with two types of controlled radical polymerization initiators. This second generation of PGNNs is poised to experience site selective expansions as a means to study the effects on network size and morphology. RAFT-PGNNs were prepared through a DA between a furan functionalized scaffold polymer and a bis-maleimide TTC. Selectivity experiments were performed to determine the optimal conditions to perform the selective expansions. Through these experiments it was determined that ZnTPP is ultimately incompatible with the bis-maleimide TTC. Further investigations into selective expansions from the TTC crosslinker must be conducted in order to achieve the desired site selective expansion. Additionally, preparation of ATRP-PGNNs and the selectivity of the ATRP expansion conditions must be evaluated.

EXPERIMENTAL

Materials:

All reagents and solvents were purchased from Sigma Aldrich and used as received unless otherwise stated. Methyl acrylate (MA), methyl methacrylate (MMA), and furfuryl methacrylate (FMA) were purified immediately before use in RAFT polymerizations by passing through a short column of inhibitor removers purchased from Sigma Aldrich. Inhibitors were not removed for

monomers used in ATRP polymerizations. TTC **1** and **1b** were synthesized as previously reported.[12] Polymerizations under green light were performed at 530 nm and polymerizations under red light were performed at 660 nm. Copper wire (5 cm, 0.25 mm) was submerged in concentrated HCl for 20 minutes, washed with water and acetone, and then dried under nitrogen immediately before use.

Material Characterization:

All ^{1}H and ^{13}C spectra were obtained using a JEOL ECA 400 (400 MHz), or a ECA-600 (600 MHz) spectrometer. Chemical shifts were measured relative to residual solvent peaks as an internal standard. TEM imaging was performed using a JEOL 2010 F Transmission Electron Microscope at 200 kV with formvar coated or holey carbon coated copper grids. Gel permeation chromatography (GPC) was performed using a Tosoh high performance GPC system HLC-8320 equipped with an auto injector, a dual differential refractive index detector and TSKgel G series columns connected in series (7.8×300 mm TSKgel G5000Hxl, TSKgel G4000Hxl, TSKgel G3000Hxl). GPC analysis was carried out in HPLC grade tetrahydrofuran (THF) with a flow rate of 1.0 mL/min at 40 °C. Molecular weights (Mn and Mw) and molecular weight distributions were calculated from polymethyl methacrylate (PMMA) standards with molecular weights of 800 to 2.2×106 g mol-1 provided by Polymer Standard Service (PSS).

Acknowledgement: All experiments were conducted alongside coauthor Enkhjargal Tsogtgerel

Synthesis:

RAFT polymerization of MMA and FMA (85/15): CPADB (151.6 mg, 0.5426 mmol) and AIBN (13.36 mg, 0.0814 mmol), MMA (3 mL, 28.16 mmol) and FMA (0.766 mL, 4.97 mmol) were dissolved in DMSO (3.766 mL) in a 4 dr vial. The reaction vessel was sealed with a rubber septum and degassed by three freeze-pump-thaw cycles, placed into an oil bath at 70°C. The reaction was left to proceed for 14 hours and then precipitated in ether. $M_{n,\,GPC}$ = 6603 g/mol, $Đ$ = 1.12.

Cu(0) mediated ATRP polymerization of MMA and FMA (85/15): Cu(II)Br_2 (2 mg, 0.0090 mmol), MMA (1 mL, 9.389 mmol), FMA (0.255 mL, 1.657 mmol) and Me_6Tren (2.88 µL, 0.0108 mmol) were dissolved in DMSO (1.255 mL) in a 1dr vial. Concurrently, in a separate vial, a stir bar wrapped with 5 cm of Copper wire was immersed in concentrated HCl and stirred for 20 minutes, washed with water and acetone and dried. The stir bar was then placed into the reaction vessel and MBPA (28.3 µL, 0.1795 mmol) was added. The reaction vessel was sealed with a rubber septum and degassed with nitrogen for 15 minutes while stirring. The reaction was left to proceed for 7 hours at rt and then precipitated in methanol. $M_{n,\,GPC}$ = 8573 g/mol, $Đ$ = 1.16.

General procedure for Diels-Alder nanonetwork formation: PMMA-*co*-PFMA and TTC (2 eq) were dissolved in anhydrous DMSO (0.02 M with respect to furan unit) stirred at 60°C for 6 hours. An aliquot was taken for ^{1}H NMR analysis. The reaction was cooled down and excess amount of furan was added to the reaction and stirred at rt for 24 hours. The reaction was then diluted with DCM and dialyzed for two days in 10kDa MWCO snakeskin tubing against 1:1 mixture of MeCN:THF.

Model reactions:

Chain extension of RAFT PMMA-*co*-PFMA with MMA: In a 1dr vial, RAFT PMMA-*co*-PFMA (66 mg, 0.01 mmol) and PheoA (0.01185 mg, 0.00002 mmol) were dissolved in 2M solution of MMA (426 µL, 4 mmol) in DMSO (426 uL). The reaction vessel was sealed with a rubber septum, degassed with nitrogen for 20 minutes and irradiated with red light for 17 hours. The reaction was quenched by exposing it to open air and precipitated in methanol.

Chain extension of ATRP PMMA-*co*-PFMA with MMA: Macroinitiator (100 mg, 0.0117 mmol), Cu(II)Br_2 (0.13 mg, 0.00058 mmol), MMA (124.1 uL, 1.165 mmol) and Me_6Tren (0.187 µL, 0.0007 mmol) were dissolved in DMSO (528.5 uL) in a 1dr vial. Concurrently, in a separate vial, a stir bar wrapped with 5 cm of Copper wire was immersed in concentrated HCl and stirred for 20 minutes, washed with water and acetone and dried. The stir bar was then placed into the reaction vessel. The reaction vessel was sealed with a rubber septum and degassed with nitrogen for 15 minutes while stirring. The reaction was left to proceed for 17.5 hours at rt° and then precipitated in methanol. $M_{n,\,GPC}$ = 10,769 g/mol, $Đ$ = 1.13

Selective chain extension of RAFT PMMA-co-PFMA with MMA in the presence of TTC 1b, mediated by PheoA: In a 1dr vial, RAFT PMMA-*co*-PFMA (66 mg, 0.01 mmol), furan capped TTC (6.6 mg, 0.01 mmol) and PheoA (0.0237 mg, 0.00004 mmol) were dissolved in 2M solution of MMA (426 µL, 4 mmol) in DMSO (2 mL). The reaction vessel was sealed with a rubber septum, degassed with nitrogen for 20 minutes and irradiated with red light for 23 hours. The reaction was quenched by exposing it to open air and precipitated in methanol. The precipitated polymer was

dried and submitted for ^{1}H NMR and GPC analysis. The supernatant was concentrated and submitted for ^{1}H NMR analysis.

Selective polymerization of MA from TTC 1b, mediated by ZnTPP in the presence of RAFT PMMA-*co*-PFMA: In a 1dr vial, RAFT PMMA-*co*-PFMA (33 mg, 0.005 mmol), furan capped TTC (6.6 mg, 0.01 mmol) and ZnTPP (0.0211 mg, 0.00003 mmol) were dissolved in a solution of MA (450 µL, 5 mmol) in DMSO (2.5 mL). The reaction vessel was sealed with a rubber septum and degassed with nitrogen for 20 minutes. The reaction was irradiated with green light for 30 minutes, 2 cm from the light source.

Scheme IV-S1. Model polymerization of MA from **1b** mediated by ZnTPP.

Polymerization of MA from 1b mediated by ZnTPP: In a 1dr vial, TTC **1b** (6.6 mg, 0.01 mmol) and ZnTPP (0.0211 mg, 0.00003 mmol) were dissolved in a solution of MA (450 µL, 5 mmol) in DMSO (450 µL). The reaction vessel was sealed with a rubber septum and degassed with nitrogen for 20 minutes. The reaction was irradiated with green light for 30 minutes, 2 cm from the light source.

GPC Analysis

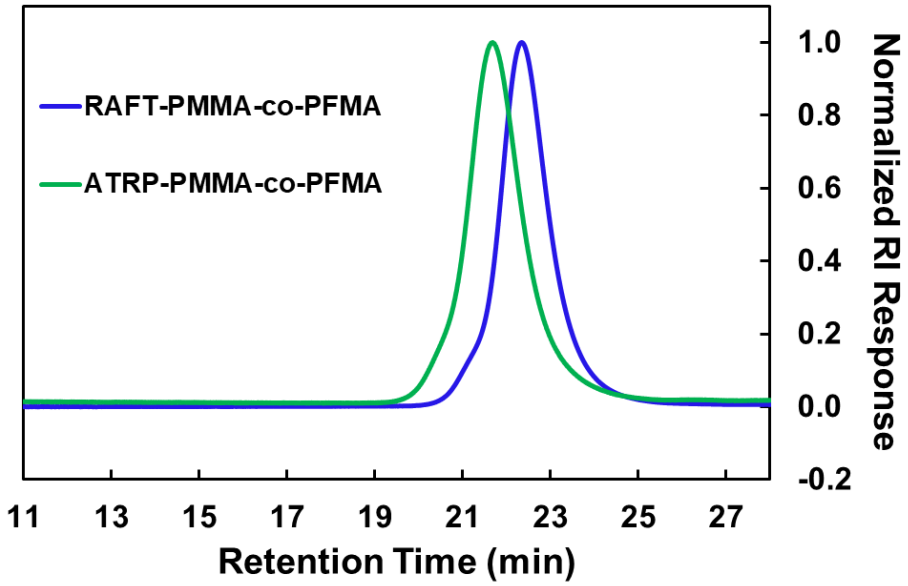

Figure IV-S1. GPC traces of RAFT and ATRP statistical copolymers with FMA.

Table IV-S1. GPC analysis of RAFT and ATRP statistical copolymers with FMA.

Entry	Sample	M_n[a] g/mol	$Đ$[a]
1	RAFT-PMMA-*co*-PFMA	6,300	1.13
2	ATRP-PMMA-*co*-PFMA	8,600	1.16

[a] Molecular weight and polydispersity measured by GPC in THF at 40°C and a flow rate of 1mL/min.

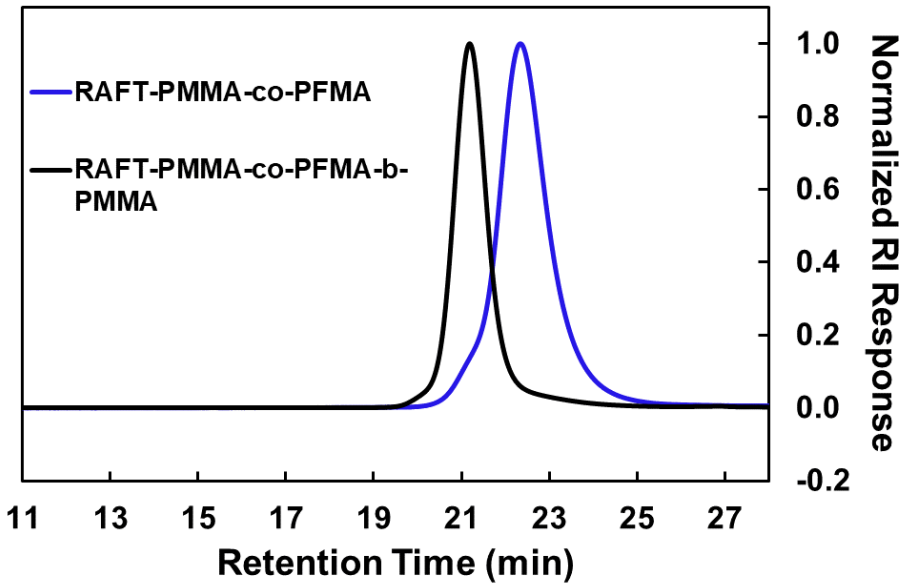

Figure IV-S2. GPC trace of RAFT-PMMA-*co*-PFMA chain extension with MMA.

Table IV-S2. GPC analysis of RAFT-PMMA-*co*-PFMA chain extension with MMA.

Entry	Sample	M_n[a] g/mol	$Đ$[a]
1	RAFT-PMMA-*co*-PFMA	6,300	1.13
2	RAFT-PMMA-*co*-PFMA-*b*-PMMA	14,600	1.10

[a] Molecular weight and polydispersity measured by GPC in THF at 40°C and a flow rate of 1mL/min

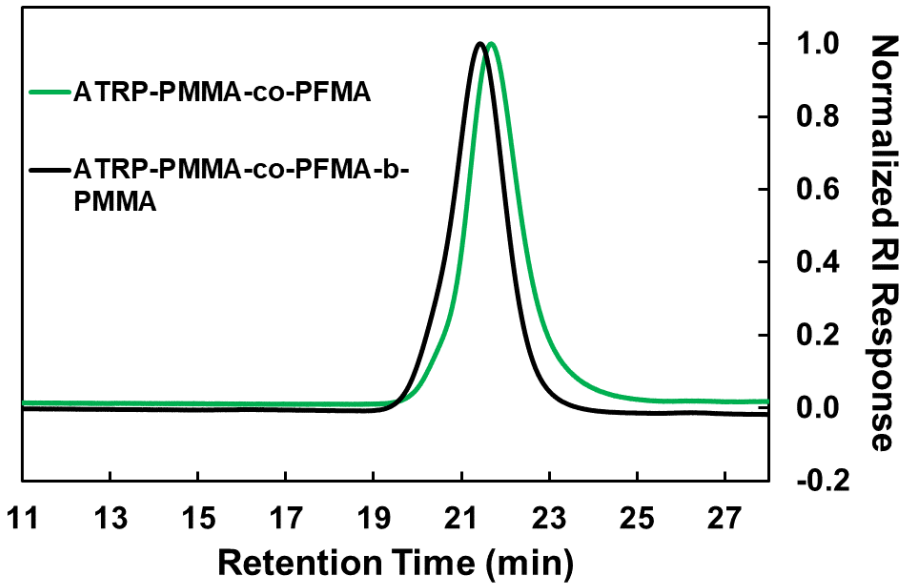

Figure IV-S3. GPC trace of ATRP-PMMA-*co*-PFMA chain extension with MMA.

Table IV-S3. GPC analysis of ATRP-PMMA-*co*-PFMA chain extension with MMA.

Entry	Sample	M_n[a] g/mol	$Đ$[a]
1	ATRP-PMMA-*co*-PFMA	8,600	1.16
2	ATRP-PMMA-*co*-PFMA-*b*-PMMA	10,800	1.13

[a] Molecular weight and polydispersity measured by GPC in THF at 40°C and a flow rate of 1mL/min.

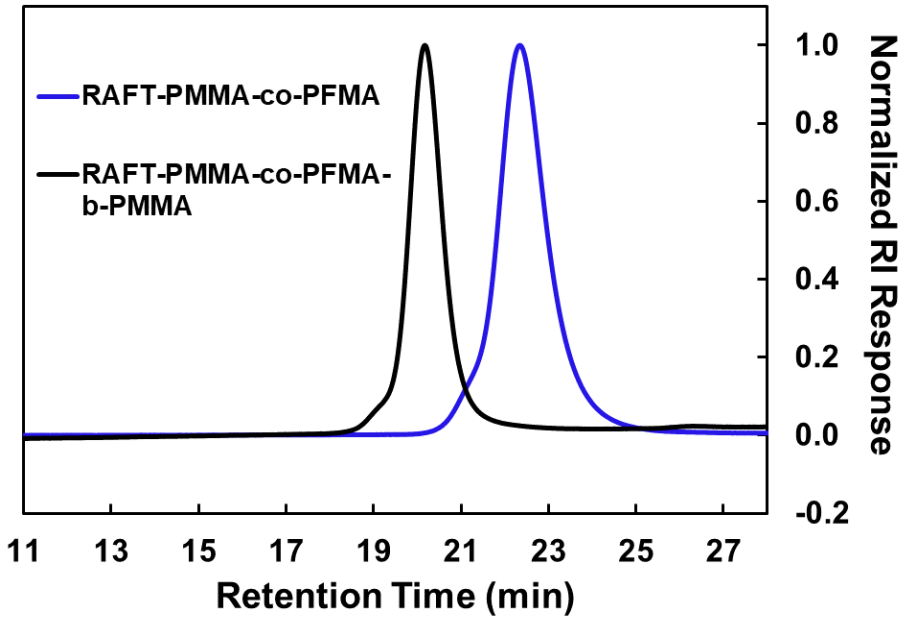

Figure IV-S4. GPC trace of RAFT-PMMA-*co*-PFMA chain extension with MMA in the presence of **1b**.

Table IV-S4. GPC analysis of RAFT-PMMA-*co*-PFMA chain extension with MMA in the presence of **1b**.

Entry	Sample	M_n[a] g/mol	$Đ$[a]
1	RAFT-PMMA-*co*-PFMA	6,300	1.13
2	RAFT-PMMA-*co*-PFMA-*b*-PMMA	20,000	1.10

[a] Molecular weight and polydispersity measured by GPC in THF at 40°C and a flow rate of 1mL/min.

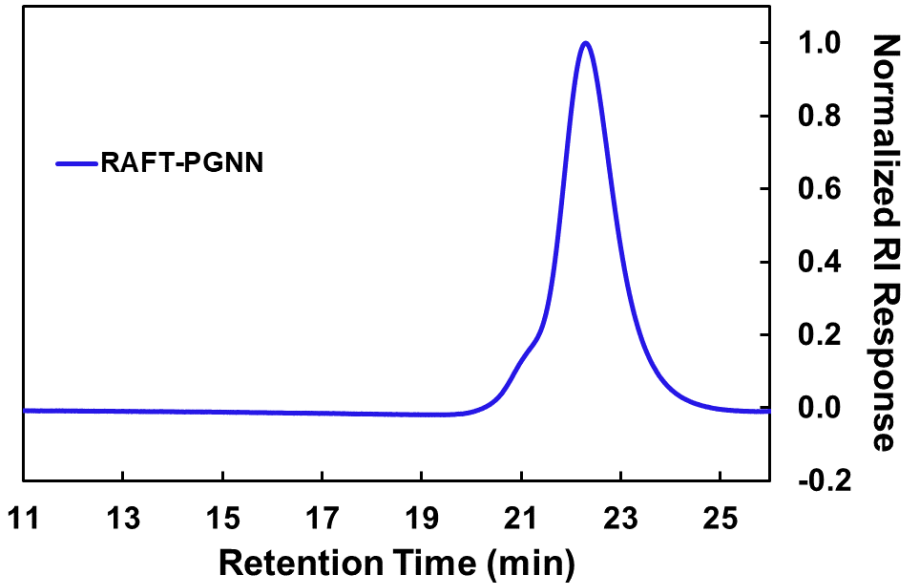

Figure IV-S5. GPC trace of RAFT-PGNN.

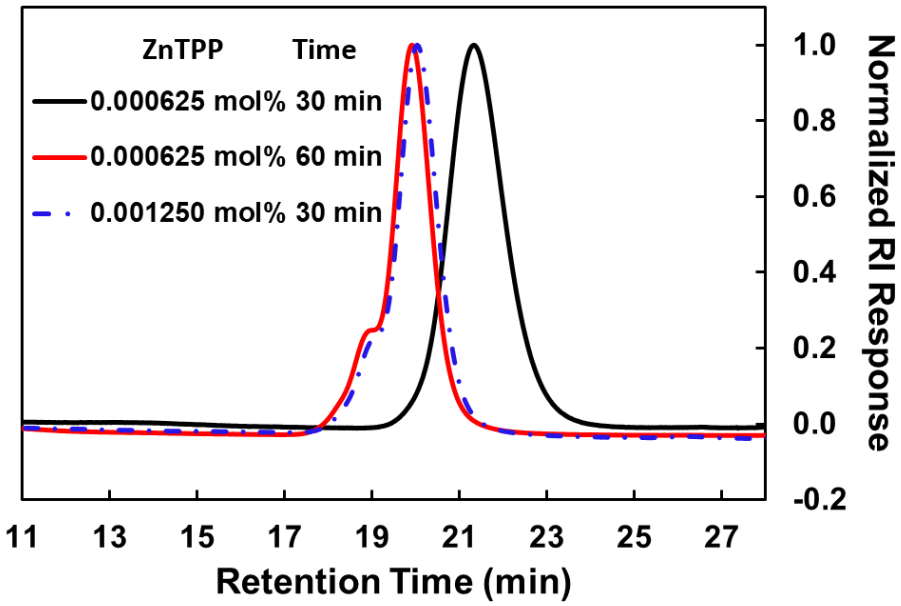

Figure IV-S6. GPC traces of MA polymerizations from **1b** mediated by ZnTPP.

Table IV-S5. GPC analysis of MA polymerizations from **1b** mediated by ZnTPP.

Entry	Sample	ZnTPP mol%	Time (min)	M_n[a] g/mol	$Đ$[a]
1	PMA	0.000625	30	10,400	1.13
2	PMA	0.000625	60	25,400	1.17
3	PMA	0.001250	30	23,400	1.16

[a] Molecular weight and polydispersity measured by GPC in THF at 40°C and a flow rate of 1mL/min.

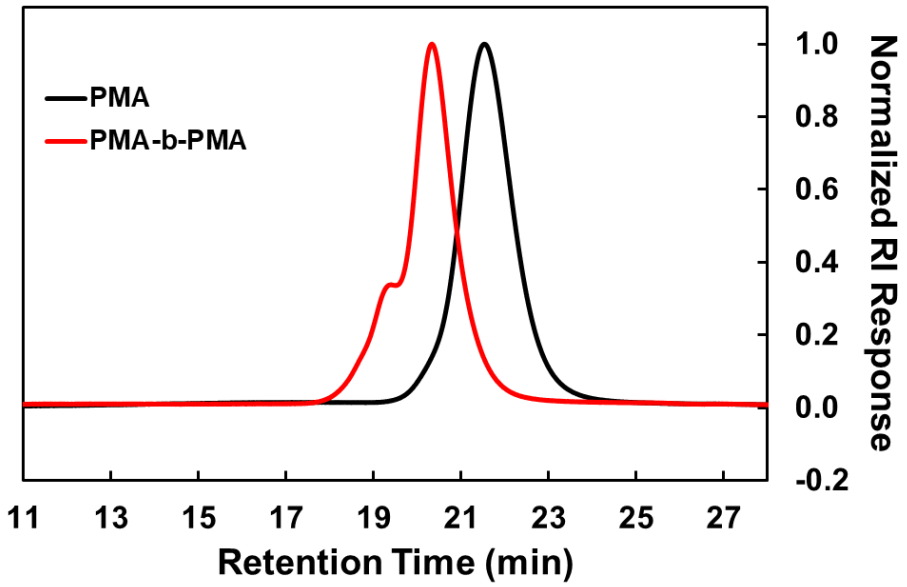

Figure IV-S7. GPC trace of PMA chain extension with MA and 0.000625 mol% ZnTPP.

Table IV-S6. GPC analysis of PMA chain extension with MA and 0.000625 mol% ZnTPP.

Entry	Sample	M_n[a] g/mol	$Đ$[a]
1	PMA	16,200	1.15
2	PMA-*b*-PMA	34,700	1.25

[a] Molecular weight and polydispersity measured by GPC in THF at 40°C and a flow rate of 1mL/min.

Table IV-S7. GPC analysis and comparison of MA polymerization with BTPA mediated by ZnTPP.

Entry	Sample	M_n[a] g/mol	$Đ$[a]
1	PMA	13,700	1.07
2	PMA from literature[13]	13,100	1.09

[a] Molecular weight and polydispersity measured by GPC in THF at 40°C and a flow rate of 1mL/min.

Selected TEM Images

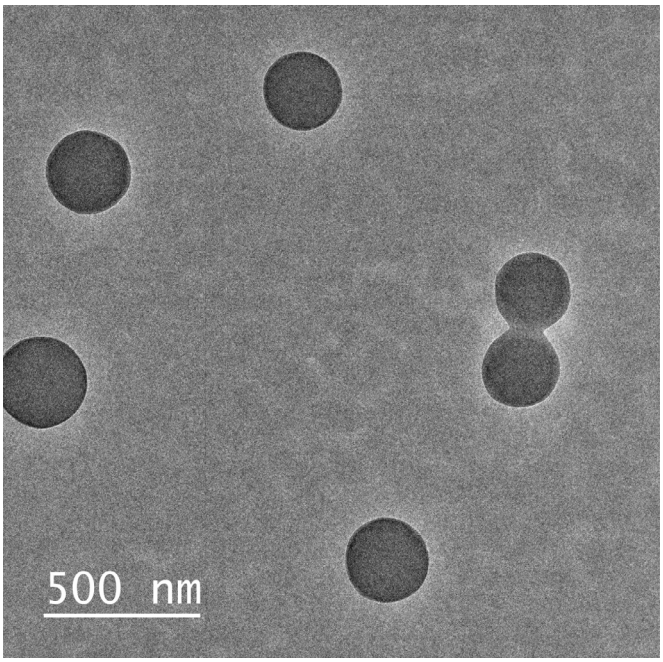

Figure IV-S8. TEM image of RAFT-PGNN.

NMR Analysis

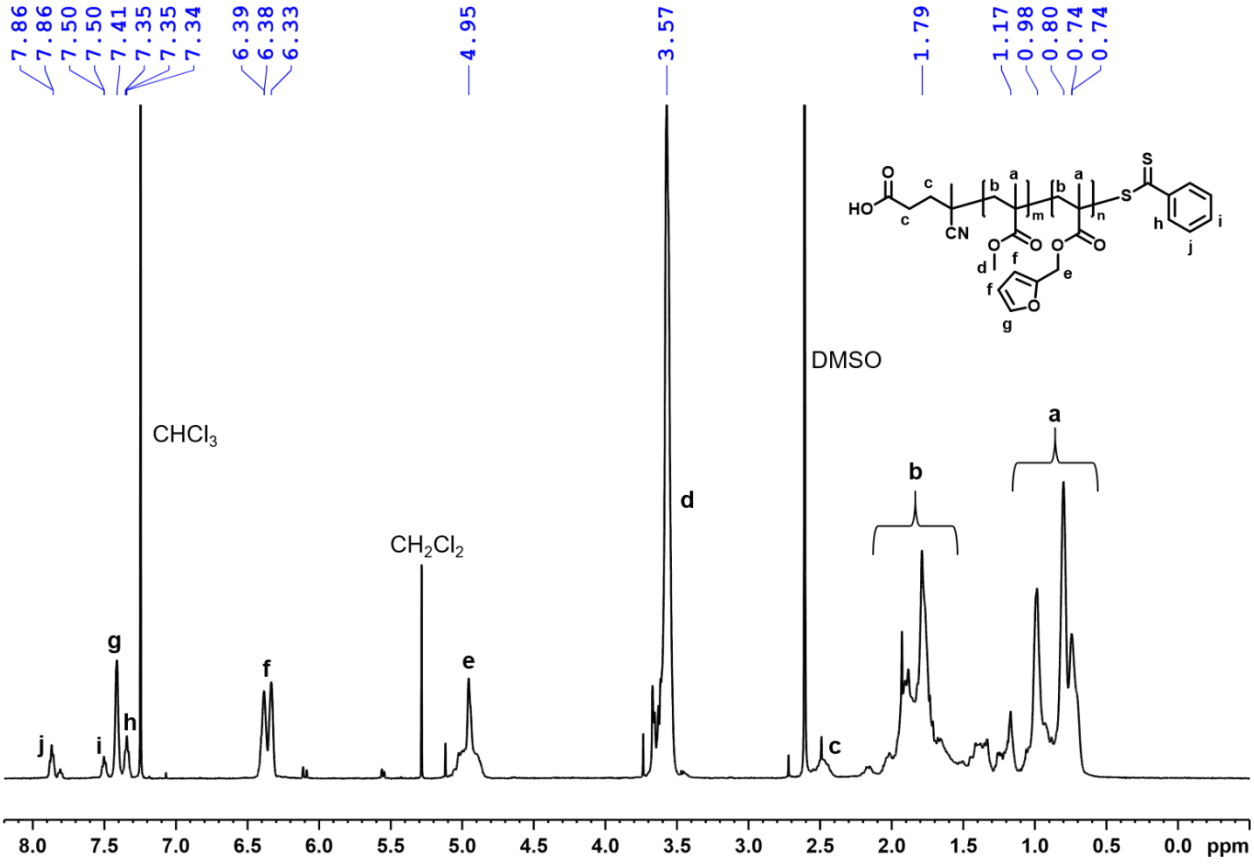

Figure IV-S9. ^{1}H NMR ($CDCl_3$, 600 MHz) of RAFT-PMMA-*co*-PFMA.

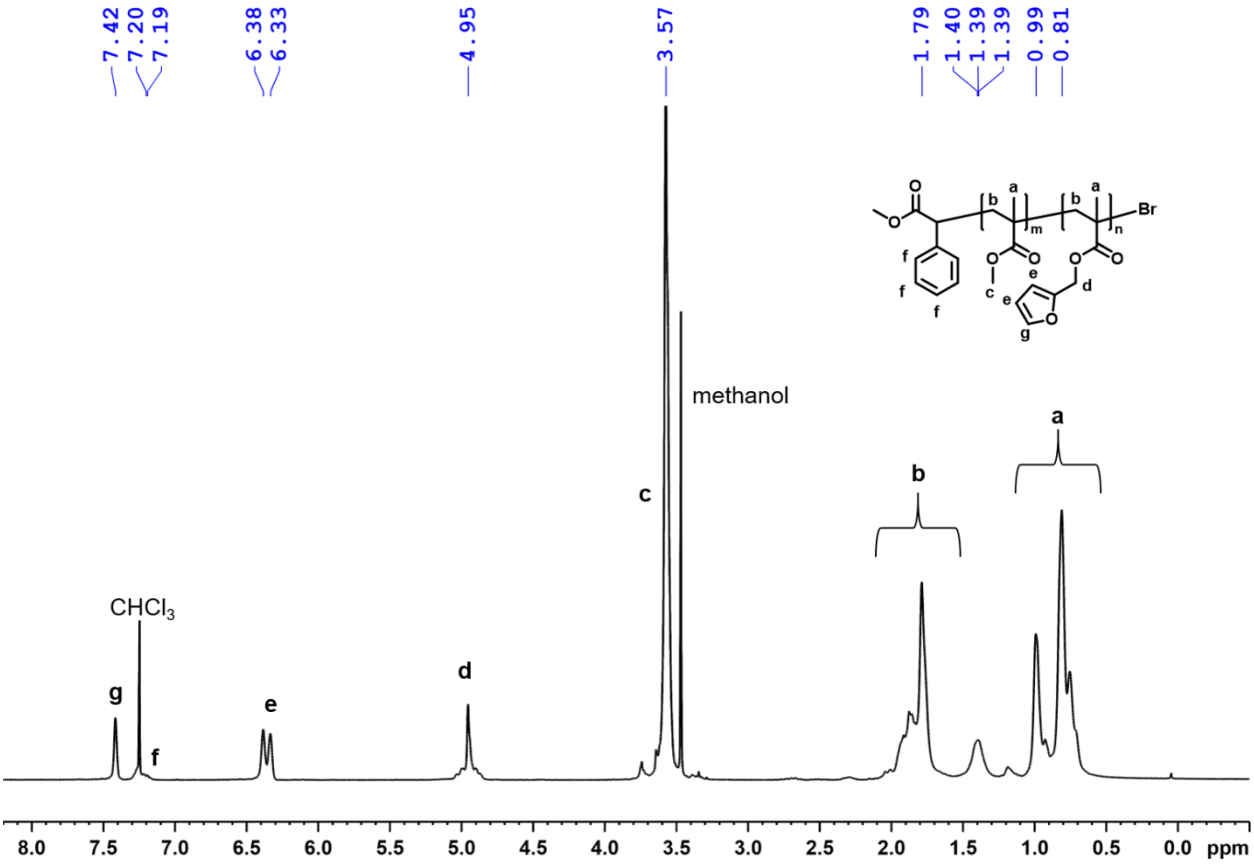

Figure IV-S10. ^{1}H NMR ($CDCl_3$, 400 MHz) of ATRP-PMMA-*co*-PFMA.

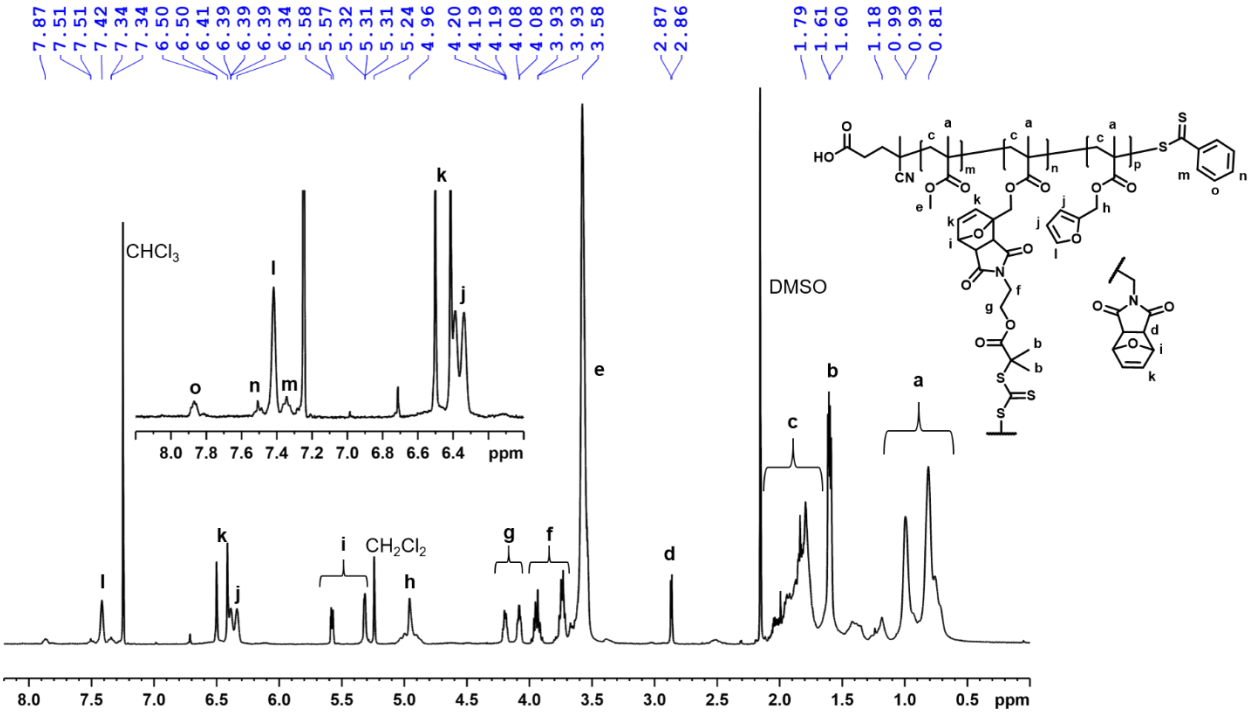

Figure IV-S11. ^{1}H NMR ($CDCl_3$, 600 MHz) of RAFT-PGNN.

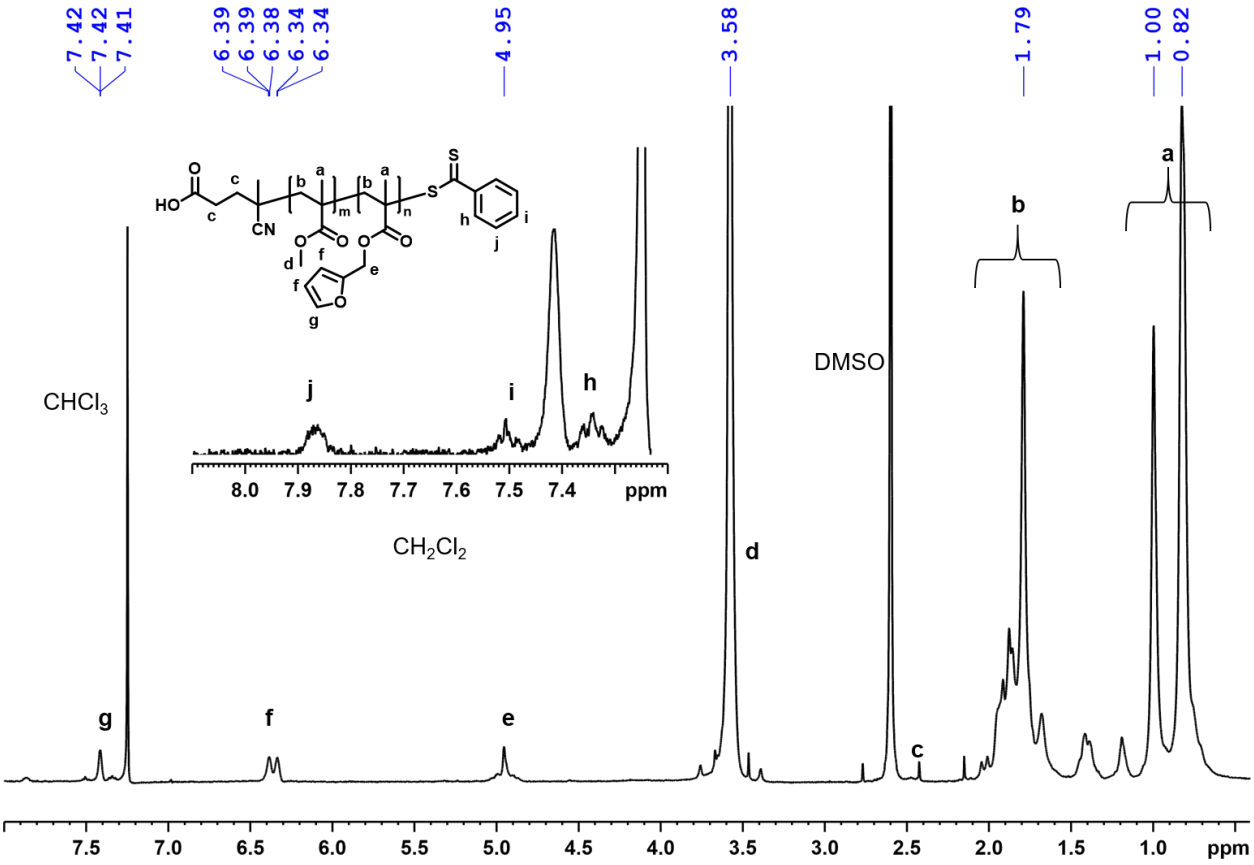

Figure IV-S12. ^{1}H NMR ($CDCl_3$, 600 MHz) of RAFT-PMMA-*co*-PFMA-*b*-PMMA produced in the presence of **1b**.

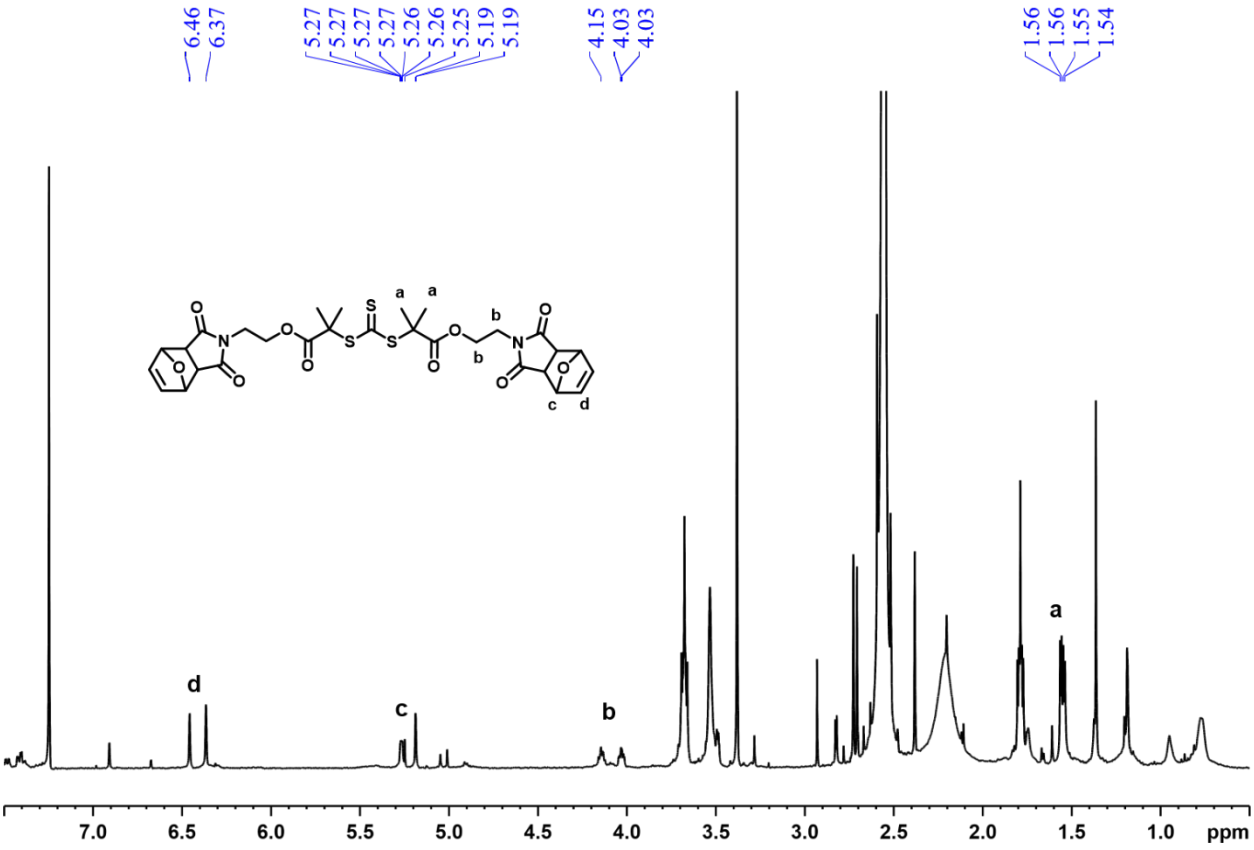

Figure IV-S13. Crude ^{1}H NMR ($CDCl_3$, 400 MHz) of concentrated supernatant produced from the chain extension of RAFT-PMMA-*co*-PFMA in the presence of **1b**.

REFERENCES

(1) Cuthbert, J.; Beziau, A.; Gottlieb, E.; Fu, L.; Yuan, R.; Balazs, A. C.; Kowalewski, T.; Matyjaszewski, K., Transformable Materials: Structurally Tailored and Engineered Macromolecular (STEM) Gels by Controlled Radical Polymerization. *Macromolecules* **2018,** *51* (10), 3808-3817.

(2) Sun, H.; Kabb, C. P.; Dai, Y.; Hill, M. R.; Ghiviriga, I.; Bapat, A. P.; Sumerlin, B. S., Macromolecular metamorphosis via stimulus-induced transformations of polymer architecture. *Nature Chemistry* **2017,** *9*, 817.

(3) He, H.; Averick, S.; Mandal, P.; Ding, H.; Li, S.; Gelb, J.; Kotwal, N.; Merkle, A.; Litster, S.; Matyjaszewski, K., Multifunctional Hydrogels with Reversible 3D Ordered Macroporous Structures. *Advanced Science* **2015,** *2* (5), 1500069.

(4) Pereira, R. F.; Sousa, A.; Barrias, C. C.; Bártolo, P. J.; Granja, P. L., A single-component hydrogel bioink for bioprinting of bioengineered 3D constructs for dermal tissue engineering. *Materials Horizons* **2018,** *5* (6), 1100-1111.

(5) Mpoukouvalas, A.; Li, W.; Graf, R.; Koynov, K.; Matyjaszewski, K., Soft Elastomers via Introduction of Poly(butyl acrylate) "Diluent" to Poly(hydroxyethyl acrylate)-Based Gel Networks. *ACS Macro Lett.* **2013,** *2* (1), 23-26.

(6) Matsukawa, K.; Masuda, T.; Akimoto, A. M.; Yoshida, R., A surface-grafted thermoresponsive hydrogel in which the surface structure dominates the bulk properties. *Chem. Commun.* **2016,** *52* (74), 11064-11067.

(7) Shanmugam, S.; Cuthbert, J.; Flum, J.; Fantin, M.; Boyer, C.; Kowalewski, T.; Matyjaszewski, K., Transformation of gels via catalyst-free selective RAFT photoactivation. *Polym. Chem.* **2019**.

(8) Chen, M.; Gu, Y.; Singh, A.; Zhong, M.; Jordan, A. M.; Biswas, S.; Korley, L. T. J.; Balazs, A. C.; Johnson, J. A., Living Additive Manufacturing: Transformation of Parent Gels into Diversely Functionalized Daughter Gels Made Possible by Visible Light Photoredox Catalysis. *ACS Central Science* **2017,** *3* (2), 124-134.

(9) Zhou, H.; Johnson, J. A., Photo-controlled Growth of Telechelic Polymers and End-linked Polymer Gels. *Angew. Chem. Int. Ed.* **2013,** *52* (8), 2235-2238.

(10) Beziau, A.; Fortney, A.; Fu, L.; Nishiura, C.; Wang, H.; Cuthbert, J.; Gottlieb, E.; Balazs, A. C.; Kowalewski, T.; Matyjaszewski, K., Photoactivated Structurally Tailored and Engineered Macromolecular (STEM) gels as precursors for materials with spatially differentiated mechanical properties. *Polymer* **2017,** *126*, 224-230.

(11) Cuthbert, J.; Martinez, M. R.; Sun, M.; Flum, J.; Li, L.; Olszewski, M.; Wang, Z.; Kowalewski, T.; Matyjaszewski, K., Non-Tacky Fluorinated and Elastomeric STEM Networks. *Macromol. Rapid Commun.* **2019,** *0* (0), 1800876.

(12) Lampley, M. W.; Harth, E., Photocontrolled Growth of Cross-Linked Nanonetworks. *ACS Macro Lett.* **2018,** *7* (6), 745-750.

(13) Shanmugam, S.; Xu, J.; Boyer, C., Exploiting Metalloporphyrins for Selective Living Radical Polymerization Tunable over Visible Wavelengths. *J. Am. Chem. Soc.* **2015,** *137* (28), 9174-9185.

(14) Xu, J.; Shanmugam, S.; Fu, C.; Aguey-Zinsou, K.-F.; Boyer, C., Selective Photoactivation: From a Single Unit Monomer Insertion Reaction to Controlled Polymer Architectures. *J. Am. Chem. Soc.* **2016,** *138* (9), 3094-3106.

(15) Theriot, J. C.; Miyake, G. M.; Boyer, C. A., N,N-Diaryl Dihydrophenazines as Photoredox Catalysts for PET-RAFT and Sequential PET-RAFT/O-ATRP. *ACS Macro Lett.* **2018,** *7* (6), 662-666.

(16) Kwak, R. N. Y.; Matyjaszewski, K., Dibromotrithiocarbonate Iniferter for Concurrent ATRP and RAFT Polymerization. Effect of Monomer, Catalyst, and Chain Transfer Agent Structure on the Polymerization Mechanism. *Macromolecules* **2008,** *41* (13), 4585-4596.

(17) Hanlon, A. M.; Martin, I.; Bright, E. R.; Chouinard, J.; Rodriguez, K. J.; Patenotte, G. E.; Berda, E. B., Exploring structural effects in single-chain "folding" mediated by intramolecular thermal Diels-Alder chemistry. *Polym. Chem.* **2017,** *8* (34), 5120-5128.

(18) Pramanik, N. B.; Mondal, P.; Mukherjee, R.; Singha, N. K., A new class of self-healable hydrophobic materials based on ABA triblock copolymer via RAFT polymerization and Diels-Alder “click chemistry”. *Polymer* **2017,** *119*, 195-205.

CHAPTER V

PROGRESS TOWARDS THE PREPARATION AND PHOTOCONTROLLED GROWTH OF SELF-ASSEMBLED PHOTORESPONSIVE MATERIALS

INTRODUCTION

There has been an ongoing interest in the manipulation of functional materials post network formation.[1-5] These manipulations have been executed with several reversible deactivation radical polymerization (RDRP) techniques, such as reversible addition-fragmentation chain-transfer (RAFT),[6] atom transfer radical polymerization (ATRP),[7] and nitroxide mediated polymerization (NMP),[8] which allowed for the controlled modification of the polymer networks. Precise manipulations of networks, both in the bulk[1, 9-13] and on the nanoscale,[14] were advanced through the development and implementation of light-mediated polymerizations[13, 15-16] which provided greater external control and thus greater spatial and temporal control.

We have recently developed a nanoparticle system crosslinked with trithiocarbonates (TTC) capable of experiencing precise manipulations through a photoredox mediated polymerization.[14] Through this process photogrowable nanonetworks (PGNNs) can be controllably altered in both size and network properties to produce differentiated progeny that inherit the properties of the newly integrated polymer chains. We now seek to investigate the effects this photogrowth process has on network architectures and morphologies.

Self-complementary quadruple hydrogen bonding motif 2-ureido-4[1H]-pyrimidinone (UPy) has been exploited to prepare a variety of reversible self-assembling supramolecular polymers, hydrogels, and nanofibers.[17-26] Ureido-pyrimidinones possess a hydrogen bond

acceptor-acceptor-donor-donor type structure that allows them to effectively dimerize through complementary hydrogen bonding (**Figure V-1A**). When urea or urethane (U) groups are positioned in close proximity to the UPy (UPy-U), additional lateral stacking is obtained through hydrogen bonding between urea or urethane groups to form stacks of Upy dimers. (**Figure V-1B**). Additionally, Bis-UPy-U compounds that possess a sufficiently long spacer between UPy moieties

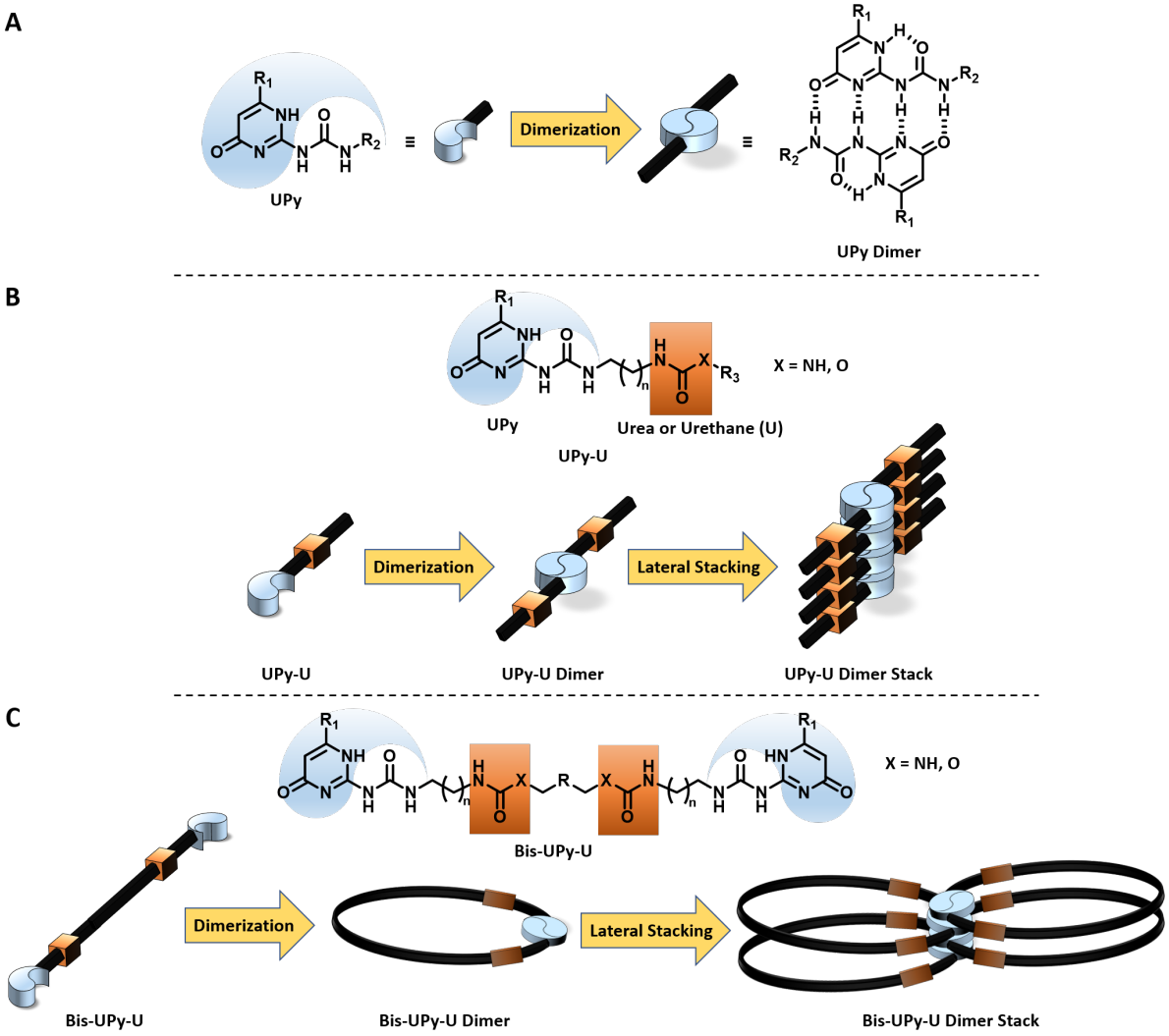

Figure V-1. (A) General structures of ureidopyrimidinone (UPy) and its dimer. (B) General structure of UPy with urea or urethane moieties and the illustration of dimerization and lateral stacking. (C) General structure of a Bis-Upy with urea or urethane and the illustration of self-dimerization and lateral stacking.

are capable of self-dimerization which have been demonstrated to undergo lateral stacking to produce nanofibers (**Figure V-1C**).[22]

We envision that the combination of our previously described photogrowth process with a UPy network will allow for the development of a photoresponsive material capable of experiencing morphological transformations from a gel to a fiber type architecture as a result of the introduction of new polymer chains between UPy units (**Figure V-2**). We sought to accomplish this by connecting UPy-Urea units with a TTC through short spacers to prevent self-dimerization. Polymerization from the TTC will increase the distance between UPy units and allow for the formation of self-dimers that can laterally stack to form nanofibers either unaided or

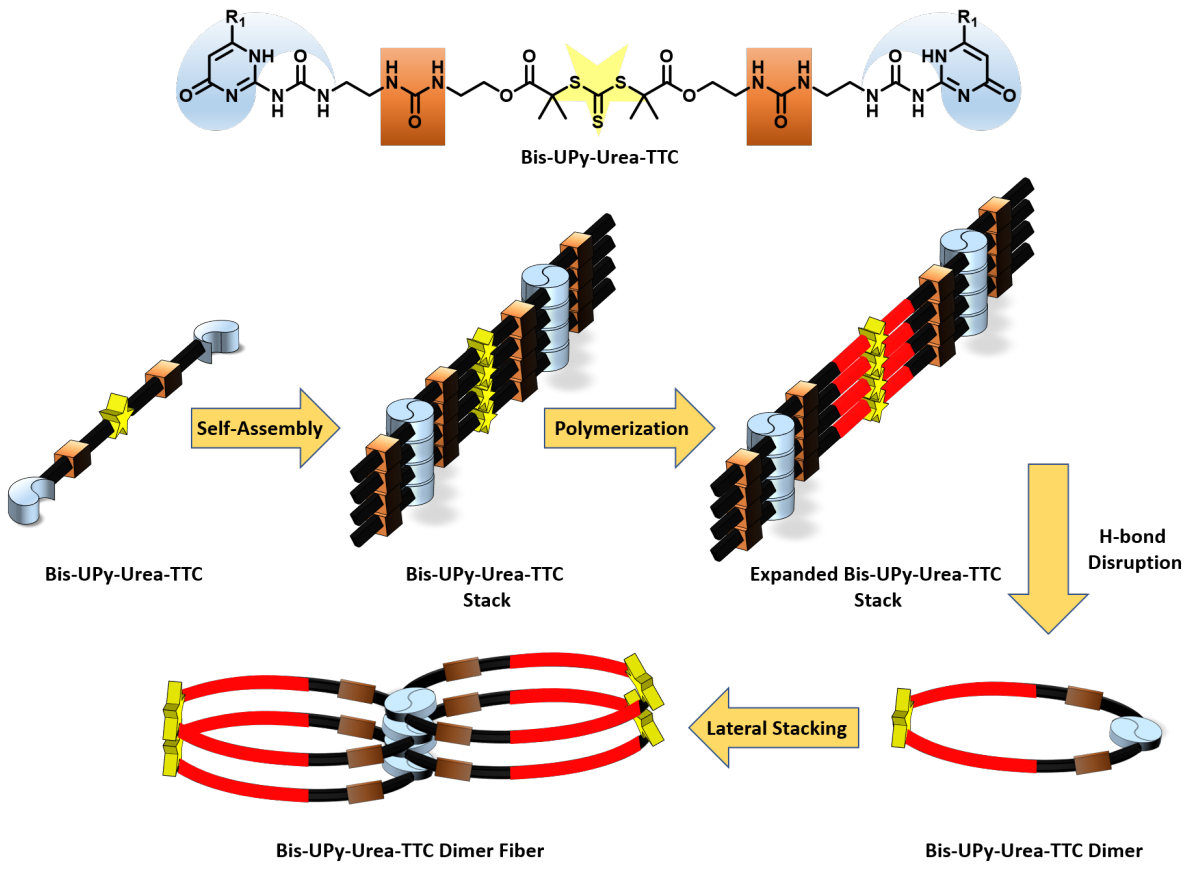

Figure V-2. General structure of the proposed Bis-UPy-Urea-TTC and the schematic description of the proposed transformation from a self-assembled gel to a self-assembled fiber facilitated by polymerization from the TTC.

promoted by hydrogen bond disruption. Herein we aim to examine the synthesis and network formation of a Bis-UPy-Urea-TTC as a means to investigate how the photogrowth process affects self-assembled supramolecular networks.

RESULTS AND DISCUSSION

Synthesis of a Bis-Ureidopyrimidinone-Urea-Trithiocarbonate

To realize this goal, we designed Bis-UPy-Urea-TTC **7**. We chose 6-methylisocytosine **1** as the foundation for our UPy unit due to its synthetic accessibility and the bis-dimethyl TTC as the TTC due to its success in our previous works.[14] We began the synthesis by first preparing 2-aminopyrimidinone **1** from the condensation of guanidine carbonate with ethyl acetoacetate. Pyrimidinone **1** was then reacted with carbonyldimidazole (CDI) to form the imidazole urea **2** which was subsequently reacted with N-Boc-ethylenediamine to produce **3**. Removal of the Boc group was performed with HCl and the hydrochloride salt **4** was used without further purification.

Scheme V-1. Steps to the synthesis of Bis-UPy-Urea-TTC **7**.

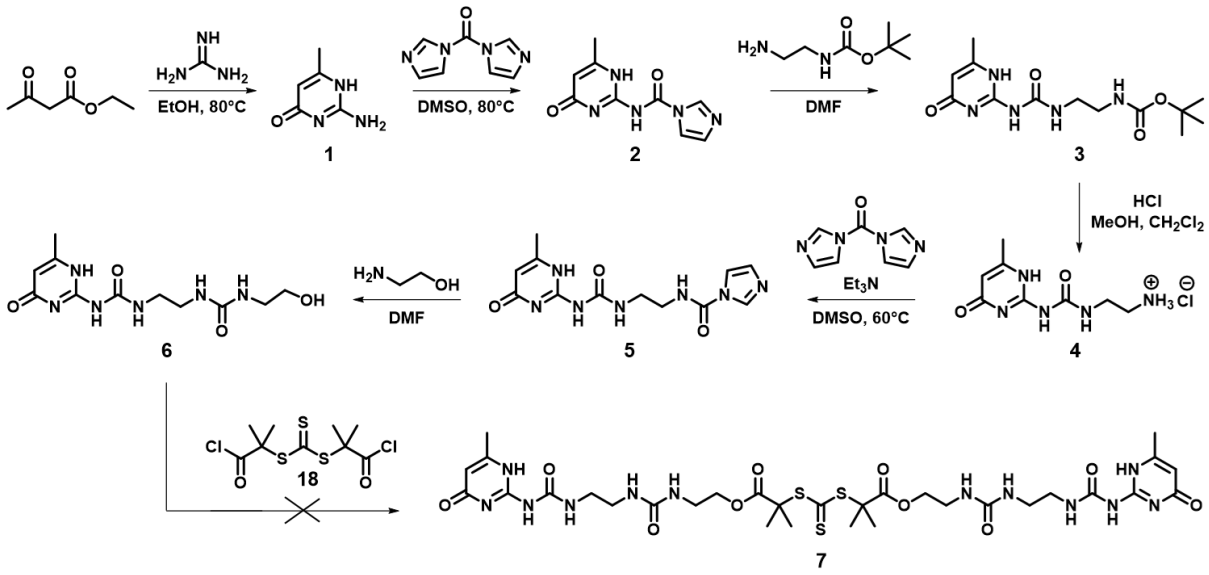

Reaction of **4** with CDI produced the UPy-Urea imidazole **5**. Formation of UPy-Urea **6** proved difficult due to the poor solubility of **5** in organic solvents, however; the reaction did proceed in dimethyl formamide (DMF) albeit with poor yields (< 40%). Unfortunately, UPy-Urea **6** proved to be largely insoluble in organic solvents and only partially soluble in dimethyl sulfoxide (DMSO). The limited solubility and poor yields for compound **6** led to the redesign of the UPy-functionalized TTC.

Substitution of the methyl group on the pyrimidinone for a larger alkyl group such as 1-ethylpentyl has been demonstrated to improve the solubility of other ureidopyrimidiones.[27] For this reason, we elected to alter the design of the Bis-UPy-Urea-TTC to include the 1-ethylpentyl substituted pyrimidinone **9** (**Scheme V-2**). Synthesis of the redesigned Upy began with the preparation of β-oxo ester **8** through the reaction of mono-ethyl malonate and 2-ethylhexanoyl chloride. Cyclization and condensation of **8** with guanidine carbonate afforded 2-

Scheme V-2. Steps to the synthesis of a Bis-UPy-Urea-TTC.

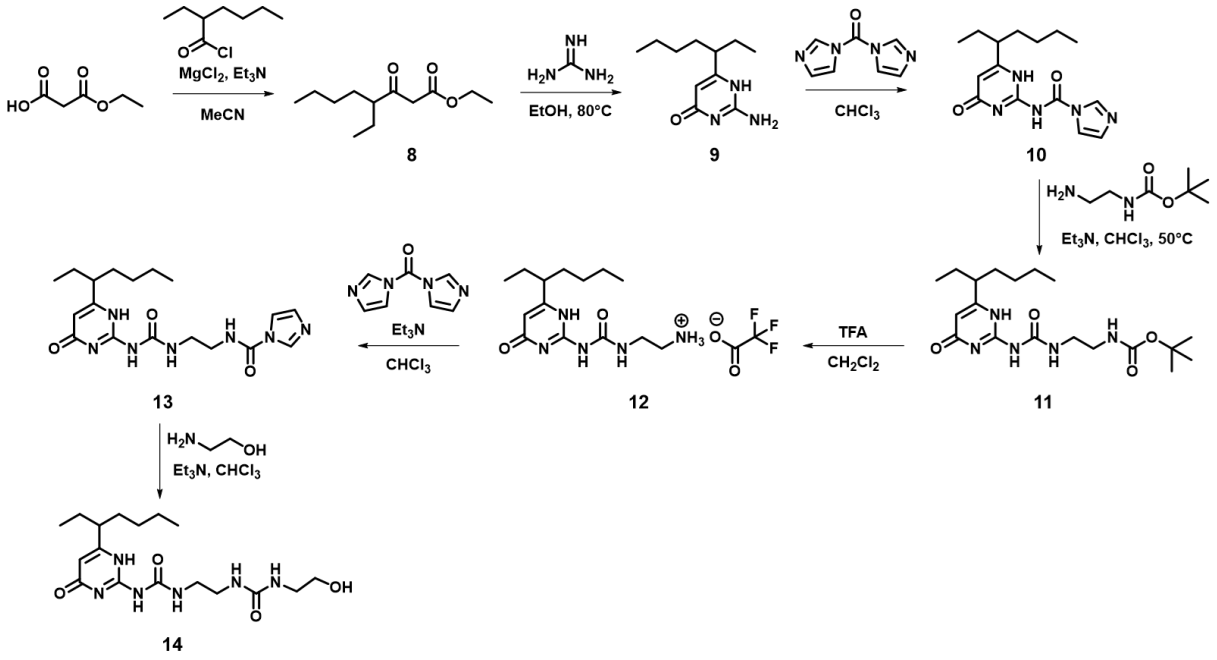

aminoureidopyrimidinone **9.** Addition of CDI followed by N-Boc-ethylenediamine yielded Boc protected UPy **11**. Deprotection of the amine with trifluoroacetic acid (TFA) followed by reaction with CDI provided UPy-Urea imidazole **13**. Preparation and purification of UPy-Urea alcohol **14** proved difficult as NMR suggested that **13** degraded during the reaction and the crude product proved to be significantly more aqueous soluble than previous steps. Additionally, the product proved difficult to purify by column chromatography with silica. The increased aqueous solubility and the difficulty with chromatography was attributed to the presences of the second urea group which increases the hydrogen bonding which in turn makes the compound difficult to work with in acidic environments. For these reasons, we elected to form the urea last.

Scheme V-3. Steps to the synthesis of Bis-UPy-Urea-TTC **17**.

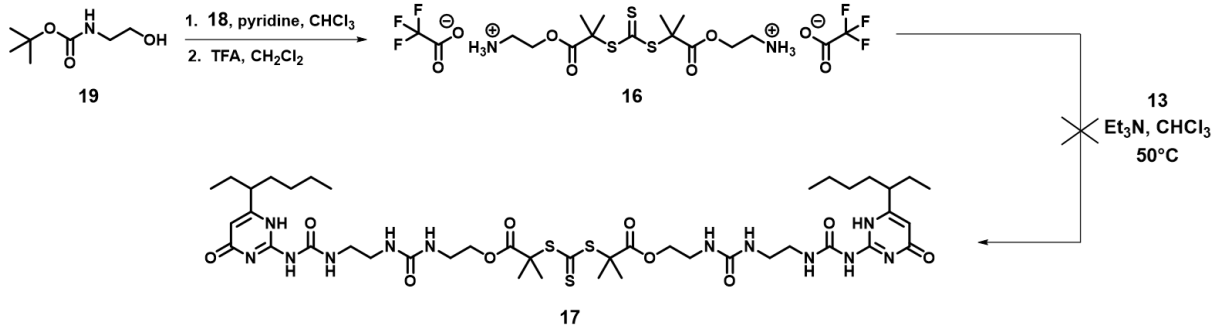

To accomplish this TTC amine salt **16** was prepared through the esterification of acid chloride **7** with N-Boc protected ethanol amine followed by deprotection with TFA (**Scheme V-3**). Importantly, no hydrolysis of the ester groups is observed if the reaction is performed under completely anhydrous conditions. Unfortunately, reaction of the amine salt **16** with UPy-Urea imidazole **13** did not produce the desired Bis-UPy-Urea-TTC **17** as degradation of **13** appears to predominate. More work needs to be done to prevent this degradation and determine if a solution is possible or if a new synthetic route is required.

CONCLUSION

Here we described the design and progress towards the preparation of a Bis-UPy-Urea-TTC. Despite the current synthetic setbacks, the preparation of a symmetrical UPy-Urea functionalized RAFT agent will be possible with some adaptations to the current synthetic route. Preparation and implementation of a Bis-UPy-Urea-TTC stands to offer the opportunity to study the manipulation of network morphology and architecture through a photogrowth process.

EXPERIMENTAL

Materials:

All reagents and solvents were purchased from Sigma Aldrich and used as received unless otherwise stated. Chloroform, acetonitrile (MeCN), and dichloromethane were all purchased as anhydrous. Compounds **1**,[28] **2**,[29] **8**,[30] **9-10**,[31] **18**,[14] and **19**[32] were prepared as previously described.

Characterization:

All ^{1}H spectra were obtained using a JEOL ECA 400 (400 MHz), or ECA-600 (600 MHz) spectrometer.

Synthesis:

tert-butyl (2-(3-(6-methyl-4-oxo-1,4-dihydropyrimidin-2-yl)ureido)ethyl)carbamate (3)

In a flame dried round bottom flask, **2** (1.72 g, 7.78 mmol, 1 eq) was suspended in DMF (13 mL) and N-Boc-ethylenediamine (1.48 mL, 9.34 mmol, 1.2 eq) was added under argon. The resulting mixture stirred for 18 hours after which a white precipitate formed. Acetone (20 mL) was added

to the reaction and the white precipitate was filtered and washed with acetone to afford **3** (2.38 g, 98%). ^{1}H NMR (400 MHz, $CDCl_3$) δ 5.82 (s, 1H), 3.34 (br s, 4H), 2.23 (s, 3H), 1.42 (s, 9H).

1-(2-aminoethyl)-3-(6-methyl-4-oxo-1,4-dihydropyrimidin-2-yl)urea hydrochloride (4)

To a round bottom flask was added **3** (2.2 g, 7.07 mmol), MeOH (20 mL), CH_2Cl_2 (20 mL), and HCl (2.5 mL). The resulting solution was stirred for 4 hours after which the reaction was concentrated and CH_2Cl_2 (20 mL) was added to precipitate the product. The suspension was then filtered to afford **4** (1.68 g, 96%). ^{1}H NMR (600 MHz, DMSO-d_6) 6.05 (s, 1H) 3.38 (q, J=6 Hz, 2H), 2.87 (q, J=6 Hz, 2H), 2.2 (s, 3H).

N-(2-(3-(6-methyl-4-oxo-1,4-dihydropyrimidin-2-yl)ureido)ethyl)-1H-imidazole-1-carboxamide (5)

To a flame dried flask, **4** (220 mg, 0.89 mmol, 1 eq), $CHCl_3$ (24 mL), and Et_3N (185 uL, 1.33 mmol, 1.5 eq) were added and the resulting mixture stirred at 60°C for 30 minutes after which CDI (187 mg, 1.15 mmol, 1.3 eq) was added. The reaction then stirred at 60°C for 1.5 hours. The reaction was cooled to room 0°C and water (40 uL) was added to decompose any remaining CDI. The reaction was then concentrated, and the mixture was carried forward without further purification. ^{1}H NMR (600 MHz, DMSO-d_6) 8.25 (s, 1H), 7.69 (s, 1H), 5.72 (s, 1H), 6.05 (s, 1H) 3.32 (s, 4H), 2.0 (s, 3H).

1-(2-(3-(2-hydroxyethyl)ureido)ethyl)-3-(6-methyl-4-oxo-1,4-dihydropyrimidin-2-yl)urea (6)

Reaction mixture of **5** was suspended in DMF (10 mL) then ethanol amine (53 uL, 0.89 mmol) and Et_3N (124 uL, 0.89 mmol) were added. The resulting mixture stirred for 24 hours and then acetone was added to precipitate the product which was then isolated by filtration to afford **6** (100 mg, 37%). ^1H NMR (400 MHz, DMSO-d_6) 5.78 (s, 1H), 3.35 (q, 6 Hz, 2H) 3.1 (m, 4H), 3.05 (q, 6 Hz, 2H), 2.1 (s, 3H).

tert-butyl (2-(3-(6-(heptan-3-yl)-4-oxo-1,4-dihydropyrimidin-2-yl)ureido)ethyl)carbamate (11)

To a flame dried flask, **10** (583 mg, 1.92 mmol, 1eq), N-Boc-ethylenediamine (339 mg, 2.11 mmol, 1.1eq), Et_3N (294 uL, 1.72 mmol, 1.1 eq), and $CHCl_3$ (5 mL) were added. The reaction stirred for 3 hours at 50°C after which the reaction washed twice with 1 M HCl and water the organic layer dried over Na_2SO_4 before concentration to provide **11** (720 mg, 95%). ^1H NMR (400 MHz, $CDCl_3$) δ 5.80 (s, 1H), 3.35 (br s, 4H), 2.29 (m, 1H), 1.54 (m, 4H), 1.42 (s, 9H), 1.25 (m, 4H), 0.87 (m, 6H).

1-(2-aminoethyl)-3-(6-(heptan-3-yl)-4-oxo-1,4-dihydropyrimidin-2-yl)urea, 2,2,2- acetate salt (12)

To a round bottom flask, **11** (600 mg, 1.52 mmol), TFA (2 mL), and CH_2Cl_2 (8 mL) were added. The reaction stirred for 2 hours after which the reaction was concentrated to afford **12** (609 mg, 98%) which was used without further purification. ^1H NMR (400 MHz, $CDCl_3$) δ 6.11 (s, 1H), 3.65 (br s, 2H), 3.30 (br s, 2H), 2.51 (m, 1H), 1.65 (m, 4H), 1.24 (m, 4H), 0.87 (m, 6H).

N-(2-(3-(6-(heptan-3-yl)-4-oxo-1,4-dihydropyrimidin-2-yl)ureido)ethyl)-1H-imidazole-1-carboxamide (13)

To a flame dried flask, **12** (373 mg, 0.91 mmol, 1 eq), CDI (191 mg, 1.18 mmol, 1.3 eq), Et_3N (164 uL, 1.18 mmol, 1.3 eq), and $CHCl_3$ (5 mL) were added. The reaction stirred 1 hour after which the reaction was diluted with $CHCl_3$ and washed with 1M HCl, then water. The organic layer was collected, dried over Na_2SO_4, and concentrated to afford **13** (304 mg, 86%). ^1H NMR (400 MHz, $CDCl_3$) δ 8.3 (s, 1H), 7.56 (s, 1H), 7.05 (s, 1H), 5.87 (s, 1H), 3.65 (br s, 2H), 3.53 (br s, 2H), 2.38 (m, 1H), 1.63 (m, 4H), 1.26 (m, 4H), 0.88 (m, 6H).

1-(6-(heptan-3-yl)-4-oxo-1,4-dihydropyrimidin-2-yl)-3-(2-(3-(2-hydroxyethyl)ureido)ethyl)urea (14)

To a flame dried flask, **13** (200 mg, 0.51 mmol, 1 eq) Et_3N (79 uL, 0.56 mmol, 1.1 eq), ethanol amine (34 uL, 0.56 mmol, 1.1 eq), and $CHCl_3$ (5 mL) were added. The reaction stirred for 24 hours after which the reaction was concentrated. Crude ^1H NMR (400 MHz, $CDCl_3$) δ 5.77 (s, 1H), 3.65 (br s, 2H), 3.50 (br s, 2H), 3.28 (m, 4H), 2.29 (m, 1H), 1.54 (m, 4H), 1.24 (m, 4H), 0.82 (m, 6H).

bis(2-((tert-butoxycarbonyl)amino)ethyl) 2,2'-(thiocarbonylbis(sulfanediyl))bis(2-methylpropanoate) (15)

To flame dried flask, **19** (1.05 g, 6.52 mmol, 2.2 eq), pyridine (525 uL, 6.52 mmol, 2.2 eq) and $CHCl_3$ (15 mL) were added. A solution of **18** (939 mg, 2.96 mmol, 1 eq) in $CHCl_3$ (5 mL) was added dropwise to the flask under argon at 0°C. The reaction stirred for 1 hour at 0°C and then at room temperature for 2 hours. The reaction was then diluted with $CHCl_3$ and washed with 1M

HCl, sat. $NaHCO_3$, and the organic layer dried over Na_2SO_4, and concentrated to afford **15** (1.56 g, 93%) ^{1}H NMR (400 MHz, $CDCl_3$) δ 4.15 (t, J=4Hz, 4H), 3.35 (q, J=5Hz, 4H), 1.65 (s, 12H), 1.42 (s, 18H).

bis(2-aminoethyl) 2,2'-(thiocarbonylbis(sulfanediyl))bis(2-methylpropanoate), 2,2,2-trifluoroacetate salt (16)

To a flame dried flask, **15** (1 g, 1.76 mmol), TFA (3 mL), and CH_2Cl_2 (12 mL) were added. The reaction stirred for 2 hours after which the solvent was removed and the product **16** (1 g, 96%) was used without further purification. ^{1}H NMR (400 MHz, $CDCl_3$) δ 4.41 (t, J=4Hz, 4H), 3.38 (q, J=5Hz, 4H), 1.69 (s, 12H).

REFERENCES

(1) Cuthbert, J.; Beziau, A.; Gottlieb, E.; Fu, L.; Yuan, R.; Balazs, A. C.; Kowalewski, T.; Matyjaszewski, K., Transformable Materials: Structurally Tailored and Engineered Macromolecular (STEM) Gels by Controlled Radical Polymerization. *Macromolecules* **2018,** *51* (10), 3808-3817.

(2) Sun, H.; Kabb, C. P.; Dai, Y.; Hill, M. R.; Ghiviriga, I.; Bapat, A. P.; Sumerlin, B. S., Macromolecular metamorphosis via stimulus-induced transformations of polymer architecture. *Nature Chemistry* **2017,** *9*, 817.

(3) Matsukawa, K.; Masuda, T.; Akimoto, A. M.; Yoshida, R., A surface-grafted thermoresponsive hydrogel in which the surface structure dominates the bulk properties. *Chem. Commun.* **2016,** *52* (74), 11064-11067.

(4) Mpoukouvalas, A.; Li, W.; Graf, R.; Koynov, K.; Matyjaszewski, K., Soft Elastomers via Introduction of Poly(butyl acrylate) "Diluent" to Poly(hydroxyethyl acrylate)-Based Gel Networks. *ACS Macro Lett.* **2013,** *2* (1), 23-26.

(5) He, H.; Averick, S.; Mandal, P.; Ding, H.; Li, S.; Gelb, J.; Kotwal, N.; Merkle, A.; Litster, S.; Matyjaszewski, K., Multifunctional Hydrogels with Reversible 3D Ordered Macroporous Structures. *Advanced Science* **2015,** *2* (5), 1500069.

(6) Boyer, C.; Bulmus, V.; Davis, T. P.; Ladmiral, V.; Liu, J.; Perrier, S., Bioapplications of RAFT Polymerization. *Chem. Rev.* **2009,** *109* (11), 5402-5436.

(7) Anastasaki, A.; Nikolaou, V.; Nurumbetov, G.; Wilson, P.; Kempe, K.; Quinn, J. F.; Davis, T. P.; Whittaker, M. R.; Haddleton, D. M., Cu(0)-Mediated Living Radical Polymerization: A Versatile Tool for Materials Synthesis. *Chem. Rev.* **2016,** *116* (3), 835-877.

(8) Harth, E.; Hawker, C. J.; Fan, W.; Waymouth, R. M., Chain End Functionalization in Nitroxide-Mediated "Living" Free Radical Polymerizations. *Macromolecules* **2001,** *34* (12), 3856-3862.

(9) Chen, M.; Gu, Y.; Singh, A.; Zhong, M.; Jordan, A. M.; Biswas, S.; Korley, L. T. J.; Balazs, A. C.; Johnson, J. A., Living Additive Manufacturing: Transformation of Parent Gels into Diversely Functionalized Daughter Gels Made Possible by Visible Light Photoredox Catalysis. *ACS Central Science* **2017,** *3* (2), 124-134.

(10) Zhou, H.; Johnson, J. A., Photo-controlled Growth of Telechelic Polymers and End-linked Polymer Gels. *Angew. Chem. Int. Ed.* **2013,** *52* (8), 2235-2238.

(11) Cuthbert, J.; Martinez, M. R.; Sun, M.; Flum, J.; Li, L.; Olszewski, M.; Wang, Z.; Kowalewski, T.; Matyjaszewski, K., Non-Tacky Fluorinated and Elastomeric STEM Networks. *Macromol. Rapid Commun.* **2019,** *0* (0), 1800876.

(12) Beziau, A.; Fortney, A.; Fu, L.; Nishiura, C.; Wang, H.; Cuthbert, J.; Gottlieb, E.; Balazs, A. C.; Kowalewski, T.; Matyjaszewski, K., Photoactivated Structurally Tailored and Engineered Macromolecular (STEM) gels as precursors for materials with spatially differentiated mechanical properties. *Polymer* **2017,** *126*, 224-230.

(13) Shanmugam, S.; Cuthbert, J.; Flum, J.; Fantin, M.; Boyer, C.; Kowalewski, T.; Matyjaszewski, K., Transformation of gels via catalyst-free selective RAFT photoactivation. *Polym. Chem.* **2019**.

(14) Lampley, M. W.; Harth, E., Photocontrolled Growth of Cross-Linked Nanonetworks. *ACS Macro Lett.* **2018,** *7* (6), 745-750.

(15) Chen, M.; MacLeod, M. J.; Johnson, J. A., Visible-Light-Controlled Living Radical Polymerization from a Trithiocarbonate Iniferter Mediated by an Organic Photoredox Catalyst. *ACS Macro Lett.* **2015,** *4* (5), 566-569.

(16) Shanmugam, S.; Cuthbert, J.; Kowalewski, T.; Boyer, C.; Matyjaszewski, K., Catalyst-Free Selective Photoactivation of RAFT Polymerization: A Facile Route for Preparation of Comblike and Bottlebrush Polymers. *Macromolecules* **2018,** *51* (19), 7776-7784.

(17) Appel, W. P. J.; Portale, G.; Wisse, E.; Dankers, P. Y. W.; Meijer, E. W., Aggregation of Ureido-Pyrimidinone Supramolecular Thermoplastic Elastomers into Nanofibers: A Kinetic Analysis. *Macromolecules* **2011,** *44* (17), 6776-6784.

(18) Wisse, E.; Spiering, A. J. H.; Dankers, P. Y. W.; Mezari, B.; Magusin, P. C. M. M.; Meijer, E. W., Multicomponent supramolecular thermoplastic elastomer with peptide-modified nanofibers. *J. Polym. Sci., Part A: Polym. Chem.* **2011,** *49* (8), 1764-1771.

(19) Celiz, A. D.; Scherman, O. A., A facile route to ureidopyrimidinone-functionalized polymers via RAFT. *J. Polym. Sci., Part A: Polym. Chem.* **2010,** *48* (24), 5833-5841.

(20) Zhu, B.; Noack, M.; Merindol, R.; Barner-Kowollik, C.; Walther, A., Light-Adaptive Supramolecular Nacre-Mimetic Nanocomposites. *Nano Lett.* **2016,** *16* (8), 5176-5182.

(21) Goor, O. J. G. M.; Hendrikse, S. I. S.; Dankers, P. Y. W.; Meijer, E. W., From supramolecular polymers to multi-component biomaterials. *Chem. Soc. Rev.* **2017,** *46* (21), 6621-6637.

(22) Bastings, M. M. C.; Koudstaal, S.; Kieltyka, R. E.; Nakano, Y.; Pape, A. C. H.; Feyen, D. A. M.; van Slochteren, F. J.; Doevendans, P. A.; Sluijter, J. P. G.; Meijer, E. W.; Chamuleau, S. A. J.; Dankers, P. Y. W., A Fast pH-Switchable and Self-Healing Supramolecular Hydrogel Carrier for Guided, Local Catheter Injection in the Infarcted Myocardium. *Advanced Healthcare Materials* **2014,** *3* (1), 70-78.

(23) Hendrikse, S. I. S.; Wijnands, S. P. W.; Lafleur, R. P. M.; Pouderoijen, M. J.; Janssen, H. M.; Dankers, P. Y. W.; Meijer, E. W., Controlling and tuning the dynamic nature of supramolecular polymers in aqueous solutions. *Chem. Commun.* **2017,** *53* (14), 2279-2282.

(24) Nieuwenhuizen, M. M. L.; de Greef, T. F. A.; van der Bruggen, R. L. J.; Paulusse, J. M. J.; Appel, W. P. J.; Smulders, M. M. J.; Sijbesma, R. P.; Meijer, E. W., Self-Assembly of Ureido-Pyrimidinone Dimers into One-Dimensional Stacks by Lateral Hydrogen Bonding. *Chemistry – A European Journal* **2010,** *16* (5), 1601-1612.

(25) Lewis, C. L.; Anthamatten, M., Synthesis, swelling behavior, and viscoelastic properties of functional poly(hydroxyethyl methacrylate) with ureidopyrimidinone side-groups. *Soft Matter* **2013,** *9* (15), 4058-4066.

(26) Zhang, G.; Chen, Y.; Deng, Y.; Ngai, T.; Wang, C., Dynamic Supramolecular Hydrogels: Regulating Hydrogel Properties through Self-Complementary Quadruple Hydrogen Bonds and Thermo-Switch. *ACS Macro Lett.* **2017,** *6* (7), 641-646.

(27) Keizer, Henk M.; Sijbesma, Rint P.; Meijer, E. W., The Convenient Synthesis of Hydrogen-Bonded Ureidopyrimidinones. *Eur. J. Org. Chem.* **2004,** *2004* (12), 2553-2555.

(28) Pilate, F.; Wen, Z.-B.; Khelifa, F.; Hui, Y.; Delpierre, S.; Dan, L.; Mincheva, R.; Dubois, P.; Yang, K.-K.; Raquez, J.-M., Design of melt-recyclable poly(ε-caprolactone)-based supramolecular shape-memory nanocomposites. *RSC Adv.* **2018,** *8* (48), 27119-27130.

(29) Zha, R. H.; de Waal, B. F. M.; Lutz, M.; Teunissen, A. J. P.; Meijer, E. W., End Groups of Functionalized Siloxane Oligomers Direct Block-Copolymeric or Liquid-Crystalline Self-Assembly Behavior. *J. Am. Chem. Soc.* **2016,** *138* (17), 5693-5698.

(30) Clay, R. J.; Collom, T. A.; Karrick, G. L.; Wemple, J., A Safe, Economical Method for the Preparation of β-Oxo Esters. *Synthesis* **1993,** *1993* (03), 290-292.

(31) Keizer, H. M.; González, J. J.; Segura, M.; Prados, P.; Sijbesma, R. P.; Meijer, E. W.; de Mendoza, J., Self-Assembled Pentamers and Hexamers Linked through Quadruple-Hydrogen-Bonded 2-Ureido-4[1H]-Pyrimidinones. *Chemistry – A European Journal* **2005,** *11* (16), 4602-4608.

(32) Devine, W. G.; Diaz-Gonzalez, R.; Ceballos-Perez, G.; Rojas, D.; Satoh, T.; Tear, W.; Ranade, R. M.; Barros-Álvarez, X.; Hol, W. G. J.; Buckner, F. S.; Navarro, M.; Pollastri, M. P., From Cells to Mice to Target: Characterization of NEU-1053 (SB-443342) and Its Analogues for Treatment of Human African Trypanosomiasis. *ACS Infectious Diseases* **2017,** *3* (3), 225-236.

Chapter VI

FUTURE DIRECTIONS

In this body of works we have successfully demonstrated the design and preparation of photoresponsive polymeric nanomaterials capable of experiencing controlled manipulations in size and network properties through the incorporation of various monomers into network crosslinks via light-mediated polymerizations. In addition to continuing the works on the site selective network expansions and the investigation into the manipulation of morphology in self-assembled materials, there exist several directions for the advancement of the developed photocontrolled growth process.

First, we have demonstrated the successful incorporation of multiblock copolymer compositions into the network architecture. Since block copolymers are known to micro-phase separate there stands an opportunity to investigate whether micro-phase separation occurs within nanonetworks expanded with block copolymer compositions. Furthermore, if phase separation is occurring it would be interesting to study how the nanonetworks are affected and if they are capable of self-assembly. Additionally, if phase separation is possible then the described photocontrolled growth process could be used to explore if the preparation of phase separated janus type nanoparticles is possible through this process.

Second, with the increased interest in network manipulations, there has been an increased interest in network defects. Given that the described photogrowable nanonetworks are fully soluble in organic solvents, they may provide useful benefits over their insoluble bulk gel counter parts when it comes to studying these network defects. Additionally, the current synthetic routes of the photogrowable networks (i.e. thiol-maleimide and Diels-Alder) inevitably produce network

defects in the form of loops. This occurs when an intramolecular crosslinking reaction takes place instead of an intermolecular crosslinking reaction. Work could be done to determine the number of loops present in the parent nanonetwork and in the produced daughter networks after expansion. Understanding how the number of loops change or how the presence of loops affects the expansion process will provide a better understanding of network defects.

Likewise, our proposed site selective expansions could provide a deeper understanding of the role that loops play during the network expansion. Expansions from the network scaffold polymers should be independent of interactions with loop defects, while expansions from the network crosslinks would be prone to interactions with loops. Comparison of the number of loops before and after network expansion from the scaffold polymer could reveal if or how the network crosslinks change as a result of these polymerizations. The ability to selectively expand from these specific sites could provide further insight into how loops and network defects affect polymerizations occurring within the network.

APPENDIX A

Curriculum Vitae

Michael W. Lampley

Ph.D. Candidate, Department of Chemistry, Vanderbilt University

(931)-242-8021 michael.w.lampley@vanderbilt.edu Linkedin.com/in/michael-w-lampley

EXECUTIVE SUMMARY

Vanderbilt Chemistry PhD, adaptable, self-starter, and problem solver with 7 years of academic research experience in organic synthesis and polymer synthesis with experimental and data analysis expertise. Seeking technical role or technical management role in a research and development setting where knowledge of polymer chemistry, nanotechnology, and organic synthesis adds value. Highlights include:

- In depth knowledge of organic chemistry
- Broad knowledge in polymer chemistry, modification, and characterization
- Good attention to detail, prioritization, and multi-tasking skills to independently advance multiple projects
- Strong oral and written communication skills demonstrated by 3 national meeting presentations and the successful funding of an NSF grant worth $450,000

EDUCATION

Ph.D., Chemistry *2019*

Vanderbilt University, Nashville, TN

Dissertation: Design and Manipulation of Photoresponsive Polymer Networks Through Light-Mediated Polymerizations
Advisor: Dr. Eva Harth

B.S., Biochemistry (summa cum laude) *2014*

Middle Tennessee State University, Murfreesboro, TN

University Honors College
Honors Thesis: “Synthesis of Cyclopropyl Peptidomimetic BACE Inhibitors”
Advisor: Dr. Norma Dunlap

WORK EXPERIENCE

Graduate Research Assistant *2014 - Present*

Vanderbilt University, Nashville, TN *and* University of Houston, Houston, TX

- Developed a "living" polymeric nanoparticle capable of experiencing precise manipulations in size and functionality through light mediated polymerizations resulting in 2 publications and the preparation of 1 manuscript
- Worked collaboratively to develop UV and visible light curable, polymer based microparticles through piezoelectric inkjet printing resulting in a publication
- Experience in controlled radical polymerizations, nanomaterials, organic synthesis and experimental design
- Mentored 3 graduate and 1 undergraduate research assistants; managed laboratory waste
- Assisted in the planning and writing of a successfully funded NSF grant
- Instrumentation: NMR, TEM, DLS, GPC, UV-Vis, and IR

Undergraduate Research Assistant *2012 -2014*

Middle Tennessee State University, Murfreesboro, TN

- Synthesized amino acid derivatives and unnatural amino acids
- Synthesized cyclopropyl peptidomimetics for activity against BACE-1
- Synthesized and characterized organic compounds to complete an 8 step synthesis

LEADERSHIP and TEACHING EXPERIENCE

Graduate Teaching Assistant *2014 –2017*

Vanderbilt University, Nashville, TN

- Conducted 2 lab sessions per semester, administered grades, and held office hours for 40 students per semester in general or organic chemistry (Fall 2014 – Summer 2017)
- Supervised and mentored over 250 undergraduates in various laboratory settings
- Achieved an average student approval rating of 4.0 on a 5 point scale

Vanderbilt University Chemistry Warren Committee *2017 – 2018*

- Organized departmental events and speakers

ACADEMIC HONORS

- Maryilyn M. and Philip M. Mathis Research Award *2014*
- First Place, MTSU Scholars Week Poster Competition *2014*
- Dan D. Scott Chemistry Scholarship *2013*

PROFESSIONAL ORGANIZATIONS

American Chemical Society *2013 - Present*

PUBLICATIONS

1. Kendrick-williams, L. L., **Lampley, M. W**., Ordonex, E., Harth, E. "Synergistic Dual Drug Delivery with Sustained-Release Formaldehyde from Polymer Prodrugs and Doxorubicin Nanoparticles for Improved Antitumor Efficacy" *Manuscript in Preparation*

2. **Lampley, M. W.,** Tsogtgerel, E., Harth E. "Nanonetwork Photogrowth Expansion: Tailoring Nanoparticle Networks' Chemical Structure and Local Topology" *Polymer Chemistry.* **2019**,10, 3841-3850
3. **Lampley, M. W**., Harth E. "Photocontrolled Growth of Cross-Linked Nanonetworks", *ACS Macro Letters*, **2018**, 7, 745-750
4. Gilmore, K. A.; **Lampley, M. W**.; Boyer, C.; Harth, E. "Matrices for combined delivery of proteins and synthetic molecules." *Advanced Drug Delivery Reviews,* **2016**
5. Spears, B.R.; Marin, M.A.; Chaker, A.N.; **Lampley, M.W**.; Harth, E. "Precise Microscale Polymeric Networks through Piezoelectronic Inkjet Printing." *ACS Biomaterials Science and Engineering*, **2016**

TECHNICAL SKILLS

Nuclear Magnetic Resonance (NMR) Spectroscopy
Gel Permeation Chromatography (GPC)
Transmission Electron Microscopy (TEM)
Dynamic Light Scattering (DLS)
Infrared Spectroscopy (IR)
Ring Opening Polymerization
RAFT Polymerization
ATRP Polymerization
UV/Vis Spectroscopy

PRESENTATIONS

- "Photocontrolled Growth of Cross-Linked Nanonetworks", oral session presented at 256th ACS National Meeting and Exposition, 2018, Boston, MA.
- Printing of Polymer Hydrogel Microparticles as Drug Delivery Vehicles. Poster session presented at: 251st ACS National Meeting and Exposition, 2016, San Diego, CA.
- Cyclopropyl Peptidomimetics as Potential HCV NS3 Protease and BACE-1 Inhibitors. Poster session presented at: 247th ACS National Meeting & Exposition, 2014 March 17; Dallas, TX